Oxidative Medicine and Cellular Longevity

Oxidants and Redox Signaling: Perspectives in Cancer Therapy, Inflammation, and Plasma Medicine

Lead Guest Editor: Sander Bekeschus
Guest Editors: Lars Bräutigam, Kristian Wende, and Eva-Maria Hanschmann

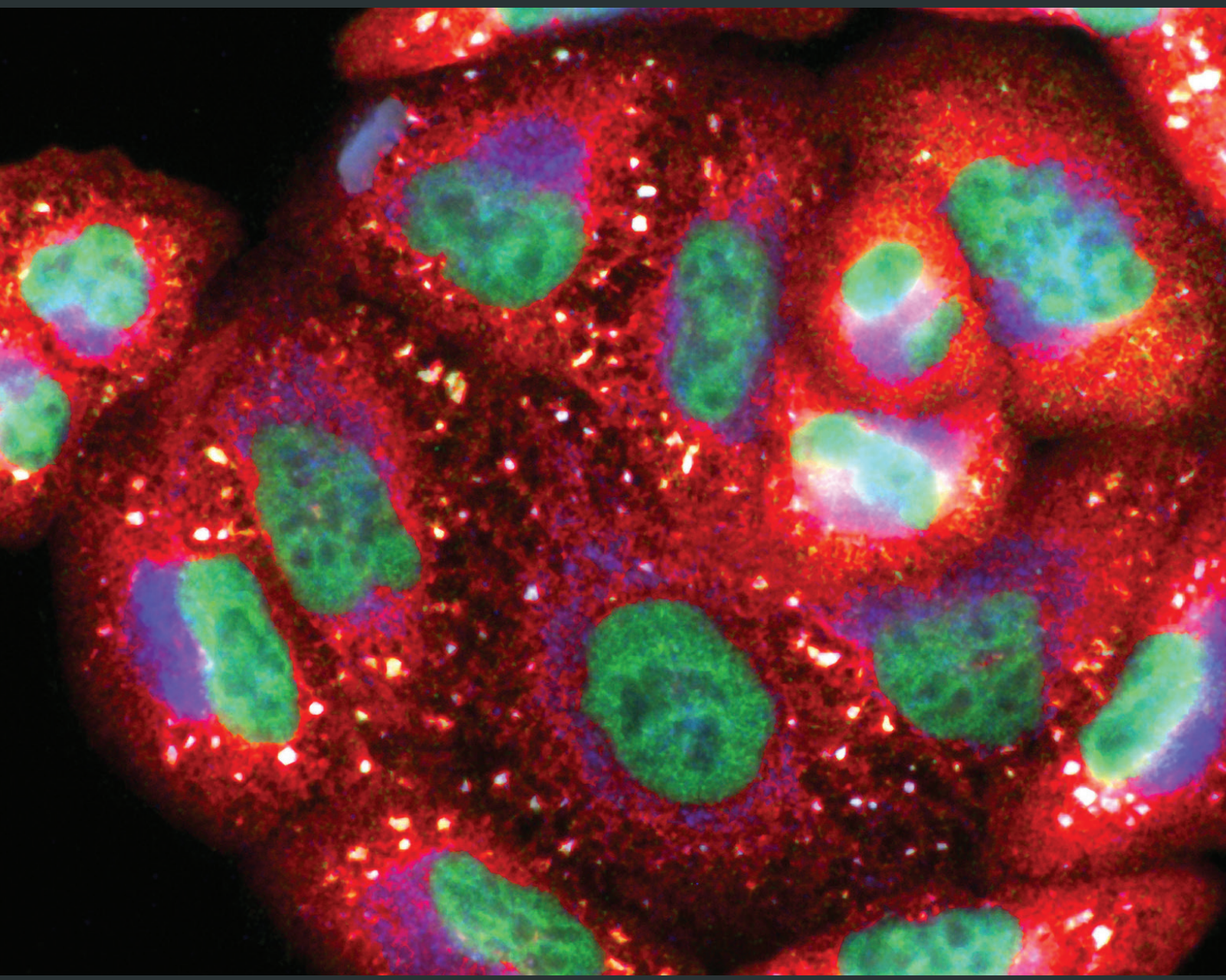

Oxidants and Redox Signaling: Perspectives in Cancer Therapy, Inflammation, and Plasma Medicine

Oxidative Medicine and Cellular Longevity

Oxidants and Redox Signaling: Perspectives in Cancer Therapy, Inflammation, and Plasma Medicine

Lead Guest Editor: Sander Bekeschus
Guest Editors: Lars Bräutigam and Kristian Wende

Editorial Board

Contents

Hindawi
Oxidative Medicine and Cellular Longevity
Volume 2017, Article ID 4020253, 2 pages
https://doi.org/10.1155/2017/4020253

Editorial

Oxidants and Redox Signaling: Perspectives in Cancer Therapy, Inflammation, and Plasma Medicine

Sander Bekeschus,[1] Lars Bräutigam,[2] Kristian Wende,[1] and Eva-Maria Hanschmann[3]

[1]*ZIK plasmatis, Leibniz Institute for Plasma Science and Technology (INP Greifswald), Greifswald, Germany*
[2]*Department of Medical Biochemistry and Biophysics, Karolinska Institutet, Stockholm, Sweden*
[3]*Department for Neurology, Heinrich Heine University Düsseldorf, Düsseldorf, Germany*

Correspondence should be addressed to Sander Bekeschus; sander.bekeschus@inp-greifswald.de

Received 17 August 2017; Accepted 17 August 2017; Published 29 October 2017

Redox signaling is a key player in the regulation of physiological processes. Current concepts in redox biology and plasma medicine emphasize the significance of redox dysregulation in inflammation and different pathologies including cancer. The identification and characterization of specific protein thiol switches and redox-regulated signaling pathways are two of the challenges in the fields. For example, tumor cells are often localized in a hypoxic environment, which leads to a unique redox signaling affecting metabolism, proliferation, metastasis, and apoptosis, as well as angiogenesis and the immune response. Deciphering and understanding the redox regulation of particular molecules and processes in a physiological and pathological context could allow the development of new therapeutic avenues. These strategies could comprise development of small molecules specifically targeting thiol switches and dysregulated redox signaling cascades, or localized generation of reactive oxygen species, for example, by cold physical plasma sources. This special issue is dedicated to oxidants and redox signaling.

One of the papers is a review article entitled "Redox Regulation of Inflammatory Processes Is Enzymatically Controlled." I. Lorenzen et al. introduce redox active molecules. They summarize distinct functions and pathological implications of the enzymes that regulate their production and decay, such as nicotinamide adenine dinucleotide phosphate oxidases (NOX), nitric oxide synthases (NOS), superoxide dismutases (SOD), and thioredoxin (TRX) family proteins. Moreover, the authors describe regulatory thiol switches in nuclear factor kappa B (NFκB), a disintegrin and metalloproteinase 17 (ADAM17), and high mobility group box 1 protein (HMGB1) as well as in pathways related to inflammatory signaling including the TLR cascades.

In the article "The Synthetic Lignan Secoisolariciresinol Diglucoside Prevents Asbestos-Induced NLRP3 Inflammasome Activation in Murine Macrophages," R. A. Pietrofesa et al. analyze the potential use of LGM2605 in chemoprevention of asbestos-induced mesothelioma. LGM2605 was formerly shown to induce gene expression of nuclear factor (erythroid-derived 2)-like 2 (Nrf2)-regulated antioxidants and to reduce cellular levels of reactive species, induced by asbestos. Here, the authors show that LGM2605 significantly reduces asbestos-induced expression of the NLRP3 inflammasome, iNOS, and NFκB, as well as the release of proinflammatory cytokines, levels of nitrates/nitrites, and NFκB activation.

The work entitled "Cold Atmospheric Plasma Induces Apoptosis and Oxidative Stress Pathway Regulation in T-Lymphoblastoid Leukemia Cells" by E. Turrini et al. aimed to mechanistically analyze the impact of cold atmospheric plasma and the induction of reactive oxygen and nitrogen species (ROS/RNS) on apoptosis, DNA damage, and the consecutive upregulation of redox-related enzymes, such as, superoxide dismutase, catalase, and glutathione reductase, thereby connecting the short-lived plasma-generated species to central cellular redox signaling pathways.

In the article "Toxicity and Immunogenicity in Murine Melanoma following Exposure to Physical Plasma-Derived Oxidants," S. Bekeschus et al. demonstrate anticancer effects

of cold physical plasma on melanoma cells in vitro. Specifically, these cells are subject to plasma-mediated oxidation, cell death, and reduced motility of the remaining viable cells. This is accompanied by alterations in biomechanical properties, that is, an increased stiffness and differential regulation of zonula occludens 1 (ZO1) proteins in melanoma cells following plasma treatment. Importantly, plasma treatment increases expression of major histocompatibility complex class I molecules and calreticulin, two major proteins for recognition and phagocytosis of antigen-presenting cells necessary to mount an immune response.

In the paper "2-Deoxy-D-glucose Restore Glucocorticoid Sensitivity in Acute Lymphoblastic Leukemia via Modification of N-linked Glycosylation in an Oxygen Tension-Independent Manner" by Z. Leni et al., a possible way is described, how to address the issue of chemoresistance in childhood leukemia. By feeding a glucose analog to different acute lymphoblastic leukemia cell lines, the authors could show efficient killing of cancer cells that was accompanied by endoplasmic reticulum stress and induction of the unfolded protein responses. Both processes are critical in eliciting immunogenic cell death that is in principle capable of driving inflammation and antitumor immune responses.

The work of L. Hu et al. entitled "The Protective Roles of ROS-Mediated Mitophagy on ^{125}I Seeds Radiation Induced Cell Death in HCT116 Cells" uncovers a critical role of phagocytosis of damaged mitochondria in irradiation-induced cancer cell death. By exposing human colon cancer cells to iodide-derived irradiation in vitro, they found an upregulation of intracellular ROS and targets (e.g., hypoxia-inducible factor α, HIF1α; BCL2/adenovirus E1B 19 kDa protein-interacting protein 3, BNIP3; NIP3-like protein X, NIX) involved in the induction of mitophagy, protecting cancer cells from cell death. The authors suggested mitophagic pathways to serve as possible drug targets in the future.

In the review article "Oxidative Stress Gene Expression Profile Correlates with Cancer Patient Poor Prognosis: Identification of Crucial Pathways Might Select Novel Therapeutic Approaches" by A. Leone et al., the authors discuss the double-face role of reactive oxygen species in cancer initiation, progression, and prognosis. Their analysis, which extends over 6 distinct tumor types, is based on cancer-type-specific oxidative stress gene profiles and data from the Cancer Genome Atlas database. Among the statistically significant genes associated with cancer initiation and progression, the authors found Forkhead box M1 (FoxM1) and thioredoxin reductase 1 (TrxR1) to be critical for the regulation of oxidative stress levels in all analyzed tumor types. Moreover, A. Leone et al. discuss how the identified signaling networks correlate to cancer stem cell signatures and provide by that knowledge on which redox pathways could be prioritized for the development of novel therapies.

Acknowledgments

The guest editorial team would like to thank all authors of the contributed papers and review articles submitted to this special issue. We are very grateful to the numerous reviewers, which have donated their time, knowledge, and experience to every single article. We hope that you will enjoy this special issue, dedicated to the exciting field of redox signaling with emphasis on cancer, inflammation, and plasma medicine.

Sander Bekeschus
Lars Bräutigam
Kristian Wende
Eva-Maria Hanschmann

Hindawi
Oxidative Medicine and Cellular Longevity
Volume 2017, Article ID 8459402, 23 pages
https://doi.org/10.1155/2017/8459402

Review Article

Redox Regulation of Inflammatory Processes Is Enzymatically Controlled

Inken Lorenzen,[1] Lisa Mullen,[2] Sander Bekeschus,[3] and Eva-Maria Hanschmann[4]

[1]*Department of Structural Biology, Institute of Zoology, Kiel University, Kiel, Germany*
[2]*Brighton and Sussex Medical School, Falmer, Brighton, UK*
[3]*Leibniz-Institute for Plasma Science and Technology (INP Greifswald), ZIK plasmatis, Greifswald, Germany*
[4]*Department of Neurology, Medical Faculty, Heinrich-Heine University, Düsseldorf, Germany*

Correspondence should be addressed to Eva-Maria Hanschmann; eva-maria.hanschmann@med.uni-duesseldorf.de

Received 3 March 2017; Revised 6 July 2017; Accepted 25 July 2017; Published 8 October 2017

Academic Editor: Shane Thomas

Redox regulation depends on the enzymatically controlled production and decay of redox active molecules. NADPH oxidases, superoxide dismutases, nitric oxide synthases, and others produce the redox active molecules superoxide, hydrogen peroxide, nitric oxide, and hydrogen sulfide. These react with target proteins inducing spatiotemporal modifications of cysteine residues within different signaling cascades. Thioredoxin family proteins are key regulators of the redox state of proteins. They regulate the formation and removal of oxidative modifications by specific thiol reduction and oxidation. All of these redox enzymes affect inflammatory processes and the innate and adaptive immune response. Interestingly, this regulation involves different mechanisms in different biological compartments and specialized cell types. The localization and activity of distinct proteins including, for instance, the transcription factor NFκB and the immune mediator HMGB1 are redox-regulated. The transmembrane protein ADAM17 releases proinflammatory mediators, such as TNFα, and is itself regulated by a thiol switch. Moreover, extracellular redox enzymes were shown to modulate the activity and migration behavior of various types of immune cells by acting as cytokines and/or chemokines. Within this review article, we will address the concept of redox signaling and the functions of both redox enzymes and redox active molecules in innate and adaptive immune responses.

1. Concept of Redox Signaling

Cells can receive and respond to distinct signals and environmental changes; they can send out signals in order to communicate with other cells. Signal transduction can depend on intracellular or membrane-bound receptors that have the ability to bind specific ligands that induce particular signaling cascades involving second messengers and rapid, reversible posttranslational modifications of transducer and effector proteins. Some signaling molecules can pass the plasma membrane and directly interact with specific targets. In the case of redox regulation, we can distinguish between different spatiotemporal modifications of cysteine residues, such as the formation of inter- or intramolecular disulfide bridges, S-glutathionylation by the formation of a mixed disulfide with glutathione (GSH), S-nitrosylation in the presence of nitric oxide (NO), the formation of sulfenic acid, for example, in the presence of hydrogen peroxide (H_2O_2), or the formation of S-sulfhydration by hydrogen sulfide (H_2S). All these modifications modify the redox state of a particular thiol group and can affect a protein in terms of structure, localization, and/or activity [1] (Figure 1). These regulatory thiol groups are known as thiol switches [2]. Interestingly, redox modifications also affect other posttranslational modifications, essential for signal transduction, for instance, phosphorylation. Redox signaling occurs upon specific stimuli and is localized in specific compartments or confined areas within a cellular compartment. The signal is sensed by a particular receptor, inducing the production and release of second messengers such as H_2O_2, NO, and H_2S. Interestingly, not all reactive oxygen, nitrogen, and sulfur species are considered signaling molecules. This is due to their high reactivity towards a wide range of unspecific targets including various biomolecules, such as DNA, lipids, and proteins, and the lack

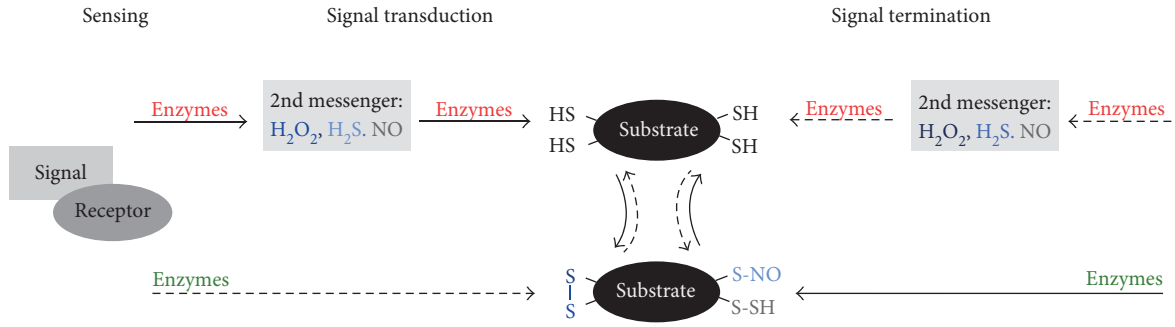

Figure 1: Concept of redox signaling. A signal is sensed by its receptor, inducing the enzymatic catalyzed production and release of second messengers (e.g., H_2O_2, NO, and H_2S). These activate a cascade of transducing proteins via specific oxidative modifications at Cys residues (e.g., disulfide formation, nitrosylation, and sulfhydration). The effector molecule induces the biological response. A signal can also induce the reduction of distinct Cys residues. The activated signaling cascade becomes terminated, and cysteinyl modifications are reversed. The involved thiol groups are known as thiol switches. Their reduction (green), as well as their oxidation (red) are regulated by different enzymes.

of regulation of their production and decay. The hydroxyl radical, for instance, is nonenzymatically produced in the Fenton reaction and reacts with basically any molecule due to its high reactivity and lack of specificity [1]. Similarly, peroxynitrite is not considered a second messenger, because it is spontaneously formed by the reaction of nitric oxide with superoxide and a strong oxidizing agent with a second-order rate constant of $10^{10}\,M^{-1}{\cdot}s^{-1}$ that also oxidizes various biomolecules (reviewed in [3, 4]). H_2O_2, NO, and H_2S activate effector molecules that induce a certain biological response via specific transducing molecules including redox couples, for example, GSH and oxidized glutathione (GSSG) and enzymes, for example, oxidoreductases of the thioredoxin (Trx) family. In the absence of the signal, the activated signaling cascade becomes terminated and cysteinyl modifications are reversed. These thiol switches have been predicted to play a role in almost every signaling cascade and are therefore essential for all biological processes. Obviously, physiological redox signaling is highly regulated and depends on the controlled oxidation as well as the specific reduction of substrates [1, 5]. The dysregulation or even disruption of redox signaling has been described as oxidative stress, a hallmark of various pathologies [6].

As mentioned above, the production and release of redox active molecules are regulated by enzymes that are located in various cellular compartments and also in the extracellular space (Figure 2). Complexes I and III of the respiratory chain and enzymes such as nicotinamide adenine dinucleotide phosphate- (NADPH-) oxidases (NOX) and xanthine oxidase produce superoxide ($O_2^{\bullet-}$). Superoxide dismutases (SOD) convert $O_2^{\bullet-}$ into H_2O_2. Different peroxidases, including catalase and the Trx family members peroxiredoxins (Prxs) and glutathione peroxidases (Gpx), reduce H_2O_2 to water. NO is synthesized by one of the three isoforms of nitric oxide synthase (NOS), that is, neuronal nNOS, inducible iNOS, and endothelial eNOS. H_2S is produced by cystathionine β-synthase, cystathionine γ-lyase, L-cysteine desulfhydrase, and 3-mercaptopyruvate sulfurtransferase (for an overview see [1] and references within). In addition to the production, the degradation of these molecules is also enzymatically regulated (Figure 2). Contrary to previous understanding, free oxygen and nitrogen species cannot generally oxidize thiol groups directly. The reaction rate of H_2O_2 with the highly abundant peroxidases of the Trx family, Prxs, ranges from 10^6 to $10^8\,M^{-1}{\cdot}s^{-1}$. The reaction rate of other reactive protein thiols and free Cys is significantly lower in a range of approximately $10^1\,M^{-1}{\cdot}s^{-1}$ [7, 8]. Due to high protein expression and reactivity, a molecule of H_2O_2 is more prone to oxidize a Prx molecule than the thiol group of any other protein. Prxs are peroxidases that can function in cellular signaling as peroxide sensors. Moreover, H_2O_2 signaling can be conducted via GPxs and GSH [9]. Trx family proteins are key regulators of redox signaling by regulating the redox state of particular substrate proteins. They catalyze disulfide reduction and isomerisation reactions and regulate deglutathionylation, as well as denitrosylation and depersulfidation. Moreover, they are also involved in the oxidation of thiols, for example, by catalyzing S-glutathionylation, transnitrosylation, and S-sulfhydration. Trx proteins contain the structural Trx fold and an active site motif that contains one or two cysteinyl residues and is essential for the catalytic monothiol and dithiol mechanisms. Substrates of Trx family proteins include enzymes such as ribonucleotide reductase [10, 11] Sirtuin-1 [12], caspase-3 [13], the mitogen-activated protein (MAP) kinase apoptosis signal-regulating kinase 1 (ASK1) [14] and mercaptopyruvate sulfur transferase (MST) [15], transcription factors such as nuclear factor kappa B (NFκB) [16], and signal transducer and activator of transcription 3 (STAT3) [17]. Moreover, components of the Wnt signaling pathway (dishevelled [18]), cytoskeletal dynamics (e.g., collapsin response mediator protein 2 [19, 20]), and innate immunity (e.g., myeloid differentiation primary response 88 (Myd88) [21] and a disintegrin and metalloproteinase 17 (ADAM17) [22]) are regulated by Trx proteins. So far, not much is known about the specificity of substrate recognition. However, it is known that not every surface-exposed Cys residue is involved in redox regulation. Lillig and Berndt have shown that the reactivity of a cysteinyl residue depends on the surrounding amino acids creating the electrostatic and hydrophobic environment of the thiol group [23]. Recently, it was demonstrated that substrate recognition depends on kinetic constraints, complementary molecular geometries, and the electrostatic surface potential of the oxidoreductase and the target protein [8, 24].

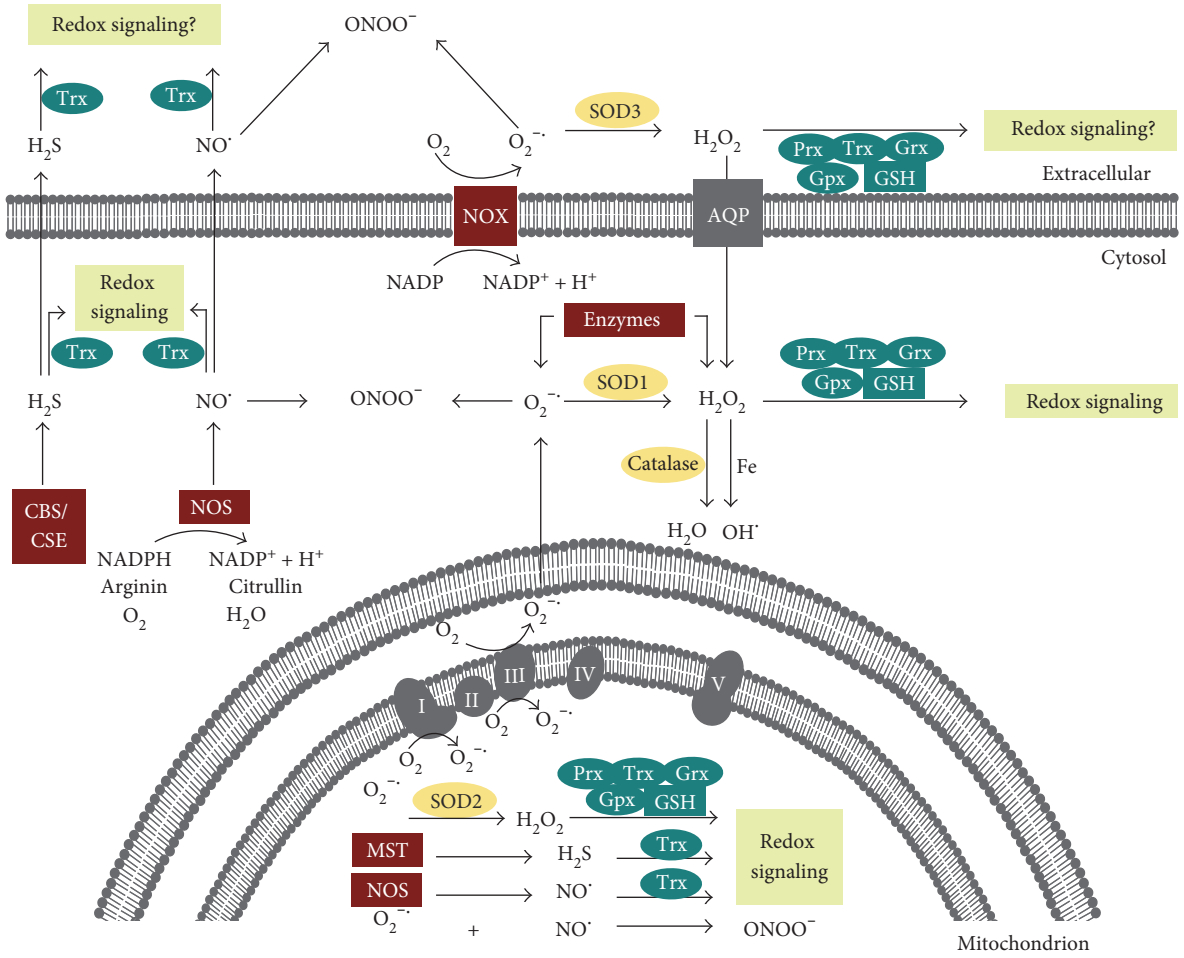

FIGURE 2: Redox regulation is enzymatically controlled. Illustration of cellular and extracellular enzymes that (i) generate redox active species (red), (ii) decompose reactive species, and are classified as antioxidants (yellow) or (iii) participate in redox signaling (blue). In the cytosol, superoxide (O_2^-) and hydrogen peroxide (H_2O_2) can be produced by specific enzymes; the cytosolic SOD1 can convert O_2^- to H_2O_2. Moreover, the NADPH and oxygen-dependent membrane protein NADPH-oxidase (NOX) can produce O_2^- that is converted to H_2O_2 by extracellular SOD3. The latter can cross the membrane via simple diffusion and aquaporins. H_2O_2 can participate in cell signaling as a second messenger via the action of the thioredoxin family members peroxiredoxin (Prx), thioredoxin (Trx), glutaredoxin (Grx), and glutathione peroxidases. These enzymes are NADPH- and mostly glutathione- (GSH-) dependent. H_2O_2 can also be reduced to water by the peroxidase catalase, which is mainly located in peroxisomes. However, in the presence of free iron, the highly reactive and damaging hydroxyl radical ($OH^\bullet$) is formed from H_2O_2 via the Fenton reaction. Nitric oxide (NO) is generated by cytosolic NO-synthase (NOS) and hydrogen sulfite (H_2S) by the enzymes cystathionine β-synthase (CBS) and cystathionine γ-lyase (CSE). Both constitute second messengers that can participate in redox signaling via the action of Trx. Note that peroxynitrite ($ONOO^-$) can spontaneously form in the presence of O_2^- and NO, inducing irreversible modifications of various biomolecules and thus not participating in redox signaling. In mitochondria, complexes I and III of the mitochondrial respiratory chain produce superoxide ($O_2^{-\bullet}$). Superoxide dismutase 2 (SOD2) converts O_2^- to H_2O_2. Mitochondrial NOS and 3-mercaptopyruvate sulfurtransferase (MST) produce NO and H_2S, respectively. Mitochondrial H_2O_2, NO, and H_2S can participate in redox signaling. Similar to the cytosol, $ONOO^-$ and $OH^\bullet$ can also be formed in the mitochondria. In the extracellular environment, NOX and SOD3 produce O_2^- and H_2O_2 and the intracellularly produced NO and H_2S can cross the plasma membrane. Members of the Trx family of proteins are found extracellular. Therefore, the intracellular concept of redox signaling might also occur in the microenvironment of the cell.

2. Redox Regulation of the Inflammatory Response

Upon tissue damage and infection, the inflammatory response is induced. This highly regulated and protective process facilitates the removal of foreign and/or damaged components, as well as tissue repair and is terminated when a return to physiological conditions is achieved. The inflammatory response is composed of distinct receptor proteins, inflammatory mediators, and specialized cell types, as well as changes in tissue homeostasis and blood flow. Initiation of inflammation is reliant on the production of a number of cytokines which are produced by activated cells of the innate immune system in response to a range of stimuli. Proinflammatory cytokines are essential for the activation of the adaptive immunity, that is, B- and T-lymphocytes. In some circumstances, the production of these proinflammatory cytokines is maintained beyond that required to facilitate

microbial destruction and tissue repair, resulting in a chronic inflammatory response where both innate and adaptive immune cells are chronically activated, inducing tissue damage and subsequent autoimmune disease. Even though the exact redox signaling cascades are not fully understood, it is well known that the production of reactive oxygen species (ROS) and reactive nitrogen species (RNS) is essential for the onset, progression, and also the termination of inflammatory processes. Redox-regulated processes involve the innate, as well as the adaptive immunity, for example, the oxidative burst of immune cells and pathogen killing, cellular signal transduction, and regulation of gene transcription, cytokine release, and antigen presentation as well as the regulation of the activation, differentiation, and migration of immune cells and wound healing [1, 25–27]. Particularly, not only NO and H_2O_2 are essential during inflammation but also H_2S has been shown to possess anti- and proinflammatory functions [28, 29]. Production of NO as a signaling molecule with microbicidal, antiviral, and antiparasital as well as immunomodulatory functions is essential for inflammatory processes (reviewed in [30, 31]). NO constitutes an important second messenger in the inflammatory response with various functions in the classical activation during the onset of the inflammation, signal transduction, revascularisation, and tissue repair [32].

Reactive species are produced by phagocytic cells of the innate immune system, such as monocytes, macrophages, neutrophils, and dendritic cells, during the oxidative burst in order to kill pathogens as well as during tissue repair [33, 34]. Myeloperoxidase (MPO) catalyzes the reaction of H_2O_2 to highly oxidizing and microbicidal hypochlorous acid (HOCl) and hypobromous acid. This reaction can also be catalyzed by the eosinophil peroxidase. Another bactericidal and fungicidal enzyme that acts in the innate immune defence is the heme protein lactoperoxidase (LPO) generating hypothiocyanite ($^{-}$OSCN) from thiocyanate (SCN^{-}) and H_2O_2. The latter is a downstream metabolite of superoxide that is enzymatically produced by the NOX enzymes Duox1 and particularly Duox2 [35, 36]. In addition, NO and further RNS have been shown to be present in the phagosome and participate in eradication of pathogens [32]. Activation of NOX and the oxidative burst occurs only upon full activation of neutrophils in the presence of pathogens. Their antimicrobial activity can be primed by inflammatory cytokines, chemokines, anaphylatoxins, or pathogen-associated molecular pattern (PAMPs), for example, compounds of bacterial cell walls such as lipopolysaccharides (LPS) and lipoteichoic acid, flagellin, and bacterial DNA that are recognized by pathogen recognition receptors such as Toll-like receptors (TLRs) and cytoplasmic NOD-like receptors (NLRs) [37]. The latter are also part of the inflammasome that facilitates the cytosolic, caspase-1-mediated maturation of inflammatory cytokines and that has been shown to be redox-regulated [38], (reviewed in [26]). Both, NLRs and TLRs also recognize endogenous damage-associated molecular patterns (DAMPs), such as the redox-regulated high mobility group protein 1 (HMGB1) or metabolites like ATP, which are also known as danger signals [39]. TLRs are not exclusively expressed in phagocytic cells and are present in the first barriers of defence, such as the skin, airway, blood vessels, and colon. TLRs are involved in ROS production. Interestingly, LPS-activated neutrophils produce H_2O_2 that induces the TLR2 expression in endothelial cells promoting the immune defence via redox-regulated signaling events [40]. The cytosolic Toll/IL-1 receptor (TIR) domain of TLRs associates with the signal transduction adaptor protein Myd88 that recruits and activates a set of proteins, inducing downstream Map kinases (e.g., JNK and p38) and the phosphorylation and degradation of IκB, NFκB activation, and expression of target genes (Figure 3) [41]. Various components of this pathway are susceptible to redox regulation and were shown to interact with Trx family proteins, including NFκB, the transcription factor that controls, for example, the expression of proinflammatory cytokines, chemokines, growth factors, prostaglandins, adhesion molecules, and NOX2 as well as iNOS and also nNOS [1, 42, 43], promoting leukocyte recruitment and activation of the surrounding tissue. Interestingly, cytokines can be expressed as cytosolic or membrane-bound "precursors" and are activated and released by redox-regulated, proteolytical cleavage via cytosolic multiprotein complexes called inflammasomes or specific proteases such as ADAM17 [26, 44–47]. Cytokines are not the only proteins that are secreted upon inflammation. A large number of proteins secreted from innate immune cells in response to inflammatory stimuli have been shown to be glutathionylated [48]. Recent studies have seen the refinement of redox proteomic techniques to interrogate those proteins, identifying a substantial number of glutathionylated proteins, both intracellular and secreted [49, 50]. Among the secreted proteins, Trx1, Trx80, Prx1, and Prx2 were detected that have cytokine and/or chemokine-like functions [1, 51]. Secreted, glutathionylated Prx2 was recently described to function as danger signal [52]. And also, the related macrophage-inhibitory factor (MIF-1) has immunomodulatory functions [1].

Redox regulation of inflammation and of immune responses is not restricted to the activation and subsequent activity of innate immune cells. Generation of both humoral and cell-mediated adaptive immunity depends on activation of T helper cells, a process heavily reliant on the redox potential of the microenvironment of these cells [53, 54]. A reducing environment is necessary for both optimal activation of T-cells [55, 56] and for the downstream proliferation of these cells [57, 58] that is essential for generating an adaptive immune response. As these effector $CD4^{+}$ T-cells are essential for inducing full activation and class switching in activated B lymphocytes, the effects of changes in the redox environment also extend to the humoral arm of the adaptive immune response. It is perhaps unsurprising that redox changes in antigen-presenting cells can also help to determine whether T-cells develop into Th1 or Th2 cells [59, 60] given the importance of the interactions between T-cells and their antigen-presenting cells in T-cell activation. Increases in cellular ROS levels have been shown to be essential, for example, during T-cell activation, antigen presentation, and receptor-mediated cell signaling. Interestingly, administration of antioxidants such as the seleno-compound ebselen inhibits and impairs these functions [1, 61]. This

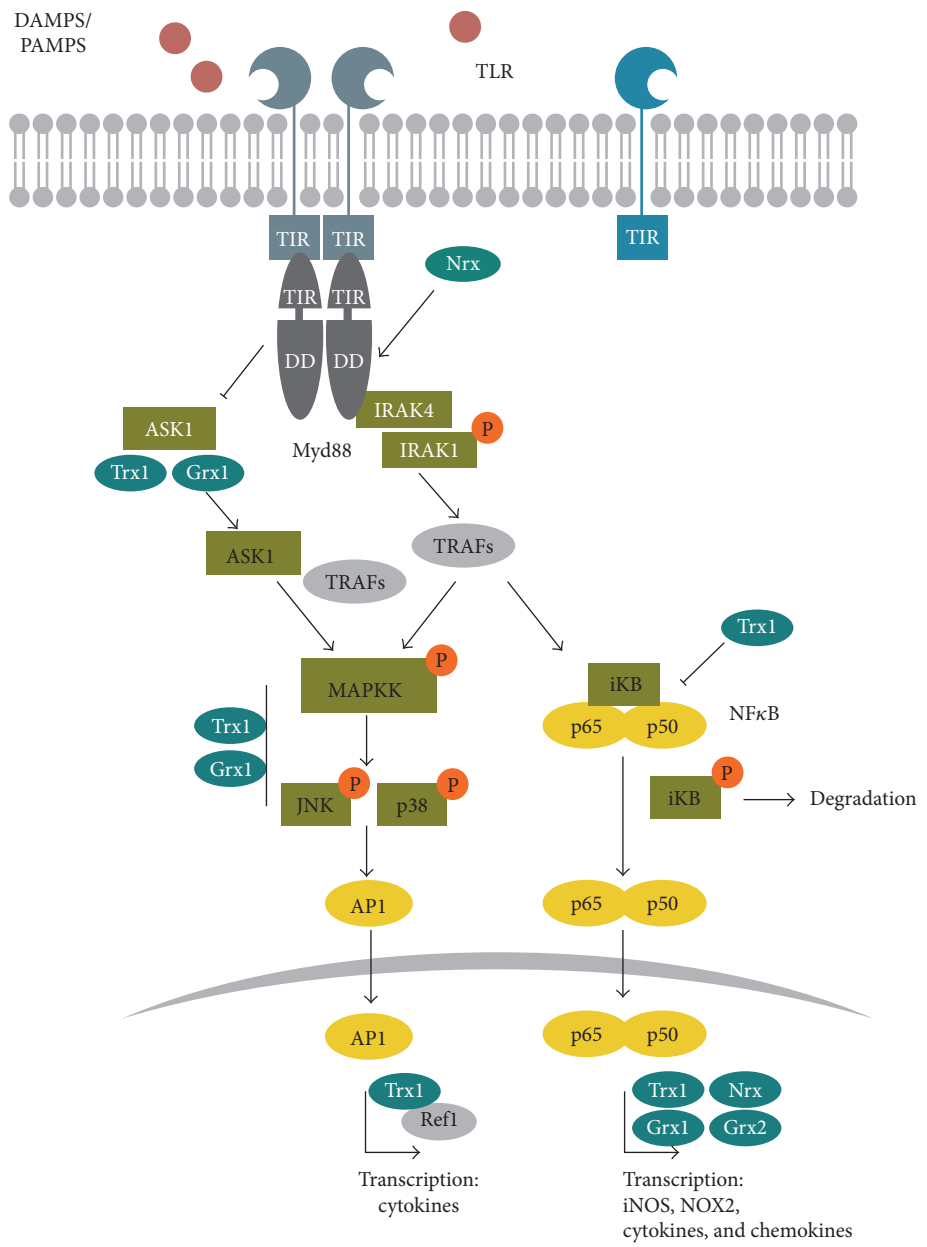

Figure 3: TLR signaling is redox-regulated. The general concept of the TLR signaling is illustrated, emphasizing the redox-regulated steps and molecules; note that this illustration is simplified and that specific TLR pathways include different proteins. PAMPs and DAMPs are recognized by their specific TLR, which can lead to homo- and heterodimerisation. Upon ligand binding, the TLR associates with the adaptor protein Myd88, which is sensitive to oxidation by hydrogen peroxide and can be regulated by Nrx. Myd88 recruits IRAK4 that phosphorylates IRAK1, which in turn activates additional proteins (e.g., TRAFs and IKK, not shown). MAP kinases and NFκB are activated. MAP kinase signaling is regulated by Trx1 and Grx1 and eventually activates the transcription factor AP1, which has two Cys residues in its DNA binding domain that are reduced by Trx1 via Ref1. The NFκB subunits p50 and p60 are kept in an inhibitory iκB/NFκB-complex in the cytosol. Reduced Trx1 inhibits the dissociation of this complex. Upon dissociation, iκB is phosphorylated and degraded by the proteasome. NF-κB translocates into the nucleus, where it binds to the DNA, a process that depends on the reduction of Cys62 and is regulated by Trx1, Grx1, and/or Nrx. An additional redox-regulated pathway involving ASK1 exists in TLR4 signaling. ASK1 is kept in an inactive complex by reduced Trx1. Upon TLR activation, Trx1 is oxidized, the complex dissociates and active ASK1 regulates JNK activity via different proteins including TRAFs.

may help to explain observations that autoimmune diseases such as rheumatoid arthritis [62] and multiple sclerosis [63] are associated with increased levels of oxidative stress. Like many autoimmune diseases and chronic inflammatory diseases, it is still unclear whether oxidative stress is a cause or effect of these conditions. However, for these particular conditions, treatment with antioxidants does actually ameliorate disease, at least in animal models [64], suggesting that oxidative stress does indeed play a role. Furthermore, one of the frontline treatments for people with multiple sclerosis,

Table 1: Thiol switches in inflammatory signaling processes.

Protein	Thiol/modification	Function	Regulation	Reference
ADAM17	C_{600}, C_{630}, C_{635}, C_{640}: intermolecular disulfides	Linear order of disulfides ($C_{600–630}$; $C_{635–640}$): open, flexible structure Overlaying disulfides ($C_{600–635}$; $C_{630–640}$): abrogates membrane binding and substrate recognition	PDI catalyzes the isomerisation from the linear to the overlaying disulfide pattern.	[135, 141]
Ask1	$C_{200, 250}$: intramolecular disulfide C_{250}: interaction with Trx1	ASK1 is involved in TLR4 signaling and is involved in TNFα-induced apoptosis. Intramolecular disulfide induces conformational changes within the Trx-binding region.	Trx1 and Grx1 bind to ASK1 and inhibit the kinase; in case of Trx1 proteasomal degradation is induced. Oxidation of Trx1/ Grx1 induces the dissociation of the complex and kinase activation.	[14, 96, 97, 257]
EGFR	C_{797}: sulfenylation	EGFR-mediated signaling; sulfenylation enhances tyrosine kinase activity.	Oxidation by H_2O_2	[90, 91]
HMGB1	C_{23}, C_{45}, C_{106}: intramolecular disulfide ($C_{23–45}$), sulfenylation(C_{106})	Fully reduced: chemotactic activity; intramolecular disulfide ($C_{23–45}$), reduced C_{106}: cytokine	Trx1 (Grx1?)	[154, 155, 157]
Myd88	8 Cys residues: (i) intermolecular disulfides (ii) nitrosylation	Intermolecular disulfides: oligomerisation during TLR signaling	Oxidation by H_2O_2 (Prx?), Nrx, Trx	[21, 93, 94]
NFκB	C_{62}: (i) glutathionylation (ii) sulfenylation	Reduced C_{62}: DNA binding and gene expression	Bound in an inactive complex by Trx1 (cytosol), reduction by Trx1, Grx1 (nucleus)	[16, 99, 101]
Src	C_{245}, C_{487}: disulfide formation	Intramolecular disulfide connects SH2 and kinase domain and stabilizes the active conformation of the kinase	Oxidation by H_2O_2	[88, 89]

dimethyl fumarate, exerts its therapeutic effects by upregulating antioxidant enzyme synthesis [65]. One possible mechanism by which oxidative stress could impact these conditions is via effects on T-cells that infiltrate the sites of disease, a recognized phenomenon in these pathologies [66]. If these cells then encounter relatively oxidizing conditions, this could influence their activation into the more inflammatory phenotypes such as Th1 and Th17 phenotypes, thereby exacerbating disease. Indeed, it has been suggested that exposure of T-cells to increased oxidative stress in rheumatoid arthritis causes them to become refractory to apoptosis leading to a perpetual immune response [67].

Within the next chapter, we will introduce distinct thiol switches and their impact on cell signaling and inflammatory processes (Table 1).

3. Thiol Switches in the Inflammatory Response

3.1. TLR Signaling. In terms of redox signaling, the production of the second messenger H_2O_2 is closely linked to the transmembrane multidomain NOX complexes. These transport electrons via NADPH, flavin-adenine dinucleotide (FAD), and heme from the cytoplasmic side of the plasma membrane to the extracellular part, where they are transferred to oxygen. By the action of extracellular SOD3, the produced superoxide is converted to H_2O_2, which passes the membrane by diffusion or via aquaporins (Figure 2). Superoxide/H_2O_2 production occurs in close proximity to the receptor complex, potentially in specific signaling platforms within lipid rafts, caveolae, or endosomes [68]. The NOX family comprises seven members, NOX1 to NOX5 and Duox1 and Duox2. The structure and regulation of the different NOXs have been extensively reviewed previously [69–72]. NOX-dependent ROS production can depend on endocytosis of activated receptor NOX complexes in redox-active endosomes, the redoxosomes. The formation of redoxosomes occurs out of lipid rafts, which contain inactive NOX as well as ligand-bound receptors that initiate NOX activity and require activated Rac1. Inhibition of endocytosis and formation of redoxosomes reduces superoxide formation and downstream activation of NFκB. For proper signaling, SOD activity and chloride channels are required, which are believed to export superoxide into the cytoplasm and import protons that stabilize the pH within the redoxosomes (reviewed in [73, 74]). Interestingly, this was demonstrated for IL-1β- and TNFα-induced signaling, but not for thrombin-activated NOX1 [74–77]. NOX1 is expressed in the colon and the vascular system and can be triggered by flagellin, via TLR5 [78], by LPS via TLR4 [79], and by CpG oligonucleotides via TLR9 [80] and is sensitive to IFNγ

[81]. NOX2 constitutes the first identified NOX, which is highly expressed in phagocytic active neutrophils and macrophages and to a much lower rate in dendritic cells [82]. NOX2 is sensitive to multiple TLRs [83] and essential for the oxidative burst. The assembly and activation of NOX2 occur upon fully activation of neutrophils in the presence of pathogens. Dendritic cells are specialized for antigen presentation, and NOX2 is needed for proper antigen presentation towards T-cells [84, 85]. In the airway epithelium, Duox1 was shown to depend on TLR4 [86]; regulating the expression of chemokines, which attract neutrophils and macrophages [83, 86, 87]. The physical interaction between the TIR domain of TLR4 and the cytoplasmic tail of NOX4 results in an activation of src, which phosphorylates IkBα, thereby activating NFκB and target genes [87]. The activity of src is regulated by tyrosine phosphorylation and can be boosted by a thiol switch [88]. Protein tyrosine phosphatases (PTPs) remove an inhibitory phosphorylation of a C-terminal Y527 residue and thus its inhibitory interaction with the SH2 domain of the kinase, followed by autophosphorylation. This active conformation of the protein is stabilized by a reversible thiol switch. C245 and C487 are oxidized and form a disulfide bond connecting the SH2 and the kinase domain. An exchange of these cysteinyl residues to alanine residues results in a redox unresponsive variant [88, 89]. Interestingly, src is not only involved in the regulation of NOX signaling but also targets the epidermal growth factor receptor (EGFR) that was also shown to undergo thiol oxidation. The targeted cysteine residue is located close to the ATP-binding site within the cytoplasmic part of the receptor protein (Figure 4). An exchange of the cysteine residue to a serine residue induces a 2.5-fold increase in the ATPase activity of EGFR [90, 91]. Besides src and EGFR, PTPs, for example, PTP1B, are targets for redox modification, that is, reversible oxidation of the catalytic active cysteine that renders the protein inactive [91, 92]. All three proteins are targeted by H_2O_2, produced by Duox1 in response to extracellular ATP, which functions as danger signal in the airway epithelium host defence [91]. These three examples show how specific and diverse redox regulation can occur during the same conditions and stimuli within a signaling cascade. Even though all transducers are oxidized at one or two particular Cys residues, the effect on the protein activity differs from being turned on or off like a redox switch to being modulated! Even though the oxidation has been shown, the exact regulatory mechanisms are still mostly elusive. It is however tempting to speculate that the oxidation by hydrogen peroxide is mediated via cytosolic Prxs and the reduction via, for example, Trx. Trx proteins have been already shown to regulate Myd88 and downstream Map kinases. Most TLRs need the adaptor protein Myd88 for signal transduction, which functions downstream of the signal-receptor complex upon ligand binding. Myd88 oligomerizes with the interleukin-1 receptor-associated kinase (IRAK) forming a signal initiation complex. The complex signal transduction involves various proteins and kinases, eventually triggering MAP kinases and NFκB signaling pathways (Figure 3) [41]. Recently, Stottmeier and Dick demonstrated that Myd88 undergoes redox regulation. In the presence of H_2O_2, Myd88 dimerizes and forms disulfide-linked conjugates with other proteins via eight conserved Cys residues (Figure 4). Interestingly, the oxidation by hydrogen peroxide is comparably sensitive to oxidation of Prx2 [93]. S-Nitrosylation of distinct Cys residues of Myd88 has also been described [94]. Nucleoredoxin (Nrx) controls TLR4 signaling by regulation of Myd88, that is, by stabilizing the interaction of Myd88 with flightless homolog 1 [21]. Moreover, Nrx was shown to regulate the adaptor protein, potentially as a disulfide reductase. Nrx is related with Trx, which additionally catalyzes de- and transnitrosylation of proteins. It is tempting to speculate that Nrx has similar catalytic mechanisms and that it could regulate Myd88 activity not only as disulfide reductase but also by regulating S-nitrosylation. Interestingly, different regulatory functions for the eight Cys residues have been introduced. Mutation of C113 inhibited NFκB signaling, whereas mutating the other Cys residues individually and especially simultaneously enhanced NFκB activity. Note that these seven Cys residues are all located in the TIR domain [93]. Different kinases, including the MAP kinases, are responsible for signal transduction and have been described to be susceptible to redox regulation. Trx1 and also Grx1 regulate ASK1 and downstream kinases such as ERK, JNK, and p38. The reduced oxidoreductases bind to ASK1 and thereby inhibit the enzymatic activity of the kinase. In case of Trx1, the protein interaction initiates ubiquitin-mediated degradation. Oxidation of the oxidoreductases induces the dissociation of the complex and restores kinase activity [1, 14, 95, 96]. Interestingly, ASK1 is involved in TLR4 signaling and has however not been shown to be essential for other TLR pathways (Figure 3) [97, 98].

Following the cascade of cell signaling-transducing molecules, effector molecules are also posttranslationally modified, for example, the transcription factor NFκB, which is highly regulated (for an overview see [36]). Comparable to other transcription factors such as AP1 and HIF1α, the DNA binding of NFκB is regulated by specific Cys residues that are susceptible to oxidation. The NFκB subunit p50 contains a cysteine residue in position 62 that promotes DNA binding in its reduced form. Alkylation, oxidation, or mutation to Ser or Ala of that particular cysteine inhibit DNA binding. It was shown that Cys62 can undergo S-glutathionylation and can also form a sulfenic acid [99]. Interestingly, various members of the Trx family have been shown to be involved in NFκB regulation. Even though it was shown that NFκB is a substrate for Trx1, Grx1, Grx2, and Nrx, the physiological impact during cellular signaling is poorly understood [1, 16, 100, 101]. Overexpression of Grx3 in T-cells on the other hand inhibited NFκB- as well as AP1-induced gene expression [102]. Besides the DNA binding, the nuclear translocation is also redox-regulated. Reduced Trx1 inhibits the dissociation of the inhibitory iκB/NFκB complex. Upon dissociation of the complex, iκB becomes phosphorylated and degraded by the proteasome. NFκB translocates into the nucleus (Figure 3). Apart from the regulation of transcription factors, gene expression can also be redox-regulated by, for example, the nuclear histone deacetylase and thus by chromatin remodelling [103].

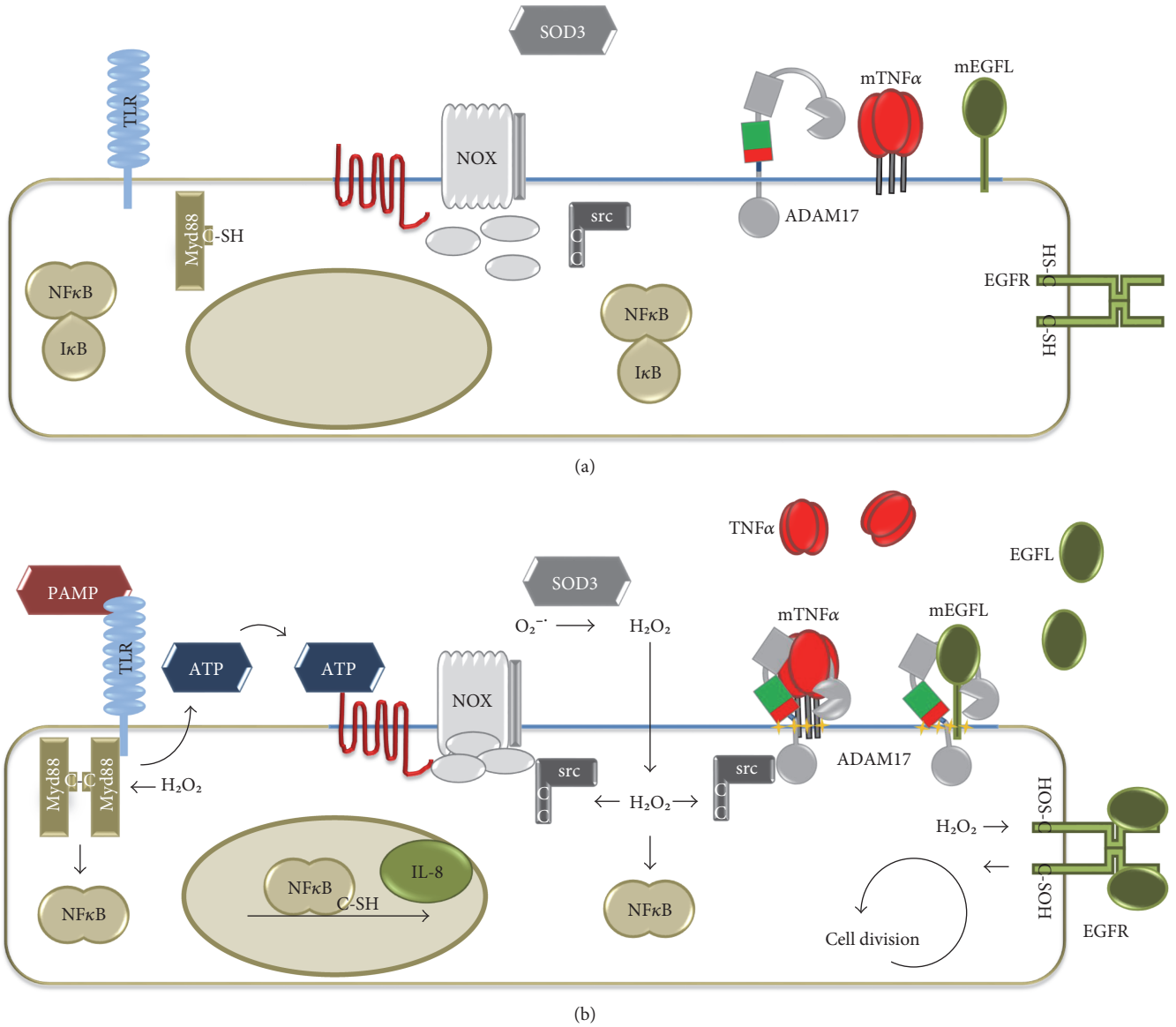

Figure 4: Pathogen detection and ROS-dependent defence and regeneration mechanisms. Epithelial cells are constantly exposed to pathogens. The redox state, the localisation, and the activity of different molecules and proteins are altered in the absence (a) or in the presence (b) of pathogens. Activation of TLRs by PAMPs and Myd88 recruitment induce secretion of ATP, which functions as danger signal and activates NOX. TLR and NOX activation both result in NFκB activation, via Myd88 or src, respectively. NFκB translocates to the nucleus and induces the expression of, for example, chemokines such as IL-8, promoting leukocyte recruitment. Myd88 dimerizes upon H_2O_2 exposure forming disulfide bridges. Src oxidation stabilizes the active conformation of the protease and the oxidation of cysteine residues near the ATP-binding site of the EGFR enhances its activity. Extracellular ATP leads to the activation of the shedding activity of ADAM17. ADAM17 releases soluble TNFα and ligands of the EGFR, such as TGFα and HB-EGF, from the cell surface, whereas TNFα promotes inflammation; signaling via the EGFR leads to regeneration due to induction of cell growth and division (mTNFα: membrane-bound TNFα; mEGFRL: membrane-bound EGFR ligands).

3.2. Redox Regulation of Inflammatory Mediators

3.2.1. The NLRP3 Inflammasome Is Redox-Regulated. ROS were shown to control the NLRP3 inflammasome, a multiprotein complex that transfers the precursor of IL-1β in its mature and active form [26]. This process was shown to be regulated via Trx1. The cytosolic oxidoreductase binds thioredoxin-interacting protein (Txnip), a protein that was suggested to act as an endogenous inhibitor of Trx [104]. In this complex, Txnip is not able to interact with and activate NLRP3. Upon oxidation of Trx1, the Trx1-Txnip complex dissociates and Txnip binds to NLRP3. Other mechanisms have been proposed in the regulation of the NLRP3 that is activated by various different stimuli, which are redox-independent or might depend on the redox regulation by Trx1 and Txnip [44].

3.2.2. Ectodomain Shedding by ADAM17—A Regulatory Thiol Switch in ADAM17 in Inflammation and Tissue Regeneration. Phagocytes release various proinflammatory

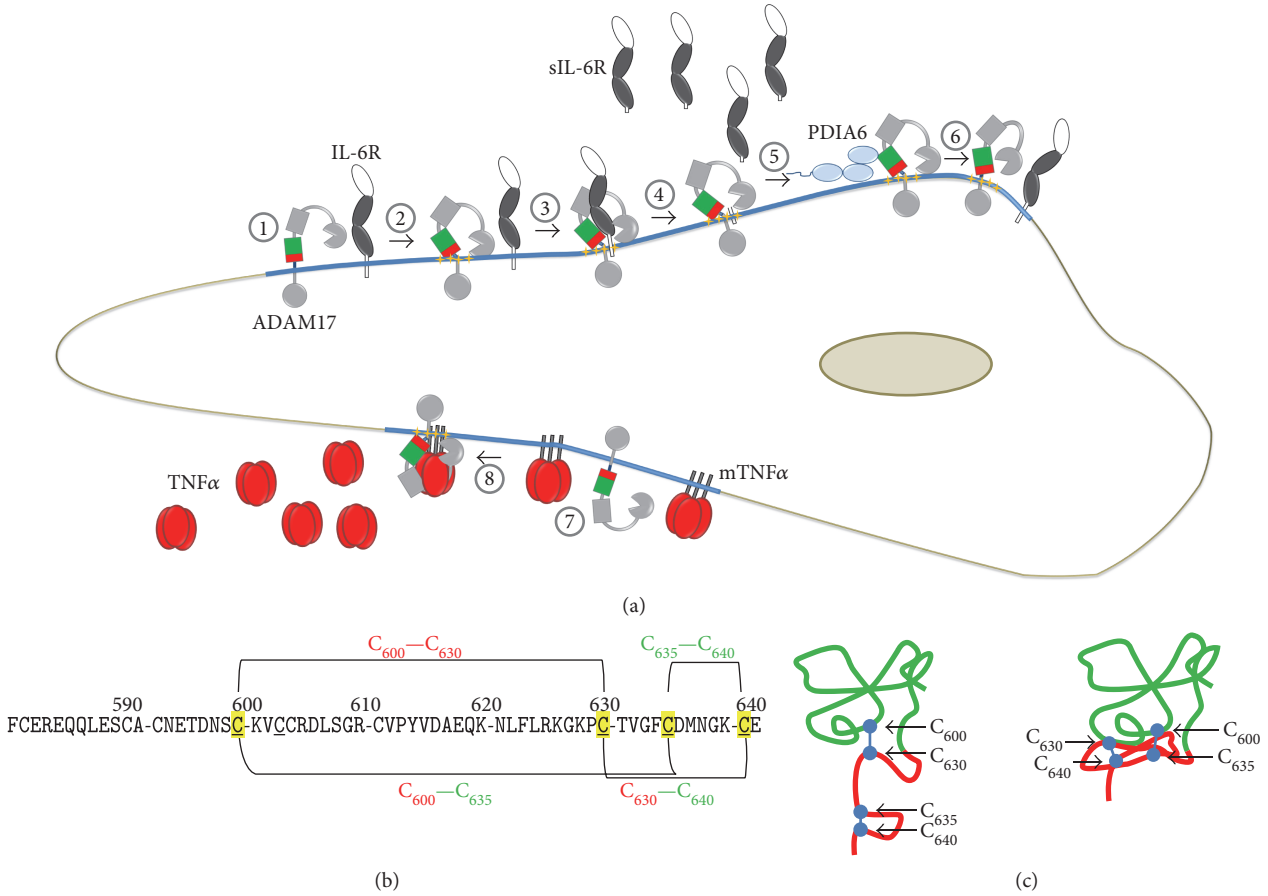

Figure 5: Thiol switch in ADAM17. (a) (1) ADAM17 is active within lipid rafts (blue line). (2) Different stimuli induce the exposure of phosphatidylserine (yellow stars), that interacts with the open and active conformation of the MPD. (3) This process allows ADAM17 to bind and (4) release substrates from the cell surface, for example, soluble interleukin 6 (sIL-6R). (5) Reduced extracellular protein disulfide isomerase PDIA6 catalyzes the disulfide isomerisation targeting the open MPD. (6) The resulting close and inactive structure of ADAM17 is not able to bind and process its substrates. (7) Membrane bound TNFα (mTNFα) is another substrate of ADAM17, (8) which is released upon activation of ADAM17 and also promotes immune response and inflammation. (b) Primary structure of the MPD of human ADAM17, indicating the disulfide bridges involved in the thiol switch. The linear pattern (C_{600}–C_{630}, C_{635}–C_{640}) constitutes the active, the overlaying pattern (C_{600}–C_{635}, C_{630}–C_{640}), the inactive conformation. (c) Structural consequence of the thiol switch of ADAM17. The red-colored part is highly flexible in the open MPD and therefore not visible in the NMR data. The right structure represents the closed conformation of ADAM17 solved by NMR, in which the red part is packed tightly to the upper, green colored part of the MPD.

mediators to promote leukocyte recruitment and activation of the surrounding tissue. In this process, the IL-6R and the membrane-bound precursor of TNFα are proteolytically cleaved by ADAM17; this shedding process leads to the generation of proinflammatory acting TNFα and sIL-6R (Figure 5). Shedding of IL-6R from apoptotic neutrophils generates an agonist of IL-6 signaling, allowing the activation of cells, which do not express the membrane-bound IL-6R, but the ubiquitously expressed signaling subunits of the IL-6 receptor complex gp130. This transsignaling mechanism promotes the attraction of monocytic cells and inflammation [46, 105, 106]. Moreover, ADAM17 cleaves members of the EGFR ligand family, which are essential for their function as growth factor and tissue regeneration [107–109]. Various ligands of the TLR and NOXs induce the activity of ADAM17 that is essential for immune response/inflammation and regeneration (Figure 4) [47, 83, 110, 111]. In the healthy airway, TLR signaling can be upstream of exogenous ATP [112, 113]. Duox1 is recruited to ATP-activated purinergic P2YR, followed by association with src, which becomes oxidized. Src in turn oxidizes and activates ADAM17, which amplifies EGFR activation and promotes immune defence and regeneration, involving an ERK1/2-dependent production of the neutrophil attractant IL-8 (Figure 4) [114, 115]. Dysregulation of this pathway has been linked to inflammatory diseases, for example, cystic fibrosis and chronic inflammatory airway disease [116–120]. LPS-induced activation of ADAM17 in macrophages was shown to rely on the activity of PKCδ and p38. This activation is TLR4- and NOX2-dependent and targets the tyrosine kinase Mer, which inhibits inflammatory signaling during efferocytosis [121]. In primary monocytes, LPS-induced activation of ADAM17 is also mediated by ROS and p38 [122]. In hepatocytes, src activates NOX1, which in turn activates ADAM17

that releases TGFα for the stimulation of the EGFR [123]. This process is caveolin-1-dependent. ADAM17, NOX1, and NOX2 are located and active within lipid rafts [75, 123–126]. The interaction of NOX1 and ADAM17 was shown by coimmunoprecipitation [127]. Interestingly, ADAM17 can also be activated by mitochondrial ROS in a src- and PKC-independent way via the activation of the P2Y receptor by ATP in fibroblast [128] and FAS-mediated apoptosis in neutrophils [129]. The activation of ADAM17 by members of the NOX family appears to be dependent on the activity of kinases such as src, PKC, p38, and/or ERK1/2. These kinases have been previously shown to be involved in the regulation of ADAM17, which is multilayered and only partially understood [130–133]. Interestingly, the extracellular part of ADAM17 is a target for regulatory events. In its mature form, the N-terminal catalytic domain is followed by a disintegrin domain, a membrane-proximal domain (MPD), and a conserved helical stalk region called conserved ADAM seventeen interaction sequence (CANDIS), a single transmembrane region and a cytoplasmic tail [134–137]. The MPD exists in two conformations that control the activity of the protease [135, 138]. A linear order of two disulfide bridges (C_{600}–C_{630} and C_{635}–C_{640}) leads to an open, flexible structure, which is able to interact with the plasma membrane and substrates [139, 140]. Reduced protein disulfide isomerase (PDI), a member of the Trx protein family, catalyzes the isomerisation to an overlaying pattern (C_{600}–C_{635} and C_{630}–C_{640}) causing a close, compact structure, which abrogates membrane binding and substrate recognition and thereby ADAM17 activity. In line, PDIA1 and PDIA6 were found to act as negative regulators [22, 135, 141] (Figure 5). The thiol switch as a general posttranslational mechanism to regulate the activity of members of the ADAM family appears to be unlikely since ADAM17 and its closest relative ADAM10 are atypical members of the protein family. The other members lack the redox-regulated MPD domain and contain a cysteine-rich and an EGF-like domain instead [134, 136]. Therefore, no comparable posttranslational thiol switch can be expected and indeed so far no posttranslational regulation of these proteases via NOX, ROS in general or specific oxidoreductases has been described to our knowledge. It is however possible that the activity of ADAM10, which contains a MPD homolog to the one of ADAM17, is regulated via a comparable thiol switch. The isolated open form of the ADAM17-MPD can be expressed as a soluble protein and the closed from can be obtained by refolding or by enzymatic catalysis by PDIs, converting the open form to the close form. So far, no open ADAM10-MPD was obtained by expression in *E. coli* (unpublished observations), indicating that no open form exists and/or that the interaction with the N-terminal located disintegrin domain might be tighter and more important for the stabilization than in ADAM17. This might point against a regulatory thiol switch of ADAM10 and fit to the observation that the activity of ADAM17 is more strongly regulated than the activity of ADAM10, which can be constitutively active. However, a thiol switch in ADAM10 cannot be excluded since reports indicate that the shedding activity of ADAM10 can indeed be stimulated by ROS [142, 143]. PDIs attack the CKVC motive in the MPD of ADAM17, which is evolutionarily conserved in vertebrates, but not present in animals such as pike, hamadryad, or drosophila. ADAM10 on the other hand contains the CHVC motif that is also conserved in evolutionary higher animals. This indicates that during evolution with increased complexity and potential higher risks of uncontrolled substrate release, a regulatory mechanism of the protease became essential. Note that the posttranslational regulation of proteins by a thiol switch in their ectodomains is not unique for metalloproteases. For example, CD30 contains no CKVC or CHVC motive and is targeted by Trx1 which results in an altered ligand binding [144], whereas ADAM17 becomes inactivated by the thiol switch, and β1 and β3 integrins become activated [145]. Intriguingly, this can be catalyzed by identical PDIs, such as PDIA1 and PDIA6. Since β1 and β3 integrins contain numerous CXXC motives, but not a CKVC motive, PDIs may recognize different CXXC motives.

3.2.3. The Immunomodulatory Functions of HMGB1 Are Regulated via Three Cys Residues. HMGB1 comprises the HMG A box essential for DNA binding, the HMG B box essential for DNA binding and proinflammatory functions (i.e., amino acids 89 to 108), and an acidic C-terminus [146]. HMGB1 conducts various functions depending on its localization. Nuclear HMGB1 is, for instance, involved in DNA organization and gene transcription; cytosolic HMGB1 regulates the inflammasome, pyroptosis, and the autophagy/apoptosis balance; and extracellular HMGB1 has been described as one of the first DAMPs with proinflammatory activities in distinct cell culture and animal models, as well as in patients suffering from sterile or infectious inflammation (reviewed in [147]). LPS-stimulated monocytes secrete HMGB1 nonclassically via exocytosis of secretory lysosomes induced by lysophosphatidylcholine that is produced comparably late during inflammation [148]. Interestingly, oleanolic acid is a natural inhibitor of HMGB1 release by LPS-stimulated RAW264.7 macrophages. Even though the exact mechanism is not fully understood, it involves the activation of Nrf2 that binds to the ARE of heme-oxygenase-1 [149]. HMGB1 is also released during necrosis or cell damage, however, not during apoptosis [150]. HMGB1 leakage has also been associated with high levels of superoxide and peroxynitrite [151]. HMGB1 has three Cys residues in the positions 23, 45, and 106. We have recently shown that TNFα-induced HMGB1 secretion from HEK293 cells does not depend on the redox state of the protein [51]. Note that the translocation from the nucleus to the cytosol depends on posttranslational modifications such as acetylation and potentially also thiol oxidation [152, 153]. Especially, the substrate interaction and the distinct functions of HMGB1 are redox-regulated. An intramolecular disulfide between Cys23 and Cys45, as well as the reduced Cys106, located in the HMG B box, is essential for TLR4/MD2 binding, macrophage activation, and cytokine release. Fully oxidized, that is, three sulfonates and fully reduced HMGB1 do not affect TLR4 signaling [154, 155]. However, the latter shows chemotactic activity by interacting with the chemokine CXCL12 that binds to the chemokine receptor CXCR4. Interestingly, a redox-

inactive mutant, containing three Ser residues instead of Cys residues, is even more active in terms of leukocyte recruitment than the fully reduced protein [151, 156, 157]. Even though the redox state of the protein has been linked to particular substrates and functions in different compartments, the regulation of the thiol switches of HMGB1 has not been fully understood. It is however clear that these switches constitute physiological mechanisms to regulate and modulate the inflammatory activities of the protein. Interestingly, HMGB1 was shown to interact with the oxidoreductase glutaredoxin [153] and also Trx1 was shown to be able to reduce the intramolecular disulfide [153, 158].

3.2.4. Extracellular Redoxins Act as Immune Mediators. Distinct members of the Trx family of proteins have been described to be secreted in various cell and animal models, as well as in patients suffering, for example, from inflammatory diseases (reviewed in [1]). Trx1 was originally known as T-cell leukemia-derived factor that was shown to induce the IL2 receptor [159] and the expression of various cytokines [160]. In addition, the truncated Trx80, formerly characterized as eosinophil cytotoxicity-enhancing factor, has been shown to be secreted functioning as cyto- and chemokine [161]. Apart from its cytokine and chemoattractant functions, there are also controversial findings that imply an anti-inflammatory role. One potential mechanism could involve the regulation of the proinflammatory macrophage migration inhibitor factor (MIF). Interestingly, MIF also belongs to the Trx family of proteins and is involved in the innate immune response [162]. Prx2 is a highly expressed intracellular peroxidase that is released from myeloid cells in response to inflammatory stimuli. Once released from cells, Prx2 has proinflammatory activity, essentially behaving as a DAMP [52]. Intriguingly, the release of Prx2 from cells under inflammatory conditions is mediated by two types of thiol modifications involving all three cysteine residues. Prx2 is released from LPS-stimulated mouse macrophages in a glutathionylated form [52]. A second thiol redox change involves oxidation of two cysteine residues forming a disulfide bond, which induces protein dimerization and results in its release from the cell via exosomes [51]. Mutation of either one of the Cys residues involved in the disulfide bridge prevents secretion of the enzyme. Recombinant Prx2 is able to stimulate the release of TNFα from both mouse macrophages and primary human monocytes [51, 52]. Prx1 is also released from mouse macrophages in response to LPS. It was detected in the secretome of LPS-stimulated cells in a glutathionylated form and also exhibits the reliance on Cys oxidation for the release from cells. Thus, it appears that redox modulation regulates the release of these enzymes from cells contributing to the local inflammatory response. In addition, redox changes provide a novel mechanism by which proteins are processed for export from cells during inflammation, at least for Prx1 and 2. As such, there is the potential for the development of novel therapeutic strategies for modulating the redox environment in order to dampen the inflammatory response. Note that also Trx1 was detected in the proteomic analysis.

4. Clinical Significance

Biomarkers for inflammatory disorders include oxidative modifications of DNA, proteins, and lipids and have been reviewed in [25]. Even though the redox state of particular proteins is not easily accessible in patient material due to a general lack of specific tools, the expression, localization, and activity of redox enzymes, for example, Trx family proteins have been studied in various diseases (Table 2) [1]. Moreover, different redox enzymes have been identified as potential targets for therapy in a number of diseases, including inflammatory disorders. The neutrophil-derived myeloperoxidase is known as one of the most potent oxidant-producing proteins. Increased MPO activity and excessive production of hypochlorous acid contribute to chronic inflammation and organ damage in many tissues [163, 164]. Elevated expression was described in cardiovascular disease [165, 166], presumably due to its oxidation of low- and high-density lipoprotein [167], as well as rheumatoid arthritis [168]. MPO also seems to be a risk factor in heart failure and acute coronary syndrome [169]. In tracheal aspirates, elevated levels of chlorinated proteins, trace markers of MPO activity, are believed to contribute to chronic lung infection in infants [170]. Accordingly, many studies have been conducted in search of nontoxic, reversible MPO inhibitors preferably binding the native protein [171–173]. Interestingly, neutrophil extracellular traps are decorated with active MPO [174] and are associated with chronic inflammation in many diseases too [175]. Neuron-derived MPO seems to contribute to Alzheimer's disease, a neurodegenerative disorder that has also been linked to neuroinflammation [176]. It is worth mentioning that elevated MPO activity is associated with an overall better outcome in specific cancer chemotherapy [177]. However, MPO is tightly linked to many clinical observations but redox signaling pathways beyond localized HOCl-mediated oxidation remain to be studied in most pathologies.

The heme protein lactoperoxidase is found in secretion liquids such as tears, milk, and saliva [178]. Saliva in particular has been thoroughly investigated in different oral diseases. The effect of orally administered LPO was weak on periodontitis and bacteriological profile [179]. However, LPO activity itself seems to be increased in periodontitis [180] although thiocyanate is not increased in this disease [181]. There is no association between recurrent aphthous stomatitis and salivary thiocyanate levels [182] but patients with aphtous ulcers have significantly lower oral LPO levels [183]. Xylitol increases oral LPO activity but not thiocyanate levels, and this may account for the cariostatic effect of xylitol. Also, compounds with a 3,4-dihydroxyphenyl structure significantly enhance LPO activity [184] but the clinical implication of this finding remains to be elucidated. Frequent tobacco consumption puts people at risk for oral cancer [185]. Saliva levels of thiocyanate are strongly increased in smokers [186] whereas LPO activity is blocked by tobacco smoke [187]. Whether LPO is crucial in oral carcinogenesis currently remains unknown.

The seven NOX members generate superoxide and secondarily H_2O_2. In chronic granulomatous disease, that is, a

Table 2: Clinical implications of redox enzymes.

Protein	Reactive species	Pathology	Levels/role	Reference
Myeloperoxidase	Production of hypochlorous and hypobromous acid	Alzheimer's disease, Parkinson's disease	Beneficial	[172, 258]
		Arteriosclerotic plaques	Increased	[259]
		Breast cancer and chemotherapy	Activity increased/beneficial	[177]
		Cardiovascular disease	Increased (plasma)	[165]
		Chronic lung infection in preterm infants	Increased (tracheal aspirates)	[170]
		Rheumatoid arthritis	Increased (plasma, synovial fluid)	[168]
Lactoperoxidase	Production of hypothiocyanate	Chronic peridontitis	Oral LPO administration had no effect on disease	[179]
		Peridontitis in diabetes mellitus type I	Activity increased (saliva)	[180]
		Recurrent aphtous stomatitis	Decreased (saliva)	[183]
		Smoking	Activity decreased (saliva)	[187]
NADPH oxidase	Production of superoxide and secondary hydrogen peroxide	Acute myocardial infarct	Increased (heart tissue), activity increased (heart tissue), increased (saphenous vein)	[192–194]
		Cardiovascular disease	Increased (serum)/detrimental	[202]
		Chronic granulomatous disease	Activity decreased (peripheral blood neutrophils)/detrimental	[189]
		Diabetes nephropathy	Increased/phase II trial completed	[199]
		Melanoma	Similar (melanoma tissue)/no correlation with invasiveness	[201]
		Retinopathy	Increased/detrimental	[260]
Nitric oxide synthase	Production of nitric oxide	Asthma	Inhibition detrimental/inhibition beneficial/inhibition had no effect	[224–226]
		Breast cancer	Increased/none	[234]
		Head and neck cancer	Increased/detrimental (in respective cancer tissue)	[235]
		Heart disease and rejected transplants	Increased (heart tissue)	[228–232]
		Melanoma	Increased/detrimental	[233]
		Migraine	Inhibition beneficial/inhibition had no effect	[220–222]
		Rheumatoid arthritis	Increased/inhibition beneficial	[227]
		Sepsis	Inhibition detrimental/beneficial/no effect (serum)	[213–217]
Peroxiredoxins	Decomposition of H_2O_2, redox signaling	Alzheimer's disease	Prx1/Prx2 increased (brain tissue), Prx2 activity decreased (blood), Prx3 decreased (brain tissue)	[241–243, 248]
		Cataracts	Prx6 decreased (eye tissue)	[250]
		Diabetes mellitus type II	Prx4 increased (serum)	[252]
		Diabetic retinopathy	Prx1 increased (vitreous biopsy)	[251]
		Glaucoma	Prx6 increased (eye tissue)	[249]
		Lung cancer	Prx1 increased, Prx3 increased (cancer tissue)	[254, 255]
		Parkinson's disease	Prx2 increased	[244]

group of hereditary defects that result in an increased susceptibility to various bacterial and fungal infections, a functional NOX attenuation leads to life-threatening infections [188]. Hereby, the degree of attenuation governs patient prognosis [189]. Genetic defects in components of NOX2 have been linked to chronic granulomatous disease [69, 84, 190]. NOX proteins have been associated with cardiovascular risk factors contributing to atherosclerosis, vascular dysfunction, hypertension, vascular hypertrophy, and thrombosis [191]. An upregulation of NOX2 was detected upon myocardial infarct in cardiomyocytes [192] and in failing, however not in nonfailing hearts [193] as well as in saphenous veins of patients with heart failure [194]. NOX2-enriched veins may contribute to endothelial dysfunction [195]. Accordingly, targeting NAPDH oxidases in cardiovascular disease was suggested to be of clinical benefit [196]. NOX can be activated in the blood vessel walls via angiotensin II [197] causing cardiovascular disease [198]. NOX is also a target in diabetic nephropathy [199], and an orally administrable inhibitor (GKT137831) has completed phase 2 trial (NCT02010242) but results have not yet been published. NOX1 inhibition is also a therapeutic strategy against hypertension [200] that is tested in clinical trials for cardiovascular conditions [201]. Particularly, the NOX inhibitor Dextromethorphan reduced hypertension in a multicenter trial [202]. In malignancies, NOX4 is elevated in brain, colorectal, gastric, lung, and pancreatic cancer [203]. Accordingly, NOX enzymes also constitute promising targets in cancer therapy [204]. Gentian violet, a NOX1 inhibitor, showed promising effects in the palliation of a melanoma patient [205]. Yet, NOX1 does not correlate with melanoma invasiveness [201]. This substance was also successfully used to treat the inflammatory skin condition erythema multiforme [206].

The importance of $NO^{\cdot}$ in human health was first suggested in human ileostomy effluents showing elevated nitrite concentrations [207]. Its role in acute and chronic inflammation [208] has been investigated ever since [209]. Elevated levels of NO contribute to pathologies linked to inflammation, for example, asthma, arthritis, multiple sclerosis, transplant rejection, stroke, and neurodegenerative diseases [30, 210]. Glucocorticoids inhibit NOS [211] and thereby production of $NO^{\bullet}$ that has been implicated in sepsis [212]. However, clinical trials on NOS inhibition gave inconclusive results demonstrating either a negative [213], a positive [214], or no effect [215] on survival of septic patients. Short-term improvement was shown following methylene blue administration [216] whereas LNNA was ineffective [217]. NOS inhibition with L-arginine analogues such as $_{L}$NMMA gave a more confident response with regard to cardiovascular parameters in septic patients [218]. However, the mortality rate in a phase III trial was elevated [219]. Nonetheless, this substance was shown to be effective in treating migraine attacks in a placebo-controlled clinical study [220]. Clinical trials using the NOS inhibitor GW274150 did not confirm these results, neither as early intervention [221] nor in a prophylactic therapy [222]. NOS genotype (high numbers of trinucleotides) and exhaled $NO^{\bullet}$ are associated with asthma [223]. The NOS inhibitor L-NIL-TA strongly reduced the amount of exhaled $NO^{\bullet}$ in asthmatic patients without measurable vascular side effects [224]. This finding was confirmed in another clinical trial using GW274150 with no significant improvement of the asthmatic symptoms [225]. Administration of $_{L}$NMMA amplified bradykinin-induced asthma in volunteers [226]. GW274150 also reduced synovial joint thickness and vascularity in patients with rheumatoid arthritis [227]. In general, NOS is linked to heart disease [228]. NOS is elevated in heart tissue of patients experiencing hibernating myocardium [229], in transplanted coronary arteries [230], in rejected transplants [231], and in tissue from human heart failure [232]. NOS expression also promotes melanoma cell proliferation and is associated with poor patient survival [233]. In breast cancer [234] but not head and neck cancer [235], NOS expression corresponds to stage and invasiveness.

Oxidants have long been suggested to play a role in the central nervous system [236]. Inflammation is a key event in the onset and stage of brain disease, such as multiple sclerosis [237]. Prx1 is expressed in glial cells, whereas Prx2 expression was predominantly found in neurons [238–240]. The expression levels of both Prx1 and Prx2 are elevated in patients suffering from Alzheimer's disease [241, 242]; moreover, Prx2 and Prx6 are more oxidized in the brain [243]. Additionally, Prx2 peroxidase activity was found to be inhibited by S-nitrosylation [244] and phosphorylation [245] in Alzheimer's disease. Prx2 expression is also increased in Parkinson's disease [246, 247], whereas the Prx3 expression is decreased in the latter [248]. Prx expression is also regulated in ocular pathologies. Alongside with inflammation, Prx6 is increased in the trabecular meshwork in glaucoma patients [249] and correlates negatively with severity of cataracts [250]. Diabetic retinopathy is associated with elevated levels of Prx1 [251], with the diabetic risk being associated with increased serum concentrations of Prx4 [252]. Peroxiredoxins are regulated in cancer, a condition that heavily modulates the inflammatory environment to enhance growth [253]. Tissue and serum of lung cancer patients showed elevated levels of Prx1 and Prx3, respectively [254, 255]. Autoantibodies against Prx6 have also been shown to be of prognostic value in esophageal cancer [256]. So far, no therapeutic strategies to target Prxs were conducted.

5. Future Perspective

It is of great interest to understand the mechanisms of cellular signaling and how they are regulated under physiological, but generally also under pathological conditions. Even though it has been established that redox regulation and oxidative Cys modifications are essential for signal transduction and cellular processes, the identification and characterization of specific thiol switches and their enzymatic regulation constitute a big challenge in the field. Particularly, the field lacks time- and spatial-resolved *in vivo* techniques for the analysis of (i) the levels and distribution of different ROS and RNS, (ii) the particular redox state of proteins, and (iii) the impact of redox signaling on complex signaling circuits and networks. The innate and the adaptive immune responses are tightly controlled and depend on the enzymatic production of superoxide, hydrogen peroxide, hydrogen sulfide, and

nitric oxide. However, not many redox-regulated protein substrates are known. Future research will identify these substrates and particular thiol switches, including intracellular, as well as membrane and extracellular proteins and the underlying regulatory mechanisms. Intriguingly, the extracellular space contains redox-active enzymes and molecules such as glutathione. It is tempting to speculate that the inflammatory response does not only constitute intracellular redox-signaling cascades but also depends on extracellular signal transduction within the microenvironment of distinct cell types.

Abbreviations

ADAM17: A disintegrin and metalloproteinase 17
DAMP: Damage-associated molecular pattern
DUOX: Dual oxidase
EGF: Epidermal growth factor
FAD: Flavin-adenine dinucleotide
Gpx: Glutathione peroxidase
Grx: Glutaredoxin
HMGB1: High-mobility group protein 1
IL: Interleukin
IRAK: Interleukin-1 receptor-associated kinase
LPO: Lactoperoxidase
LPS: Lipopolysaccharide
MAPK: Mitogen-activated protein kinase
MIF: Macrophage migration inhibitor factor
MPD: Membrane-proximal domain
MPO: Neutrophil-derived myeloperoxidase
Myd88: Myeloid differentiation primary response 88
NLR: NOD-like receptors
NOS: Nitric oxide synthase
NOX: NADPH oxidase
Nrx: Nucleoredoxin
PAMP: Pathogen-associated molecular pattern
Prx: Peroxiredoxin
SOD: Superoxide dismutase
TIR: Toll/IL-1 receptor
TNF: Tumor necrosis factor
TLR: Toll-like receptor
Trx: Thioredoxin
Txnip: Thioredoxin-interacting protein
ROS: Reactive oxygen species
RNS: Reactive nitrogen species.

Conflicts of Interest

The authors declare that there is no conflict of interests regarding the publication of this paper.

Acknowledgments

Inken Lorenzen and Eva-Maria Hanschmann gratefully acknowledge the financial support by the priority program (SPP) 1710, founded by the German Research Foundation (DFG) to investigate thiol switches in cellular physiology. Lisa Mullen gratefully acknowledges financial support from the Brighton and Sussex Medical School, the University of Sussex Research Development Fund and the University of Brighton. Sander Bekeschus was supported by the German Federal Ministry of Education and Research (BMBF; grant no. 03Z22DN11).

References

[1] E.-M. Hanschmann, J. R. Godoy, C. Berndt, C. Hudemann, and C. H. Lillig, "Thioredoxins, glutaredoxins, and peroxiredoxins—molecular mechanisms and health significance: from cofactors to antioxidants to redox signaling," *Antioxidants & Redox Signaling*, vol. 19, no. 13, pp. 1539–1605, 2013.

[2] L. I. Leichert and T. P. Dick, "Incidence and physiological relevance of protein thiol switches," *Biological Chemistry*, vol. 396, no. 5, pp. 389–399, 2015.

[3] L.-O. Klotz, P. Schroeder, and H. Sies, "Peroxynitrite signaling: receptor tyrosine kinases and activation of stress-responsive pathways," *Free Radical Biology & Medicine*, vol. 33, no. 6, pp. 737–743, 2002.

[4] P. Calcerrada, G. Peluffo, and R. Radi, "Nitric oxide-derived oxidants with a focus on peroxynitrite: molecular targets, cellular responses and therapeutic implications," *Current Pharmaceutical Design*, vol. 17, no. 35, pp. 3905–3932, 2011.

[5] C. Berndt, C. H. Lillig, and L. Flohé, "Redox regulation by glutathione needs enzymes," *Frontiers in Pharmacology*, vol. 5, p. 168, 2014.

[6] D. P. Jones, "Redefining oxidative stress," *Antioxidants & Redox Signaling*, vol. 8, no. 9-10, pp. 1865–1879, 2006.

[7] C. C. Winterbourn and D. Metodiewa, "Reactivity of biologically important thiol compounds with superoxide and hydrogen peroxide," *Free Radical Biology and Medicine*, vol. 27, no. 3-4, pp. 322–328, 1999.

[8] M. Deponte and C. H. Lillig, "Enzymatic control of cysteinyl thiol switches in proteins," *Biological Chemistry*, vol. 396, no. 5, pp. 401–413, 2015.

[9] L. E. S. Netto and F. Antunes, "The roles of peroxiredoxin and thioredoxin in hydrogen peroxide sensing and in signal transduction," *Molecules and Cells*, vol. 39, no. 1, pp. 65–71, 2016.

[10] T. C. Laurent, E. C. Moore, and P. Reichard, "Enzymatic synthesis of deoxyribonucleotides. IV. Isolation and characterization of thioredoxin, the hydrogen donor from Escherichia coli b," *The Journal of Biological Chemistry*, vol. 239, pp. 3436–3444, 1964.

[11] A. Holmgren, "Glutathione-dependent synthesis of deoxyribonucleotides. Characterization of the enzymatic mechanism of *Escherichia coli* glutaredoxin," *The Journal of Biological Chemistry*, vol. 254, no. 9, pp. 3672–3678, 1979.

[12] L. Bräutigam, L. D. Jensen, G. Poschmann et al., "Glutaredoxin regulates vascular development by reversible glutathionylation of sirtuin 1," *Proceedings of the National Academy of Sciences of the United States of America*, vol. 110, no. 50, pp. 20057–20062, 2013.

[13] D. A. Mitchell and M. A. Marletta, "Thioredoxin catalyzes the S-nitrosation of the caspase-3 active site cysteine," *Nature Chemical Biology*, vol. 1, no. 3, pp. 154–158, 2005.

[14] M. Saitoh, H. Nishitoh, M. Fujii et al., "Mammalian thioredoxin is a direct inhibitor of apoptosis signal-regulating kinase (ASK) 1," *The EMBO Journal*, vol. 17, no. 9, pp. 2596–2606, 1998.

[15] Y. Mikami, N. Shibuya, Y. Kimura, N. Nagahara, Y. Ogasawara, and H. Kimura, "Thioredoxin and dihydrolipoic acid

are required for 3-mercaptopyruvate sulfurtransferase to produce hydrogen sulfide," *The Biochemical Journal*, vol. 439, no. 3, pp. 479–485, 2011.

[16] J. R. Matthews, N. Wakasugi, J. L. Virelizier, J. Yodoi, and R. T. Hay, "Thioredoxin regulates the DNA binding activity of NF-κB by reduction of a disulphide bond involving cysteine 62," *Nucleic Acids Research*, vol. 20, no. 15, pp. 3821–3830, 1992.

[17] M. C. Sobotta, W. Liou, S. Stöcker et al., "Peroxiredoxin-2 and STAT3 form a redox relay for H2O2 signaling," *Nature Chemical Biology*, vol. 11, no. 1, pp. 64–70, 2015.

[18] Y. Funato, T. Michiue, M. Asashima, and H. Miki, "The thioredoxin-related redox-regulating protein nucleoredoxin inhibits Wnt-beta-catenin signalling through dishevelled," *Nature Cell Biology*, vol. 8, no. 5, pp. 501–508, 2006.

[19] L. Bräutigam, L. D. Schütte, J. R. Godoy et al., "Vertebrate-specific glutaredoxin is essential for brain development," *Proceedings of the National Academy of Sciences of the United States of America*, vol. 108, no. 51, pp. 20532–20537, 2011.

[20] M. Gellert, S. Venz, J. Mitlöhner, C. Cott, E.-M. Hanschmann, and C. H. Lillig, "Identification of a dithiol-disulfide switch in collapsin response mediator protein 2 (CRMP2) that is toggled in a model of neuronal differentiation," *The Journal of Biological Chemistry*, vol. 288, no. 49, pp. 35117–35125, 2013.

[21] T. Hayashi, Y. Funato, T. Terabayashi et al., "Nucleoredoxin negatively regulates Toll-like receptor 4 signaling via recruitment of flightless-I to myeloid differentiation primary response gene (88)," *The Journal of Biological Chemistry*, vol. 285, no. 24, pp. 18586–18593, 2010.

[22] S. H. Willems, C. J. Tape, P. L. Stanley et al., "Thiol isomerases negatively regulate the cellular shedding activity of ADAM17," *The Biochemical Journal*, vol. 428, no. 3, pp. 439–450, 2010.

[23] C. H. Lillig and C. Berndt, "Glutaredoxins in thiol/disulfide exchange," *Antioxidants & Redox Signaling*, vol. 18, no. 13, pp. 1654–1665, 2013.

[24] C. Berndt, J.-D. Schwenn, and C. H. Lillig, "The specificity of thioredoxins and glutaredoxins is determined by electrostatic and geometric complementarity," *Chemical Science*, vol. 6, no. 12, pp. 7049–7058, 2015.

[25] Y. Lei, K. Wang, L. Deng, Y. Chen, E. C. Nice, and C. Huang, "Redox regulation of inflammation: old elements, a new story," *Medicinal Research Reviews*, vol. 35, no. 2, pp. 306–340, 2015.

[26] J. M. Abais, M. Xia, Y. Zhang, K. M. Boini, and P.-L. Li, "Redox regulation of NLRP3 inflammasomes: ROS as trigger or effector?," *Antioxidants & Redox Signaling*, vol. 22, no. 13, pp. 1111–1129, 2015.

[27] C. K. Sen and S. Roy, "Redox signals in wound healing," *Biochimica et Biophysica Acta (BBA) - General Subjects*, vol. 1780, no. 11, pp. 1348–1361, 2008.

[28] O. Kabil, N. Motl, and R. Banerjee, "H2S and its role in redox signaling," *Biochimica et Biophysica Acta (BBA) - Proteins and Proteomics*, vol. 1844, no. 8, pp. 1355–1366, 2014.

[29] M. Bhatia, "H2S and inflammation: an overview," *Handbook of Experimental Pharmacology*, vol. 230, pp. 165–180, 2015.

[30] H. Kleinert, A. Pautz, K. Linker, and P. M. Schwarz, "Regulation of the expression of inducible nitric oxide synthase," *European Journal of Pharmacology*, vol. 500, no. 1–3, pp. 255–266, 2004.

[31] A. Pautz, J. Art, S. Hahn, S. Nowag, C. Voss, and H. Kleinert, "Regulation of the expression of inducible nitric oxide synthase," *Nitric Oxide: Biology and Chemistry*, vol. 23, no. 2, pp. 75–93, 2010.

[32] D. A. Wink, H. B. Hines, R. Y. Cheng et al., "Nitric oxide and redox mechanisms in the immune response," *Journal of Leukocyte Biology*, vol. 89, no. 6, pp. 873–891, 2011.

[33] B. Brüne, N. Dehne, N. Grossmann et al., "Redox control of inflammation in macrophages," *Antioxidants & Redox Signaling*, vol. 19, no. 6, pp. 595–637, 2013.

[34] Z. Prokopowicz, J. Marcinkiewicz, D. R. Katz, and B. M. Chain, "Neutrophil myeloperoxidase: soldier and statesman," *Archivum Immunologiae et Therapiae Experimentalis (Warsz)*, vol. 60, no. 1, pp. 43–54, 2012.

[35] P. Nagy, S. S. Alguindigue, and M. T. Ashby, "Lactoperoxidase-catalyzed oxidation of thiocyanate by hydrogen peroxide: a reinvestigation of hypothiocyanite by nuclear magnetic resonance and optical spectroscopy," *Biochemistry (Moscow)*, vol. 45, no. 41, pp. 12610–12616, 2006.

[36] M. V. Gattas, R. Forteza, M. A. Fragoso et al., "Oxidative epithelial host defense is regulated by infectious and inflammatory stimuli," *Free Radical Biology & Medicine*, vol. 47, no. 10, pp. 1450–1458, 2009.

[37] M. Jaeger, M. H. T. Stappers, L. A. B. Joosten, I. C. Gyssens, and M. G. Netea, "Genetic variation in pattern recognition receptors: functional consequences and susceptibility to infectious disease," *Future Microbiology*, vol. 10, no. 6, pp. 989–1008, 2015.

[38] B. K. Davis, H. Wen, and J. P.-Y. Ting, "The inflammasome NLRs in immunity, inflammation, and associated diseases," *Annual Review of Immunology*, vol. 29, pp. 707–735, 2011.

[39] P. Matzinger, "Tolerance, danger, and the extended family," *Annual Review of Immunology*, vol. 12, pp. 991–1045, 1994.

[40] J. Fan, R. S. Frey, and A. B. Malik, "TLR4 signaling induces TLR2 expression in endothelial cells via neutrophil NADPH oxidase," *The Journal of Clinical Investigation*, vol. 112, no. 8, pp. 1234–1243, 2003.

[41] J. Brown, H. Wang, G. N. Hajishengallis, and M. Martin, "TLR-signaling networks," *Journal of Dental Research*, vol. 90, no. 4, pp. 417–427, 2011.

[42] T. Lawrence, "The nuclear factor NF-kappaB pathway in inflammation," *Cold Spring Harbor Perspectives in Biology*, vol. 1, no. 6, article a001651, 2009.

[43] M. J. Morgan and Z. Liu, "Crosstalk of reactive oxygen species and NF-κB signaling," *Cell Research*, vol. 21, no. 1, pp. 103–115, 2011.

[44] A. Abderrazak, T. Syrovets, D. Couchie et al., "NLRP3 inflammasome: from a danger signal sensor to a regulatory node of oxidative stress and inflammatory diseases," *Redox Biology*, vol. 4, pp. 296–307, 2015.

[45] M. L. Moss, S. L. Jin, M. E. Milla et al.et al., "Cloning of a disintegrin metalloproteinase that processes precursor tumour-necrosis factor-alpha," *Nature*, vol. 385, no. 6618, pp. 733–736, 1997.

[46] A. Chalaris, B. Rabe, K. Paliga et al., "Apoptosis is a natural stimulus of IL6R shedding and contributes to the proinflammatory trans-signaling function of neutrophils," *Blood*, vol. 110, no. 6, pp. 1748–1755, 2007.

[47] J. H. Bell, A. H. Herrera, Y. Li, and B. Walcheck, "Role of ADAM17 in the ectodomain shedding of TNF-alpha and its

receptors by neutrophils and macrophages," *Journal of Leukocyte Biology*, vol. 82, no. 1, pp. 173–176, 2007.

[48] P. Ghezzi, "Protein glutathionylation in health and disease," *Biochimica et Biophysica Acta (BBA) - General Subjects*, vol. 1830, no. 5, pp. 3165–3172, 2013.

[49] L. Mullen, M. Seavill, R. Hammouz et al., "Development of 'redox arrays' for identifying novel glutathionylated proteins in the secretome," *Scientific Reports*, vol. 5, article 14630, 2015.

[50] P. Checconi, S. Salzano, L. Bowler et al., "Redox proteomics of the inflammatory secretome identifies a common set of redoxins and other glutathionylated proteins released in inflammation, influenza virus infection and oxidative stress," *PLoS One*, vol. 10, no. 5, article e0127086, 2015.

[51] L. Mullen, E.-M. Hanschmann, C. H. Lillig, L. A. Herzenberg, and P. Ghezzi, "Cysteine oxidation targets peroxiredoxins 1 and 2 for exosomal release through a novel mechanism of redox-dependent secretion," *Molecular Medicine Cambridge, Mass*, vol. 21, no. 1, pp. 98–108, 2015.

[52] S. Salzano, P. Checconi, E. M. Hanschmann et al., "Linkage of inflammation and oxidative stress via release of glutathionylated peroxiredoxin-2, which acts as a danger signal," *Proceedings of the National Academy of Sciences of the United States of America*, vol. 111, no. 33, pp. 12157–12162, 2014.

[53] Z. Yan, S. K. Garg, J. Kipnis, and R. Banerjee, "Extracellular redox modulation by regulatory T cells," *Nature Chemical Biology*, vol. 5, no. 10, pp. 721–723, 2009.

[54] L. Simeoni and I. Bogeski, "Redox regulation of T-cell receptor signaling," *Biological Chemistry*, vol. 396, no. 5, pp. 555–568, 2015.

[55] G. Angelini, S. Gardella, M. Ardy et al., "Antigen-presenting dendritic cells provide the reducing extracellular microenvironment required for T lymphocyte activation," *Proceedings of the National Academy of Sciences of the United States of America*, vol. 99, no. 3, pp. 1491–1496, 2002.

[56] P. Castellani, G. Angelini, L. Delfino, A. Matucci, and A. Rubartelli, "The thiol redox state of lymphoid organs is modified by immunization: role of different immune cell populations," *European Journal of Immunology*, vol. 38, no. 9, pp. 2419–2425, 2008.

[57] J. P. Secrist, L. A. Burns, L. Karnitz, G. A. Koretzky, and R. T. Abraham, "Stimulatory effects of the protein tyrosine phosphatase inhibitor, pervanadate, on T-cell activation events," *The Journal of Biological Chemistry*, vol. 268, no. 8, pp. 5886–5893, 1993.

[58] M. Suthanthiran, M. E. Anderson, V. K. Sharma, and A. Meister, "Glutathione regulates activation-dependent DNA synthesis in highly purified normal human T lymphocytes stimulated via the CD2 and CD3 antigens," *Proceedings of the National Academy of Sciences*, vol. 87, no. 9, pp. 3343–3347, 1990.

[59] A. A. Hasan, A. M. Ghaemmaghami, L. Fairclough, A. Robins, H. F. Sewell, and F. Shakib, "Allergen-driven suppression of thiol production by human dendritic cells and the effect of thiols on T cell function," *Immunobiology*, vol. 214, no. 1, pp. 2–16, 2009.

[60] J. D. Peterson, L. A. Herzenberg, K. Vasquez, and C. Waltenbaugh, "Glutathione levels in antigen-presenting cells modulate Th1 versus Th2 response patterns," *Proceedings of the National Academy of Sciences*, vol. 95, no. 6, pp. 3071–3076, 1998.

[61] H. M. Tse, M. J. Milton, S. Schreiner, J. L. Profozich, M. Trucco, and J. D. Piganelli, "Disruption of innate-mediated proinflammatory cytokine and reactive oxygen species third signal leads to antigen-specific hyporesponsiveness," *Journal of Immunology Baltimore*, vol. 178, no. 2, pp. 908–917, 2007.

[62] T. Jikimoto, Y. Nishikubo, M. Koshiba et al., "Thioredoxin as a biomarker for oxidative stress in patients with rheumatoid arthritis," *Molecular Immunology*, vol. 38, no. 10, pp. 765–772, 2002.

[63] B. Adamczyk and M. Adamczyk-Sowa, "New insights into the role of oxidative stress mechanisms in the pathophysiology and treatment of multiple sclerosis," *Oxidative Medicine and Cellular Longevity*, vol. 2016, Article ID 1973834, 18 pages, 2016.

[64] L. Dai, A. Claxson, S. L. Marklund et al., "Amelioration of antigen-induced arthritis in rats by transfer of extracellular superoxide dismutase and catalase genes," *Gene Therapy*, vol. 10, no. 7, pp. 550–558, 2003.

[65] K. Kasarełło, A. Cudnoch-Jędrzejewska, A. Członkowski, and D. Mirowska-Guzel, "Mechanism of action of three newly registered drugs for multiple sclerosis treatment," *Pharmacological Reports*, vol. 69, no. 4, pp. 702–708, 2017.

[66] G. F. Wu and E. Alvarez, "The immunopathophysiology of multiple sclerosis," *Neurologic Clinics*, vol. 29, no. 2, pp. 257–278, 2011.

[67] H. R. Griffiths, "ROS as signalling molecules in T cells–evidence for abnormal redox signalling in the autoimmune disease, rheumatoid arthritis," *Redox Report Communications Free Radical Research*, vol. 10, no. 6, pp. 273–280, 2005.

[68] M. Ushio-Fukai, "Localizing NADPH oxidase-derived ROS," *Sciences STKE Signal Transduction Knowledge Environment*, vol. 2006, no. 349, article re8, 2006.

[69] A. Panday, M. K. Sahoo, D. Osorio, and S. Batra, "NADPH oxidases: an overview from structure to innate immunity-associated pathologies," *Cellular & Molecular Immunology*, vol. 12, no. 1, pp. 5–23, 2015.

[70] S. Pendyala and V. Natarajan, "Redox regulation of Nox proteins," *Respiratory Physiology & Neurobiology*, vol. 174, no. 3, pp. 265–271, 2010.

[71] P. Nunes, N. Demaurex, and M. C. Dinauer, "Regulation of the NADPH oxidase and associated ion fluxes during phagocytosis," *Traffic*, vol. 14, no. 11, pp. 1118–1131, 2013.

[72] R. Paletta-Silva, N. Rocco-Machado, and J. R. Meyer-Fernandes, "NADPH oxidase biology and the regulation of tyrosine kinase receptor signaling and cancer drug cytotoxicity," *International Journal of Molecular Sciences*, vol. 14, no. 2, pp. 3683–3704, 2013.

[73] F. D. Oakley, D. Abbott, Q. Li, and J. F. Engelhardt, "Signaling components of redox active endosomes: the redoxosomes," *Antioxidants & Redox Signaling*, vol. 11, no. 6, pp. 1313–1333, 2009.

[74] N. Y. Spencer and J. F. Engelhardt, "The basic biology of redoxosomes in cytokine-mediated signal transduction and implications for disease-specific therapies," *Biochemistry (Moscow)*, vol. 53, no. 10, pp. 1551–1564, 2014.

[75] F. J. Miller Jr., X. Chu, B. Stanic et al., "A differential role for endocytosis in receptor-mediated activation of Nox1," *Antioxidants & Redox Signaling*, vol. 12, no. 5, pp. 583–593, 2010.

[76] Q. Li, M. M. Harraz, W. Zhou et al., "Nox2 and Rac1 regulate H2O2-dependent recruitment of TRAF6 to endosomal interleukin-1 receptor complexes," *Molecular and Cellular Biology*, vol. 26, no. 1, pp. 140–154, 2006.

[77] F. D. Oakley, R. L. Smith, and J. F. Engelhardt, "Lipid rafts and caveolin-1 coordinate interleukin-1beta (IL-1beta)-dependent activation of NFkappaB by controlling endocytosis of Nox2 and IL-1beta receptor 1 from the plasma membrane," *The Journal of Biological Chemistry*, vol. 284, no. 48, pp. 33255–33264, 2009.

[78] T. Kawahara, Y. Kuwano, S. Teshima-Kondo et al., "Role of nicotinamide adenine dinucleotide phosphate oxidase 1 in oxidative burst response to Toll-like receptor 5 signaling in large intestinal epithelial cells," *The Journal of Immunology*, vol. 172, no. 5, pp. 3051–3058, 2004.

[79] S. Teshima, H. Kutsumi, T. Kawahara, K. Kishi, and K. Rokutan, "Regulation of growth and apoptosis of cultured guinea pig gastric mucosal cells by mitogenic oxidase 1," *American Journal of Physiology - Gastrointestinal and Liver Physiology*, vol. 279, no. 6, pp. G1169–G1176, 2000.

[80] J. G. Lee, S. H. Lee, D. W. Park et al., "Toll-like receptor 9-stimulated monocyte chemoattractant protein-1 is mediated via JNK-cytosolic phospholipase A_2-ROS signaling," *Cellular Signalling*, vol. 20, no. 1, pp. 105–111, 2008.

[81] M. Geiszt, J. B. Kopp, P. Várnai, and T. L. Leto, "Identification of renox, an NAD(P)H oxidase in kidney," *Proceedings of the National Academy of Sciences of the United States of America*, vol. 97, no. 14, pp. 8010–8014, 2000.

[82] S. Elsen, J. Doussière, C. L. Villiers et al., "Cryptic O_2^--generating NADPH oxidase in dendritic cells," *Journal of Cell Science*, vol. 117, Part 11, pp. 2215–2226, 2004.

[83] J. L. Koff, M. X. G. Shao, I. F. Ueki, and J. A. Nadel, "Multiple TLRs activate EGFR via a signaling cascade to produce innate immune responses in airway epithelium," *American Journal of Physiology - Lung Cellular and Molecular Physiology*, vol. 294, no. 6, pp. L1068–L1075, 2008.

[84] E. Ogier-Denis, S. B. Mkaddem, and A. Vandewalle, "NOX enzymes and Toll-like receptor signaling," *Seminars in Immunopathology*, vol. 30, no. 3, pp. 291–300, 2008.

[85] A. Savina, C. Jancic, S. Hugues et al., "NOX2 controls phagosomal pH to regulate antigen processing during cross-presentation by dendritic cells," *Cell*, vol. 126, no. 1, pp. 205–218, 2006.

[86] S. Chang, A. Linderholm, and R. Harper, "DUOX-mediated signaling is not required for LPS-induced neutrophilic response in the airways," *PLoS One*, vol. 10, no. 7, article e0131810, 2015.

[87] H. S. Park, J. N. Chun, H. Y. Jung, C. Choi, and Y. S. Bae, "Role of NADPH oxidase 4 in lipopolysaccharide-induced proinflammatory responses by human aortic endothelial cells," *Cardiovascular Research*, vol. 72, no. 3, pp. 447–455, 2006.

[88] E. Giannoni, F. Buricchi, G. Raugei, G. Ramponi, and P. Chiarugi, "Intracellular reactive oxygen species activate Src tyrosine kinase during cell adhesion and anchorage-dependent cell growth," *Molecular and Cellular Biology*, vol. 25, no. 15, pp. 6391–6403, 2005.

[89] P. Chiarugi, "Src redox regulation: there is more than meets the eye," *Molecules and Cells*, vol. 26, no. 4, pp. 329–337, 2008.

[90] C. E. Paulsen, T. H. Truong, F. J. Garcia et al., "Peroxide-dependent sulfenylation of the EGFR catalytic site enhances kinase activity," *Nature Chemical Biology*, vol. 8, no. 1, pp. 57–64, 2011.

[91] D. E. Heppner, M. Hristova, C. M. Dustin, K. Danyal, A. Habibovic, and A. van der Vliet, "The NADPH oxidases DUOX1 and NOX2 play distinct roles in redox regulation of epidermal growth factor receptor signaling," *The Journal of Biological Chemistry*, vol. 291, no. 44, pp. 23282–23293, 2016.

[92] H. Sies, "Hydrogen peroxide as a central redox signaling molecule in physiological oxidative stress: oxidative eustress," *Redox Biology*, vol. 11, pp. 613–619, 2017.

[93] B. Stottmeier and T. P. Dick, "Redox sensitivity of the MyD88 immune signaling adapter," *Free Radical Biology & Medicine*, vol. 101, pp. 93–101, 2016.

[94] T. Into, M. Inomata, M. Nakashima, K. Shibata, H. Häcker, and K. Matsushita, "Regulation of MyD88-dependent signaling events by S nitrosylation retards toll-like receptor signal transduction and initiation of acute-phase immune responses," *Molecular and Cellular Biology*, vol. 28, no. 4, pp. 1338–1347, 2008.

[95] A. Matsuzawa and H. Ichijo, "Redox control of cell fate by MAP kinase: physiological roles of ASK1-MAP kinase pathway in stress signaling," *Biochimica et Biophysica Acta (BBA) - General Subjects*, vol. 1780, no. 11, pp. 1325–1336, 2008.

[96] J. J. Song and Y. J. Lee, "Differential role of glutaredoxin and thioredoxin in metabolic oxidative stress-induced activation of apoptosis signal-regulating kinase 1," *The Biochemical Journal*, vol. 373, Part 3, pp. 845–853, 2003.

[97] A. Matsuzawa, K. Saegusa, T. Noguchi et al., "ROS-dependent activation of the TRAF6-ASK1-p38 pathway is selectively required for TLR4-mediated innate immunity," *Nature Immunology*, vol. 6, no. 6, pp. 587–592, 2005.

[98] X. Guo, C. Harada, K. Namekata et al., "Regulation of the severity of neuroinflammation and demyelination by TLR-ASK1-p38 pathway," *EMBO Molecular Medicine*, vol. 2, no. 12, pp. 504–515, 2010.

[99] E. Pineda-Molina, P. Klatt, J. Vázquez et al., "Glutathionylation of the p50 subunit of NF-κB: a mechanism for redox-induced inhibition of DNA binding," *Biochemistry*, vol. 40, no. 47, pp. 14134–14142, 2001.

[100] D. Daily, A. Vlamis-Gardikas, D. Offen et al., "Glutaredoxin protects cerebellar granule neurons from dopamine-induced apoptosis by activating NF-κB via Ref-1," *Journal of Biological Chemistry*, vol. 276, no. 2, pp. 1335–1344, 2001.

[101] K. Hirota, M. Matsui, M. Murata et al., "Nucleoredoxin, glutaredoxin, and thioredoxin differentially regulate NF-κB, AP-1, and CREB activation in HEK293 cells," *Biochemical and Biophysical Research Communications*, vol. 274, no. 1, pp. 177–182, 2000.

[102] S. Witte, M. Villalba, K. Bi, Y. Liu, N. Isakov, and A. Altman, "Inhibition of the c-Jun N-terminal kinase/AP-1 and NF-κB pathways by PICOT, a novel protein kinase C-interacting protein with a thioredoxin homology domain," *The Journal of Biological Chemistry*, vol. 275, no. 3, pp. 1902–1909, 2000.

[103] I. Rahman, J. Marwick, and P. Kirkham, "Redox modulation of chromatin remodeling: impact on histone acetylation and deacetylation, NF-κB and pro-inflammatory gene expression," *Biochemical Pharmacology*, vol. 68, no. 6, pp. 1255–1267, 2004.

[104] A. Nishiyama, M. Matsui, S. Iwata et al., "Identification of thioredoxin-binding protein-2/vitamin D_3 up-regulated protein 1 as a negative regulator of thioredoxin function and expression," *Journal of Biological Chemistry*, vol. 274, no. 31, pp. 21645–21650, 1999.

[105] S. Rose-John, "IL-6 trans-signaling via the soluble IL-6 receptor: importance for the pro-inflammatory activities of IL-6," *International Journal of Biological Sciences*, vol. 8, no. 9, pp. 1237–1247, 2012.

[106] F. Schaper and S. Rose-John, "Interleukin-6: biology, signaling and strategies of blockade," *Cytokine & Growth Factor Reviews*, vol. 26, no. 5, pp. 475–487, 2015.

[107] J. J. Peschon, J. L. Slack, P. Reddy et al., "An essential role for ectodomain shedding in mammalian development," *Science*, vol. 282, no. 5392, pp. 1281–1284, 1998.

[108] C. P. Blobel, "ADAMs: key components in EGFR signalling and development," *Nature Reviews Molecular Cell Biology*, vol. 6, no. 1, pp. 32–43, 2005.

[109] A. Chalaris, N. Adam, C. Sina et al., "Critical role of the disintegrin metalloprotease ADAM17 for intestinal inflammation and regeneration in mice," *The Journal of Experimental Medicine*, vol. 207, no. 8, pp. 1617–1624, 2010.

[110] M. A. West, A. R. Prescott, K. M. Chan et al., "TLR ligand-induced podosome disassembly in dendritic cells is ADAM17 dependent," *The Journal of Cell Biology*, vol. 182, no. 5, pp. 993–1005, 2008.

[111] R. S. Chanthaphavong, P. A. Loughran, T. Y. S. Lee, M. J. Scott, and T. R. Billiar, "A role for cGMP in inducible nitric-oxide synthase (iNOS)-induced tumor necrosis factor (TNF) α-converting enzyme (TACE/ADAM17) activation, translocation, and TNF receptor 1 (TNFR1) shedding in hepatocytes," *The Journal of Biological Chemistry*, vol. 287, no. 43, pp. 35887–35898, 2012.

[112] A. Piccini, S. Carta, S. Tassi, D. Lasiglié, G. Fossati, and A. Rubartelli, "ATP is released by monocytes stimulated with pathogen-sensing receptor ligands and induces IL-1β and IL-18 secretion in an autocrine way," *Proceedings of the National Academy of Sciences*, vol. 105, no. 23, pp. 8067–8072, 2008.

[113] E. Asgari, G. Le Friec, H. Yamamoto et al., "C3a modulates IL-1β secretion in human monocytes by regulating ATP efflux and subsequent NLRP3 inflammasome activation," *Blood*, vol. 122, no. 20, pp. 3473–3481, 2013.

[114] A. W. Boots, M. Hristova, D. I. Kasahara, G. R. M. M. Haenen, A. Bast, and A. van der Vliet, "ATP-mediated activation of the NADPH oxidase DUOX1 mediates airway epithelial responses to bacterial stimuli," *The Journal of Biological Chemistry*, vol. 284, no. 26, pp. 17858–17867, 2009.

[115] D. Sham, U. V. Wesley, M. Hristova, and A. van der Vliet, "ATP-mediated transactivation of the epidermal growth factor receptor in airway epithelial cells involves DUOX1-dependent oxidation of Src and ADAM17," *PLoS One*, vol. 8, no. 1, article e54391, 2013.

[116] H. Nakamura, K. Yoshimura, N. G. McElvaney, and R. G. Crystal, "Neutrophil elastase in respiratory epithelial lining fluid of individuals with cystic fibrosis induces interleukin-8 gene expression in a human bronchial epithelial cell line," *The Journal of Clinical Investigation*, vol. 89, no. 5, pp. 1478–1484, 1992.

[117] J. V. Fahy, K. W. Kim, J. Liu, and H. A. Boushey, "Prominent neutrophilic inflammation in sputum from subjects with asthma exacerbation," *Journal of Allergy and Clinical Immunology*, vol. 95, no. 4, pp. 843–852, 1995.

[118] M. X. G. Shao and J. A. Nadel, "Neutrophil elastase induces MUC5AC mucin production in human airway epithelial cells via a cascade involving protein kinase C, reactive oxygen species, and TNF-α-converting enzyme," *The Journal of Immunology*, vol. 175, no. 6, pp. 4009–4016, 2005.

[119] M. X. G. Shao and J. A. Nadel, "Dual oxidase 1-dependent MUC5AC mucin expression in cultured human airway epithelial cells," *Proceedings of the National Academy of Sciences of the United States of America*, vol. 102, no. 3, pp. 767–772, 2005.

[120] I. Kuwahara, E. P. Lillehoj, T. Koga, Y. Isohama, T. Miyata, and K. C. Kim, "The signaling pathway involved in neutrophil elastase stimulated MUC1 transcription," *American Journal of Respiratory Cell and Molecular Biology*, vol. 37, no. 6, pp. 691–698, 2007.

[121] E. Thorp, T. Vaisar, M. Subramanian, L. Mautner, C. Blobel, and I. Tabas, "Shedding of the Mer tyrosine kinase receptor is mediated by ADAM17 protein through a pathway involving reactive oxygen species, protein kinase Cδ, and p38 mitogen-activated protein kinase (MAPK)," *The Journal of Biological Chemistry*, vol. 286, no. 38, pp. 33335–33344, 2011.

[122] A. J. Scott, K. P. O'Dea, D. O'Callaghan et al., "Reactive oxygen species and p38 mitogen-activated protein kinase mediate tumor necrosis factor α-converting enzyme (TACE/ADAM-17) activation in primary human monocytes," *The Journal of Biological Chemistry*, vol. 286, no. 41, pp. 35466–35476, 2011.

[123] J. Moreno-Càceres, J. Mainez, R. Mayoral, P. Martín-Sanz, G. Egea, and I. Fabregat, "Caveolin-1-dependent activation of the metalloprotease TACE/ADAM17 by TGF-β in hepatocytes requires activation of Src and the NADPH oxidase NOX1," *The FEBS Journal*, vol. 283, no. 7, pp. 1300–1310, 2016.

[124] E. Tellier, M. Canault, L. Rebsomen et al., "The shedding activity of ADAM17 is sequestered in lipid rafts," *Experimental Cell Research*, vol. 312, no. 20, pp. 3969–3980, 2006.

[125] D. Shao, A. W. Segal, and L. V. Dekker, "Lipid rafts determine efficiency of NADPH oxidase activation in neutrophils," *FEBS Letters*, vol. 550, no. 1–3, pp. 101–106, 2003.

[126] F. Vilhardt and B. van Deurs, "The phagocyte NADPH oxidase depends on cholesterol-enriched membrane microdomains for assembly," *The EMBO Journal*, vol. 23, no. 4, pp. 739–748, 2004.

[127] H. P. Wang, X. Wang, L. F. Gong et al., "Nox1 promotes colon cancer cell metastasis via activation of the ADAM17 pathway," *European Review for Medical and Pharmacological Sciences*, vol. 20, no. 21, pp. 4474–4481, 2016.

[128] T. J. Myers, L. H. Brennaman, M. Stevenson et al., "Mitochondrial reactive oxygen species mediate GPCR-induced TACE/ADAM17-dependent transforming growth factor-α shedding," *Molecular Biology of the Cell*, vol. 20, no. 24, pp. 5236–5249, 2009.

[129] Y. Wang, J. D. Robertson, and B. Walcheck, "Different signaling pathways stimulate a disintegrin and metalloprotease-17 (ADAM17) in neutrophils during apoptosis and activation," *The Journal of Biological Chemistry*, vol. 286, no. 45, pp. 38980–38988, 2011.

[130] T. Maretzky, W. Zhou, X.-Y. Huang, and C. P. Blobel, "A transforming Src mutant increases the bioavailability of

EGFR ligands via stimulation of the cell-surface metalloproteinase ADAM17," *Oncogene*, vol. 30, no. 5, pp. 611–618, 2011.

[131] S. Van Schaeybroeck, D. M. Kelly, J. Kyula et al., "Src and ADAM-17-mediated shedding of transforming growth factor-alpha is a mechanism of acute resistance to TRAIL," *Cancer Research*, vol. 68, no. 20, pp. 8312–8321, 2008.

[132] P. Xu and R. Derynck, "Direct activation of TACE-mediated ectodomain shedding by p38 MAP kinase regulates EGF receptor-dependent cell proliferation," *Molecular Cell*, vol. 37, no. 4, pp. 551–566, 2010.

[133] S. M. Soond, B. Everson, D. W. H. Riches, and G. Murphy, "ERK-mediated phosphorylation of Thr735 in TNFα-converting enzyme and its potential role in TACE protein trafficking," *Journal of Cell Science*, vol. 118, Part 11, pp. 2371–2380, 2005.

[134] P. W. Janes, N. Saha, W. A. Barton et al., "Adam meets Eph: an ADAM substrate recognition module acts as a molecular switch for ephrin cleavage in trans," *Cell*, vol. 123, no. 2, pp. 291–304, 2005.

[135] S. Düsterhöft, S. Jung, C. W. Hung et al., "Membrane-proximal domain of a disintegrin and metalloprotease-17 represents the putative molecular switch of its shedding activity operated by protein-disulfide isomerase," *Journal of the American Chemical Society*, vol. 135, no. 15, pp. 5776–5781, 2013.

[136] S. Takeda, "Three-dimensional domain architecture of the ADAM family proteinases," *Seminars in Cell & Developmental Biology*, vol. 20, no. 2, pp. 146–152, 2009.

[137] S. Düsterhöft, K. Höbel, M. Oldefest et al., "A disintegrin and metalloprotease 17 dynamic interaction sequence, the sweet tooth for the human interleukin 6 receptor," *The Journal of Biological Chemistry*, vol. 289, no. 23, pp. 16336–16348, 2014.

[138] Y. Wang, A. H. Herrera, Y. Li, K. K. Belani, and B. Walcheck, "Regulation of mature ADAM17 by redox agents for L-selectin shedding," *Journal of Immunology*, vol. 182, no. 4, pp. 2449–2457, 2009.

[139] S. Düsterhöft, M. Michalek, F. Kordowski et al., "Extracellular juxtamembrane segment of ADAM17 interacts with membranes and is essential for its shedding activity," *Biochemistry (Moscow)*, vol. 54, no. 38, pp. 5791–5801, 2015.

[140] A. Sommer, F. Kordowski, J. Büch et al., "Phosphatidylserine exposure is required for ADAM17 sheddase function," *Nature Communications*, vol. 7, article 11523, 2016.

[141] T. W. Kim, H. H. Ryu, S. Y. Li et al., "PDIA6 regulation of ADAM17 shedding activity and EGFR-mediated migration and invasion of glioblastoma cells," *Journal of Neurosurgery*, vol. 126, no. 6, pp. 1829–1838, 2017.

[142] Y. Liu, W. Hao, A. Dawson, S. Liu, and K. Fassbender, "Expression of amyotrophic lateral sclerosis-linked SOD1 mutant increases the neurotoxic potential of microglia via TLR2," *The Journal of Biological Chemistry*, vol. 284, no. 6, pp. 3691–3699, 2009.

[143] M. P. Sanderson, C. A. Abbott, H. Tada, M. Seno, P. J. Dempsey, and A. J. Dunbar, "Hydrogen peroxide and endothelin-1 are novel activators of betacellulin ectodomain shedding," *Journal of Cellular Biochemistry*, vol. 99, no. 2, pp. 609–623, 2006.

[144] U. Schwertassek, Y. Balmer, M. Gutscher et al., "Selective redox regulation of cytokine receptor signaling by extracellular thioredoxin-1," *The EMBO Journal*, vol. 26, no. 13, pp. 3086–3097, 2007.

[145] P. A. Jordan and J. M. Gibbins, "Extracellular disulfide exchange and the regulation of cellular function," *Antioxidants & Redox Signaling*, vol. 8, no. 3-4, pp. 312–324, 2006.

[146] J. Li, R. Kokkola, S. Tabibzadeh et al., "Structural basis for the proinflammatory cytokine activity of high mobility group box 1," *Molecular Medicine*, vol. 9, no. 1-2, pp. 37–45, 2003.

[147] H. Yang, H. Wang, S. S. Chavan, and U. Andersson, "High mobility group box protein 1 (HMGB1): the prototypical endogenous danger molecule," *Molecular Medicine*, vol. 21, Supplement 1, pp. S6–S12, 2015.

[148] S. Gardella, C. Andrei, D. Ferrera et al., "The nuclear protein HMGB1 is secreted by monocytes via a non-classical, vesicle-mediated secretory pathway," *EMBO Reports*, vol. 3, no. 10, pp. 995–1001, 2002.

[149] K. Kawahara, T. Hashiguchi, K. Masuda et al., "Mechanism of HMGB1 release inhibition from RAW264.7 cells by oleanolic acid in Prunus mume Sieb. et Zucc," *International Journal of Molecular Medicine*, vol. 23, no. 5, pp. 615–620, 2009.

[150] P. Scaffidi, T. Misteli, and M. E. Bianchi, "Release of chromatin protein HMGB1 by necrotic cells triggers inflammation," *Nature*, vol. 418, no. 6894, pp. 191–195, 2002.

[151] C. Janko, M. Filipović, L. E. Munoz et al., "Redox modulation of HMGB1-related signaling," *Antioxidants & Redox Signaling*, vol. 20, no. 7, pp. 1075–1085, 2014.

[152] D. Tang, R. Kang, K. M. Livesey, H. J. Zeh, and M. T. Lotze, "High mobility group box 1 (HMGB1) activates an autophagic response to oxidative stress," *Antioxidants & Redox Signaling*, vol. 15, no. 8, pp. 2185–2195, 2011.

[153] G. Hoppe, K. E. Talcott, S. K. Bhattacharya, J. W. Crabb, and J. E. Sears, "Molecular basis for the redox control of nuclear transport of the structural chromatin protein Hmgb1," *Experimental Cell Research*, vol. 312, no. 18, pp. 3526–3538, 2006.

[154] H. Yang, H. S. Hreggvidsdottir, K. Palmblad et al., "A critical cysteine is required for HMGB1 binding to Toll-like receptor 4 and activation of macrophage cytokine release," *Proceedings of the National Academy of Sciences of the United States of America*, vol. 107, no. 26, pp. 11942–11947, 2010.

[155] H. Yang, P. Lundbäck, L. Ottosson et al., "Redox modification of cysteine residues regulates the cytokine activity of high mobility group box-1 (HMGB1)," *Molecular Medicine*, vol. 18, pp. 250–259, 2012.

[156] E. Venereau, M. Casalgrandi, M. Schiraldi et al., "Mutually exclusive redox forms of HMGB1 promote cell recruitment or proinflammatory cytokine release," *The Journal of Experimental Medicine*, vol. 209, no. 9, pp. 1519–1528, 2012.

[157] H. Yang, D. J. Antoine, U. Andersson, and K. J. Tracey, "The many faces of HMGB1: molecular structure-functional activity in inflammation, apoptosis, and chemotaxis," *Journal of Leukocyte Biology*, vol. 93, no. 6, pp. 865–873, 2013.

[158] D. Sahu, P. Debnath, Y. Takayama, and J. Iwahara, "Redox properties of the A-domain of the HMGB1 protein," *FEBS Letters*, vol. 582, no. 29, pp. 3973–3978, 2008.

[159] Y. Tagaya, Y. Maeda, A. Mitsui et al., "ATL-derived factor (ADF), an IL-2 receptor/Tac inducer homologous to thioredoxin; possible involvement of dithiol-reduction in the IL-2 receptor induction," *The EMBO Journal*, vol. 8, no. 3, pp. 757–764, 1989.

[160] H. Schenk, M. Vogt, W. Dröge, and K. Schulze-Osthoff, "Thioredoxin as a potent costimulus of cytokine expression," *Journal of Immunology*, vol. 156, no. 2, pp. 765–771, 1996.

[161] K. Pekkari and A. Holmgren, "Truncated thioredoxin: physiological functions and mechanism," *Antioxidants & Redox Signaling*, vol. 6, no. 1, pp. 53–61, 2004.

[162] A. Son, N. Kato, T. Horibe et al., "Direct association of thioredoxin-1 (TRX) with macrophage migration inhibitory factor (MIF): regulatory role of TRX on MIF internalization and signaling," *Antioxidants & Redox Signaling*, vol. 11, no. 10, pp. 2595–2605, 2009.

[163] W. M. Nauseef, "Neutrophils, from cradle to grave and beyond," *Immunological Reviews*, vol. 273, no. 1, pp. 5–10, 2016.

[164] The resurrection of myeloperoxidase as a therapeutic target | JACC: basic to translational science," 2017, http://www.basictranslational.onlinejacc.org/content/1/7/644.

[165] J. Olza, C. M. Aguilera, M. Gil-Campos et al., "Myeloperoxidase is an early biomarker of inflammation and cardiovascular risk in prepubertal obese children," *Diabetes Care*, vol. 35, no. 11, pp. 2373–2376, 2012.

[166] R. K. Schindhelm, L. P. van der Zwan, T. Teerlink, and P. G. Scheffer, "Myeloperoxidase: a useful biomarker for cardiovascular disease risk stratification?," *Clinical Chemistry*, vol. 55, no. 8, pp. 1462–1470, 2009.

[167] A. Daugherty, J. L. Dunn, D. L. Rateri, and J. W. Heinecke, "Myeloperoxidase, a catalyst for lipoprotein oxidation, is expressed in human atherosclerotic lesions," *The Journal of Clinical Investigation*, vol. 94, no. 1, pp. 437–444, 1994.

[168] L. K. Stamp, I. Khalilova, J. M. Tarr et al., "Myeloperoxidase and oxidative stress in rheumatoid arthritis," *Rheumatology*, vol. 51, no. 10, pp. 1796–1803, 2012.

[169] C. Sinning, R. Schnabel, W. F. Peacock, and S. Blankenberg, "Up-and-coming markers: myeloperoxidase, a novel biomarker test for heart failure and acute coronary syndrome application?," *Congestive Heart Failure*, vol. 14, no. 4, Supplement 1, pp. 46–48, 2008.

[170] I. H. Buss, R. Senthilmohan, B. A. Darlow, N. Mogridge, A. J. Kettle, and C. C. Winterbourn, "3-Chlorotyrosine as a marker of protein damage by myeloperoxidase in tracheal aspirates from preterm infants: association with adverse respiratory outcome," *Pediatric Research*, vol. 53, no. 3, pp. 455–462, 2003.

[171] A. J. Kettle and C. C. Winterbourn, "Mechanism of inhibition of myeloperoxidase by anti-inflammatory drugs," *Biochemical Pharmacology*, vol. 41, no. 10, pp. 1485–1492, 1991.

[172] A. Jucaite, P. Svenningsson, J. O. Rinne et al., "Effect of the myeloperoxidase inhibitor AZD3241 on microglia: a PET study in Parkinson's disease," *Brain: A Journal of Neurology*, vol. 138, Part 9, pp. 2687–2700, 2015.

[173] L. V. Forbes, T. Sjögren, F. Auchère et al., "Potent reversible inhibition of myeloperoxidase by aromatic hydroxamates," *The Journal of Biological Chemistry*, vol. 288, no. 51, pp. 36636–36647, 2013.

[174] H. Parker, A. M. Albrett, A. J. Kettle, and C. C. Winterbourn, "Myeloperoxidase associated with neutrophil extracellular traps is active and mediates bacterial killing in the presence of hydrogen peroxide," *Journal of Leukocyte Biology*, vol. 91, no. 3, pp. 369–376, 2012.

[175] B. Pinegin, N. Vorobjeva, and V. Pinegin, "Neutrophil extracellular traps and their role in the development of chronic inflammation and autoimmunity," *Autoimmunity Reviews*, vol. 14, no. 7, pp. 633–640, 2015.

[176] P. S. Green, A. J. Mendez, J. S. Jacob et al., "Neuronal expression of myeloperoxidase is increased in Alzheimer's disease," *Journal of Neurochemistry*, vol. 90, no. 3, pp. 724–733, 2004.

[177] C. B. Ambrosone, W. E. Barlow, W. Reynolds et al., "Myeloperoxidase genotypes and enhanced efficacy of chemotherapy for early-stage breast cancer in SWOG-8897," *Journal of Clinical Oncology: Official Journal of the American Society of Clinical Oncology*, vol. 27, no. 30, pp. 4973–4979, 2009.

[178] P. G. Furtmüller, W. Jantschko, G. Regelsberger, C. Jakopitsch, J. Arnhold, and C. Obinger, "Reaction of lactoperoxidase compound I with halides and thiocyanate," *Biochemistry*, vol. 41, no. 39, pp. 11895–11900, 2002.

[179] E. Shimizu, T. Kobayashi, H. Wakabayashi, K. Yamauchi, K. Iwatsuki, and H. Yoshie, "Effects of orally administered lactoferrin and lactoperoxidase-containing tablets on clinical and bacteriological profiles in chronic periodontitis patients," *International Journal Dentistry*, vol. 2011, Article ID 405139, 9 pages, 2011.

[180] Y. Güven, I. Satman, N. Dinççağ, and S. Alptekin, "Salivary peroxidase activity in whole saliva of patients with insulin-dependent (type-1) diabetes mellitus," *Journal of Clinical Periodontology*, vol. 23, no. 9, pp. 879–881, 1996.

[181] C. V. Kalburgi, K. L. Naik, M. V. Kokatnur, and S. Warad, "Estimation and correlation of salivary thiocyanate levels in healthy and different forms of tobacco users having chronic periodontitis: a cross-sectional biochemical study," *Contemporary Clinical Dentistry*, vol. 5, no. 2, pp. 182–186, 2014.

[182] K. Cherubini, C. S. Lorandi, S. M. Krapf et al., "Association between recurrent aphthous stomatitis and salivary thiocyanate levels," *Journal of Oral Science*, vol. 48, no. 3, pp. 153–156, 2006.

[183] G. C. Kiran and B. A. Reginald, "Aphthous ulcers, salivary peroxidase and stress: are they related?," *Journal of Oral Maxillofacial Pathology*, vol. 19, no. 1, pp. 37–41, 2015.

[184] J. Flemmig, D. Rusch, M. E. Czerwińska, H.-W. Rauwald, and J. Arnhold, "Components of a standardised olive leaf dry extract (Ph. Eur.) promote hypothiocyanite production by lactoperoxidase," *Archives of Biochemistry and Biophysics*, vol. 549, pp. 17–25, 2014.

[185] T. Bundgaard, J. Wildt, M. Frydenberg, O. Elbrønd, and J. E. Nielsen, "Case-control study of squamous cell cancer of the oral cavity in Denmark," *Cancer Causes Control*, vol. 6, no. 1, pp. 57–67, 1995.

[186] R. V. Luepker, T. F. Pechacek, D. M. Murray, C. A. Johnson, F. Hund, and D. R. Jacobs, "Saliva thiocyanate: a chemical indicator of cigarette smoking in adolescents," *American Journal of Public Health*, vol. 71, no. 12, pp. 1320–1324, 1981.

[187] A. Z. Reznick, I. Klein, J. P. Eiserich, C. E. Cross, and R. M. Nagler, "Inhibition of oral peroxidase activity by cigarette smoke: in vivo and in vitro studies," *Free Radical Biology & Medicine*, vol. 34, no. 3, pp. 377–384, 2003.

[188] E. B. de Oliveira-Junior, J. Bustamante, P. E. Newburger, and A. Condino-Neto, "The human NADPH oxidase: primary and secondary defects impairing the respiratory burst function and the microbicidal ability of phagocytes," *Scandinavian Journal of Immunology*, vol. 73, no. 5, pp. 420–427, 2011.

[189] D. B. Kuhns, W. G. Alvord, T. Heller et al., "Residual NADPH oxidase and survival in chronic granulomatous

disease," *The New England Journal of Medicine*, vol. 363, no. 27, pp. 2600–2610, 2010.

[190] L. A. Allen, F. R. DeLeo, A. Gallois, S. Toyoshima, K. Suzuki, and W. M. Nauseef, "Transient association of the nicotinamide adenine dinucleotide phosphate oxidase subunits p47phox and p67phox with phagosomes in neutrophils from patients with X-linked chronic granulomatous disease," *Blood*, vol. 93, no. 10, pp. 3521–3530, 1999.

[191] I. Takac, K. Schröder, and R. P. Brandes, "The Nox family of NADPH oxidases: friend or foe of the vascular system?," *Current Hypertension Reports*, vol. 14, no. 1, pp. 70–78, 2012.

[192] P. A. Krijnen, C. Meischl, C. E. Hack et al., "Increased Nox2 expression in human cardiomyocytes after acute myocardial infarction," *Journal of Clinical Pathology*, vol. 56, no. 3, pp. 194–199, 2003.

[193] C. Heymes, J. K. Bendall, P. Ratajczak et al., "Increased myocardial NADPH oxidase activity in human heart failure," *Journal of the American College of Cardiology*, vol. 41, no. 12, pp. 2164–2171, 2003.

[194] R. Dworakowski, S. Walker, A. Momin et al., "Reduced nicotinamide adenine dinucleotide phosphate oxidase-derived superoxide and vascular endothelial dysfunction in human heart failure," *Journal of the American College of Cardiology*, vol. 51, no. 14, pp. 1349–1356, 2008.

[195] T. J. Guzik, N. E. West, E. Black et al., "Vascular superoxide production by NAD(P)H oxidase: association with endothelial dysfunction and clinical risk factors," *Circulation Research*, vol. 86, no. 9, pp. E85–E90, 2000.

[196] J. Streeter, W. Thiel, K. Brieger, and F. J. Miller, "Opportunity Nox: the future of NADPH oxidases as therapeutic targets in cardiovascular disease," *Cardiovascular Therapeutics*, vol. 31, no. 3, pp. 125–137, 2013.

[197] C. Berry, C. A. Hamilton, M. J. Brosnan et al., "Investigation into the sources of superoxide in human blood vessels: angiotensin II increases superoxide production in human internal mammary arteries," *Circulation*, vol. 101, no. 18, pp. 2206–2212, 2000.

[198] B. Guzik, M. Chwała, P. Matusik et al., "Mechanisms of increased vascular superoxide production in human varicose veins," *Polskie Archiwum Medycyny Wewnętrznej*, vol. 121, no. 9, pp. 279–286, 2011.

[199] Y. Gorin and K. Block, "Nox as a target for diabetic complications," *Clinical Science*, vol. 125, no. 8, pp. 361–382, 2013.

[200] J.-J. Peng, B. Liu, J.-Y. Xu, J. Peng, and X.-J. Luo, "NADPH oxidase: its potential role in promotion of pulmonary arterial hypertension," *Naunyn-Schmiedeberg's Archives of Pharmacology*, vol. 390, no. 4, pp. 331–338, 2017.

[201] F. Liu-Smith, R. Dellinger, and F. L. Meyskens, "Updates of reactive oxygen species in melanoma etiology and progression," *Archives of Biochemistry and Biophysics*, vol. 563, pp. 51–55, 2014.

[202] W. H. Yin, P. Chen, H. I. Yeh et al., "Combination with low-dose dextromethorphan improves the effect of amlodipine monotherapy in clinical hypertension: a first-in-human, concept-proven, prospective, dose-escalation, multicenter study," *Medicine (Baltimore)*, vol. 95, no. 12, article e3234, 2016.

[203] J. L. Meitzler, S. Antony, Y. Wu et al., "NADPH oxidases: a perspective on reactive oxygen species production in tumor biology," *Antioxidants & Redox Signaling*, vol. 20, no. 17, pp. 2873–2889, 2014.

[204] M. Ushio-Fukai and Y. Nakamura, "Reactive oxygen species and angiogenesis: NADPH oxidase as target for cancer therapy," *Cancer Letters*, vol. 266, no. 1, pp. 37–52, 2008.

[205] J. L. Arbiser, M. Bips, A. Seidler, M. Y. Bonner, and C. Kovach, "Combination therapy of imiquimod and gentian violet for cutaneous melanoma metastases," *Journal of the American Academy of Dermatology*, vol. 67, no. 2, pp. e81–e83, 2012.

[206] R. K. Murthy, L. Van, and J. L. Arbiser, "Treatment of extensive erythema multiforme with topical gentian violet," *Experimental Dermatology*, vol. 26, no. 5, pp. 431-432, 2017.

[207] S. R. Tannenbaum, D. Fett, V. R. Young, P. D. Land, and W. R. Bruce, "Nitrite and nitrate are formed by endogenous synthesis in the human intestine," *Science*, vol. 200, no. 4349, pp. 1487–1489, 1978.

[208] C. Bogdan, "Nitric oxide and the immune response," *Nature Immunology*, vol. 2, no. 10, pp. 907–916, 2001.

[209] K. A. Kirkebøen and O. A. Strand, "The role of nitric oxide in sepsis–an overview," *Acta Anaesthesiologica Scandinavica*, vol. 43, no. 3, pp. 275–288, 1999.

[210] S. R. Jaffrey and S. H. Snyder, "Nitric oxide: a neural messenger," *Annual Review of Cell and Developmental Biology*, vol. 11, pp. 417–440, 1995.

[211] H. Kleinert, C. Euchenhofer, I. Ihrig-Biedert, and U. Förstermann, "Glucocorticoids inhibit the induction of nitric oxide synthase II by down-regulating cytokine-induced activity of transcription factor nuclear factor-kappa B," *Molecular Pharmacology*, vol. 49, no. 1, pp. 15–21, 1996.

[212] M. A. Titheradge, "Nitric oxide in septic shock," *Biochimica et Biophysica Acta (BBA) - Bioenergetics*, vol. 1411, no. 2-3, pp. 437–455, 1999.

[213] B. E. Kreger, D. E. Craven, and W. R. McCabe, "Gram-negative bacteremia. IV. Re-evaluation of clinical features and treatment in 612 patients," *The American Journal of Medicine*, vol. 68, no. 3, pp. 344–355, 1980.

[214] J. H. Christy, "Treatment of gram-negative shock," *The American Journal of Medicine*, vol. 50, no. 1, pp. 77–88, 1971.

[215] C. L. Sprung, P. V. Caralis, E. H. Marcial et al., "The effects of high-dose corticosteroids in patients with septic shock. A prospective, controlled study," *The New England Journal of Medicine*, vol. 311, no. 18, pp. 1137–1143, 1984.

[216] B. Gachot, J. P. Bedos, B. Veber, M. Wolff, and B. Regnier, "Short-term effects of methylene blue on hemodynamics and gas exchange in humans with septic shock," *Intensive Care Medicine*, vol. 21, no. 12, pp. 1027–1031, 1995.

[217] J. M. Fukuto, K. S. Wood, R. E. Byrns, and L. J. Ignarro, "NG-amino-L-arginine: a new potent antagonist of L-arginine-mediated endothelium-dependent relaxation," *Biochemical and Biophysical Research Communications*, vol. 168, no. 2, pp. 458–465, 1990.

[218] A. Petros, D. Bennett, and P. Vallance, "Effect of nitric oxide synthase inhibitors on hypotension in patients with septic shock," *The Lancet*, vol. 338, no. 8782-8783, pp. 1557-1558, 1991.

[219] A. López, J. A. Lorente, J. Steingrub et al., "Multiple-center, randomized, placebo-controlled, double-blind study of the nitric oxide synthase inhibitor 546C88: effect on survival in patients with septic shock," *Critical Care Medicine*, vol. 32, no. 1, pp. 21–30, 2004.

[220] L. H. Lassen, M. Ashina, I. Christiansen et al., "Nitric oxide synthase inhibition: a new principle in the treatment of migraine attacks," *Cephalalgia*, vol. 18, no. 1, pp. 27–32, 1998.

[221] J. Palmer, F. Guillard, B. Laurijssens, A. Wentz, R. Dixon, and P. Williams, "A randomised, single-blind, placebo-controlled, adaptive clinical trial of gw274150, a selective iNOS inhibitor, in the treatment of acute migraine," *Cephalalgia*, vol. 29, no. 1, p. 124, 2009.

[222] H. O. Høivik, B. E. Laurijssens, L. O. Harnisch et al., "Lack of efficacy of the selective iNOS inhibitor GW274150 in prophylaxis of migraine headache," *Cephalalgia*, vol. 30, no. 12, pp. 1458–1467, 2010.

[223] M. E. Wechsler, H. Grasemann, A. Deykin et al., "Exhaled nitric oxide in patients with asthma: association with NOS1 genotype," *American Journal of Respiratory and Critical Care Medicine*, vol. 162, no. 6, pp. 2043–2047, 2000.

[224] T. T. Hansel, S. A. Kharitonov, L. E. Donnelly et al., "A selective inhibitor of inducible nitric oxide synthase inhibits exhaled breath nitric oxide in healthy volunteers and asthmatics," *FASEB Journal*, vol. 17, no. 10, pp. 1298–1300, 2003.

[225] D. Singh, D. Richards, R. G. Knowles et al., "Selective inducible nitric oxide synthase inhibition has no effect on allergen challenge in asthma," *American Journal of Respiratory and Critical Care Medicine*, vol. 176, no. 10, pp. 988–993, 2007.

[226] F. L. Ricciardolo, P. Geppetti, A. Mistretta et al., "Randomised double-blind placebo-controlled study of the effect of inhibition of nitric oxide synthesis in bradykinin-induced asthma," *The Lancet*, vol. 348, no. 9024, pp. 374–377, 1996.

[227] M. Seymour, F. Pétavy, F. Chiesa et al., "Ultrasonographic measures of synovitis in an early phase clinical trial: a double-blind, randomised, placebo and comparator controlled phase IIa trial of GW274150 (a selective inducible nitric oxide synthase inhibitor) in rheumatoid arthritis," *Clinical and Experimental Rheumatology*, vol. 30, no. 2, pp. 254–261, 2012.

[228] P. Pacher, J. S. Beckman, and L. Liaudet, "Nitric oxide and peroxynitrite in health and disease," *Physiological Reviews*, vol. 87, no. 1, pp. 315–424, 2007.

[229] C. S. Baker, D. P. Dutka, D. Pagano et al., "Immunocytochemical evidence for inducible nitric oxide synthase and cyclooxygenase-2 expression with nitrotyrosine formation in human hibernating myocardium," *Basic Research in Cardiology*, vol. 97, no. 5, pp. 409–415, 2002.

[230] S. Ravalli, A. Albala, M. Ming et al., "Inducible nitric oxide synthase expression in smooth muscle cells and macrophages of human transplant coronary artery disease," *Circulation*, vol. 97, no. 23, pp. 2338–2345, 1998.

[231] M. J. Szabolcs, S. Ravalli, O. Minanov, R. R. Sciacca, R. E. Michler, and P. J. Cannon, "Apoptosis and increased expression of inducible nitric oxide synthase in human allograft rejection," *Transplantation*, vol. 65, no. 6, pp. 804–812, 1998.

[232] G. A. Haywood, P. S. Tsao, H. E. von der Leyen et al., "Expression of inducible nitric oxide synthase in human heart failure," *Circulation*, vol. 93, no. 6, pp. 1087–1094, 1996.

[233] S. Ekmekcioglu, J. Ellerhorst, C. M. Smid et al., "Inducible nitric oxide synthase and nitrotyrosine in human metastatic melanoma tumors correlate with poor survival," *Clinical Cancer Research*, vol. 6, no. 12, pp. 4768–4775, 2000.

[234] M. Vakkala, K. Kahlos, E. Lakari, P. Pääkkö, V. Kinnula, and Y. Soini, "Inducible nitric oxide synthase expression, apoptosis, and angiogenesis in in situ and invasive breast carcinomas," *Clinical Cancer Research*, vol. 6, no. 6, pp. 2408–2416, 2000.

[235] M. J. Pukkila, J. K. Kellokoski, J. A. Virtaniemi et al., "Inducible nitric oxide synthase expression in pharyngeal squamous cell carcinoma: relation to p53 expression, clinicopathological data, and survival," *The Laryngoscope*, vol. 112, no. 6, pp. 1084–1088, 2002.

[236] B. Halliwell, "Free radicals, reactive oxygen species and human disease: a critical evaluation with special reference to atherosclerosis," *British Journal of Experimental Pathology*, vol. 70, no. 6, pp. 737–757, 1989.

[237] F. Zipp and O. Aktas, "The brain as a target of inflammation: common pathways link inflammatory and neurodegenerative diseases," *Trends in Neurosciences*, vol. 29, no. 9, pp. 518–527, 2006.

[238] T. A. Sarafian, M. A. Verity, H. V. Vinters et al., "Differential expression of peroxiredoxin subtypes in human brain cell types," *Journal of Neuroscience Research*, vol. 56, no. 2, pp. 206–212, 1999.

[239] H. Mizusawa, T. Ishii, and S. Bannai, "Peroxiredoxin I (macrophage 23 kDa stress protein) is highly and widely expressed in the rat nervous system," *Neuroscience Letters*, vol. 283, no. 1, pp. 57–60, 2000.

[240] S. Kato, M. Kato, Y. Abe et al., "Redox system expression in the motor neurons in amyotrophic lateral sclerosis (ALS): immunohistochemical studies on sporadic ALS, superoxide dismutase 1 (SOD1)-mutated familial ALS, and SOD1-mutated ALS animal models," *Acta Neuropatholica*, vol. 110, no. 2, pp. 101–112, 2005.

[241] R. C. Cumming, R. Dargusch, W. H. Fischer, and D. Schubert, "Increase in expression levels and resistance to sulfhydryl oxidation of peroxiredoxin isoforms in amyloid beta-resistant nerve cells," *The Journal of Biological Chemistry*, vol. 282, no. 42, pp. 30523–30534, 2007.

[242] K. Krapfenbauer, E. Engidawork, N. Cairns, M. Fountoulakis, and G. Lubec, "Aberrant expression of peroxiredoxin subtypes in neurodegenerative disorders," *Brain Research*, vol. 967, no. 1-2, pp. 152–160, 2003.

[243] Y. Yoshida, A. Yoshikawa, T. Kinumi et al., "Hydroxyoctadecadienoic acid and oxidatively modified peroxiredoxins in the blood of Alzheimer's disease patients and their potential as biomarkers," *Neurobiology of Aging*, vol. 30, no. 2, pp. 174–185, 2009.

[244] J. Fang, T. Nakamura, D.-H. Cho, Z. Gu, and S. A. Lipton, "S-nitrosylation of peroxiredoxin 2 promotes oxidative stress-induced neuronal cell death in Parkinson's disease," *Proceedings of the National Academy of Sciences of the United States of America*, vol. 104, no. 47, pp. 18742–18747, 2007.

[245] D. Qu, J. Rashidian, M. P. Mount et al., "Role of Cdk5-mediated phosphorylation of Prx2 in MPTP toxicity and Parkinson's disease," *Neuron*, vol. 55, no. 1, pp. 37–52, 2007.

[246] M. Basso, S. Giraudo, D. Corpillo, B. Bergamasco, L. Lopiano, and M. Fasano, "Proteome analysis of human substantia nigra in Parkinson's disease," *Proteomics*, vol. 4, no. 12, pp. 3943–3952, 2004.

[247] D. Butterfield, R. Sultana, and H. Poon, "Redox proteomics: a new approach to investigate oxidative stress in Alzheimer's disease," in *Neurodegenerative Disorders, Aging and Antioxidants*, Marcel Dekker Inc, New York, NY, USA, 2006.

[248] S. H. Kim, M. Fountoulakis, N. Cairns, and G. Lubec, "Protein levels of human peroxiredoxin subtypes in brains of patients with Alzheimer's disease and Down syndrome,"

Journal of Neural Transmission Supplementum, no. 61, pp. 223–235, 2001.

[249] N. Fatma, E. Kubo, C. B. Toris, W. D. Stamer, C. B. Camras, and D. P. Singh, "PRDX6 attenuates oxidative stress- and TGFbeta-induced abnormalities of human trabecular meshwork cells," *Free Radical Research*, vol. 43, no. 9, pp. 783–795, 2009.

[250] N. Hasanova, E. Kubo, Y. Kumamoto, Y. Takamura, and Y. Akagi, "Age-related cataracts and Prdx6: correlation between severity of lens opacity, age and the level of Prdx 6 expression," *The British Journal of Ophthalmology*, vol. 93, no. 8, pp. 1081–1084, 2009.

[251] B.-B. Gao, X. Chen, N. Timothy, L. P. Aiello, and E. P. Feener, "Characterization of the vitreous proteome in diabetes without diabetic retinopathy and diabetes with proliferative diabetic retinopathy," *Journal of Proteome Research*, vol. 7, no. 6, pp. 2516–2525, 2008.

[252] A. Abbasi, E. Corpeleijn, R. T. Gansevoort et al., "Circulating peroxiredoxin 4 and type 2 diabetes risk: the prevention of renal and vascular endstage disease (PREVEND) study," *Diabetologia*, vol. 57, no. 9, pp. 1842–1849, 2014.

[253] S. F. Moss and M. J. Blaser, "Mechanisms of disease: inflammation and the origins of cancer," *Nature Clinical Practice Oncology*, vol. 2, no. 2, pp. 90–97, 2005, quiz 1 p following 113.

[254] Y. S. Kim, H. L. Lee, K. B. Lee et al., "Nuclear factor E2-related factor 2 dependent overexpression of sulfiredoxin and peroxiredoxin III in human lung cancer," *The Korean Journal of Internal Medicine*, vol. 26, no. 3, pp. 304–313, 2011.

[255] J. W. Chang, S. H. Lee, J. Y. Jeong et al., "Peroxiredoxin-I is an autoimmunogenic tumor antigen in non-small cell lung cancer," *FEBS Letters*, vol. 579, no. 13, pp. 2873–2877, 2005.

[256] Y. W. Xu, Y. H. Peng, B. Chen et al., "Autoantibodies as potential biomarkers for the early detection of esophageal squamous cell carcinoma," *The American Journal of Gastroenterology*, vol. 109, no. 1, pp. 36–45, 2014.

[257] S. Kylarova, D. Kosek, O. Petrvalska et al., "Cysteine residues mediate high-affinity binding of thioredoxin to ASK1," *The FEBS Journal*, vol. 283, no. 20, pp. 3821–3838, 2016.

[258] T. M. Jeitner, M. Kalogiannis, B. F. Krasnikov, I. Gomlin, M. R. Peltier, and G. R. Moran, "Linking inflammation and Parkinson disease: hypochlorous acid generates parkinsonian poisons," *Toxicological Sciences*, vol. 151, no. 2, pp. 388–402, 2016.

[259] V. Nambi, "The use of myeloperoxidase as a risk marker for atherosclerosis," *Current Atherosclerosis Reports*, vol. 7, no. 2, pp. 127–131, 2005.

[260] J. L. Wilkinson-Berka, I. Rana, R. Armani, and A. Agrotis, "Reactive oxygen species, Nox and angiotensin II in angiogenesis: implications for retinopathy," *Clinical Science*, vol. 124, no. 10, pp. 597–615, 2013.

Hindawi
Oxidative Medicine and Cellular Longevity
Volume 2017, Article ID 7395238, 14 pages
https://doi.org/10.1155/2017/7395238

Research Article

The Synthetic Lignan Secoisolariciresinol Diglucoside Prevents Asbestos-Induced NLRP3 Inflammasome Activation in Murine Macrophages

Ralph A. Pietrofesa,[1] Patrick Woodruff,[1] Wei-Ting Hwang,[2] Priyal Patel,[3] Shampa Chatterjee,[3] Steven M. Albelda,[1] and Melpo Christofidou-Solomidou[1]

[1]*Division of Pulmonary, Allergy, and Critical Care Medicine and the Department of Medicine, University of Pennsylvania Perelman School of Medicine, Philadelphia, PA 19104, USA*
[2]*Department of Biostatistics and Epidemiology, University of Pennsylvania Perelman School of Medicine, Philadelphia, PA 19104, USA*
[3]*Institute for Environmental Medicine, Department of Physiology, University of Pennsylvania Perelman School of Medicine, Philadelphia, PA 19104, USA*

Correspondence should be addressed to Melpo Christofidou-Solomidou; melpo@mail.med.upenn.edu

Received 30 March 2017; Accepted 12 July 2017; Published 13 September 2017

Academic Editor: Eva-Maria Hanschmann

Background. The interaction of asbestos with macrophages drives two key processes that are linked to malignancy: (1) the generation of reactive oxygen species (ROS)/reactive nitrogen species (RNS) and (2) the activation of an inflammation cascade that drives acute and chronic inflammation, with the NLRP3 inflammasome playing a key role. Synthetic secoisolariciresinol diglucoside (SDG), LGM2605, is a nontoxic lignan with anti-inflammatory and antioxidant properties and was evaluated for protection from asbestos in murine peritoneal macrophages (MF). *Methods*. MFs were exposed to crocidolite asbestos ± LGM2605 given 4 hours prior to exposure and evaluated at various times for NLRP3 expression, secretion of inflammasome-activated cytokines (IL-1β and IL-18), proinflammatory cytokines (IL-6, TNFα, and HMGB1), NF-κB activation, and levels of total nitrates/nitrites. *Results*. Asbestos induces a significant ($p < 0.0001$) increase in the NLRP3 subunit, release of proinflammatory cytokines, NLRP3-activated cytokines, NF-κB, and levels of nitrates/nitrites. LGM2605 significantly reduced NLRP3 ranging from 40 to 81%, IL-1β by 89–96%, and TNFα by 67–78%, as well as activated NF-κB by 48-49% while decreasing levels of nitrates/nitrites by 85–93%. *Conclusions*. LGM2605 reduced asbestos-induced NLRP3 expression, proinflammatory cytokine release, NF-κB activation, and nitrosative stress in MFs supporting its possible use in preventing the asbestos-induced inflammatory cascade leading to malignancy.

1. Introduction

Recent studies have indicated that the pathogenesis of asbestos-induced cancers involves chronic inflammation which is facilitated by the cytokines interleukin-1 beta (IL-1β), the chemokine tumor necrosis factor alpha (TNFα), and high mobility group box-1 (HMGB1) and eventual oxidative tissue damage caused by persistent asbestos fibers [1, 2]. Inhaled asbestos fibers permeate into the lung and ultimately to the pleural surface, where they are taken up by tissue phagocytes, primarily macrophages [3, 4]. Macrophages exposed to asbestos then undergo frustrated phagocytosis of elongated fibers [5]. Frustrated phagocytosis of asbestos fibers by macrophages and mesothelial cells generates intracellular reactive oxygen species (ROS) and reactive nitrogen species (RNS) which, besides being deleterious due to direct oxidative damage, also activate proinflammatory transcription factors such as NF-κB, leading to the generation of numerous proinflammatory cytokines. Furthermore, oxidants and inflammatory moieties contribute to DNA

damage and ultimately lead to malignant transformation of mesothelial cells [6]. Asbestos-activated macrophages also contribute to tumorigenesis by overproduction of ROS/RNS that can in turn induce further DNA damage and lead to potential genomic instability [7]. Work by Yang and coworkers expanded the old hypothesis of ROS-induced tumorigenesis to attribute a key role for HMGB-1 in this process [8].

Inflammation plays a key role in the pathology of asbestos-induced lung cancers; indeed, asbestos-induced inflammation is considered to be a critical event in the development of malignant mesothelioma (MM) [9, 10]. This inflammation has largely been attributed to the activation of the NF-κB and subsequent induction of inflammatory genes. Lately, there is increasing evidence of a role for the activated NLRP3 inflammasome in sustaining and amplifying inflammation caused by asbestos [11–13].

The NLRP3 inflammasome is part of the innate immune system. The NLRP3 subunit is a receptor on immune and other cells and forms a macromolecular complex in response to external stimuli. This complex, which is comprised of the NLRP3 subunit and adaptor proteins, functions as a scaffold for inactive caspase-1 that is activated upon binding to the inflammasome. Active caspase-1 cleaves the proinflammatory IL-1 family of cytokines into their bioactive forms, IL-1β and IL-18. These active cytokines are primary drivers of cell death and inflammation. We have shown in our previous work [14] that LGM2605 inhibits asbestos-induced cell death in murine macrophages.

Thus, a well-tolerated and safe agent with anti-inflammatory properties that targets the NLRP3 inflammasome could potentially be used to prevent the onset of inflammation signals that lead to the development of malignant mesothelioma (MM) in asbestos-exposed populations. MM is on the rise across the US and Western Europe [15] with more than 7000 reported cases annually. This necessitates the identification of a protective agent which can block the pathology of MM.

Previous studies in various models of inflammation-induced lung disease, including ischemia/reperfusion [16] and radiation-induced fibrosis [17], suggested that the flaxseed lignan secoisolariciresinol diglucoside (SDG) has these requisite anti-inflammatory and antioxidant properties [18, 19]. We thus hypothesized that SDG or an SDG-rich flaxseed lignan component (FLC) formulation administered via the diet might be useful in the chemoprevention of asbestos-induced malignant mesothelioma and have begun a series of studies to test the validity of this idea. Earlier, we carried out an *in vivo* study in which we evaluated the usefulness of an FLC-supplemented diet in a murine model of acute asbestos-induced peritoneal inflammation. Three days after intraperitoneal instillation of asbestos into mice, we observed both inflammation and oxidative/nitrosative stress in the peritoneal fluid. The FLC diet led to marked reductions in total white blood cell influx and proinflammatory IL-1β, IL-6, TNFα, and HMGB1 cytokine release [20].

These findings indicated a protective role for SDG-rich formulations in asbestos-induced inflammation; however, the mechanisms or cell types that conferred this protection were not clear. The contribution of the main flaxseed lignan, that is, the purified compound SDG, was also not known. The effect of SDG in combating asbestos-induced inflammation signaling needs to be studied to facilitate the use of SDG as a preventive or protective agent against asbestos-induced lung damage. SDG was chemically synthesized (LGM2605) by a proprietary pathway [18], to enable evaluation through animal testing in anticipation of eventual clinical usefulness. Synthetic secoisolariciresinol diglucoside (SDG), LGM2605, is a nontoxic lignan with anti-inflammatory and antioxidant properties and was evaluated for protection from asbestos in murine peritoneal macrophages (MF). LGM2605 was found to be similar to natural SDG (extracted from whole grain flaxseed), acting as a free radical scavenger and an antioxidant, with DNA-protective activity [19]. Importantly, our recent study also found that LGM2605 possessed potent cell protective properties [21] and, when tested on asbestos-activated elicited murine macrophages, it induced cell protective defenses, such as cellular Nrf2 activation and the expression of phase II antioxidant enzymes, HO-1 and Nqo1, and reduced asbestos-induced ROS generation and markers of oxidative stress [14]. Thus, we carried out the present study to determine whether inhibition of inflammasome activation was implicated in the mechanism of LGM2605 protection from asbestos exposure of macrophages. Our objectives were (1) to characterize the inflammatory pathway triggered in murine peritoneal macrophages following asbestos exposure, (2) to evaluate the effect of LGM2605 in modulating this inflammation, and (3) to evaluate the chemopreventive properties of LGM2605 by determining whether it acts via inhibition of asbestos-induced inflammasome activation.

2. Materials and Methods

2.1. Harvesting of Murine Peritoneal Macrophages. Murine peritoneal macrophages (MF) were harvested from the peritoneum following elicitation using thioglycollate broth according to the method described by Zhang et al., [22] whereby a uniform MF population is obtained. Mice were used at 13 weeks of age under animal protocols approved by the Institutional Animal Care and Use Committee (IACUC) of the University of Pennsylvania (Philadelphia, PA). Animals were housed in conventional cages under standardized conditions with controlled temperature and humidity, and a 12-12-hour day-night light cycle. Animals had free access to water and mouse chow. Mice were injected, via intraperitoneal (IP) injection, with 1 ml of a 3% solution of thioglycollate broth in 0.5 ml phosphate-buffered saline (PBS). Three days following thioglycollate exposure, mice were euthanized using an overdose of ketamine (160 mg/kg) and xylazine (25 mg/kg). Peritoneal lavage (PL) was then performed through a 20-gauge angiocatheter (BD Pharmingen, San Diego, CA, USA), with the intraperitoneal instillation of 3 ml Hank's balanced salt solution (HBSS, Ca^{2+}, Mg^{2+} free). An aliquot of peritoneal lavage fluid (PLF) was immediately separated to measure total cell counts (cells/ml PLF) using a Coulter Cell and Particle Counter (Beckman Coulter, Miami, FL, USA). Murine peritoneal macrophages were pooled and plated in 1 ml of cell culture medium (phenol-free RPMI supplemented with 1% FBS and supplemented

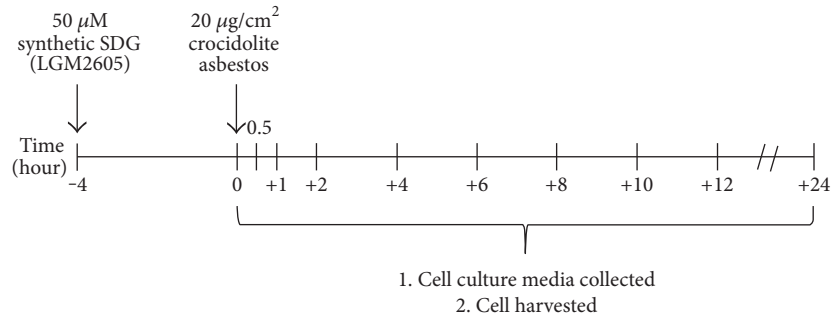

Figure 1: The LGM2605 pretreatment regimen used in this study. Macrophages subjected to asbestos exposure with or without LGM2605. Elicited murine peritoneal macrophages were exposed to 50 μM LGM2605 4 hours prior to exposure to crocidolite asbestos fibers (20 μg/cm^2). Culture medium and cells were harvested at 0, 0.5, 1, 2, 4, 6, 8, 10, 12, and 24 hours post asbestos exposure.

with penicillin (100 units/ml) and streptomycin (100 μg/ml) and L-glutamine (2 mm)) in a 6-well plate (2×10^6 cells/well) and allowed to adhere to the bottom of the wells. Overall, 10–20 million cells are obtained from each mouse. Elicited peritoneal macrophages were used to determine the effects of LGM2605 in preventing asbestos-induced inflammasome activation, cytokine secretion, antioxidant response, and asbestos-induced cytotoxicity.

2.2. Crocidolite Asbestos Exposure. Elicited peritoneal macrophages were exposed to sterile UICC crocidolite (SPI Supplies, West Chester, PA, USA) asbestos fibers that were baked overnight, resuspended in 1X PBS at a stock concentration of 800 μg/ml, and sonicated for 30 minutes. The solution of asbestos fibers was exposed to ultraviolet light prior to use in cell culture experiments. For all experiments, murine peritoneal macrophages were exposed to crocidolite asbestos fibers at a concentration of 20 μg/cm^2 based on our previous studies [14].

2.3. LGM2605 Exposure. Chemical synthesis of secoisolariciresinol diglucoside has been previously described [18]. Briefly, LGM2605 was synthesized from vanillin via secoisolariciresinol and a glucosyl donor (perbenzoyl-protected trichloroacetimidate under the influence of TMSOTf) through a concise route that involved chromatographic separation of diastereomeric diglucoside derivatives. LGM2605 was reconstituted to a stock concentration of 10 mM, and cells were exposed to 50 μM LGM2605 4 hours prior to asbestos exposure (see Figure 1). The 50 μM dose of LGM2605 exposure was selected based on an earlier study in which this dose was sufficient to diminish asbestos-induced ROS generation by macrophages to levels that were comparable to naïve macrophages [14].

2.4. Microscopic Visualization of the NLRP3 Subunit of the Inflammasome in Murine Macrophages by Fluorescence Imaging. Elicited murine peritoneal macrophages exposed to crocidolite asbestos fibers at a concentration of 20 μg/cm^2 were assessed for induction of the NLRP3 inflammasome 24 hours following asbestos exposure. This was done by fixing the cells (1 : 1 methanol-acetone fixation) and immunostaining for the NLRP3 subunit by using polyclonal anti-NLRP3 primary antibody (catalogue number 15101S, Cell Signaling Technology, Danvers, MA, USA) and the goat anti-rabbit-Alexa 488 secondary antibody (Abcam, Cambridge, MA, USA) followed by imaging on a Zeiss LSM510 scanning laser microscope. All images were acquired at the same exposure and offset settings using LSM Metamorph Imaging® software (Molecular Devices, Sunnyvale, CA, USA). The fluorescent images of cells were processed and quantitated for NLRP3 expression by the use of ImageJ software (NIH). The intensity of cells in each field was integrated to obtain the total fluorescence intensity of a particular field. Three to four fields were imaged for each condition (control, LGM2605 only, asbestos treated, asbestos, and LGM2605) for $n = 3$ independent experiments.

2.5. Determination of Asbestos-Induced Proinflammatory Cytokine Release from Murine Peritoneal Macrophages. Levels of proinflammatory cytokines, IL-1β, IL-6, IL-18, tumor necrosis factor alpha (TNFα), and high mobility group box 1 (HMGB1), were determined in cell culture medium at multiple time points post asbestos exposure (0, 0.5, 1, 2, 4, 6, 8, 12, and 24 hours post asbestos) using enzyme-linked immunosorbent assays (ELISA). Samples were run undiluted in triplicate, and assays were performed according to manufacturer's instructions. Levels of IL-1β, IL-6, IL-18, and TNFα are reported as picograms per milliliter (pg/ml) of culture medium, and levels of HMGB1 released into the culture medium are reported as nanograms per milliliter (ng/ml). ELISA kits (TNFα and IL-1β) were purchased from BD biosciences (San Jose, CA, USA), MBL International (Woburn, MA, USA) (mouse IL-18 ELISA Kit), R&D systems (Minneapolis, MN, USA) (mouse IL-6 Quantikine ELISA Kit), and Chondrex Inc. (Redmond, WA, USA) (HMGB1 Detection Kit).

2.6. Analysis of Nitrate/Nitrite Levels in Cell Culture Medium. Levels of nitrates and nitrites, metabolites of nitric oxide, in the culture medium were determined using a nitrate/nitrite colorimetric assay kit (Cayman Chemical, Ann Arbor, MI, USA) according to the manufacturer's protocol. The assay kit quantifies levels of total nitrates/nitrites (stable breakdown products of nitric oxide) by first converting nitrates to nitrites using nitrate reductase and then measuring total nitrites by adding Greiss Reagent to the reaction mixture, which produces a purple azo compound in the presence of

nitrites that can be measured spectrophotometrically. The absorbance of the azo chromophore was measured at 540 nm measured using a SpectraMax i3x Multi-Mode microplate reader (Molecular Devices, Sunnyvale, CA, USA). Cell culture medium samples were run undiluted, and the data are reported as the concentration (μM) of total nitrate/nitrites in the cell culture medium.

2.7. NF-κB Transcription Factor Analysis. The presence of nuclear factor kappa-light-chain-enhancer of activated B cells (NF-κB) p65 subunit was determined in nuclear extracts isolated from macrophages exposed to asbestos and harvested at 1, 2, 4, 6, 8, and 12 hours post asbestos exposure. Cytoplasmic and nuclear extracts were prepared using a commercially available nuclear extraction kit (Cayman Chemical, Ann Arbor, MI, USA). Transcription factor assay kits (Cayman Chemical, Ann Arbor, MI, USA) were used to detect nuclear NF-κB. The transcription factor assay kits utilize a specific double-stranded DNA sequence containing the NF-κB response element. The data are reported as the ratio of the absorbance at 450 nm (OD_{450}) to the protein extract concentration (μg).

2.8. RNA Isolation and Gene Expression Analysis. Total RNA was isolated from murine peritoneal macrophages using a commercially available kit, RNeasy Plus Mini Kit, supplied by Qiagen (Valencia, CA, USA). Total RNA was quantified using a NanoDrop 2000 apparatus (ThermoFisher Scientific, Waltham, MA, USA). Reverse transcription of RNA to cDNA was then performed on a Veriti® Thermal Cycler using the high capacity RNA to cDNA kit supplied by Applied Biosystems. Quantitative polymerase chain reaction was performed using TaqMan® Probe-Based Gene Expression Assays supplied by Applied Biosystems, Life Technologies (Carlsbad, CA, USA). Individual TaqMan gene expression assays were selected for proinflammatory cytokines (IL-1β, IL-6, IL-18, TNFα, and HMGB1), for inducible nitric oxide synthase (iNOS) and for NF-κB. Quantitative real-time PCR was performed using 50 ng of cDNA per reaction well on a StepOnePlus™ Real-Time PCR System (Applied Biosystems, Life Technologies, Carlsbad, CA, USA). Gene expression data were normalized to β-actin RNA housekeeping gene and calibrated to the control samples (CTL at time 0) according to the ΔΔCT method as previously described [14].

2.9. Western Blot Analysis. Immunoblot analysis of murine peritoneal macrophages at 0, 8, and 24 hours post asbestos exposure was performed as previously described [21] using primary antibodies against NLRP3 (catalogue number 15101S, Cell Signaling Technology, Danvers, MA, USA) and iNOS (catalogue number 13120, Cell Signaling Technology, Danvers, MA, USA). Membranes were developed using Western Lighting Chemiluminescence Reagent Plus (PerkinElmer Life Sciences, Boston, MA, USA) and quantified by densitometric analysis of 110 kDa band for NLRP3 and 130 kDa band for iNOS. Densitometric analysis of western blots with β-actin normalization of protein expression was performed using Gel-Pro Analyzer software (version 6.0, MediaCybernetics, Silver Spring, MD, USA).

2.10. Statistical Analysis. All data were analyzed using two-way analysis of variance (ANOVA) to test for the main effects of time and treatment on study outcome measures. Posttests (Tukey's multiple comparison tests) were conducted analyzing significant differences among treatment groups (CTL, LGM2605, ASB, and ASB + LGM2605) within each respective time point. Statistically significant differences were determined using GraphPad Prism version 6.00 for Windows, GraphPad Software, La Jolla, California, USA. Results are reported as mean ± the standard error of the mean (SEM) from three separate experiments. Levels of target gene mRNA are reported as the mean fold change ± SEM from CTL macrophages at time 0 (not exposed to asbestos and not treated with LGM2605). Statistically significant differences were determined at p value < 0.05.

3. Results

To determine the usefulness of LGM2605 in preventing asbestos-induced inflammation and oxidative cell damage, we utilized elicited murine peritoneal macrophages (MFs) as a model of tissue phagocyte response to the presence of asbestos in the pleural space using a regimen as outlined in Figure 1.

3.1. LGM2605 Blunts the Asbestos-Induced Expression of the Inflammasome. The NLRP3 subunit of the inflammasome was observed to be expressed at low levels in naïve cells (green fluorescence). Upon asbestos treatment, NLRP3 expression increased significantly ($p < 0.05$) as observed from the increased green fluorescence intensity in cells (Figures 2(a) and 2(b)). Green fluorescence was reflective of the expression of the NLRP3 subunit, while propidium iodide was used to delineate the nuclei of the cells. The fluorescence signal was along the cell membrane and also within intracellular structures. Pretreatment with LGM2605 reduced NLRP3 expression (by 40–81%) to levels comparable to untreated cells.

Induction of the inflammasome by asbestos and inhibition by LGM2605 were also confirmed by Western blotting (Figures 2(c) and 2(d)). Specifically, levels of NLRP3 increased on average 1.63 ± 0.06-fold over control at 24 hours post asbestos exposure. LGM2605 treatment significantly ($p < 0.01$) reduced asbestos-induced NLRP3 expression (1.11 ± 0.09-fold over control). Data are presented as mean ± SEM.

3.2. LGM2605 Blunts the Asbestos-Induced Release and Expression of Inflammasome-Activated Cytokines. Asbestos exposure has been reported to activate the NLRP3 inflammasome and lead to the production and release of proinflammatory cytokines, IL-1β and IL-18 [11, 12]. Levels of IL-1β and IL-18 thus were determined up to 24 hours post asbestos exposure, along with their respective gene expression levels (Figure 3). Minimal IL-1β or IL-18 was released by control (nonasbestos treated) cells or by cells treated with LMG2605 alone. Levels of IL-1β rapidly increased within the first 6 hours post asbestos exposure (from 4.04 ± 0.13 pg/ml at baseline

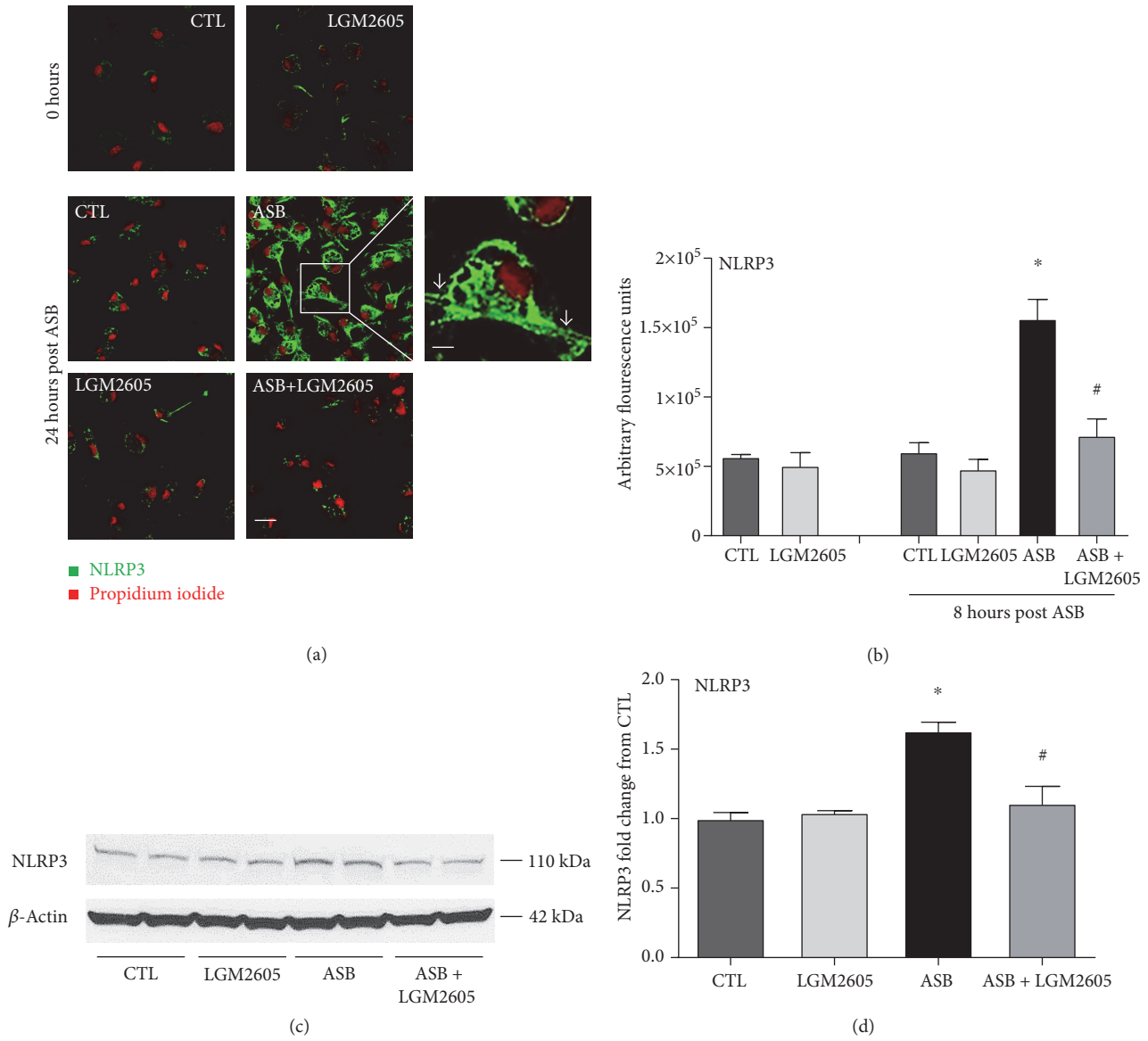

Figure 2: LGM2605 blocks the induction of the NLRP3 subunit of the inflammasome. Murine peritoneal macrophages exposed to LGM2605 4 hours prior to exposure to asbestos fibers were assessed for NLRP3 inflammasome by monitoring the induction of the NLRP3 subunit (green fluorescence) by laser scanning fluorescence microscopy at 24 hours as compared to 0 hours (a). A nuclear stain in the form of propidium iodide (PI) was used to delineate the cells. Magnification 200x; scale is 10 μm. Enlarged inset is at magnification 600x; scale is 30 μm. Grey arrows indicate asbestos fiber engulfed by the macrophage. Quantification of NLRP3 immunostaining (b). Date are presented as arbitrary fluorescence units and as mean ± SEM. Protein levels of the NLRP3 subunit of the inflammasome were evaluated by Western blotting for NLRP3 (c and d). (c) depicts a representative Western blot from three separate experiments at 24 hours. (d) displays mean ± SEM fold change of NLRP3 from CTL. *Statistically significant difference ($p < 0.05$) between ASB- and CTL-treated cells. #Statistically significant difference ($p < 0.05$) between ASB- and ASB + LGM2605-treated cells.

to 586.13 ± 4.61 pg/ml) and then plateaued through 24 hours (Figure 3(a)). Levels of IL-18 increased linearly over time up to 24 hours post asbestos (from 1.65 ± 0.10 pg/ml at baseline to 424.62 ± 8.80 pg/ml) (Figure 3(c)). Pretreatment with LGM2605 significantly ($p < 0.0001$) reduced levels of IL-1β (Figure 3(a)) and IL-18 (Figure 3(c)) by 89–96% and 84–95%, respectively. We also determined mRNA levels of IL-1β and IL-18 from treated macrophages at 8 and 24 hours post asbestos exposure. Although gene expression levels of both IL-1β and Il-18 were elevated (mean fold change ranging from 1.58- to 2.26-fold increase from CTL at time 0), treatment with LGM2605 significantly ($p < 0.05$) reduced levels of both IL-1β and Il-18 (by ~89–96%), similar to baseline values (Figures 3(b) and 3(d)). Data are presented as mean ± SEM as well as activated NF-κB by 48-49% while decreasing levels of nitrates/nitrites by 85–93%.

3.3. Asbestos-Induced Proinflammatory Cytokine Release and Expression Is Ameliorated by LGM2605. The inflammatory response post asbestos exposure was further characterized

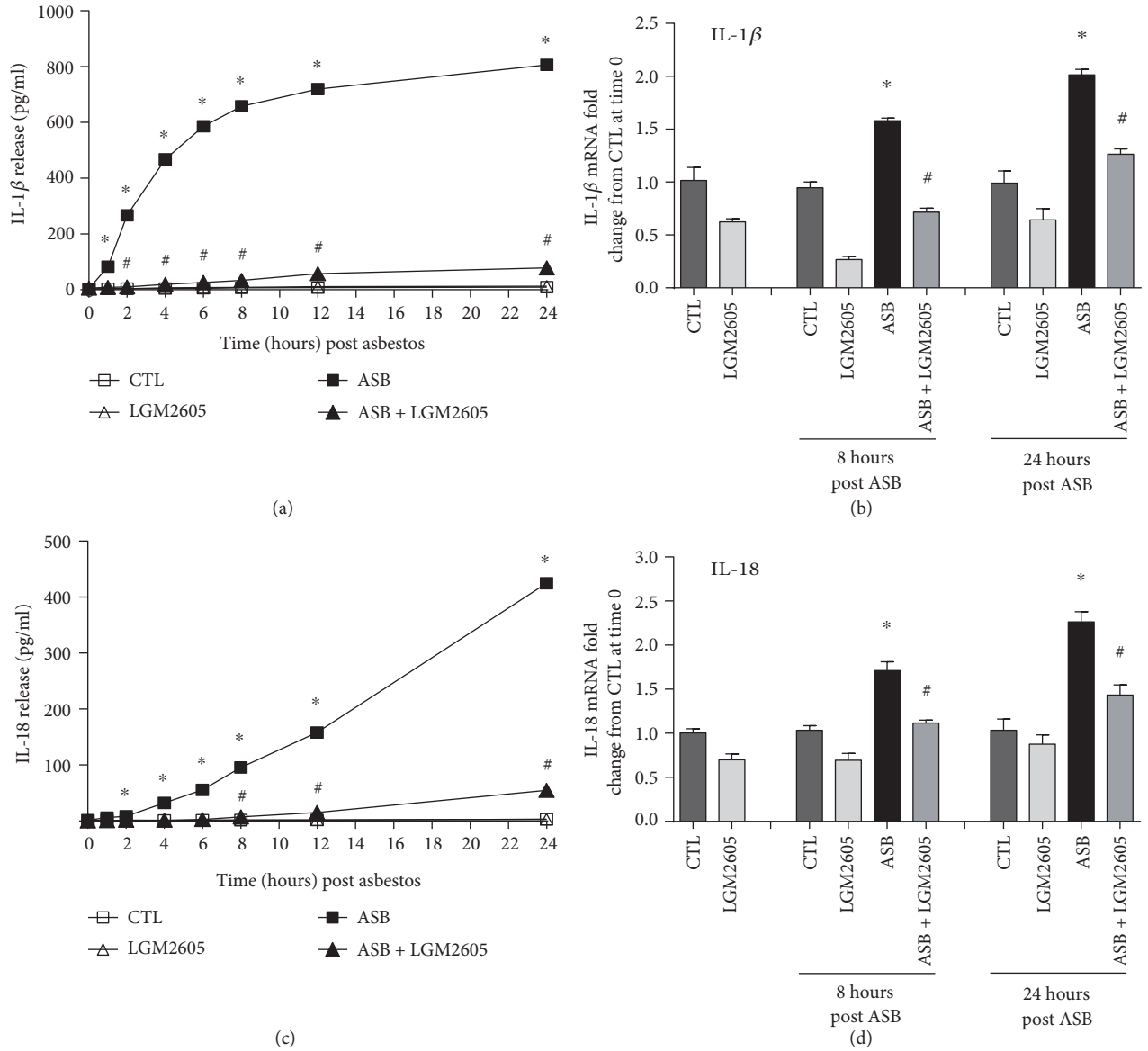

Figure 3: Inflammasome activation following asbestos exposure leads to IL-1β and IL-18 secretion via activated caspase-1. Release of IL-1β (a) and IL-18 (c) was determined at 0, 1, 2, 4, 6, 8, 12, and 24 hours post asbestos exposure. Samples were run undiluted in triplicate, and cytokine concentrations (pg/ml) are presented as mean ± SEM. Macrophage mRNA expression of IL-1β (b) and IL-18 (d) was determined at 0, 8, and 24 hours post asbestos exposure using qPCR. Levels of target gene mRNA were normalized to 18S ribosomal RNA, and values are expressed as mean fold change from CTL at time 0. Data are presented as mean ± SEM. *Statistically significant difference ($p < 0.05$) between ASB- and CTL-treated cells. #Statistically significant difference ($p < 0.05$) between ASB- and ASB + LGM2605-treated cells.

by determining the protein and mRNA levels of the proinflammatory cytokines IL-6, TNFα, and HMGB1 (Figure 4). Minimal amounts of IL-6, TNFα, and HMGB1 were released by control (nonasbestos treated) cells or by cells treated with LMG2605 alone. Protein levels of IL-6 (Figure 4(a)) and TNFα (Figure 4(c)) peaked at 24 hours post asbestos exposure (455.99 ± 3.03 and 695.34 ± 5.80 pg/ml, resp.) and were significantly ($p < 0.0001$) reduced by 62 and 66%, respectively, among macrophages treated with LGM2605 (172.98 ± 2.76 and 227.89 ± 3.30 pg/ml, resp.). Although the asbestos-induced increase in levels of IL-6 and TNFα followed similar kinetics, levels of HMGB1 peaked 30 minutes post asbestos exposure (39.85 ± 1.12 ng/ml) and gradually decreased over time (16.24 ± 0.25 ng/ml at 24 hours post asbestos) (Figure 4(e)). The initial increase in HMGB1 at 30 minutes post asbestos exposure was significantly ($p < 0.0001$) reduced by LGM2605 (ranging from 73 to 75%). Additionally, although levels of IL-6 (Figure 4(b)), TNFα (Figure 4(d)), and HMGB1 (Figure 4(f)) mRNA from asbestos-exposed macrophages were significantly ($p < 0.05$) elevated (1.92-, 5.81-, and 1.87-fold) from untreated macrophages at 24 hours post asbestos exposure, mRNA levels from LGM2605-treated macrophages (1.25-, 2.10-, and 1.00-fold from control, resp.) were significantly ($p < 0.05$) decreased from mRNA levels of asbestos-only-exposed macrophages. Data are presented as mean ± SEM.

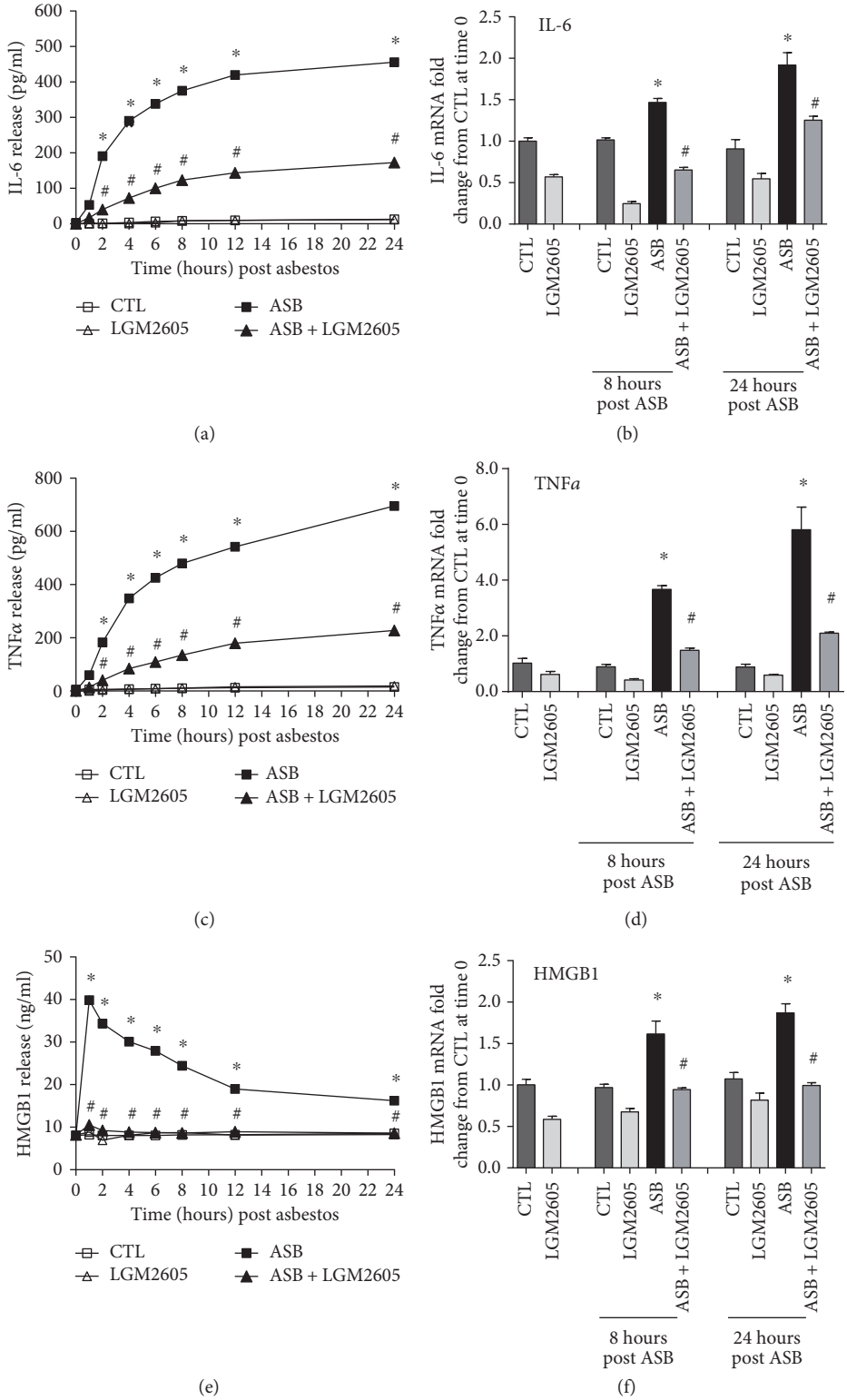

Figure 4: Asbestos-induced proinflammatory cytokine secretion is blunted by LGM2605. Release of IL-6 (a), TNFα (c), and HMGB1 (e) was determined at 0, 1, 2, 4, 6, 8, 12, and 24 hours post asbestos exposure. Samples were run undiluted in triplicate, and cytokine concentrations (pg/ml for IL-6 and TNFα and ng/ml for HMGB1) are presented as mean ± SEM. Macrophage mRNA expression of IL-6 (b), TNFα (d), and HMGB1 (f) was determined at 0, 8, and 24 hours post asbestos exposure using qPCR. Levels of target gene mRNA were normalized to β-actin RNA, and values are expressed as mean fold change from CTL at time 0. Data are presented as mean ± SEM. *Statistically significant difference ($p < 0.05$) between ASB- and CTL-treated cells. #Statistically significant difference ($p < 0.05$) between ASB- and ASB + LGM2605-treated cells.

3.4. LGM2605 Prevents Asbestos-Induced Oxidative/Nitrosative Stress and Activation of NF-κB. We evaluated levels of total nitrates and nitrites in the cell culture medium as a marker of nitrosative stress following asbestos exposure (Figure 5(a)). Minimal nitrates/nitrites were released by control (nonasbestos treated) cells or by cells treated with LMG2605 alone. Asbestos exposure led to a significant increase in the concentration of nitrates/nitrites ($465.99 \pm 4.20\,\mu$M at 24 hours post asbestos) that was significantly blunted (by 85–93%) by the administration of LGM2605 ($34.87 \pm 0.55\,\mu$M (Figure 5(a)).

We further investigated the observation of decreased nitrosative stress with LGM2605 treatment by determining protein and mRNA levels of inducible nitric oxide synthase in asbestos-exposed macrophages. After 8 and 24 hours of exposure to asbestos, mRNA levels of iNOS were significantly ($p < 0.05$) elevated above untreated macrophages (5.41 ± 0.38- and 8.78 ± 0.85-fold change, resp.) (Figure 5(b)). Alternatively, iNOS gene expression was significantly decreased among LGM2605-treated macrophages exposed to asbestos at both 8 and 24 hours post asbestos (1.84 ± 0.09- and 2.20 ± 0.32-fold change, resp.). Furthermore, although we were able to detect levels of iNOS in macrophages exposed to crocidolite asbestos fibers, iNOS was not detectable in asbestos-exposed macrophages treated with LGM2605 (Figure 5(c)).

The observed decreased expression of iNOS prompted us to further explore molecular targets upstream of iNOS that may be altered by LGM2605. We measured levels of active NF-κB in macrophage nuclear extracts and determined the kinetics of NF-κB nuclear accumulation following asbestos exposure. Following asbestos exposure, we saw significantly ($p < 0.0001$) increased levels of NF-κB present in nuclear extracts from asbestos-exposed macrophages, with the highest concentration occurring after 2 hours postexposure (Figure 5(d)). Gene expression levels of nuclear NF-κB were further induced by asbestos when measured after 8 and 24 hours of exposure (1.67 ± 0.20- and 6.64 ± 0.47-fold change, resp.) (Figure 5(e)). Importantly, treatment of macrophages with LGM2605 significantly ($p < 0.05$) reduced asbestos-induced activation and expression of NF-κB (by ~48%).

4. Discussion

Asbestos exposure is a well-established driver of malignant mesothelioma (MM) via an inflammation cascade. Chronic inflammation is believed to play a critical role in the onset and development of MM [6, 9]. In recent years, it has become clear that one of the key inflammatory moieties driving asbestos-induced damage and fibrosis is the induction of the inflammasome [10–13]. As there is no current cure for asbestos-related lung/pleural diseases, blocking the inflammasome may be a potential strategy to reduce the onset of inflammation [23].

Asbestos fibers have been shown to participate in redox reactions to generate several free radicals, including hydroxyl radicals, generated either through a redox reaction or by catalyzing a Fenton-like reaction in exposed cells [24]. These species, collectively called ROS, induce direct oxidative and nitrosative stress besides activating inflammation-signaling pathways. Asbestos fiber internalization generates a significant increase in intracellular ROS, and there is considerable evidence that asbestos-initiated chronic oxidative stress contributes to carcinogenesis and fibrosis by promoting oxidative DNA damage and regulating redox signaling pathways in exposed cells [25].

LGM2605 is a synthetic version of the lignan secoisolariciresinol diglucoside (SDG) which is derived from the natural plant flaxseed. After ingestion, SDG is converted to secoisolariciresinol, which is further metabolized to the entero lignans enterodiol and enterolactone. Our previous work on SDG (and SDG metabolites) shows that this compound can provide protection against oxidative lung injury via multiple mechanisms such as its ability to scavenge ROS and other active radicals and upregulate antioxidant genes via induction of Nrf2 (the transcription factor that regulates antioxidant defense), as well as by reducing the expression and activity of proinflammatory moieties [14, 19, 26].

Our earlier *in vivo* study showed that an SDG-rich formulation given in the diet reduced abdominal inflammation in asbestos-exposed mice. This work is a follow-up investigation to evaluate the mechanisms by which SDG (LGM2605) reduces inflammation *in vivo*. We used murine peritoneal macrophages as an *in vitro* model, as peritoneal macrophages are the major cell type that contributes to both local and systemic inflammatory responses upon contact with foreign agents/pathogens. In this capacity, these cells often drive various inflammatory pathologies. Furthermore, they are involved in the clearance of foreign particles and cellular debris, as well as pathogenic agents. The dose of LGM2605 used here was $50\,\mu$M based on an earlier study where this dose was sufficient to scavenge ROS in asbestos-treated macrophages [14]. Even lower doses ($<1\,\mu$M) were shown to be effective in ROS scavenging, such as ROS generated from radiation exposure of cells [17].

Our findings highlight the pluripotent properties of LGM2605 (see Figure 6) in an *in vitro* model of asbestos exposure. Specifically, redox signaling following asbestos exposure is thought to occur through 3 primary mechanisms: (1) ROS release from macrophages following frustrated phagocytosis of the asbestos fiber [27], (2) generation of reactive oxygen species (especially the DNA-damaging hydroxyl radical) due to the high iron content (~27–30%) of crocidolite asbestos [28, 29] that can be redox activated, and (3) mitochondrial-derived ROS release from macrophages following asbestos exposure. Furthermore, asbestos fibers have been shown to induce the generation of hydrogen peroxide, superoxide radical, and reactive nitrogen species that may lead to both extracellular cell signaling (ROS interaction with the TNF receptor) and intracellular cell signaling (NLRP3 inflammasome activation).

Thus, in the current study, we observed the ability of LGM2605 to blunt asbestos-induced inflammation and alter the inflammatory processes that contribute to cytokine production and secretion. Importantly, LGM2605 inhibited activation of NF-κB although the mechanism by which this occurs is not clear. We presume that reduced activation of NF-κB is via the scavenging of ROS (either directly or by

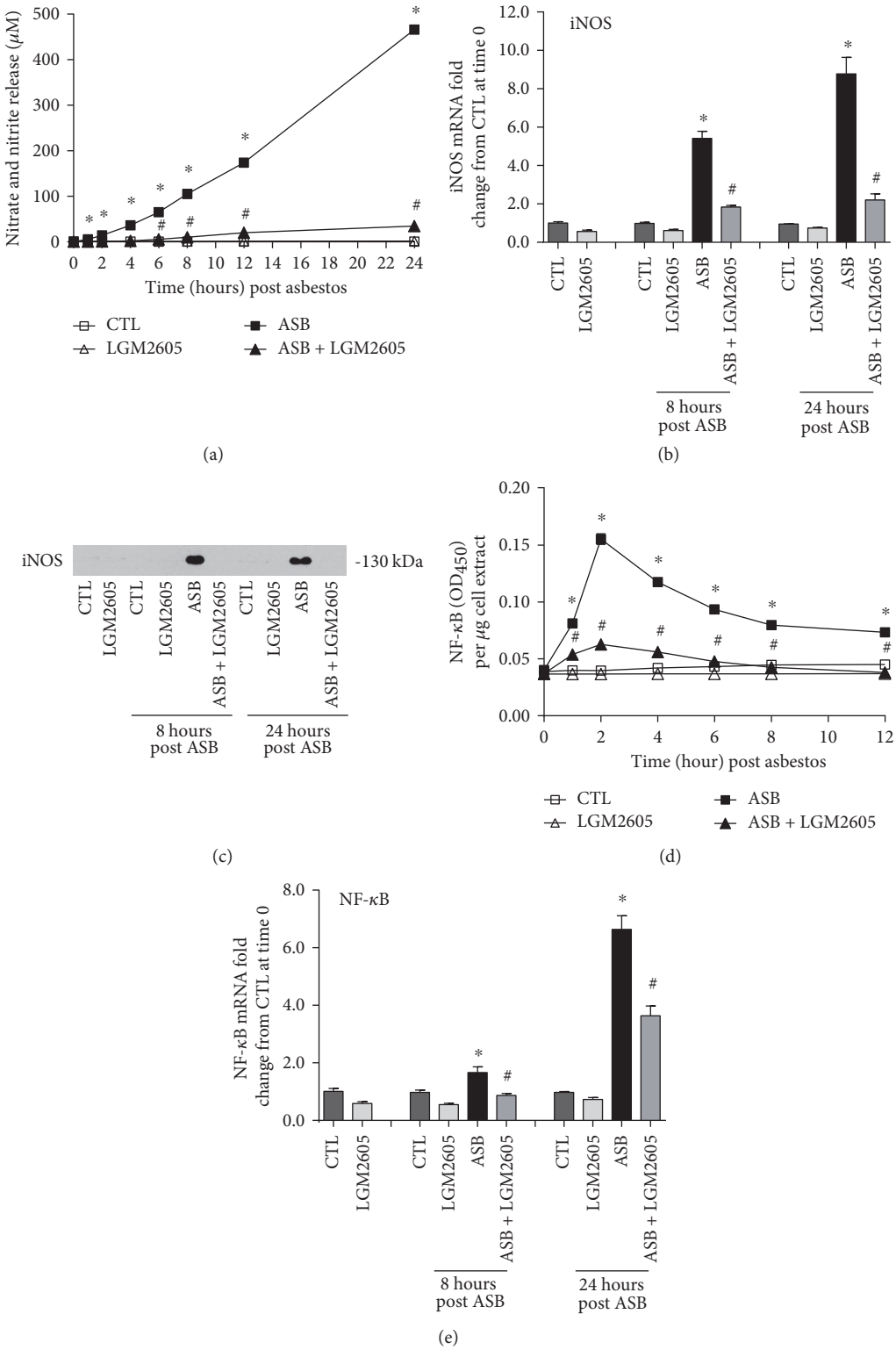

Figure 5: LGM2605 inhibits NF-κB expression and prevents asbestos-induced iNOS expression and nitric oxide production by murine peritoneal macrophages. The concentrations (μM) of nitrates and nitrites (a) were determined in cell culture medium at 0, 1, 2, 4, 6, 8, 12, and 24 hours post asbestos exposure. Macrophage mRNA expression iNOS (b) was determined at 0, 8, and 24 hours post asbestos exposure using qPCR and protein levels of iNOS were evaluated by Western blotting for iNOS (c) (molecular weight 130 kDa). Levels of active nuclear NF-κB (d) were determined at 0, 1, 2, 4, 6, 8, and 12 hours post asbestos exposure, while mRNA expression of NF-κB (e) was determined at 0, 8, and 24 hours post asbestos exposure using qPCR. Levels of target gene mRNA were normalized to β-actin RNA, and values are expressed as mean fold change from CTL at time 0. Data are presented as mean ± SEM. *Statistically significant difference ($p < 0.05$) between ASB- and CTL-treated cells. #Statistically significant difference ($p < 0.05$) between ASB- and ASB + LGM2605-treated cells.

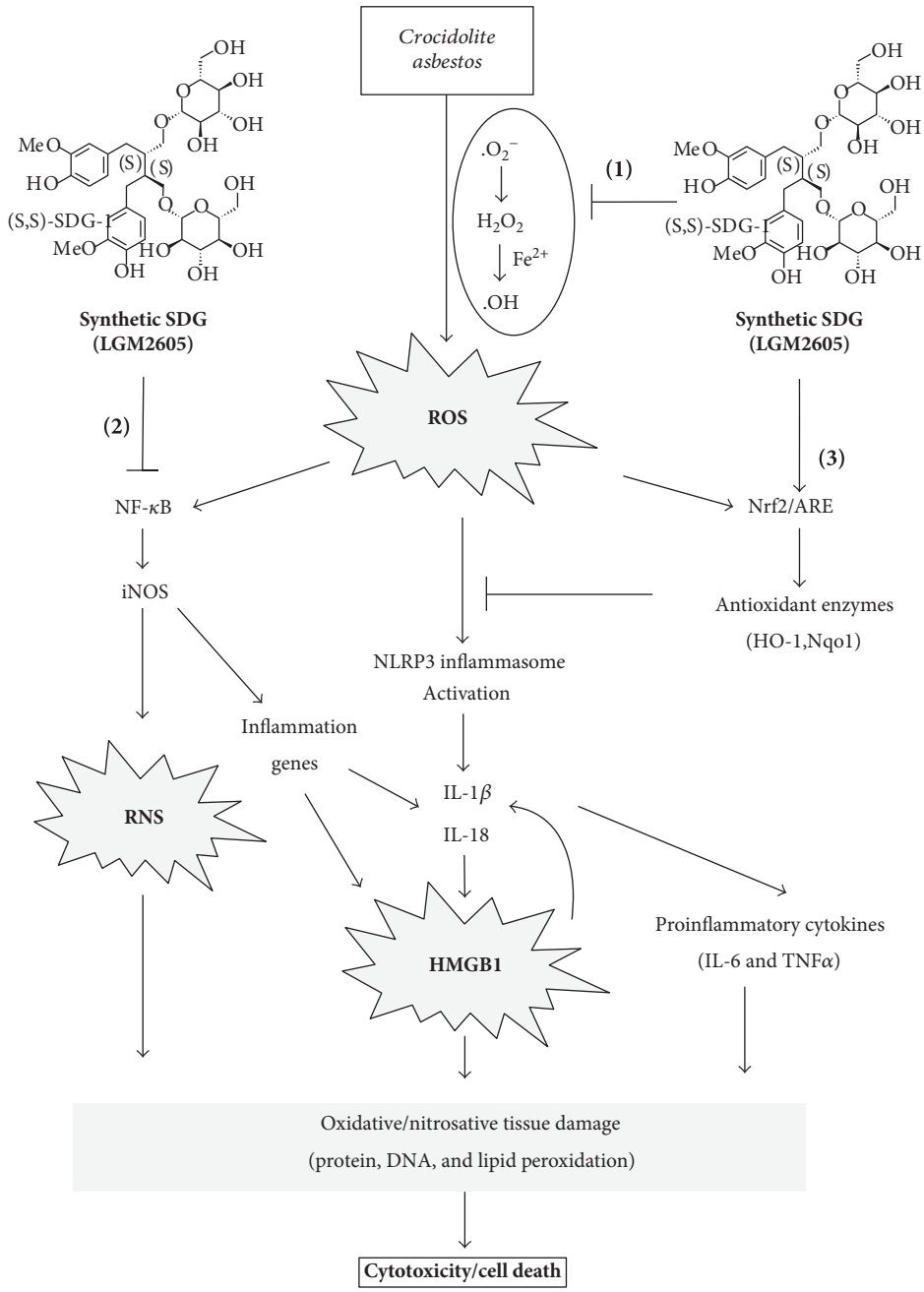

Figure 6: Role of the LGM2605 in preventing asbestos-induced inflammation, oxidative/nitrosative cell damage, cell injury, and cell death proposed mechanism of asbestos-induced inflammation and oxidative/nitrosative stress and the protective effect of LGM2605. Asbestos exposure leads to the production of ROS (such as H_2O_2, $^{\cdot}OH$) that activates an inflammatory cascade, of which the NLRP3 inflammasome is involved. NLRP3 activation leads to the release of cytokines IL-1β and IL-18. These cytokines drive inflammation-induced cell death. Under these conditions, the damage-associated molecular pattern protein HMGB1 is either released by dead cells or passively secreted from inflamed cells. HMGB1 release can also lead to a feed forward cycle of IL-1β and IL-18 induction and activation. Importantly, asbestos-induced inflammation is largely driven by HMGB1 and the NLRP3 inflammasome. Frustrated phagocytosis of asbestos fibers may lead to cell necrosis and the subsequent release of HMGB1, which promotes the activation of the NLRP3 inflammasome. Asbestos-induced ROS generation exacerbates this signaling cascade and further promotes malignant transformation. Combined, HMGB1 and NLRP3 inflammasome activation, induces a proinflammatory signaling cascade that ultimately leads to IL-1β and TNFα secretion and NF-κB activation. LGM2605 exhibits a pluripotent role in preventing ROS/RNS generation and inflammation following asbestos exposure through several mechanisms: (1) LGM2605 directly scavenges free radicals (ROS, such as H_2O_2, $^{\cdot}OH$) and mitigates asbestos-induced ROS/RNS generation, (2) LGM2605 inhibits the proinflammatory NF-κB pathway presumably via reduced levels of ROS (either due to direct scavenging or due to increased antioxidant enzyme expression) or via direct inhibition of the transcription factor. LGM2605 decreased the levels of NLRP3 inflammasome (protein), HMGB1 (protein and mRNA), and the levels of iNOS (protein and mRNA), and (3) LGM2605 activates Nrf2 and induces the expression of cellular antioxidant and detoxification enzymes.

increased cellular antioxidant status) or via inhibiting the transcription factor itself. Inhibition of NF-κB caused the lowering of key inflammasome-activated cytokines IL-1β and IL-18, suggesting further modulation of the NLRP3 inflammasome by LGM2605. LGM2605 reduced HMGB1 (protein and mRNA) levels indicating that HMGB1 induced the secretion of inflammatory cytokines. Asbestos-induced ROS generation may lead to NF-κB activation through ROS signaling via the TNF receptor. Asbestos induces a multitude of redox cell signaling pathways through direct interaction of the asbestos fiber with the cell membrane, extracellular ROS generation and interaction with cell receptors, and intracellular ROS generation. Ultimately, the cell signaling pathways influenced by asbestos fiber exposure are key pathways implicated in gene expression and cell fate. The inflammatory cascade initiated within the macrophage involves both asbestos-induced NALP3 inflammasome activation and ROS-induced TNFα and NF-κB signaling. Secretion of IL-1β and TNFα is directly implicated in asbestos-induced carcinogenesis. Pretreatment with LGM2605 not only decreases asbestos-induced ROS generation but also reduces levels of HMGB1 and TNFα, which are implicated in NF-κB activation.

Additionally, LGM2605 reduced levels of asbestos-induced oxidative and nitrosative stress by decreasing expression of iNOS and enhancing levels of key antioxidant enzymes involved in the detoxification of reactive oxygen species. We have previously reported on the ROS scavenging ability of LGM2605 in asbestos-exposed macrophages [14]. Specifically, LGM2605 significantly reduced asbestos-induced ROS and upregulated expression of Nrf2 phase II detoxification enzymes, ultimately reducing cellular injury and cell death indicated by LDH release.

Based on our earlier work, it is clear that several free radicals (H_2O_2, O_2, and ·OH), collectively called ROS, are scavenged by LGM2605 in cell-free systems. In asbestos-treated cells, we have previously reported a decrease in H_2O_2 production [14], but the effect on other radicals per se was not studied. The contribution of peroxynitrite versus ROS-induced damage with asbestos treatment is also not very clear. However, based on our studies, it emerges that LGM2605 is protective against asbestos-induced damage by blocking key elements of oxidative and nitrosative stress that have been reported elsewhere to participate in inflammation, cell death, and tissue damage.

Asbestos exposure leads to increases in the levels of ROS, such as superoxide anion ($O_2-\cdot$), hydroxyl radical (·OH), and hydrogen peroxide (H_2O_2) both inside the cell and in the extracellular matrix due to the surface reactivity of the crocidolite asbestos. The hydroxyl radical (·OH) scavenging ability of SDG has previously been reported by Prasad [30, 31]. Furthermore, Kitts and colleagues evaluated the hydroxyl and peroxyl radical scavenging activity of SDG [32] and reported on the effectiveness of SDG in reducing lipid peroxidation and deoxyribose oxidation. Hu et al. reported on the effectiveness of SDG against 1,1-diphenyl-2-picrylhydrazyl (DPPH·) and 2,2′-azo-bis (2-amidinopropane) dihydrochloride (AAPH) peroxyl radicals [33]. Furthermore, we have previously reported on the antioxidant properties of synthetic SDG (LGM2605) showing powerful scavenging activity against hydroxyl radicals, peroxyl radicals, and DPPH radicals [18].

Taken together, via a multiprong mechanism of action described in Figure 6, LGM2605 reduced asbestos-induced NLRP3 inflammasome expression, proinflammatory cytokine release, and markers of injury and nitrosative stress in murine peritoneal macrophages supporting its possible use in preventing the asbestos-induced inflammatory cascade. Combined, our findings support the usefulness of LGM2605 as a potential chemopreventive agent in reducing the early inflammatory and cytotoxic effects that occur following asbestos exposure.

SDG, an antioxidant isolated from flaxseed, is metabolized by intestinal bacteria to enterodiol (ED) and enterolactone (EL) which are bioactive. However, SDG also has strong direct antioxidant properties *in vitro* without the need for metabolic activation [17]. The antioxidant activities of these three lignans (SDG, EL, and ED) were shown by their ability to inhibit linoleic acid lipid peroxidation, indicating direct hydroxyl radical scavenging activity [31, 32]. Since oxidant stress is implicated in the etiology of cancer, the therapeutic or preventive use of dietary flaxseed or flaxseed-derived lignans has been considered in certain malignancies such as in lung cancer [34, 35].

Our initial findings showed that treatment with the LGM2605 significantly inhibited the release of inflammasome-activated cytokines, IL-1β and IL-18. However, macrophages treated with LGM2605 also displayed significantly reduced levels of other proinflammatory cytokines, such as TNFα and IL-6, suggesting that both the NF-κB system and NLRP3 inflammasome pathway are blocked by LGM2605. Additionally, LGM2605 blocked the asbestos-induced release of HMGB1, which is either released passively by dead cells or secreted actively by stressed cells. Our earlier data showed that asbestos induces cell death (LDH release) which is ameliorated by the action of LGM2605, so clearly, cell death does presumably play a role in the increase of HMGB1 levels. Our current study shows HMGB1 mRNA and protein levels declined with LGM2605 treatment indicating that this agent blocks the induction of this danger-associated molecular pattern (DAMP) protein (Figures 4(e) and 4(f)). However, regardless of the mechanism of its release, HMGB1 outside the cell behaves as a DAMP protein or alarmin that activates the innate immune system either alone or in conjunction with cytokines and appears to be critical in the malignant transformation of mesothelial cells. HMGB1 amplifies the inflammatory response in general (by chemotaxing leukocytes (including neutrophils and mast cells [36]) and activating NF-κB) but also serves as an important protumorigenic cytokine that enhances the growth, survival, and invasiveness of the mesothelial cells [1]. Therefore, the fact that LGM2605 reduces HMGB1 via either reducing its release by stressed cells or by reducing cell death implies that this agent (LGM2605) can effectively "block" the asbestos-induced inflammatory signaling cascade that leads to activation of innate immune response and subsequent malignant transformation.

The activation of the NLRP3 inflammasome that drives maturation of proinflammatory cytokines such as

interleukin-1β (IL-1β) and IL-18, and leads to cell death (pyroptosis) has been reported elsewhere to be ROS regulated. Indeed, ROS have been reported to be crucial in triggering NLRP3 inflammasome formation and activation in response to both exogenous stimuli and endogenous signals in the form of damage-associated molecular patterns secreted by apoptotic cells [37]. Inhibition of NADPH oxidase-derived ROS prevented ATP-induced caspase-1 activation and IL-1β production in alveolar macrophages [38].

Our previous work shows increased ROS generation following asbestos exposure, which presumably participates in NLRP3 induction, as pretreatment with the ROS scavenger LGM2605, which reduced its activation as monitored by IL-1β and IL-18. Earlier studies reported the importance of NADPH oxidase-derived ROS in activating NLRP3 in response to ATP, asbestos, and silica [11]. Indeed, monocyte THP-1 cells that produced caspase 1 (i.e., showed NLRP3 inflammasome activation) in response to asbestos or silica showed a blunted response in specific knockdown of NADPH oxidase subunit p22phox or when treated with ROS scavengers (N-acetylcysteine and ammonium pyrrolidine dithiocarbamate) [11].

While induction and activation of the NLRP3 inflammasome are accepted to be redox regulated, the exact mechanism by which this occurs is not clear. One possibility is via the thioredoxin-interacting protein (TXNIP) that has been shown elsewhere to be associated with NLRP3 as a binding partner in a NLRP3-TXNIP complex [39]. TXNIP is a negative regulator of the antioxidant thioredoxin (TRX), and the dissociation of TXNIP from TRX is a ROS dependent process [39]. Thus, high levels of ROS lead to dissociation of TXNIP from TRX thus potentially allowing TXNIP to bind to NLRP3.

We report the ability of LGM2605 to both scavenge free radicals and detoxify ROS through direct and indirect molecular effects. We have previously reported the direct free radical scavenging ability of LGM2605 in a murine endothelial cell model of gamma radiation-induced ROS [17] and, therefore, studied this potential mechanism in our system. As shown in Figure 6, LGM2605 likely acted as a direct free radical scavenger and antioxidant in a dose-responsive manner. In addition to the direct free radical scavenging ability of LGM2605, we have shown that flaxseed, and its bioactive lignan component, can activate Nrf2 [16, 17, 21, 40]. Nrf2 is a master transcriptional regulator of carcinogen detoxifying and antioxidant enzymes (such as HO1 and NQO1) and plays a major role in tissue protection. These findings are in agreement with those of Velalopoulou et al., where LGM2605 protected normal lung cells from radiation-induced DNA damage through direct free radical scavenging and boosting of endogenous antioxidant enzyme gene expression [21].

5. Conclusion

An ideal agent used for the chemoprevention of asbestos-induced mesothelioma must be nontoxic, tolerable, and effective in interfering in asbestos-induced carcinogenesis. LGM2605 reduced proinflammatory cytokine release and markers of oxidative and nitrosative stress in murine peritoneal macrophages and may impede the asbestos-induced inflammatory cascade on the way to malignancy. Importantly, the ability of LGM2605 to interfere in multiple molecular pathways (boosting antioxidant defenses and blocking inflammation) provides strong evidence for its potential usefulness in chronic *in vivo* models of asbestos-induced mesothelioma.

Abbreviations

ASB: Asbestos
CTL: Control
DAMP: Danger-associated molecular pattern
ED: Enterodiol
EL: Enterolactone
ELISA: Enzyme-linked immunosorbent assays
FLC: Flaxseed lignan component
HMGB1: High mobility group box 1
HO-1: Heme oxygenase-1
IACUC: Institutional Animal Care and Use Committee
IL-1β: Interleukin-1β
IL-6: Interleukin-6
IL-18: Interleukin-18
iNOS: Inducible nitric oxide synthase
IP: Intraperitoneal
LC/MS/MS: Liquid chromatography/tandem mass spectrometry
LDH: Lactate dehydrogenase
LGM2605: Synthetic secoisolariciresinol diglucoside
MF: Macrophages
MDA: Malondialdehyde
MM: Malignant mesothelioma
NF-κB: Nuclear factor kappa-light-chain-enhancer of activated B cells
Nrf2: Nuclear factor E2-related factor 2
Nqo1: NADPH:quinone oxidoreductase-1
PBS: Phosphate-buffered saline
PL: Peritoneal lavage
PLF: Peritoneal lavage fluid
qPCR: Quantitative polymerase chain reaction
RNS: Reactive nitrogen species
ROS: Reactive oxygen species
SDG: Secoisolariciresinol diglucoside
TNFα: Tumor necrosis factor alpha
WBC: White blood cells.

Disclosure

The contents are solely the responsibility of the authors and do not necessarily represent the official views of the NIEHS, NIH.

Conflicts of Interest

Melpo Christofidou-Solomidou (MCS) reports grants from the NIH during the conduct of the study. In addition, Melpo Christofidou-Solomidou has patents no. PCT/US14/41636 and no. PCT/US15/22501 pending and has a founder equity

position in LignaMed, LLC. All other coauthors report no actual, potential, or perceived conflict of interest with regard to this manuscript.

Authors' Contributions

Ralph A. Pietrofesa performed biochemical assays, conducted data analysis and interpretation, and assisted with manuscript preparation. Patrick Woodruff assisted in data analysis and interpretation and assisted with manuscript preparation. Wei-Ting Hwang assisted in data analysis and interpretation and assisted with manuscript preparation. Priyal Patel performed fluorescence microscopy and conducted data analysis. Shampa Chatterjee designed individual experiments, assisted in data analysis and interpretation, and assisted with manuscript preparation. Steven M. Albelda designed the study and individual experiments, assisted in data analysis and interpretation, and assisted with manuscript preparation. Melpo Christofidou-Solomidou designed the study and the individual experiments, analyzed and interpreted data, wrote the manuscript, and supervised the lab personnel. All coauthors reviewed the manuscript before submission and approved the final version.

Acknowledgments

This work was funded in part by NIH–R01 CA133470 (Melpo Christofidou-Solomidou), NIH–1R21AT008291-02 (Melpo Christofidou-Solomidou), NIH–R03 CA180548 (Melpo Christofidou-Solomidou), and NIH–1P42ES023720-01 (Melpo Christofidou-Solomidou) and by pilot project support from NIH–1P30 ES013508-02 awarded to Melpo Christofidou-Solomidou.

References

[1] M. Carbone and H. Yang, "Molecular pathways: targeting mechanisms of asbestos and erionite carcinogenesis in mesothelioma," *Clinical Cancer Research*, vol. 18, no. 3, pp. 598–604, 2012.

[2] M. Neri, D. Ugolini, S. Boccia et al., "Chemoprevention of asbestos-linked cancers: a systematic review," *Anticancer Research*, vol. 32, no. 3, pp. 1005–1013, 2012.

[3] H. Bielefeldt-Ohmann, D. R. Fitzpatrick, A. L. Marzo et al., "Patho- and immunobiology of malignant mesothelioma: characterisation of tumour infiltrating leucocytes and cytokine production in a murine model," *Cancer Immunology, Immunotherapy*, vol. 39, no. 6, pp. 347–359, 1994.

[4] P. A. Moalli, J. L. MacDonald, L. A. Goodglick, and A. B. Kane, "Acute injury and regeneration of the mesothelium in response to asbestos fibers," *The American Journal of Pathology*, vol. 128, no. 3, pp. 426–445, 1987.

[5] H. Bielefeldt-Ohmann, A. G. Jarnicki, and D. R. Fitzpatrick, "Molecular pathobiology and immunology of malignant mesothelioma," *The Journal of Pathology*, vol. 178, no. 4, pp. 369–378, 1996.

[6] M. E. Ramos-Nino, J. R. Testa, D. A. Altomare et al., "Cellular and molecular parameters of mesothelioma," *Journal of Cellular Biochemistry*, vol. 98, no. 4, pp. 723–734, 2006.

[7] F. Colotta, P. Allavena, A. Sica, C. Garlanda, and A. Mantovani, "Cancer-related inflammation, the seventh hallmark of cancer: links to genetic instability," *Carcinogenesis*, vol. 30, no. 7, pp. 1073–1081, 2009.

[8] H. Yang, Z. Rivera, S. Jube et al., "Programmed necrosis induced by asbestos in human mesothelial cells causes high-mobility group box 1 protein release and resultant inflammation," *Proceedings of the National Academy of Sciences of the United States of America*, vol. 107, no. 28, pp. 12611–12616, 2010.

[9] J. M. Hillegass, A. Shukla, S. A. Lathrop et al., "Inflammation precedes the development of human malignant mesotheliomas in a SCID mouse xenograft model," *Annals of the New York Academy of Sciences*, vol. 1203, pp. 7–14, 2010.

[10] M. Sayan and B. T. Mossman, "The NLRP3 inflammasome in pathogenic particle and fibre-associated lung inflammation and diseases," *Particle and Fibre Toxicology*, vol. 13, no. 1, p. 51, 2016.

[11] C. Dostert, V. Petrilli, R. V. Bruggen, C. Steele, B. T. Mossman, and J. Tschopp, "Innate immune activation through Nalp3 inflammasome sensing of asbestos and silica," *Science*, vol. 320, no. 5876, pp. 674–677, 2008.

[12] J. Palomaki, E. Valimaki, J. Sund et al., "Long, needle-like carbon nanotubes and asbestos activate the NLRP3 inflammasome through a similar mechanism," *ACS Nano*, vol. 5, no. 9, pp. 6861–6870, 2011.

[13] J. K. Thompson, M. B. MacPherson, S. L. Beuschel, and A. Shukla, "Asbestos-induced mesothelial to fibroblastic transition is modulated by the inflammasome," *The American Journal of Pathology*, vol. 187, no. 3, pp. 665–678, 2017.

[14] R. A. Pietrofesa, A. Velalopoulou, S. M. Albelda, and M. Christofidou-Solomidou, "Asbestos induces oxidative stress and activation of Nrf2 signaling in murine macrophages: chemopreventive role of the synthetic lignan secoisolariciresinol diglucoside (LGM2605)," *International Journal of Molecular Sciences*, vol. 17, no. 3, p. 322, 2016.

[15] A. Scherpereel, P. Astoul, P. Baas et al., "Guidelines of the European Respiratory Society and the European Society of Thoracic Surgeons for the management of malignant pleural mesothelioma," *The European Respiratory Journal*, vol. 35, no. 3, pp. 479–495, 2010.

[16] J. C. Lee, F. Bhora, J. Sun et al., "Dietary flaxseed enhances antioxidant defenses and is protective in a mouse model of lung ischemia-reperfusion injury," *American Journal of Physiology. Lung Cellular and Molecular Physiology*, vol. 294, no. 2, pp. L255–L265, 2008.

[17] J. C. Lee, R. Krochak, A. Blouin et al., "Dietary flaxseed prevents radiation-induced oxidative lung damage, inflammation and fibrosis in a mouse model of thoracic radiation injury," *Cancer Biology & Therapy*, vol. 8, no. 1, pp. 47–53, 2009.

[18] O. P. Mishra, N. Simmons, S. Tyagi et al., "Synthesis and antioxidant evaluation of (S,S)- and (R,R)-secoisolariciresinol diglucosides (SDGs)," *Bioorganic & Medicinal Chemistry Letters*, vol. 23, no. 19, pp. 5325–5328, 2013.

[19] O. P. Mishra, R. Pietrofesa, and M. Christofidou-Solomidou, "Novel synthetic (S,S) and (R,R)-secoisolariciresinol diglucosides (SDGs) protect naked plasmid and genomic DNA from gamma radiation damage," *Radiation Research*, vol. 182, no. 1, pp. 102–110, 2014.

[20] R. A. Pietrofesa, A. Velalopoulou, E. Arguiri et al., "Flaxseed lignans enriched in secoisolariciresinol diglucoside prevent

acute asbestos-induced peritoneal inflammation in mice," *Carcinogenesis*, vol. 37, no. 2, pp. 177–187, 2016.

[21] A. Velalopoulou, S. Tyagi, R. A. Pietrofesa, E. Arguiri, and M. Christofidou-Solomidou, "The flaxseed-derived lignan phenolic secoisolariciresinol diglucoside (SDG) protects non-malignant lung cells from radiation damage," *International Journal of Molecular Sciences*, vol. 17, no. 1, 2016.

[22] X. Zhang, R. Goncalves, and D. M. Mosser, "The isolation and characterization of murine macrophages," *Current Protocols in Immunology*, Chapter 14, Unit 14 11, 2008.

[23] Y. Kadariya, C. W. Menges, J. Talarchek et al., "Inflammation-related IL1beta/IL1R signaling promotes the development of asbestos-induced malignant mesothelioma," *Cancer Prevention Research*, vol. 9, no. 5, pp. 406–414, 2016.

[24] D. J. Blake, C. M. Bolin, D. P. Cox, F. Cardozo-Pelaez, and J. C. Pfau, "Internalization of Libby amphibole asbestos and induction of oxidative stress in murine macrophages," *Toxicological Sciences*, vol. 99, no. 1, pp. 277–288, 2007.

[25] S. X. Huang, M. A. Partridge, S. A. Ghandhi, M. M. Davidson, S. A. Amundson, and T. K. Hei, "Mitochondria-derived reactive intermediate species mediate asbestos-induced genotoxicity and oxidative stress-responsive signaling pathways," *Environmental Health Perspectives*, vol. 120, no. 6, pp. 840–847, 2012.

[26] O. P. Mishra, A. V. Popov, R. A. Pietrofesa, and M. Christofidou-Solomidou, "Gamma-irradiation produces active chlorine species (ACS) in physiological solutions: secoisolariciresinol diglucoside (SDG) scavenges ACS - a novel mechanism of DNA radioprotection," *Biochimica et Biophysica Acta (BBA) - General Subjects*, vol. 1860, no. 9, pp. 1884–1897, 2016.

[27] M. E. Ramos-Nino, A. Haegens, A. Shukla, and B. T. Mossman, "Role of mitogen-activated protein kinases (MAPK) in cell injury and proliferation by environmental particulates," *Molecular and Cellular Biochemistry*, vol. 234, no. 1, pp. 111–118, 2002.

[28] B. T. Mossman, S. Faux, Y. Janssen et al., "Cell signaling pathways elicited by asbestos," *Environmental Health Perspectives*, vol. 105, Supplement 5, pp. 1121–1125, 1997.

[29] N. H. Heintz, Y. M. Janssen-Heininger, and B. T. Mossman, "Asbestos, lung cancers, and mesotheliomas: from molecular approaches to targeting tumor survival pathways," *American Journal of Respiratory Cell and Molecular Biology*, vol. 42, no. 2, pp. 133–139, 2010.

[30] K. Prasad, "Hydroxyl radical-scavenging property of secoisolariciresinol diglucoside (SDG) isolated from flax-seed," *Molecular and Cellular Biochemistry*, vol. 168, no. 1-2, pp. 117–123, 1997.

[31] K. Prasad, "Antioxidant activity of secoisolariciresinol diglucoside-derived metabolites, secoisolariciresinol, enterodiol, and enterolactone," *International Journal of Angiology*, vol. 9, no. 4, pp. 220–225, 2000.

[32] D. D. Kitts, Y. V. Yuan, A. N. Wijewickreme, and L. U. Thompson, "Antioxidant activity of the flaxseed lignan secoisolariciresinol diglycoside and its mammalian lignan metabolites enterodiol and enterolactone," *Molecular and Cellular Biochemistry*, vol. 202, no. 1-2, pp. 91–100, 1999.

[33] C. Hu, Y. V. Yuan, and D. D. Kitts, "Antioxidant activities of the flaxseed lignan secoisolariciresinol diglucoside, its aglycone secoisolariciresinol and the mammalian lignans enterodiol and enterolactone in vitro," *Food and Chemical Toxicology*, vol. 45, no. 11, pp. 2219–2227, 2007.

[34] S. Chikara, K. Lindsey, P. Borowicz, M. Christofidou-Solomidou, and K. M. Reindl, "Enterolactone alters FAK-Src signaling and suppresses migration and invasion of lung cancer cell lines," *BMC Complementary and Alternative Medicine*, vol. 17, no. 1, p. 30, 2017.

[35] S. Chikara, K. Lindsey, H. Dhillon et al., "Enterolactone induces G1-phase cell cycle arrest in nonsmall cell lung cancer cells by downregulating cyclins and cyclin-dependent kinases," *Nutrition and Cancer*, vol. 69, no. 4, pp. 652–662, 2017.

[36] G. L. Hold and E. M. El-Omar, "Genetic aspects of inflammation and cancer," *The Biochemical Journal*, vol. 410, no. 2, pp. 225–235, 2008.

[37] J. Tschopp and K. Schroder, "NLRP3 inflammasome activation: the convergence of multiple signalling pathways on ROS production?," *Nature Reviews. Immunology*, vol. 10, no. 3, pp. 210–215, 2010.

[38] C. M. Cruz, A. Rinna, H. J. Forman, A. L. Ventura, P. M. Persechini, and D. M. Ojcius, "ATP activates a reactive oxygen species-dependent oxidative stress response and secretion of proinflammatory cytokines in macrophages," *The Journal of Biological Chemistry*, vol. 282, no. 5, pp. 2871–2879, 2007.

[39] R. Zhou, A. Tardivel, B. Thorens, I. Choi, and J. Tschopp, "Thioredoxin-interacting protein links oxidative stress to inflammasome activation," *Nature Immunology*, vol. 11, no. 2, pp. 136–140, 2010.

[40] P. Kinniry, Y. Amrani, A. Vachani et al., "Dietary flaxseed supplementation ameliorates inflammation and oxidative tissue damage in experimental models of acute lung injury in mice," *The Journal of Nutrition*, vol. 136, no. 6, pp. 1545–1551, 2006.

Hindawi
Oxidative Medicine and Cellular Longevity
Volume 2017, Article ID 4271065, 13 pages
https://doi.org/10.1155/2017/4271065

Research Article

Cold Atmospheric Plasma Induces Apoptosis and Oxidative Stress Pathway Regulation in T-Lymphoblastoid Leukemia Cells

Eleonora Turrini,[1] Romolo Laurita,[2] Augusto Stancampiano,[2] Elena Catanzaro,[1] Cinzia Calcabrini,[1] Francesca Maffei,[1] Matteo Gherardi,[2] Vittorio Colombo,[2] and Carmela Fimognari[1]

[1]*Department for Life Quality Studies, Alma Mater Studiorum-Università di Bologna, C.so D'Augusto 237, 47921 Rimini, Italy*
[2]*Department of Industrial Engineering, Alma Mater Studiorum-Università di Bologna, Via Saragozza 8, 40123 Bologna, Italy*

Correspondence should be addressed to Eleonora Turrini; eleonora.turrini@unibo.it

Received 2 March 2017; Revised 18 May 2017; Accepted 19 June 2017; Published 29 August 2017

Academic Editor: Eva-Maria Hanschmann

Cold atmospheric plasma (CAP) has shown its antitumor activity in both *in vitro* and *in vivo* systems. However, the mechanisms at the basis of CAP-cell interaction are not yet completely understood. The aim of this study is to investigate CAP proapoptotic effect and identify some of the molecular mechanisms triggered by CAP in human T-lymphoblastoid leukemia cells. CAP treatment was performed by means of a wand electrode DBD source driven by nanosecond high-voltage pulses under different operating conditions. The biological endpoints were assessed through flow cytometry and real-time PCR. CAP caused apoptosis in Jurkat cells mediated by p53 upregulation. To test the involvement of intrinsic and/or extrinsic pathway, the expression of Bax/Bcl-2 and caspase-8 was analyzed. The activation of caspase-8 and the upregulation of Bax and Bcl-2 were observed. Moreover, CAP treatment increased ROS intracellular level. The situation reverts after a longer time of treatment. This is probably due to compensatory cellular mechanisms such as the posttranscriptional upregulation of SOD1, CAT, and GSR2. According to ROS increase, CAP induced a significant increase in DNA damage at all treatment conditions. In conclusion, our results provide a deeper understanding of CAP potential in the oncological field and pose the basis for the evaluation of its toxicological profile.

1. Introduction

Previous researches have repeatedly proven the anticancer effects of cold atmospheric plasmas (CAPs). Plasma effect on cancer cells is mediated by biologically active factors such as electric field [1–3], charged particles (ions and electrons), photons and UV radiations, free radicals, and reactive oxygen and nitrogen species (RONS) [4], including atomic oxygen (O), hydroxyl radical (·OH), superoxide (O_2^-), hydrogen peroxide (H_2O_2), atomic nitrogen (N), and nitric oxide (NO), generated both in gas and liquid phases [5]. Moreover, this blend of reactive species plays a major role in the induction of apoptosis in cancer cells directly exposed to CAP [6–9] or indirectly treated by means of plasma-activated liquids [10–18]. In particular, plasma treatment of complete cell medium induces the increase of extracellular RONS concentration [19] and this plays a crucial role in the effects of CAP on cells [20]. The anticancer effects mediated by reactive species are imputable to biochemical changes induced in the cells by the gas phase RONS and liquid phase RONS products [21]. Different studies demonstrated that RONS generated by plasma treatment can trigger cell signaling pathways involving JNK and p38 [22] and p53 [23], thus, promoting mitochondrial perturbation and activation of caspases [8], finally leading to apoptosis. The alteration of redox signaling induced by CAP treatment correlates not only with the induction of apoptosis but also with DNA damage [24], via DNA strand break formation and consequent activation of DNA damage checkpoints [8]. The antitumor effect of CAP was also explored on *in vivo* models.

Vandamme et al. [25] evaluated the potential antitumor effect of an *in vivo* plasma treatment on a U87-luc glioma tumor xenograft, showing a significant reduction of tumor mass after 5 days of plasma treatment. Likewise, Chernets et al. demonstrated that plasma induced tumor suppression of subdermal melanoma in mouse model, via the increase of RONS levels [7]. Furthermore, a significant inhibition of tumor growth in *in vivo* model was shown by plasma-activated Ringer's lactate solution [12] and plasma-activated cell culture medium [26, 27]. Several studies demonstrated that the antitumor effect of plasma-activated liquids can be attributable to RONS and to the activation of solution component (e.g., L-sodium lactate) [12].

Clinical applications of plasma in the treatment of tumor are still missing, but a recent work of Metelmann et al. [28] reported a superficial partial remission of tumor on patients afflicted with advanced squamous cell carcinoma after CAP treatment. Recent papers proposed CAP as a promising anticancer strategy not only for its cytotoxic potential but also for its ability to simultaneously activate the immune system against cancer, which in turn determines the long-term success of anticancer therapy system [29]. In fact, redox molecules, such as, NO and ROS, and redox chemistry have a key role as immunomodulators in tumor and pathogen killing [30]. The optimization of plasma parameters would allow the induction of immunogenic cell death in tumors locally that will trigger a specific and protective immune response systematically [31].

Thus, plasma could be proposed as an interesting anticancer treatment, but it is necessary to deepen the understanding on the mechanisms and the specific components of CAP responsible of its anticancer effects. In this study, we investigated the proapoptotic effect of CAP and its ability to modulate the oxidative stress pathway in human T-lymphoblastoid leukemia cells (Jurkat cells) and identified some of the molecular mechanisms triggered by CAP treatment. We demonstrated that the exposure of complete medium to CAP produced by a nanosecond-pulsed DBD induced the generation of several RONS; among these species, nitrites and hydrogen peroxide are considered the most significant RONS contributing to plasma toxicity on cancer cells.

2. Materials and Methods

2.1. Cell Culture. Jurkat cells were purchased from LGC Standards (Teddington, UK) and cultured in RPMI 1640 supplemented with 10% heat-inactivated fetal calf serum, 1% antibiotics [penicillin 5000 IU/streptomycin 5 mg/mL], and 1% L-glutamine solution (all purchased from Biochrom, Billerica, MA, USA). Cultured cells were maintained in 5% CO_2 and humidified air at 37°C.

2.2. Detection of Hydrogen Peroxides and Nitrites in Plasma-Treated Medium. The Amplex® Red Hydrogen Peroxide Assay Kit (Thermo Fisher Scientific, Waltham, MA, USA) and Nitrate/Nitrite Colorimetric Assay (Roche, Basel, Switzerland) were used according to the manufacturer's protocol to measure the concentrations of hydrogen peroxide and nitrites induced by plasma treatment in 1 mL complete cell culture medium. Plasma-treated medium was diluted 100-fold in PBS immediately after treatment, to obtain a solution with hydrogen peroxide concentration below 10 μM and avoid any influence of pH on the measurement. The absorbances were measured photometrically with a microplate reader (Rayto, Shenzhen, P.R. China).

2.3. Cell Treatment with CAP. 5×10^5 cells in 1 mL complete medium were seeded in a monolayer through centrifugation and directly exposed to plasma treatment in a 24-well plate. The adopted plasma source is a nanosecond-pulsed dielectric barrier discharge (DBD) consisting of a cylindrical internal brass electrode covered by a glass test tube with a semispherical tip as dielectric (1 mm thick) [32]. Two operating conditions were selected following preliminary experiments, as already reported by the authors [11]; the first one consists in a 60″ treatment keeping a distance of 1.25 mm between the tip of plasma source and the surface of the cell medium (gap) (T1); while the second treatment condition consisted in a 120″ treatment performed setting the gap at 2.50 mm (T2). For each of the two operating conditions, preliminary experiments were performed, demonstrating that for the achievement of similar cellular effects, it is necessary to increase the exposure times when using greater distances and reduce them when using smaller distances [11]. During treatment time, peak voltage (PV) and pulse repetition frequency (PRF) were kept constant at 20 kV and 500 Hz, respectively.

2.4. Analysis of Cell Death Mechanisms. After treatment, aliquots of 2.0×10^4 cells were stained with Guava Nexin Reagent (100 μL) (Merck Millipore, Billerica, MA, USA), containing annexin V phycoerythrin and 7-amino-actinomycin D (7-AAD). Three cell populations can be detected: nonapoptotic live cells (annexin$^-$/7-AAD$^-$), early apoptotic cells (annexin$^+$/7-AAD$^-$), and late apoptotic or necrotic cells (annexin$^+$/7-AAD$^+$). Cells were incubated for 20 min at room temperature in the dark and analyzed by flow cytometry. H_2O_2 300 μM was used as positive control.

2.5. Detection of Intracellular ROS. 3 or 6 h after CAP treatment, cells were incubated with 2′,7′-dichlorodihydrofluorescein diacetate (H_2DCFDA, 10 μM) (Sigma-Aldrich, St. Louis, Missouri, USA) for 20 min at 37°C, 5% CO_2 in the dark. H_2DCFDA is a nonpolar and nonfluorescent molecule able to diffuse in living cells, where it is hydrolyzed at 2′,7′-diclodihydrofluorescrin (H_2DCF) by intracellular esterases and trapped into cells. In the presence of ROS, H_2DCF is oxidized to the fluorescent molecule 2′,7′-diclorofluorescein (DCF), which can be detected by flow cytometry. The fluorescence intensity of DCF is proportional to intracellular ROS levels.

2.6. DNA Damage Assays. A complementary experimental approach was used to detect the primary DNA damage (H2A.X histone phosphorylation assay), as opposed to the mutational effects (micronucleus test) that can result from DNA damage.

Phosphorylation of histone p-H2A.X was used as marker of CAP genotoxic potential using FlowCellect™ Histone

H2A.X Phosphorylation Assay Kit (Merck Millipore), 6 and 24 h after treatment with CAP. The kit components include the fixation buffer (Part number CS202122) and 1x permeabilization buffer (Part number CS203284), both ready to use. After washing, 1×10^6 cells were suspended in 1 mL fixation buffer and incubated 20 min on ice. After washing with 1x assay buffer, samples were permeabilized using 1 mL permeabilization buffer and incubated for 20 min on ice according to the manufacturer's instructions. After washing, each sample was resuspended in 95 μL of assay buffer and 5 μL of anti-histone H2A.X antibody. The antibody used to detect H2A.X phosphorylated was 20x anti-histone H2A.X-Alexa Fluor® 488 (Part number CS208216). Samples were incubated for 30 minutes in the dark at room temperature. After washing, cells were suspended in 1x assay buffer and analyzed via flow cytometry. Ethyl methanesulphonate (EMS) 240 μg/mL was used as positive control. Some experiments were performed with N-acetylcysteine (NAC) (1 h, 10 mM).

2.7. MN Assay. For micronucleus test, Jurkat cells were treated with CAP and incubated for 24 h to allow cell replication. At the end of the incubation, 0.5×10^6 cells were stained according to the manufacturer's instruction of the in Vitro Microflow kit (Litron Laboratories, Rochester, NY, USA). Briefly, cells were first stained with nucleic acid dye A solution (300 μL), containing ethidium monoazide (EMA) that crosses the compromised membrane of apoptotic and necrotic cells. Since EMA needs photoactivation to covalently bind DNA, cells were kept on ice and photoactivated. Complete lysis solution 1 (500 μL) was added to digest the cytoplasmatic membrane and release nuclei and micronuclei (MN). To complete membrane lysis and obtain the complete release of nuclei and MN, cells were then treated with complete lysis solution 2 (500 μL). Both cell lysis solutions contain the dye SYTOX green that labels chromatin. The double staining with EMA and SYTOX green of chromatin allows discriminating nuclei and MN in living cells (SYTOX green$^+$) from fragments derived from damaged chromatin of dead/dying cells (EMA$^+$/SYOTX green$^+$). At the end of the incubation, cells were analyzed by flow cytometry. MN were distinguished from nuclei for their smaller dimension and thus for their lower fluorescence: MN exhibit 1/100th to 1/10th of the intensity of duplicated nuclei [33]. EMS (240 μg/mL) was used as positive control. The gating strategy is carefully described in the protocol of the in Vitro Microflow kit (Litron Laboratories). Using a negative control for setup, samples were acquired adjusting forward scatter (FSC) and side scatter (SSC) voltages to bring nuclei into view. The lower bounds of the region were approximately 2 logs lower in FSC and SSC than the bottom left edge of the nucleus events. Then, EMA fluorescence was set according to discriminate nuclei from healthy and dead cells. The position of the "FSC versus SYTOX" region was adjusted until nuclei were positioned. Much of the chromatin associated with dead/dying cells fell above an appropriately located "FSC versus SYTOX" region. Then, the position of the "SSC versus SYTOX" region was adjusted until nuclei were positioned. Much of the chromatin associated with dead/dying cells fell above an appropriately located "SSC versus SYTOX" region. The final plot gave results on the number of MN and nucleated cells, showing SYTOX green versus FCS. From this test, cell cycle perturbations were recorded by studying fluorescence histograms of SYTOX green, a nucleic acid dye.

To validate the results obtained by in Vitro Microflow kit, the analysis of MN in binucleated cells was performed by adding cytochalasin B (Sigma-Aldrich; final concentration of 6 μg/mL) after 44 h of culture [34]. At the end of the 72 h incubation period, Jurkat cells were fixed with ice-cold methanol/acetic acid (1 : 1). The fixed cells were put directly on slides using a cytospin and stained with May-Grünwald-Giemsa. All slides were coded before scoring. The criteria for scoring micronuclei were as described by Fenech [35]. At least 2000 binucleated lymphocytes were examined per concentration (two cultures per concentration) for the presence of one, two, or more micronuclei.

2.8. Analysis of p53, Bax, Bcl-2, and Caspase-8 Protein Levels. 24 and 48 h after cell treatment, the analysis of protein levels involved in the apoptotic process was performed. Briefly, 0.5×10^6 cells were fixed using a 4% paraformaldehyde solution in PBS 1x and permeabilized in 90% ice-cold methanol solution. Cells were then incubated with the following antibodies: p53 (1 : 200, Santa Cruz Biotechnology, Dallas, TX, USA), Bax (1 : 200, Santa Cruz Biotechnology), and Alexa Fluor 488-labeled Bcl-2 (1 : 200, BioLegend, San Diego, CA, USA). The cells, except those stained with Bcl-2, were washed, incubated with fluorescein isothiocyanate-labeled secondary antibody (1 : 100, Sigma-Aldrich), and analyzed by flow cytometry. Sulforaphane was used as positive control. Mean fluorescence intensity values were calculated. Nonspecific binding was excluded by isotype-matched negative control (1 : 100, eBioscience, San Diego, CA, USA). The expression of caspase-8 was detected by using leucine-glutamic acid-threonine-aspartic acid (LETD) caspase-8-preferred substrate linked to a fluoromethylketone (FMK) that reacts covalently with the catalytic cysteine residue in the active enzymatic center. 6-Carboxyfluorescein (FAM) was used as fluorescent reporter. 24 and 48 h after CAP treatment, nonpermeabilized cells were stained with 10 μL of freshly prepared 10x working dilution of FAM-LETD-FMK solution (Merck Millipore) and incubated for 1 h at 37°C in the dark. At the end of incubation, cells were washed and suspended in 150 μL of 7-AAD diluted 1 : 200 in 1x working dilution wash buffer (Merck Millipore), incubated for 5 min at room temperature in the dark, and analyzed via flow cytometry. Staurosporine was used as positive control.

2.9. Real-Time PCR. Total RNA was isolated using Agilent Total RNA isolation Mini Kit (Agilent Technologies, Santa Clara, CA, USA), according to the manufacturer's instructions. Briefly, 350 μL of lysis buffer was added to cell pellet and the cell homogenate centrifuged through a miniprefiltration column. The eluate was mixed with an equal volume of 70% ethanol solution, incubated for 5 min at room temperature, and centrifuged through a mini-isolation column. The eluate was discharged, and after column washing, the RNA was eluted by adding nuclease-free water and stored

at −20°C. cDNA was synthesized using High Capacity cDNA Reverse Transcription Kit (Life Technologies, Carlsbad, CA, USA). Briefly, 200 ng total RNA was added to 10 μL reaction kit mixture with RNAse inhibitor, according to manufacturer's recommendations. Changes in mRNA expression were measured by using TaqMan® gene expression assay (Life Technologies) and Real-Time PCR (Step One, Life Technologies). The variation in the expression of the following genes was analyzed: TP53 (Hs01034349_m1), Bax (Hs00180269_m1), Bcl-2 (Hs00608023_m1), SOD1 (Hs00533490_m1), CAT (Hs00156308_m1), and GSR2 (Hs00167317_m1). 18S ribosomal RNA and actin beta (ACTB) (Hs99999901_s1 and Hs99999903_m1, resp.) were used as endogenous controls. Each measurement was performed in triplicate. Data were analyzed through the $2^{-\Delta\Delta Ct}$ method.

2.10. Statistical Analysis. The results are expressed as mean ± SEM of at least 3 independent experiments. Statistical analysis was performed using repeated ANOVA, followed by Bonferroni as posttest, using GraphPad InStat version 5.00 (GraphPad Prism, La Jolla, CA, USA). $P < 0.05$ was considered significant.

3. Results

3.1. CAP Induces Hydrogen Peroxide and Nitrite Production in Treated Medium. Since the effects of plasma on cancer cells seem to be mediated by reactive species, we first studied the ability of CAP to produce H_2O_2 and NO_2- in medium. In Figure 1, we show the concentrations of hydrogen peroxides and nitrites in 1 mL of complete cell culture medium after plasma treatments, recorded by a specific colorimetric kit. Hydrogen peroxides and nitrites are not present in the untreated medium. Both CAP treatment conditions, T1 and T2, induced the production of similar concentrations of hydrogen peroxides (about 310 μM). On the other hand, nitrites concentration induced by T2 was significantly higher (up to about 1068 μM) compared to the concentration produced by T1 (about 556 μM).

3.2. CAP Induces Apoptosis in Jurkat Cells. One of the most relevant mechanisms of action of anticancer drugs is the induction of apoptosis. Thus, we investigated the ability of CAP to induce apoptosis by flow cytometry. A significant increase in apoptotic cells was found in samples after treatment under both the tested CAP operating conditions. As an example, 17.1% of apoptotic cells was observed 24 h after CAP exposure at T1 (versus 6.0% of the untreated cells) and 26.6% 48 h after CAP exposure at T2 treatment condition (versus 11.3% of the untreated cells) (Figure 2).

To evaluate the apoptotic mechanisms evoked by CAP, the expression of key genes involved in the apoptotic pathway was analyzed. CAP increased p53 protein expression 48 h after treatment. p53 expression in cells treated under condition T2 resulted in a 1.74-fold increase compared to the untreated cells, whose expression was normalized to 1 (Figure 3(a)). No modulation for p53 was observed at RNA level for all tested treatment conditions (Figure 3(b)).

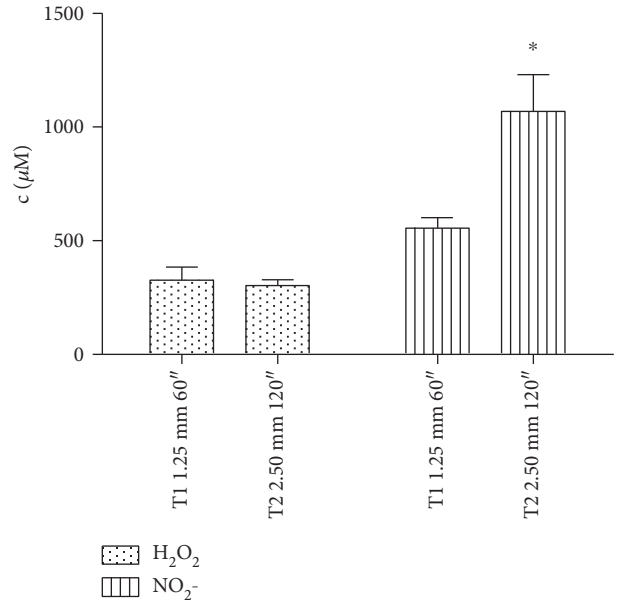

Figure 1: Hydrogen peroxide and nitrite concentration in plasma-treated complete medium, measured by specific colorimetric kits. Shown data are the mean of three different experiments. $^*P < 0.05$ versus T1 nitrite.

To explore the involvement of the intrinsic and/or extrinsic pathway in CAP-induced apoptosis, the expression of Bax/Bcl-2 and caspase-8 was analyzed. An increase in Bax and Bcl-2 expression was observed, with the highest effect in cells treated under the T2 condition and 48 h after CAP exposure. Bax and Bcl-2 expression resulted 1.66-fold and 1.63-fold higher, respectively, than the untreated cells (Figures 3(c) and 3(e)). Sulforaphane, used as positive control, increased the expression of Bax by about 3 times after 48 h treatment versus the untreated cells. Of note, the Bax/Bcl-2 ratio was not significantly changed following CAP treatment (Figure 3(g)). Any variation was observed for RNA expression of Bax neither 6 nor 24 h after CAP treatment (Figure 3(d)). The modulation of Bcl-2 by CAP treatment was more complex. Bcl-2 was downregulated 6 h after treatment using both the operating conditions but upregulated 24 h after CAP treatment (Figure 3(f)). The expression of caspase-8 was significantly increased both 24 and 48 h after CAP treatment and in both conditions. In particular, after 24 h T1 CAP treatment, the expression was 1.36-fold higher than the untreated cells (Figure 3(h)). Staurosporine, used as positive control for caspase-8, induced a 4-fold increase after 48 h of treatment, compared to the untreated cells.

3.3. CAP Increases Intracellular ROS Levels and Modulates the Oxidative Stress Pathway. We previously demonstrated that CAP produces H_2O_2 and NO_2- in medium. For this reason, we studied the effects of CAP on the modulation of intracellular ROS levels. The cytofluorimetric measurement of 2′,7′-diclorofluorescein (DCF) indicated a significant increase in intracellular ROS levels after CAP treatment. In particular, 3 h after CAP exposure, ROS levels were 1.89-fold and 1.45-fold higher in cells treated at T1 and T2 operative

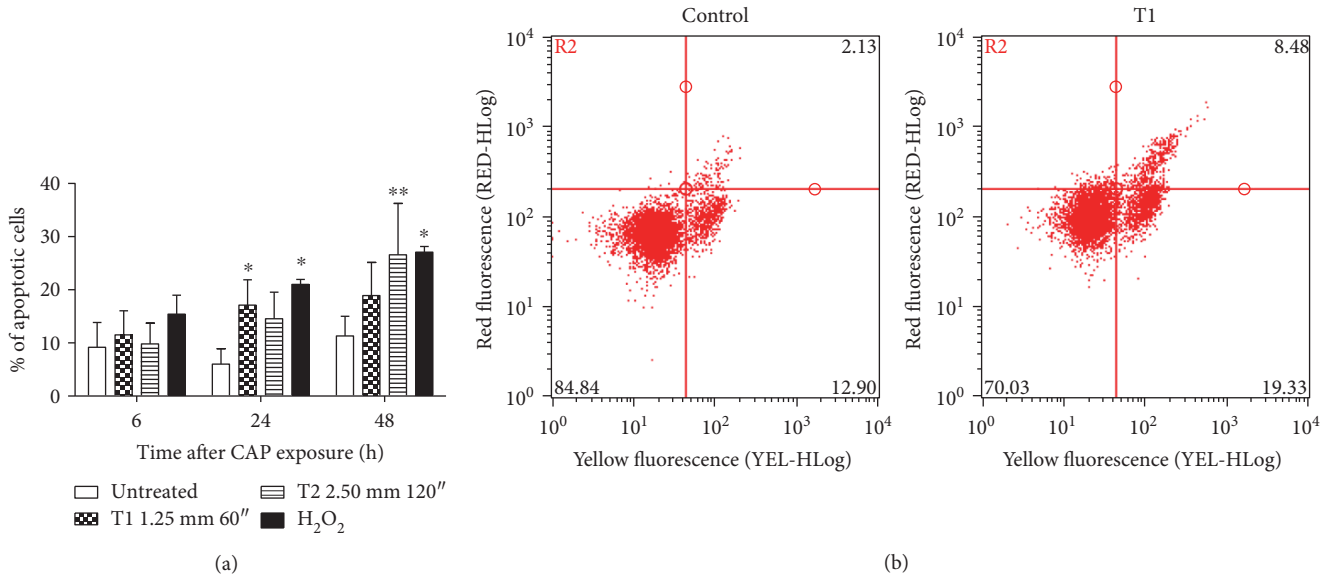

Figure 2: (a) % of apoptotic cells 6, 24, and 48 h after CAP treatment of Jurkat cells under T1 (1.25 mm 60″) and T2 (2.50 mm 120″) conditions (mean of three different experiments). H_2O_2 300 μM was used as positive control. (b) Representative dot plot of annexin V (yellow fluorescence) versus 7-amino-actinomycin D (7AAD, red fluorescence) for the untreated cells and cells 24 h after CAP treatment under T1 condition. $^*P < 0.05$; $^{**}P < 0.01$ versus the untreated cells.

conditions, respectively, compared to control (Figure 4(a)). However, 6 h after CAP treatment, a significant reduction of intracellular ROS levels was observed in both the investigated cases (Figure 4(a)). Thus, the ability of CAP treatment to modulate the oxidative stress pathway was analyzed. A posttranscriptional modulation of SOD1 was observed, as indicated by the 1.5-fold higher expression than the untreated cells 24 h after treatment at the T2 condition (Figure 4(b)). An upregulation of CAT and GSR2 was also detected after CAP exposure. The highest effect was observed for both genes 24 h after the T2 CAP treatment (3.52- and 2.31-fold higher than the untreated cells, resp.) (Figures 4(c) and 4(d)).

3.4. CAP Has a Genotoxic and Mutagenic Effect. Since we demonstrated that CAP is able to generate RONS, its genotoxic potential should be carefully examined. For this reason, in the final part of our study, we used different tests of genotoxicity with the aim to detect the net and actual mutagenic effect of the plethora of lesions caused by CAP and to directly relate the DNA damage to the mutagenic effect. To investigate whether CAP was able to induce DNA damage, the phosphorylation of H2A.X (p-H2A.X) was analyzed. 6 h after CAP exposure, a 2.16-fold increase in p-H2A.X compared to the untreated cells was observed. 24 h after CAP treatment, the level of p-H2A.X was significant only under the T2 condition (Figures 5(a) and 5(b)). In order to assess the role of ROS on p-H2A.X assay, we pretreated cells with N-acetylcysteine (NAC) 10 mM for 1 h and then with CAP. After 6 h from treatment, we observed a decrease in p-H2A.X in cells pretreated with NAC and then exposed to CAP compared to cells treated only with CAP at the T1 condition (1.61-fold versus 1.9-fold compared to the untreated cells) (Figure 5(c)).

To understand whether CAP causes retained alterations in DNA sequence and thus a mutagenic effect, the generation of micronuclei (MN) was analyzed. 24 h after CAP exposure, a 3.2-fold increase in the frequency of MN was observed at the T1 condition (MN 0.24% versus 0.08% of the untreated cells) and a 10.2-fold increase at the T2 (MN 0.78%), compared to the untreated cells. The increase in MN frequency induced by EMS, used as positive control, was 5.3-fold compared to the untreated cultures (Figures 6(a) and 6(b)). The correlation index between the p-H2A.X expression and the MN frequency calculated by GraphPad InStat version 5.00 at 24 h posttreatment was 0.79. The 0.79 value indicates a strong positive linear relationship between the genotoxicity and mutagenicity of CAP. The MN test performed on binucleated cells by microscopic analysis confirmed the mutagenic effect of CAP (Figure 6(c)).

By analyzing the fluorescence histograms of SYTOX green, a nucleic acid dye, we demonstrated that the treatment of Jurkat cells with CAP inhibited cell-cycle progression and induced an accumulation of cells in the G2/M phase. For example, both CAP treatments under T1 and T2 conditions increased the percentage of cells in G2/M phase (69% and 72%, resp., versus 40% of the untreated cells), with a compensatory decrease of cells in S phase (6% and 9%, resp., versus 22% of control) and G0/G1 phase (25% and 19%, resp., versus 38% of the untreated cells).

4. Discussion

The effects of CAP on cancer cells were observed in an *in vitro* leukemia model. Complete medium containing serum was treated by means of DBD with two different operative conditions using different treatment time and gap that are known to play a crucial role in the RONS generation, as reported by Kuchenbecker et al. [36]. The plasma treatments induced the production of similar concentrations of hydrogen peroxide and higher concentration of nitrite in the T2 condition (120″). This difference on RONS concentrations

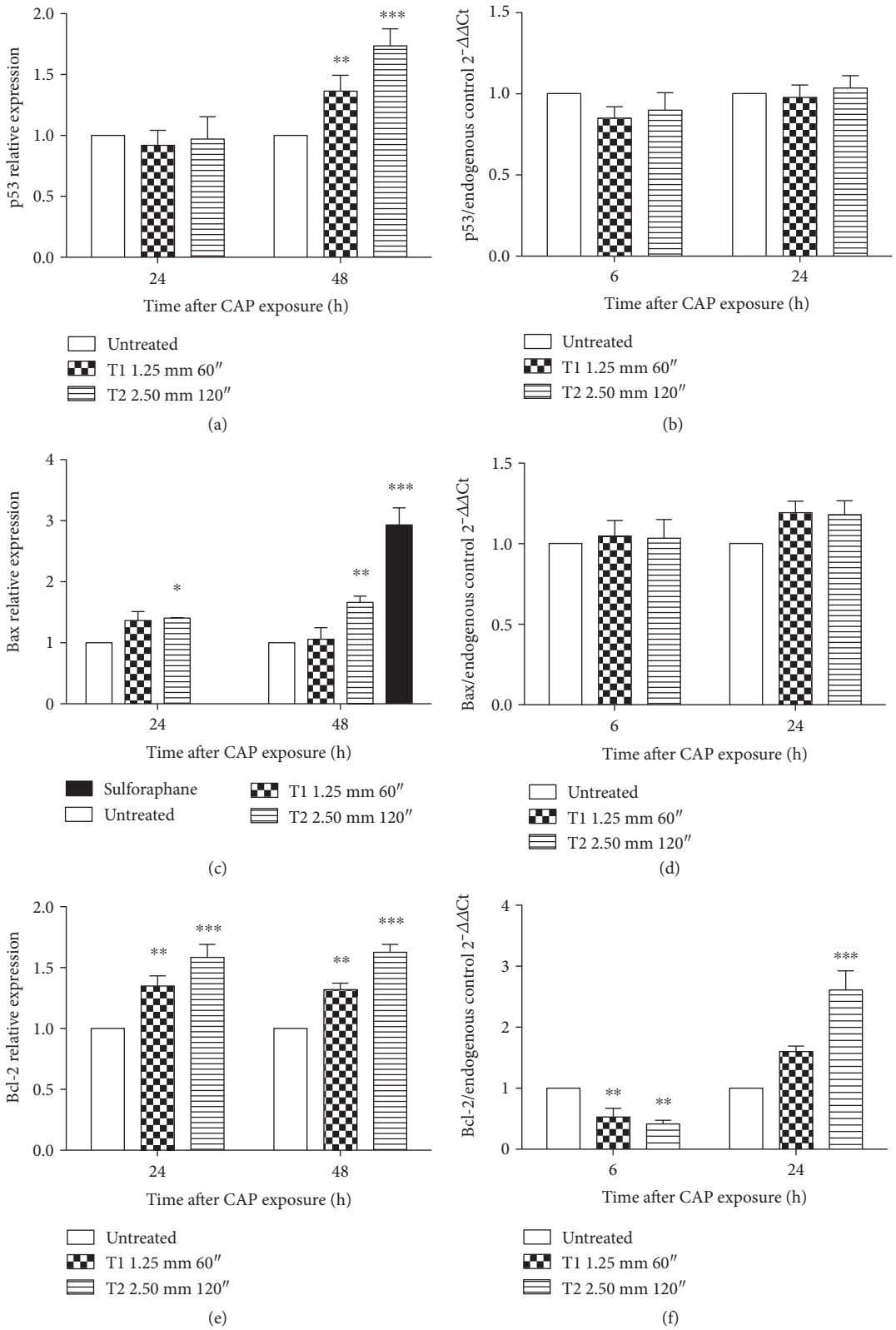

Figure 3: Continued.

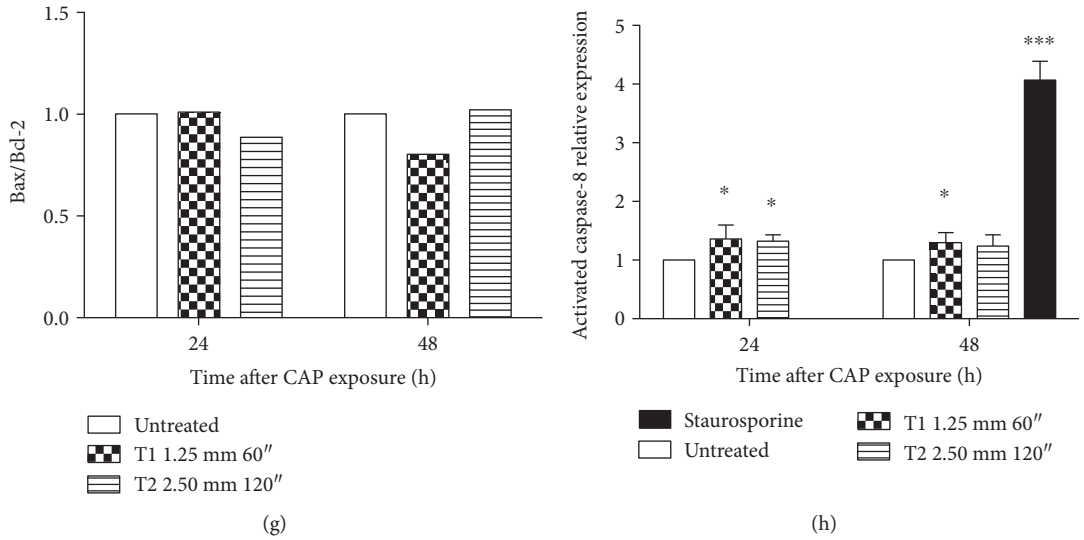

Figure 3: Effects of CAP on gene involved in the apoptotic pathway in Jurkat cells. Relative protein expression of (a) p53, (c) Bax (sulforaphane was used as positive control), and (e) Bcl-2 after 24 and 48 h after CAP exposure. mRNA expression of (b) p53, (d) Bax, and (f) Bcl-2 6 and 24 h after CAP exposure at T1 and T2 conditions. 18S ribosomal RNA and actin beta (ACTB) were used as endogenous controls. (g) Bax/Bcl-2 ratio. (h) Relative expression of caspase-8 24 and 48 h after CAP treatment. Staurosporine was used as positive control. Data are the mean of at least three different experiments. $^{*}P < 0.05$; $^{**}P < 0.01$; $^{***}P < 0.001$ versus the untreated cells.

could be related to the presence of serum in the treated medium that is known to scavenge hydrogen peroxide [24] while not affecting the nitrite accumulation. Furthermore, we hypothesize that the increase in nitrite concentration after T2 treatment could be ascribed to the higher gap (2.50 mm), which enhances the interaction between plasma and nitrogen in air.

The observed overexpression of p53 indicates the contribution of this protein to CAP-induced apoptosis. Apoptosis could be mediated by mitochondrial/intrinsic pathway or receptor/extrinsic pathway [37]. p53, a crucial protein in both mechanisms, has been identified as one of the most targetable molecules for developing anticancer treatment. Its activation, usually in response to DNA damage, and relevant signaling are key steps to induce apoptosis [38]. Apoptosis is a defense mechanism against stressed, damaged, and/or stimulated cells, and different regulatory pathways are involved to orchestrate this mechanism of cell death [37]. The involvement of the intrinsic pathway on CAP-induced apoptosis was verified through the analysis of Bax and Bcl-2 expression. Bax and Bcl-2 are two of the major proteins of Bcl-2 family and their ratio, meaning the balance of the expression between pro- and anti-apoptotic pathways determines apoptosis execution in response to external stimuli, thus, cell fate [39, 40]. The protein expression of Bax resulted significantly upregulated after CAP treatment, but no modulation was observed at RNA level. Moreover, CAP provoked an upregulation of Bcl-2 at protein level, but the effect was different at RNA level. In fact, mRNA expression was downregulated 6 h after treatment and upregulated longer time (i.e., 24 h) after CAP treatment. To understand how cells respond to stress, we quantified both protein and RNA expression. The different modulation of Bax and Bcl-2 at mRNA and protein levels recorded in our study could be due to the tiny mechanisms involved in the posttranscriptional regulation to turn mRNA into protein and the different time of proteins' turnover [41]. The observed increase in Bcl-2 protein observed in our experimental setting may also serve as a compensatory protection of Jurkat cells upon CAP insult. The increase in Bcl-2 expression could be justified by its involvement in the modulation of cellular oxidative stress, beside its well-established role as antiapoptotic protein [42]. In fact, it has been demonstrated that Bcl-2-overexpressing cells show a significant, but subpathological, enhancement of ROS output that, in turn, stimulates the antioxidant defense. Furthermore, the different regulations of Bcl-2 mRNA at different time points may be due to the different mechanisms of compensation triggered by stress or adaptation signaling in cancer cells, such as epigenetic mechanisms [43]. Other studies showed how CAP treatment reduced the mitochondrial membrane potential, downregulated the expression of Bcl-2 that, in our experimental system, we observed at RNA level, activated PARP, and released apoptosis-inducing factor from the mitochondria [13]. However, some limitations in our study deserve a consideration. The activation of the proapoptotic function of Bax can be regulated by interdependent mechanisms including post-translational modifications like phosphorylation. Protein kinase Cζ plays a critical role in promoting cell survival. It may phosphorylate and interact with Bax. Through these mechanisms, it leads to sequestration of Bax in cytoplasm and abrogation of its proapoptotic function [44]. We did not analyze the phosphorylation status of Bax with regard to protein and mRNA expression and its role in the modulation of apoptosis induced in cells treated with CAP.

The significant increase in caspase-8 activation and p53 upregulation indicates the involvement of the extrinsic pathway by CAP treatment. The cross talk between extrinsic and

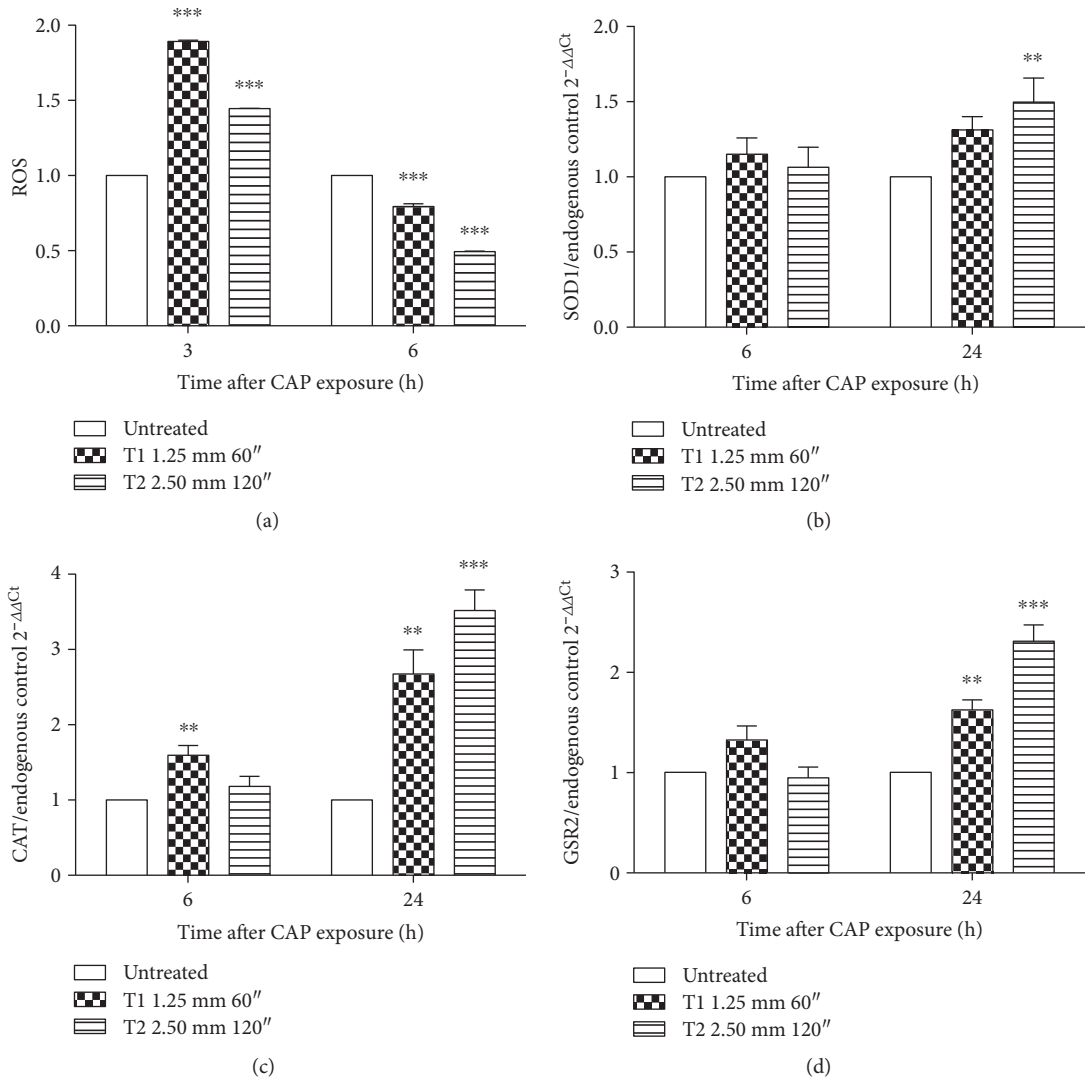

Figure 4: Effect of CAP on ROS levels and antioxidant enzymes. (a) Intracellular levels of ROS in Jurkat cells after CAP exposure for 3 and 6 h, measured via 2′,7′-diclorofluorescein (DCF) fluorescence. Relative mRNA expression of (b) SOD1, (c) CAT, and (d) GSR2 6 and 24 h after CAP treatment. 18S ribosomal RNA and actin beta (ACTB) were used as endogenous controls. Data are the mean of three different experiments. $^{**}P < 0.01$; $^{***}P < 0.001$ versus the untreated cells.

intrinsic pathways of apoptosis is regulated by Bid, a proapoptotic member of Bcl-2 family. The cleavage of Bid is mediated by caspase-8, which induces apoptosis by releasing cytochrome c from the mitochondria [37]. Other studies on DBD plasma demonstrated that the increased transcription of Bax and caspase-8 on U937 (human monocytic lymphoma) cells contributes to plasma-induced apoptosis [45].

Our results are in the agreement with previous studies on the effects of plasma on Jurkat cells. Bundscherer and colleagues investigated the effects of nonthermal plasma, using the kinpen, in Jurkat cells and demonstrated an increase in apoptotic events, depending on plasma treatment time. They confirmed the proapoptotic effect of plasma, which is due to the activation of caspase-3 and MAPK signaling pathway [46]. Cell death induced by CAP on Jurkat cells was also reported using a volume barrier discharge device in which the target is located between the two electrodes. No effects were observed when low energy (128 J/cm^2) was used to generate plasma discharge, but an apoptotic pattern was registered for medium energy (255 J/cm^2) and a purely necrotic pattern for high energy (425 J/cm^2) [47]. In our experimental system, a significant increase in necrotic events was observed when cells were treated with DBD for longer time (i.e., 120″) at the shortest distance from the medium (1.25 mm) after 24 h from treatment.

Oxidative stress has a major role in many biological processes [48]. The increase in ROS levels is involved in different physiological processes, such as proliferation and differentiation, while, over a certain intracellular level, ROS are responsible for cytotoxic and cytostatic effects [49]. Targeting oxidative equilibrium of tumor cells is currently a recognized approach to kill cancer cells [50, 51]. In fact, tumor cells are usually characterized by an increased basal oxidative stress, making them vulnerable to chemotherapeutic agents that further enhance ROS levels [52]. RONS generation has been actually proposed as a new theory behind CAP

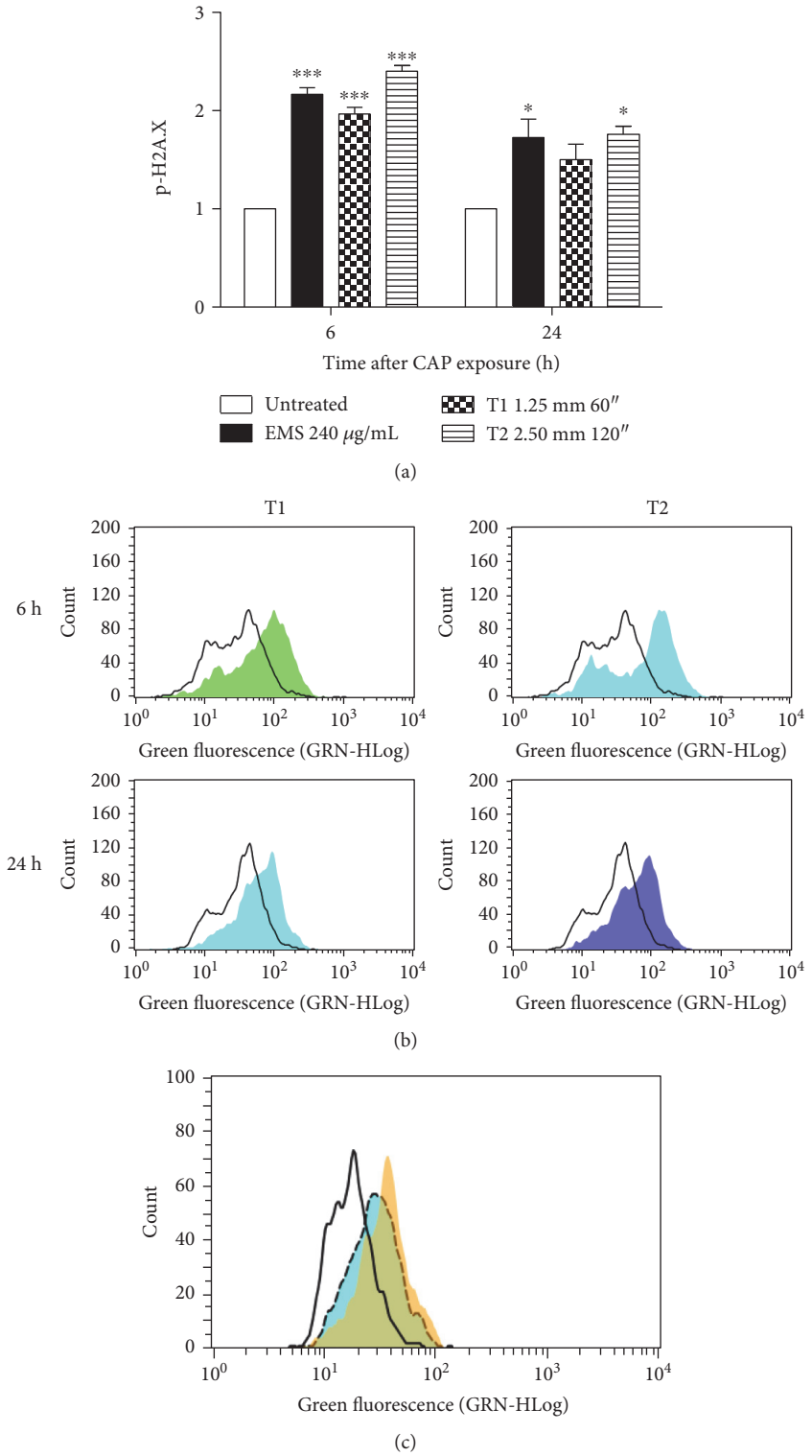

Figure 5: (a) Relative expression of p-H2A.X in Jurkat cells 6 and 24 h after CAP exposure. Ethyl methanesulfonate (EMS) was used as positive control. Data are the mean of three different experiments. (b) Representative histograms of p-H2A.X expression after 6 and 24 h at T1 and T2 treatment conditions. (c) Histogram of p-H2A.X expression representative of three different experiments performed with similar results. Black line: untreated cells; yellow histogram: cells after T1 CAP treatment; dashed line: cells pretreated with N-acetylcysteine (NAC) 10 mM and then exposed to CAP. $^{*}P < 0.05$; $^{***}P < 0.001$ versus the untreated cells.

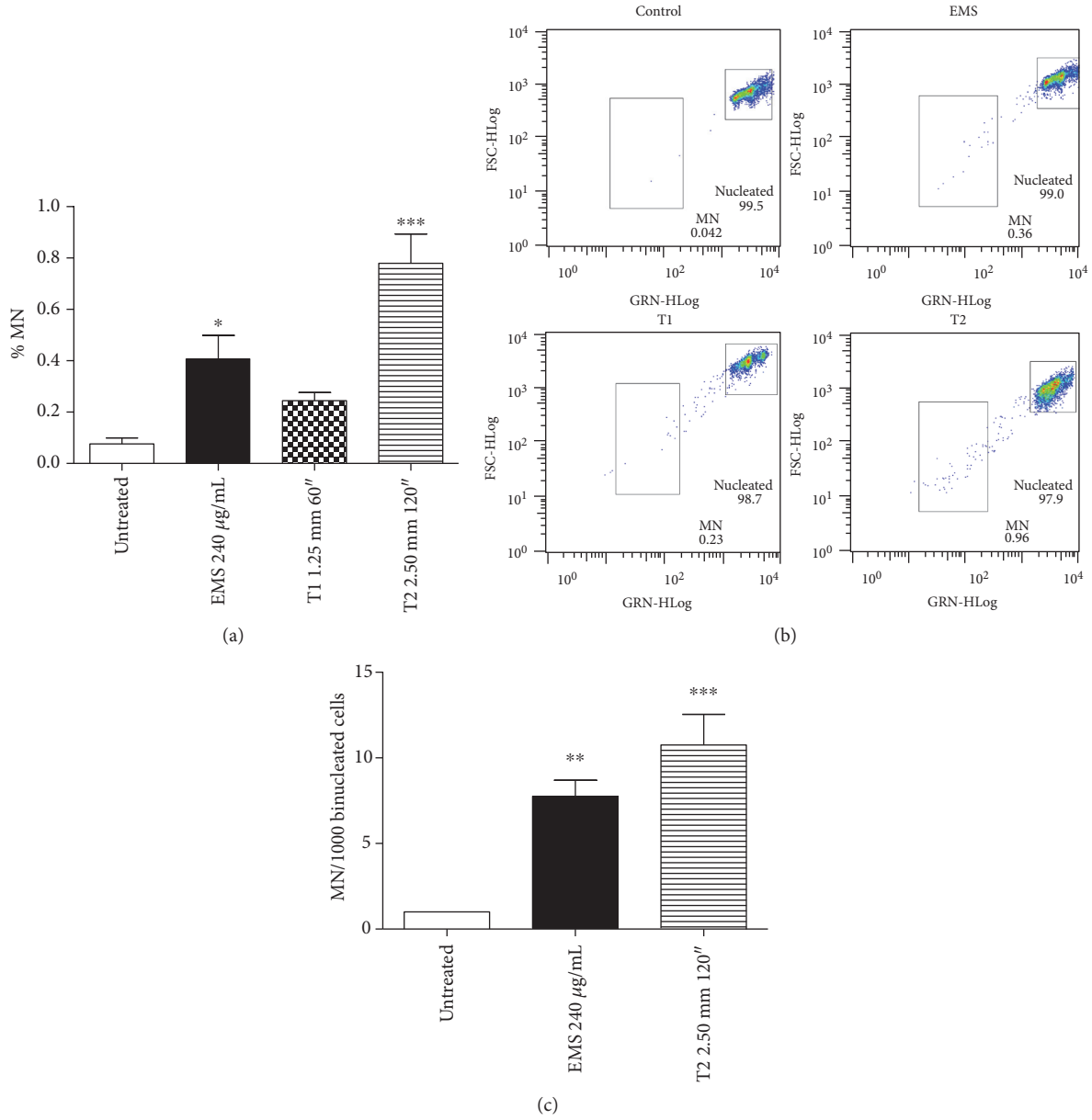

Figure 6: Induction of micronuclei (MN) 24 h after CAP exposure in Jurkat cells. Ethyl methanesulfonate (EMS) was used as positive control. (a) % of MN recorded flow cytometrically by SYTOX green/EMA. Data are the mean of three different experiments. (b) Representative results of the final gate of SYTOX fluorescence (GRN) versus forward scatter (FSC) of control, EMS, and CAP treatments under T1 and T2 conditions. (c) MN recorded microscopically on binucleated cells. $^{*}P < 0.05$; $^{**}P < 0.01$; and $^{***}P < 0.001$ versus the untreated cells.

selectivity [53]. We observed a significant increase in intracellular ROS levels after CAP treatment, according to literature data [23, 54], hence, potentially leading to a selective death of tumor cells. In our experimental settings, CAP modulated the intracellular ROS levels 3 h after treatment, whereas 6 h after plasma treatment, ROS were restored at levels similar or even lower than those of the pretreatment condition. This may be probably due to cellular compensatory mechanisms [55], such as the observed posttranscriptional regulation of SOD1, CAT, and GSR2. The major cellular defense against $O_2^{\bullet-}$ and peroxynitrite is a group of oxidoreductases known as SODs, which catalyze the dismutation of $O_2^{\bullet-}$ into oxygen and H_2O_2 that is detoxified to water by catalases and peroxidases [56]. GSH and GSH-dependent enzymes including GSR play a key role in cellular detoxification processes that enable organism to cope with various internal and environmental stressors [57]. The antioxidant response is therefore orchestrated from different enzymes that together in combined action give the antioxidant effect. The observed upregulation of SOD1, CAT, and GSR2 enzymes at RNA level supports the hypothesis that the combined interaction of plasma constituents, electric field, ions, and electrons with the biological cellular components induces oxidative stress.

However, the detailed biological mechanisms by which CAP can induce apoptosis is not yet clear [58]. As

previously mentioned, CAP affects cells both via direct and indirect treatments. In particular, H_2O_2-cooperating active species seem to be responsible to induce membrane alteration, increasing the permeability to other extracellular reactive species and further modulating intracellular ROS levels [13].

Due to the capacity of CAP to generate RONS, we evaluated its genotoxic potential through the analysis of premutational and mutational events. The phosphorylation of H2A.X is a reliable marker of genotoxicity and useful to predict the genotoxic potential of a compound [59]. In our study, CAP treatment induced a significant increase in the level of p-H2A.X under all tested treatment conditions, with higher values at 6 h as compared to 24 h after plasma treatment. Notably, the phosphorylation assay is a clear index of the ability of a xenobiotic, or in this case, a physical treatment, to interact with the DNA, thus causing a premutational lesion that could still be repaired by the DNA repair systems [60]. Furthermore, the decrease in DNA damage recorded 24 h after CAP exposure could be justified by the decrease in intracellular ROS levels observed at the same time point [61]. The reduction in p-H2A.X expression recorded after pretreatment of cells with NAC suggests that intracellular ROS levels play a role in the DNA damage induced by CAP. The evidence that scavenging proteins limited the effect of nonthermal plasma was previously reported. For example, Ma and colleagues showed that the cytotoxic effect of CAP is dose dependently reduced by the presence of ROS scavengers [23]. However, in our experimental settings, NAC did not fully abolish H2A.X phosphorylation. This means that other CAP components may interact with DNA. Furthermore, a growing body of evidence demonstrated that p-H2A.X is always induced when DNA double-strand breaks (DSBs) are provoked, but p-H2A.X should not be considered an unequivocal marker of DSBs and could not be a participant in the DNA damage response [62, 63]. To understand whether the CAP-induced DNA lesions are turned into mutations, the MN test was performed. To the best of our knowledge, this is the first report describing that CAP exposure significantly increased the frequency of MN on Jurkat cells at both exposure conditions, thus indicating a mutagenic and irreversible effect for CAP. The recovery of damaged cells under conditions where cell death occurred by apoptosis [64] suggests that the destruction of genetically damaged cells by the apoptosis effector pathways is not completely efficient. A huge amount of data demonstrated the genotoxic effects of plasma treatments in both prokaryotic and eukaryotic systems, but due to the complexity of DNA-plasma interaction, sometimes conflicting results are reported. Some studies showed the lack of mutagenic effect of plasma. For example, the treatment with the argon plasma jet kinpen did not display a mutagenic potential [65–67]. Taking into account the heterogeneity of plasma composition, each plasma source should be tested for both efficacy and safety aspects [24].

In conclusion, our results provide a deeper understanding of the potential of CAP as a promising physic-pharmacologic strategy in the oncological field and pose the basis for the evaluation of its toxicological profile.

Disclosure

These data were presented, in part, at the 6th International Conference on Plasma Medicine (ICPM6), September 4–9, 2016, Bratislava, Slovakia.

Conflicts of Interest

The authors declare that they have no conflicts of interest.

Acknowledgments

This work was supported by the National SIR Grant (RBSI14DBMB) "Non-thermal plasma as an innovative anticancer strategy: in vitro and ex vivo studies on leukemia models" and by COST Action TD1208 "Electrical discharges with liquids for future applications."

References

[1] T. Darny, J. M. Pouvesle, V. Puech, C. Douat, S. Dozias, and E. Robert, "Analysis of conductive target influence in plasma jet experiments through helium metastable and electric field measurements," *Plasma Sources Science and Technology*, vol. 26, no. 4, article 045008, 2017.

[2] A. Lin, B. Truong, S. Patel et al., "Nanosecond-pulsed DBD plasma-generated reactive oxygen species trigger immunogenic cell death in A549 lung carcinoma cells through intracellular oxidative stress," *International Journal of Molecular Sciences*, vol. 18, no. 5, p. 966, 2017.

[3] S. A. Norberg, E. Johnsen, and M. J. Kushner, "Helium atmospheric pressure plasma jets interacting with wet cells: delivery of electric fields," *Journal of Physics D: Applied Physics*, vol. 49, no. 18, article 185201, 2016.

[4] X. Lu, G. V. Naidis, M. Laroussi, S. Reuter, D. B. Graves, and K. Ostrikov, "Reactive species in non-equilibrium atmospheric-pressure plasmas: generation, transport, and biological effects," *Physics Reports*, vol. 630, pp. 1–84, 2016.

[5] A. M. Hirst, F. M. Frame, M. Arya, N. J. Maitland, and D. O'Connell, "Low temperature plasmas as emerging cancer therapeutics: the state of play and thoughts for the future," *Tumor Biology*, vol. 37, no. 6, pp. 7021–7031, 2016.

[6] M. Akhlaghi, H. Rajaei, A. S. Mashayekh et al., "Determination of the optimum conditions for lung cancer cells treatment using cold atmospheric plasma," *Physics of Plasmas*, vol. 23, no. 10, article 103512, 2016.

[7] N. Chernets, D. S. Kurpad, V. Alexeev, D. B. Rodrigues, and T. A. Freeman, "Reaction chemistry generated by nanosecond pulsed dielectric barrier discharge treatment is responsible for the tumor eradication in the B16 melanoma mouse model," *Plasma Processes and Polymers*, vol. 12, no. 12, pp. 1400–1409, 2015.

[8] W. H. Chung, "Mechanisms of a novel anticancer therapeutic strategy involving atmospheric pressure plasma-mediated apoptosis and DNA strand break formation," *Archives of Pharmacal Research*, vol. 39, no. 1, pp. 1–9, 2016.

[9] G. Fridman, A. Shereshevsky, M. M. Jost et al., "Floating electrode dielectric barrier discharge plasma in air promoting apoptotic behavior in melanoma skin cancer cell lines," *Plasma Chemistry and Plasma Processing*, vol. 27, no. 2, pp. 163–176, 2007.

[10] Z. Chen, L. Lin, X. Cheng, E. Gjika, and M. Keidar, "Treatment of gastric cancer cells with nonthermal atmospheric plasma generated in water," *Biointerphases*, vol. 11, no. 3, article 031010, 2016.

[11] M. Gherardi, E. Turrini, R. Laurita et al., "Atmospheric non-equilibrium plasma promotes cell death and cell-cycle arrest in a lymphoma cell line," *Plasma Processes and Polymers*, vol. 12, no. 12, pp. 1354–1363, 2015.

[12] H. Tanaka, K. Nakamura, M. Mizuno et al., "Non-thermal atmospheric pressure plasma activates lactate in Ringer's solution for anti-tumor effects," *Scientific Reports*, vol. 6, article 36282, 2016.

[13] T. Adachi, H. Tanaka, S. Nonomura, H. Hara, S. Kondo, and M. Hori, "Plasma-activated medium induces A549 cell injury via a spiral apoptotic cascade involving the mitochondrial-nuclear network," *Free Radical Biology and Medicine*, vol. 79, pp. 28–44, 2015.

[14] K. Torii, S. Yamada, K. Nakamura et al., "Effectiveness of plasma treatment on gastric cancer cells," *Gastric Cancer*, vol. 18, no. 3, pp. 635–643, 2015.

[15] N. Kumar, J. H. Park, S. N. Jeon, B. S. Park, E. H. Choi, and P. Attri, "The action of microsecond-pulsed plasma-activated media on the inactivation of human lung cancer cells," *Journal of Physics D: Applied Physics*, vol. 49, no. 11, article 115401, 2016.

[16] J. Florian, N. Merbahi, and M. Yousfi, "Genotoxic and cytotoxic effects of plasma-activated media on multicellular tumor spheroids," *Plasma Medicine*, vol. 6, no. 1, pp. 47–57, 2016.

[17] D. Yan, N. Nourmohammadi, A. Talbot, J. H. Sherman, and M. Keidar, "The strong anti-glioblastoma capacity of the plasma-stimulated lysine-rich medium," *Journal of Physics D: Applied Physics*, vol. 49, no. 27, article 274001, 2016.

[18] D. Yan, N. Nourmohammadi, K. Bian, F. Murad, J. H. Sherman, and M. Keidar, "Stabilizing the cold plasma-stimulated medium by regulating medium's composition," *Scientific Reports*, vol. 6, article 26016, 2016.

[19] P. Bao, X. Lu, M. He, and D. Liu, "Kinetic analysis of delivery of plasma reactive species into cells immersed in culture media," *IEEE Transactions on Plasma Science*, vol. 44, no. 11, pp. 2673–2681, 2016.

[20] K. Wende, P. Williams, J. Dalluge et al., "Identification of the biologically active liquid chemistry induced by a nonthermal atmospheric pressure plasma jet," *Biointerphases*, vol. 10, no. 2, article 029518, 2015.

[21] D. B. Graves, "Reactive species from cold atmospheric plasma: implications for cancer therapy," *Plasma Processes and Polymers*, vol. 11, no. 12, pp. 1120–1127, 2014.

[22] H. J. Ahn, K. I. Kim, N. N. Hoan et al., "Targeting cancer cells with reactive oxygen and nitrogen species generated by atmospheric-pressure air plasma," *PLoS One*, vol. 9, no. 1, article e86173, 2014.

[23] Y. Ma, C. S. Ha, S. W. Hwang et al., "Non-thermal atmospheric pressure plasma preferentially induces apoptosis in p53-mutated cancer cells by activating ROS stress-response pathways," *PLoS One*, vol. 9, no. 4, article e91947, 2014.

[24] D. Boehm, C. Heslin, P. J. Cullen, and P. Bourke, "Cytotoxic and mutagenic potential of solutions exposed to cold atmospheric plasma," *Scientific Reports*, vol. 6, article 21464, 2016.

[25] M. Vandamme, E. Robert, S. Pesnel et al., "Antitumor effect of plasma treatment on U87 glioma xenografts: preliminary results," *Plasma Processes and Polymers*, vol. 7, no. 3-4, pp. 264–273, 2010.

[26] S. Takeda, S. Yamada, N. Hattori et al., "Intraperitoneal administration of plasma-activated medium: proposal of a novel treatment option for peritoneal metastasis from gastric cancer," *Annals of Surgical Oncology*, vol. 24, no. 5, pp. 1188–1194, 2017.

[27] F. Utsumi, H. Kajiyama, K. Nakamura et al., "Effect of indirect nonequilibrium atmospheric pressure plasma on anti-proliferative activity against chronic chemo-resistant ovarian cancer cells in vitro and in vivo," *PLoS One*, vol. 8, no. 12, article e81576, 2013.

[28] H. R. Metelmann, D. S. Nedrelow, C. Seebauer et al., "Head and neck cancer treatment and physical plasma," *Clinical Plasma Medicine*, vol. 3, no. 1, pp. 17–23, 2015.

[29] V. Miller, A. Lin, and A. Fridman, "Why target immune cells for plasma treatment of cancer," *Plasma Chemistry and Plasma Processing*, vol. 36, no. 1, pp. 259–268, 2016.

[30] D. A. Wink, H. B. Hines, R. Y. Cheng et al., "Nitric oxide and redox mechanisms in the immune response," *Journal of Leukocyte Biology*, vol. 89, no. 6, pp. 873–891, 2011.

[31] V. Miller, A. Lin, G. Fridman, D. Dobrynin, and A. Fridman, "Plasma stimulation of migration of macrophages," *Plasma Processes and Polymers*, vol. 11, no. 12, pp. 1193–1197, 2014.

[32] R. Laurita, F. Alviano, C. Marchionni et al., "A study of the effect on human mesenchymal stem cells of an atmospheric pressure plasma source driven by different voltage waveforms," *Journal of Physics D: Applied Physics*, vol. 49, no. 36, article 364003, 2016.

[33] S. M. Bryce, J. C. Bemis, S. L. Avlasevich, and S. D. Dertinger, "in vitro micronucleus assay scored by flow cytometry provides a comprehensive evaluation of cytogenetic damage and cytotoxicity," *Mutation Research/Genetic Toxicology and Environmental Mutagenesis*, vol. 630, no. 1, pp. 78–91, 2007.

[34] M. Fenech and A. A. Morley, "Measurement of micronuclei in lymphocytes," *Mutation Research/Environmental Mutagenesis and Related Subjects*, vol. 147, no. 1-2, pp. 29–36, 1985.

[35] M. Fenech, "The cytokinesis-block micronucleus technique: a detailed description of the method and its application to genotoxicity studies in human populations," *Mutation Research/Fundamental and Molecular Mechanisms of Mutagenesis*, vol. 285, no. 1, pp. 35–44, 1993.

[36] M. Kuchenbecker, N. Bibinov, A. Kaemlimg, D. Wandke, P. Awakowicz, and W. Viöl, "Characterization of DBD plasma source for biomedical applications," *Journal of Physics D: Applied Physics*, vol. 42, no. 4, article 045212, 2009.

[37] Y. Kiraz, A. Adan, M. Kartal Yandim, and Y. Baran, "Major apoptotic mechanisms and genes involved in apoptosis," *Tumor Biology*, vol. 37, no. 7, pp. 8471–8486, 2016.

[38] P. Bragado, A. Armesilla, A. Silva, and A. Porras, "Apoptosis by cisplatin requires p53 mediated p38α MAPK activation through ROS generation," *Apoptosis*, vol. 12, no. 9, pp. 1733–1742, 2007.

[39] M. Raisova, A. M. Hossini, J. Eberle et al., "The Bax/Bcl-2 ratio determines the susceptibility of human melanoma cells to CD95/Fas-mediated apoptosis," *Journal of Investigative Dermatology*, vol. 117, no. 2, pp. 333–340, 2001.

[40] J. M. Adams and S. Cory, "The Bcl-2 protein family: arbiters of cell survival," *Science*, vol. 281, no. 5381, pp. 1322–1326, 1998.

[41] D. Greenbaum, C. Colangelo, K. Williams, and M. Gerstein, "Comparing protein abundance and mRNA expression levels on a genomic scale," *Genome Biology*, vol. 4, no. 9, p. 117, 2003.

[42] D. W. Voehringer and R. E. Meyn, "Redox aspects of Bcl-2 function," *Antioxidants and Redox Signaling*, vol. 2, no. 3, pp. 537–550, 2000.

[43] S. Willimott and S. D. Wagner, "Post-transcriptional and post-translational regulation of Bcl2," *Biochemical Society Transactions*, vol. 38, no. 6, pp. 1571–1575, 2010.

[44] M. Xin, F. Gao, W. S. May, T. Flagg, and X. Deng, "Protein kinase Cζ abrogates the proapoptotic function of Bax through phosphorylation," *Journal of Biological Chemistry*, vol. 282, no. 29, pp. 21268–21277, 2007.

[45] N. Kaushik, N. Kumar, C. H. Kim, N. K. Kaushik, and E. H. Choi, "Dielectric barrier discharge plasma efficiently delivers an apoptotic response in human monocytic lymphoma," *Plasma Processes and Polymers*, vol. 11, no. 12, pp. 1175–1187, 2014.

[46] L. Bundscherer, K. Wende, K. Ottmüller et al., "Impact of non-thermal plasma treatment on MAPK signaling pathways of human immune cell lines," *Immunobiology*, vol. 218, no. 10, pp. 1248–1255, 2013.

[47] A. Duval, I. Marinov, G. Bousquet et al., "Cell death induced on cell cultures and nude mouse skin by non-thermal, nanosecond-pulsed generated plasma," *PLoS One*, vol. 8, no. 12, article e83001, 2013.

[48] P. Sestili and C. Fimognari, "Cytotoxic and antitumor activity of sulforaphane: the role of reactive oxygen species," *BioMed Research International*, vol. 2015, Article ID 402386, 9 pages, 2015.

[49] R. B. Hamanaka and N. S. Chandel, "Mitochondrial reactive oxygen species regulate cellular signaling and dictate biological outcomes," *Trends in Biochemical Sciences*, vol. 35, no. 9, pp. 505–513, 2010.

[50] L. Raj, T. Ide, A. U. Gurkar et al., "Selective killing of cancer cells by a small molecule targeting the stress response to ROS," *Nature*, vol. 475, no. 7355, pp. 231–234, 2011.

[51] H. W. Lee, G. Y. Park, Y. S. Seo, Y. H. Im, S. B. Shim, and H. J. Lee, "Modelling of atmospheric pressure plasmas for biomedical applications," *Journal of Physics D: Applied Physics*, vol. 44, no. 5, article 053001, 2011.

[52] P. T. Schumacker, "Reactive oxygen species in cancer cells: live by the sword, die by the sword," *Cancer Cell*, vol. 10, no. 3, pp. 175-176, 2006.

[53] G. Bauer and D. B. Graves, "Mechanisms of selective antitumor action of cold atmospheric plasma-derived reactive oxygen and nitrogen species," *Plasma Processes and Polymers*, vol. 13, no. 12, pp. 1157–1178, 2016.

[54] S. Kalghatgi, C. M. Kelly, E. Cerchar et al., "Effects of non-thermal plasma on mammalian cells," *PLoS One*, vol. 6, no. 1, article e16270, 2011.

[55] G. Y. Liou and P. Storz, "Reactive oxygen species in cancer," *Free Radical Research*, vol. 44, no. 5, pp. 479–496, 2010.

[56] T. Fukai and M. Ushio-Fukai, "Superoxide dismutases: role in redox signaling, vascular function, and diseases," *Antioxidants & Redox Signaling*, vol. 15, no. 6, pp. 1583–1606, 2011.

[57] K. Lüersen, D. Stegehake, J. Daniel et al., "The glutathione reductase GSR-1 determines stress tolerance and longevity in *Caenorhabditis elegans*," *PLoS One*, vol. 8, no. 4, article e60731, 2013.

[58] E. A. Ratovitski, X. Cheng, D. Yan et al., "Anti-cancer therapies of 21st century: novel approach to treat human cancers using cold atmospheric plasma," *Plasma Processes and Polymers*, vol. 11, no. 12, pp. 1128–1137, 2014.

[59] G. P. Watters, D. J. Smart, J. S. Harvey, and C. A. Austin, "H2AX phosphorylation as a genotoxicity endpoint," *Mutation Research/Genetic Toxicology and Environmental Mutagenesis*, vol. 679, no. 1, pp. 50–58, 2009.

[60] T. T. Paull, E. P. Rogakou, V. Yamazaki, C. U. Kirchgessner, M. Gellert, and W. M. Bonner, "A critical role for histone H2AX in recruitment of repair factors to nuclear foci after DNA damage," *Current Biology*, vol. 10, no. 15, pp. 886–895, 2000.

[61] K. P. Arjunan, V. K. Sharma, and S. Ptasinska, "Effects of atmospheric pressure plasmas on isolated and cellular DNA-a review," *International Journal of Molecular Sciences*, vol. 16, no. 2, pp. 2971–3016, 2015.

[62] P. Rybak, A. Hoang, L. Bujnowicz et al., "Low level phosphorylation of histone H2AX on serine 139 (gammaH2AX) is not associated with DNA double-strand breaks," *Oncotarget*, vol. 7, no. 31, pp. 49574–49587, 2016.

[63] J. E. Cleaver, "γH2Ax: biomarker of damage or functional participant in DNA repair "all that glitters is not gold!"," *Photochemistry and Photobiology*, vol. 87, no. 6, pp. 1230–1239, 2011.

[64] W. P. Roos and B. Kaina, "DNA damage-induced cell death: from specific DNA lesions to the DNA damage response and apoptosis," *Cancer Letters*, vol. 332, no. 2, pp. 237–248, 2013.

[65] V. Boxhammer, Y. F. Li, J. Köritzer et al., "Investigation of the mutagenic potential of cold atmospheric plasma at bactericidal dosages," *Mutation Research/Genetic Toxicology and Environmental Mutagenesis*, vol. 753, no. 1, pp. 23–28, 2013.

[66] K. Wende, S. Bekeschus, A. Schmidt et al., "Risk assessment of a cold argon plasma jet in respect to its mutagenicity," *Mutation Research/Genetic Toxicology and Environmental Mutagenesis*, vol. 798, pp. 48–54, 2016.

[67] S. Kluge, S. Bekeschus, C. Bender et al., "Investigating the mutagenicity of a cold argon-plasma jet in an HET-MN model," *PLoS One*, vol. 11, no. 9, article e0160667, 2016.

Hindawi
Oxidative Medicine and Cellular Longevity
Volume 2017, Article ID 2487297, 15 pages
https://doi.org/10.1155/2017/2487297

Research Article

2-Deoxy-D-glucose Restore Glucocorticoid Sensitivity in Acute Lymphoblastic Leukemia via Modification of N-Linked Glycosylation in an Oxygen Tension-Independent Manner

Zaira Leni,[1] Paulina Ćwiek,[1] Valeriya Dimitrova,[1] Andrea S. Dulcey,[1] Nicola Zamboni,[2] Cedric Simillion,[3] Geetha Rossi,[1] Kurt Leibundgut,[1] and Alexandre Arcaro[1]

[1]*Division of Pediatric Hematology/Oncology, Bern University Hospital, Bern, Switzerland*
[2]*Institute of Molecular Systems Biology, ETH Zürich, Zürich, Switzerland*
[3]*Department of Clinical Research, University of Bern, Bern, Switzerland*

Correspondence should be addressed to Zaira Leni; leni.zaira@dkf.unibe.ch

Received 3 March 2017; Revised 24 April 2017; Accepted 8 May 2017; Published 26 July 2017

Academic Editor: Sander Bekeschus

In childhood acute lymphoblastic leukemia, treatment failure is associated with resistance to glucocorticoid agents. Resistance to this class of drugs represents one of the strongest indicators of poor clinical outcome. We show that leukemic cells, which are resistant to the glucocorticoid drug methylprednisolone, display a higher demand of glucose associated with a deregulation of metabolic pathways, in comparison to sensitive cells. Interestingly, a combinatorial treatment of glucocorticoid and the glucose analog 2-deoxy-D-glucose displayed a synergistic effect in methylprednisolone-resistant cells, in an oxygen tension-independent manner. Unlike solid tumors, where 2-deoxy-D-glucose promotes inhibition of glycolysis by hexokinase II exclusively under hypoxic conditions, we were able to show that the antileukemic effects of 2-deoxy-D-glucose are far more complex in leukemia. We demonstrate a hexokinase II-independent cell viability decrease and apoptosis induction of the glucose analog in leukemia. Additionally, due to the structural similarity of 2-deoxy-D-glucose with mannose, we could confirm that the mechanism by which 2-deoxy-D-glucose predominantly acts in leukemia is via modification in N-linked glycosylation, leading to endoplasmic reticulum stress and consequently induction of the unfolded protein response.

1. Introduction

Acute lymphoblastic leukemia (ALL) is the second most common cause of death in children and adolescents, behind accidents. Significant advances have been made in the successful treatment of childhood-ALL (ch-ALL), leading to an overall survival rate approaching 90% in children [1]. Despite this success, a subset of patients remains refractory to chemotherapy and suffers from relapse which is associated with poor outcome. The conventional ch-ALL treatment consists of several classes of chemotherapeutic agents including glucocorticoids (GCs) and fails in approximately 20% of the patients [2–4]. Resistance to GCs, such as methylprednisolone (MP), is related to unfavorable prognosis. Therefore, it is important to develop alternative therapies that can overcome MP resistance. Previous reports have suggested that leukemic cells from ALL patients resistant to GC treatment present an increase in glycolytic rate [5, 6]. Moreover, it has been shown that solid tumors have altered rates of glucose transport and glycolysis in comparison to their nonmalignant counterparts [7–10]. The treatment of ch-ALL with the glycolysis inhibitor 2-deoxy-D-glucose (2-DG) provided the first evidence that ALL have a similar metabolic shift as solid tumors [11]. 2-DG has been extensively described to competitively inhibit hexokinase (HK) and glucose phosphoisomerase (PGI) in solid tumors [12]. Indeed, 2-DG can enter into the cell through glucose transporter GLUT-1, where it is converted to 2-deoxy-D-glucose-6-phosphate (2-DG6P) by HK. Unlike the endogenous substrate, G6P, 2-DG6P cannot be further metabolized by the second enzyme in the glycolytic pathway, PGI. It has been shown that in solid tumors, 2-DG6P accumulation inhibits glycolysis which

represents the main mechanism of 2-DG cytotoxicity [13]. Furthermore, it has been previously reported that in cancer cells growing under hypoxic conditions, 2-DG causes apoptosis by inhibiting glycolysis [12]. In this study, we demonstrate that, in contrast to solid tumors, 2-DG induces apoptosis in ch-ALL cell lines in combination with MP under normal oxygen tension. In addition, we report that the cytotoxic activity of 2-DG in leukemia cell line is not primary through glycolysis inhibition, since silencing of *HKII* does not interfere with 2-DG-mediated decrease in cell viability. We hypothesize that, in leukemia cells, 2-DG predominantly acts as an inhibitor of N-linked glycosylation (NLG) due to its structural similarity with mannose. 2-DG can be fraudulently incorporated in the place of mannose on the oligosaccharide chain and lead to accumulation of misfolded proteins [12]. The accumulation of misfolded proteins in the lumen of the endoplasmic reticulum (ER) leads to ER stress and, as a consequence, the induction of the unfolded protein response (UPR) [13]. Taken together, the cytotoxic activity of 2-DG in selected ch-ALL cells under aerobic conditions is caused by interfering with NLG rather than inhibition of glycolysis. Furthermore, we discovered an additional mechanism of 2-DG action, which involves glycogen synthase kinase-3 (GSK-3) in the context of MP resistance in ch-ALL cell lines.

2. Material and Methods

2.1. Calculation of Synergy. Synergistic effects of drugs were evaluated as equipotent drug concentrations by the equation developed by Berenbaum [14]. A dose-response curve was constructed for each single drug and combinations of two drugs together. The values calculated according to the Berenbaum equation are referred to as a synergy factor (F_{syn}). A value < 1 indicates synergy, F_{syn} equal to 1 indicates an additive effect, and $F_{syn} > 1$ represents an antagonist effect.

2.2. Glucose-Consumption Assay. Glucose levels were measured with the glucose assay kit (Sigma, Buchs, Switzerland), as described by the manufacturer. Briefly, 5×10^5 cells were cultured and after 96 h medium was collected and incubated for 30 minutes with glucose assay buffer (1.5 mM NAD, 1 mM ATP, 1 U/ml hexokinase and 1 U/ml glucose-6-phosphate dehydrogenase). During this time, glucose is phosphorylated to glucose-6-phosphate (G6P), and the latter is then oxidized to 6-phosphate glucoronate in the presence of NAD. Conversion of NAD to NADH was measured by the increase in absorbance at 340 nm, which is directly proportional to the glucose concentration. To calculate glucose consumption, values were compared with media (RPMI or IMDM) glucose levels and corrected for cell growth.

2.3. Flow Cytometry. Apoptosis was assessed by fluorescence-activated cell sorting (FACS) after treatment with MP and 2-DG or the combination of drugs. Cells were harvested, pelleted by centrifugation, and washed with phosphate-buffered saline (PBS). Subsequently, leukemic cells were resuspended in 100 μl of binding buffer (1.4 M NaCl, 25 mM CaCl, 0.1 M Hepes; pH 7.4) and stained with FITC-labeled Annexin-V-fluorescein isothiocyanate (Biotium, Hayward, CA, USA) and 7-Aminoactinomycin D (7-AAD) according to the manufacturer's protocol (BD Biosciences, Mississauga, ON) and analyzed on a Becton-Dickinson LSR II flow cytometer using BD FACSDiva software (version 6.1.3; Becton Dickinson AG, Allschwil, Switzerland) and FlowJo software (version 5.4+; Three Star Inc., Ashland, OR, USA). PE Active Caspase-3 Apoptotic kit (BD Pharmigen, San Diego, CA, USA) according with manufacture's instruction was used to confirm apoptosis. Flow cytometry analysis measurements were performed in singlet with three repetitions of each individual experiment.

2.4. Nucleofection. Silencing of *HKII* gene by small interfering RNA (siRNA) was performed by nucleofection using the Amaxa Nucleofector II (Amaxa Biosystems, Cologne, Germany), following the manufacturer's instructions. Each sample was transfected with 300 nM siRNA (HKII: siRNA IDs 6562) (Ambion, Applied Biosystem, USA) using the program X-01 of the Nucleofector II. The transfection efficiency was evaluated by quantitative RT-PCR after 24 h. Following the same procedure, protein extracts were analyzed by Western blotting 48 h after transfection, and the impact on cell viability was evaluated by using the MTS assay (Promega, Madison, WI, USA).

2.5. Microarray Analysis. The raw data in the form of Affymetrix.CEL hybridisation files from the dataset of Haferlach et al. [15] were downloaded from the ArrayExpress database (accession E-GEOD-13159). The data was background-corrected and normalized using the Robust Microarray Analysis method. Gene summarization was done using the alternative CDF files provided by Dai et al. [16]. Differential gene expression of 121 ch-ALL samples carrying the translocation t(9;22) (Philadelphia chromosome positive) and 236 ch-ALL samples without this translocation compared to 72 healthy bone marrow samples was calculated using the limma R-package.

2.6. Metabolite Profiling. A total of 234 samples from SUP-15, SD1, and REH leukemia cell lines were treated with vehicle (Benzyl alcohol, AB), MP, and 2-DG or the combination for 0, 6, 12, 18, 24, and 48 h. Cells were extracted using a modified version of a previously described protocol. Briefly, rapid inactivation of metabolism was obtained by a two-step process consisting of initial quenching of the cells, followed by extraction of the metabolites. Quenching procedure: 2×10^6 cells were washed twice with 150 μl of ammonium carbonate (75 mM, pH 7.4) prewarmed at 75°C and shaken on a heating block. Cells were pelleted by centrifugation and snap-frozen in liquid nitrogen. For metabolite extraction, pellets were treated twice with 150 μl of hot extraction solution (75°C, 70% *v*/*v* pure ethanol) and placed in a heating block (75°C) for 3 minutes. The collected supernatants were completely dried under vacuum. Dry extracts were stored at −80°C until metabolomics analysis. Nontargeted metabolome profiling was done by flow injection—time-of-flight analysis in negative mode on an

Agilent 6550 QTOF instrument (Agilent, Santa Clara CA, USA).

2.7. Clustering Analysis and Metabolite Pathway Analysis. The ion intensities were first log-transformed and then averaged over all technical replicates per condition, resulting in a matrix with 60 columns for 4 treatments, 3 cell lines and 5 time points, and 827 rows for as many ions. For each noncontrol condition—that is, any treatment with MP, 2-DG, or 2-DG+MP—log-fold change values were calculated by subtracting the log-transformed intensities from the corresponding, that is, same cell line and time point, control sample. This operation resulted in a matrix with 45 columns—3 cell lines x 3 treatments x 5 time points—and 827 rows. Of these 827 ions, we retained only those with significantly changing intensities, either over time or across different treatments compared to the control treatment, using the limma method [17]. Using an adjusted p value cutoff of 0.01, 649 ions were retained. Next, k-medoids clustering was performed to detect groups of similarly regulated ions using the correlation distance as distance metric. Using the silhouette width quality score, the optimal number of clusters to create was found to be 5. We then used the SetRank algorithm to look for overrepresented pathways in each cluster, using metabolite annotation from the KEGG and Reactome databases [18, 19].

2.8. High-Throughput Protein Kinase Inhibitors Screen. REH and SD1 leukemia cells were screened with a library of 365 GlaxoSmithKline Published Kinase Inhibitor Set (GSK, PLC United Kingdom) [20]. The cells were plated at a minimum density of 30,000 cells per well, in 96-well plates in triplicates. Cells were treated with MP (150 μg/ml for REH and 100 μg/ml for SD1) alone and/or in combination with the kinase inhibitors at the final concentration of 1 μM. Dimethyl sulfoxide (DMSO, Sigma-Aldrich Chemie Gmbh, Buchs, Switzerland) as a negative control was added to each plate of the library. Validation of the hit candidates was evaluated after 72 h using the MTS assay. SB-360741 a 3-anilino-4-arylmalemide, GSK-3 inhibitor was selected and further validated in SD1 and REH cell lines.

2.9. Statistical Analysis. All statistics were performed in GraphPad Prism software (La Jolla, CA, USA). The statistical significance of differences between groups was assessed by two-way analysis of variance (ANOVA) correct for Bonferroni's multiple comparison test. p values of <0.05 were considered significant.

3. Results

3.1. 2-DG Modulates MP-Induced Cytotoxicity in Resistant ch-ALL Cell Lines. 2-DG, a synthetic glucose analog with a primary function to inhibit glycolysis, has been reported to synergize with standard anticancer treatments in the induction of cell death in several carcinoma types [10, 21, 22]. MP resistance in leukemia has been associated with an increased expression of genes involved in glucose metabolism. Moreover, inhibition of glycolysis was shown to sensitize leukemia cells to prednisone [5]. Single treatment with MP was administrated to three leukemia cell lines, and according to their responses, they were classified as sensitive (SUP-B15), intermediate (SD1), and resistant (REH) cells toward MP (Figure 1). To determine the effects of 2-DG, SUP-B15, SD1, and REH, cells were exposed to increasing concentration of the glucose analog and their growth and cytotoxic responses were assessed (Figure 1). SUP-B15 and SD1 displayed a dose-dependent decrease in cell viability (Figures 1(a) and 1(b)) in response to the glycolysis inhibitor. The REH cell line showed a higher resistance towards 2-DG (Figure 1(c)). Thus, it was necessary to increase the dose of the glucose analog in order to obtain the same biological effect. To further investigate if the observed synergism of chemotherapy and 2-DG reported in carcinoma cells could also be observed in the case of GCs sensitization towards MP, 2-DG was administrated with sublethal concentrations of MP. Coincubation of 2-DG and MP displayed increased cytotoxicity in all leukemia cell lines tested. All three leukemia cell lines displayed synergistic effects between the two drugs, with values of $F_{syn} = 0.86$, 0.95, and 0.58 for SUP-B15, SD1, and REH, respectively (Figure 2). Moreover, SD1 displayed a dose-dependent viability decrease upon combinatorial treatment with all three concentrations of 2-DG tested (Figure 2(b)), while the effect on REH cell line was independent of the dose of 2-DG (Figure 2(c)). In contrast, the synergistic effect in SUP-B15 was observed only at the higher concentration of 2-DG (0.25 mM) (Figure 2(a)).

3.2. 2-DG Inhibits Glucose Consumption, Utilization, and Uptake. To determine whether metabolic changes are associated with glucocorticoid resistance in ch-ALL and to further investigate the hypothesis that this cancer relies on glycolysis to produce ATP and biomass, we analyzed the glucose uptake in a panel of leukemia cell lines (Figure 3). The cells were cultured in normal media in the presence or absence of single drugs or combinatorial drug treatments. Despite the broad spectrum of treatment concentrations, the SUP-B15 cell line did not display any differences in glucose uptake upon treatment with MP (Figure 3(a)), 2-DG (Figure 3(b)), or the combination suggesting that the survival of this cell line does not rely exclusively on glycolysis (Figure 3(d)). This observation can be in part explained by SUP-B15 sensitivity to MP. In contrast, SD1 and REH cells displayed an increase in glucose consumption and a significant rescue of the glucose uptake upon 2-DG treatment (Figures 3(b) and 3(c)) at the concentration of 1 mM. Moreover, the combinatorial treatment of MP (50 μg/ml) and 2-DG (0.5 mM) was able to revert the glucose uptake significantly, after 96 h exposure (Figures 3(e) and 3(f)).

3.3. 2-DG Sensitizes Resistant ch-ALL Cell Lines to MP-Induced Apoptosis. To analyze the mechanism of action of the combinatorial treatment of 2-DG and MP as a cause of cell viability decrease, a flow cytometry analysis of apoptotic markers (Annexin-V, 7-AAD) was performed. Induction of apoptosis was detected in all three leukemia cell lines after 12 h and 24 h (Figures 4(a) and 4(b)). An increase in early apoptosis (Annexin-V-positive cells) was observed after 12 h in the intermediate and resistant cell lines

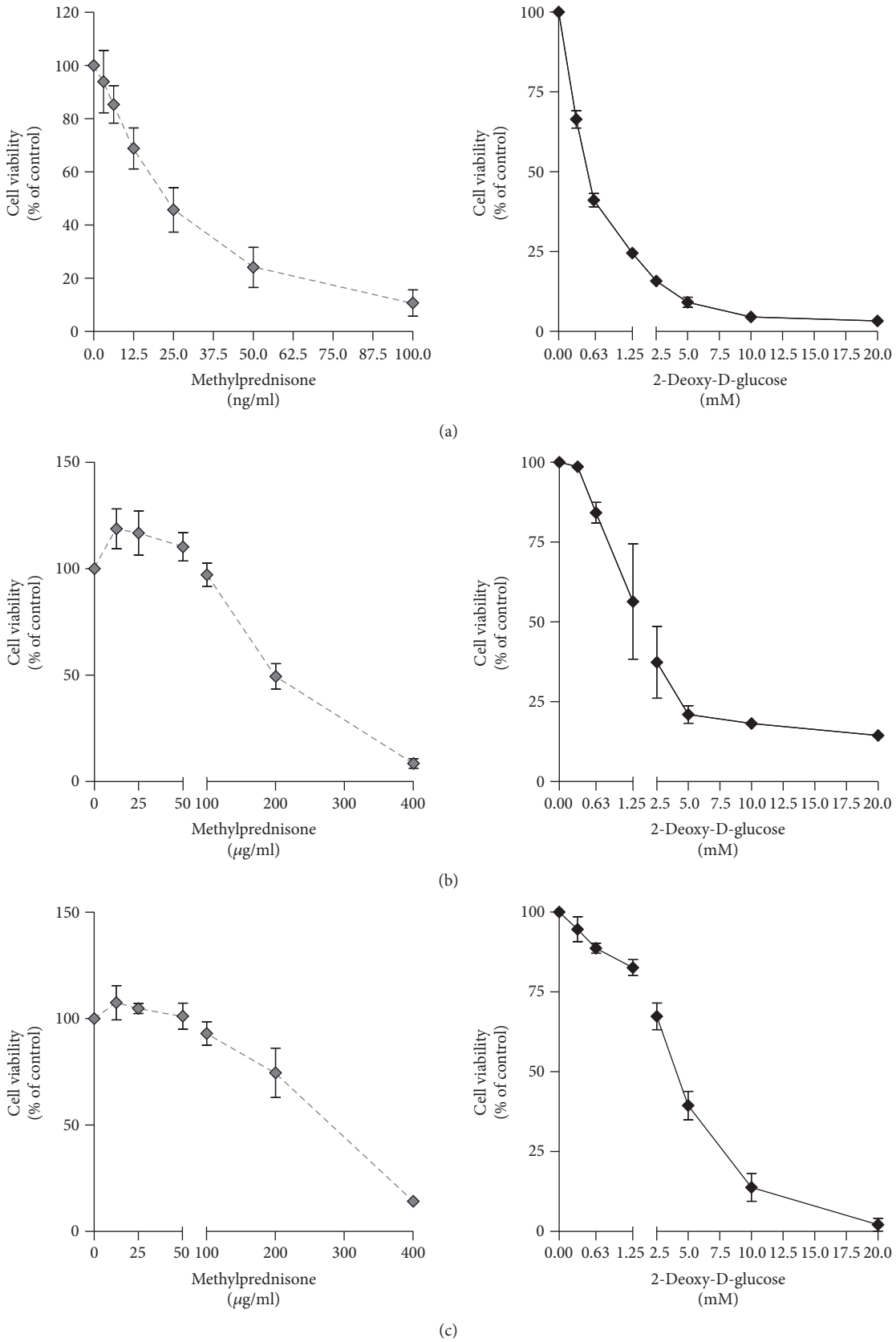

Figure 1: Effects of MP and 2-DG single treatment in a panel of ch-ALL cell lines. Cell viability was evaluated in (a) SUP-B15, (b) SD1, and (c) REH cells treated for 72 h with MP and 2-DG at the indicated concentrations. Error bars represent the SD of the mean of three independent experiments ($n = 3$).

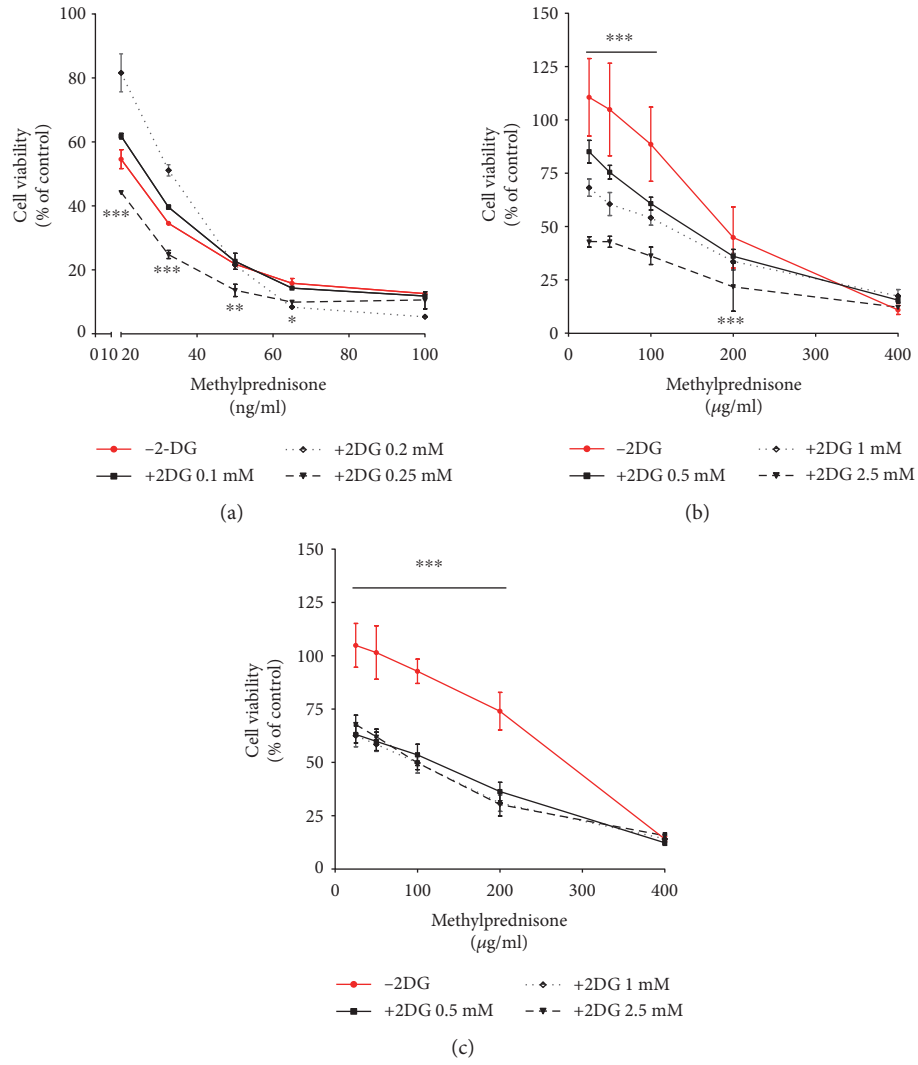

Figure 2: Synergistic effect of MP and 2-DG in ch-ALL cell lines. The responses of a panel of leukemia cell lines to MP alone and in combination with 2-DG: (a) 0.1 mM, 0.2 mM, and 0.25 mM of 2-DG for SUP-B15 and (b, c) 0.5 mM, 1 mM, and 2.5 mM of 2-DG for SD1 and REH was measured after 72 h using the MTS assay. Cell viability was normalized to untreated cells (100%). Data represent the SD of the mean of three independent experiments ($n = 3$). $^{*}p \leq 0.05$, $^{**}p \leq 0.01$, $^{***}p \leq 0.001$ compared to single treatment (−2-DG) as determined by two-way ANOVA analysis of variance using Bonferroni's multiple comparison test.

(Figure 4(a)). Unlike SD1 and REH, SUP-B15 displayed an increase in late apoptosis upon 12 h of treatment. Interestingly, combinatorial treatments induced early and late apoptosis in all three leukemia cell lines (Figure 4(b)). Taken together, these results confirm that MP treatment in combination with 2-DG not only leads to increased apoptotic activity in leukemia cell lines, but also tends to overcome MP-resistance in SD1 and REH by inducing a decrease in cell viability. This supports the hypothesis that inhibition of metabolism with 2-DG impairs proliferation and triggers cell death in ch-ALL cells. To confirm our data, we measured apoptotic markers upon single and combinatorial treatment at the protein level. An induction of apoptosis was observed in all three leukemia cell lines upon 24 h of treatment, indicated by the increased levels of cleaved PARP protein, a nuclear enzyme involved in DNA repair (Figure 4(c)). SUP-B15 displayed a similar induction of cleaved PARP upon single or combinatorial treatment while SD1 demonstrated an induction of apoptosis upon 2-DG treatment and the combinatorial treatment (Figure 4(c)). REH displayed apoptosis only following combinatorial treatment (Figure 4(c)). Moreover, the levels of active caspase-3 were assessed after 24 h of treatment. In line with our previous results, activation of caspase-3 in the SUP-B15 cell line was found upon all treatment conditions, while in SD1 and REH, a significant activation was observed only upon combinatorial treatment (Figure 4(d)). Regression analysis confirmed that the reduction in cell viability is in part due to the induction of apoptosis (Additional file 1: Figure S1 available online at https://doi.org/10.1155/2017/2487297).

3.4. 2-DG-Induced Cytotoxicity Is Exerted in a Hexokinase-Independent (HK) Manner in Leukemia Cell Lines. We used the cDNA microarray data set from Haferlach et al. [15] to

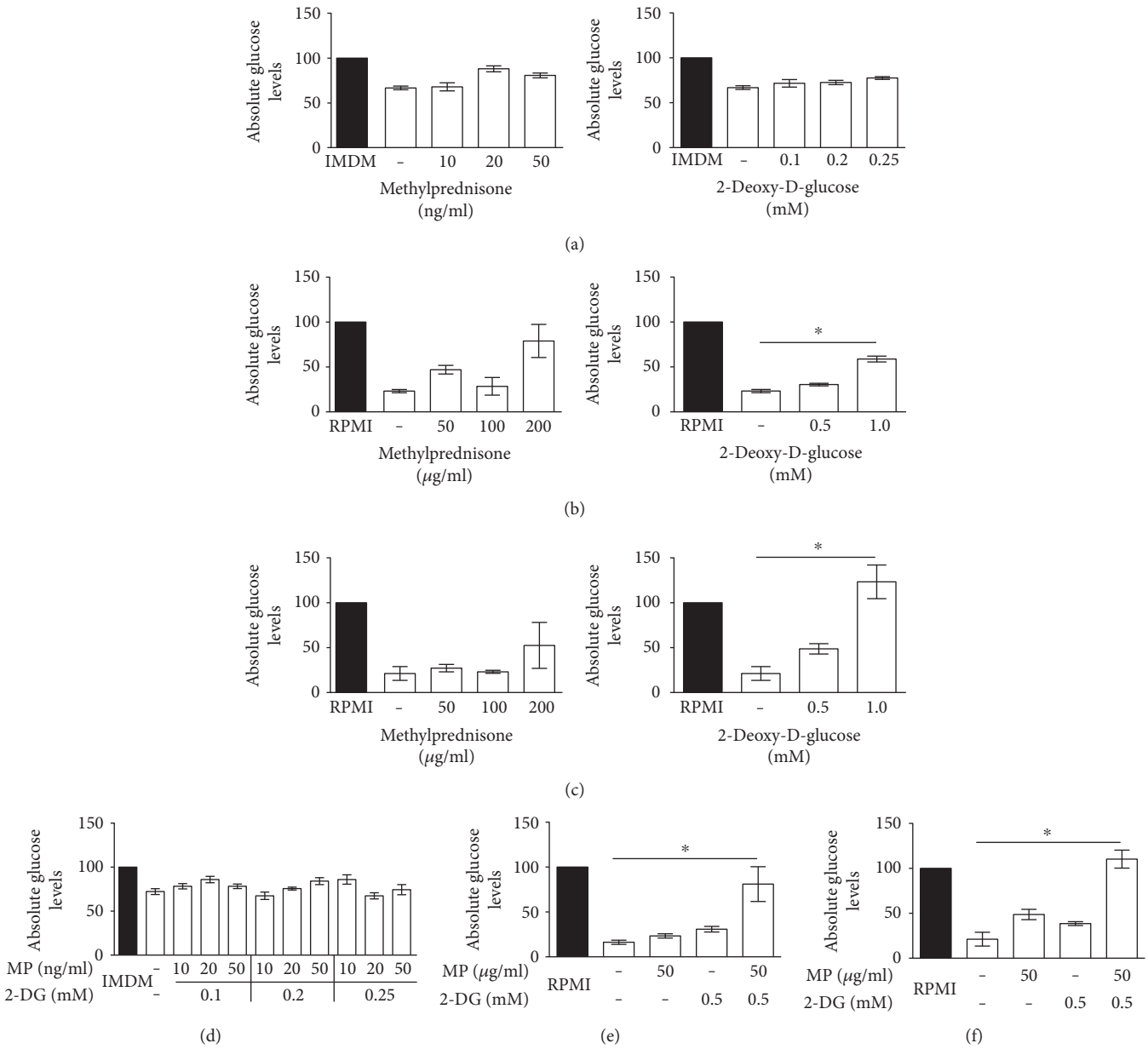

Figure 3: Glucose consumption in a panel of ch-ALL cell lines. The absolute glucose levels were measured in the cell media after incubation with MP, 2-DG, or combinatorial treatment. Kinetic measurements of glucose uptake were performed; only data from 96 h are shown. (a) SUP-B15, (b) SD1, and (c) REH cell lines were treated with increasing concentration of MP (left graph) and 2-DG (right graph). RPMI and IMDM controls represent the amount of glucose present in the culture medium incubated for 96 h in the absence of treatment. The effects of combined drug treatments on glucose levels are shown in (d), (e), and (f) for SUP-B15, SD1, and REH, respectively. The conversion of glucose to glucose-6-phosphoglucoronate (G6P) and NADH was evaluated. The concentration of NADH was measured. Graphs represent the SD of the mean of at least two independent experiments ($n = 2$). $^{*}p \leq 0.05$ using two-way analysis of variance (ANOVA) using Bonferroni's multiple comparison test.

analyze differences in gene expression in patients of two ch-ALL subgroups in comparison with healthy bone marrow samples. The wide cohort of ch-ALL patient samples analyzed in our laboratory (data not shown) displayed a general downregulation of the genes involved in the glycolytic pathway (Additional file 1: Figures 2a and 2b). Surprisingly, all three hexokinase isoforms (HKI, HKII, and HKIII) are significantly downregulated in both ch-ALL subgroups examined compare to healthy bone marrow (all p value $>10^{-10}$) (Additional file 1: Figure 2a). The hexokinase isoforms II (HKII) and III (HKIII) are enzymes responsible for the conversion of glucose to glucose-6-phosphate (G6P), which is considered as the first limiting step of glycolysis. In line with this result, further evidence revealed that in our panel of leukemia cell lines, the expression of HK isoforms was downregulated (Additional file 1: Figure 2c). We thus speculated that in our leukemia in vitro model, HKII is not required for 2-DG-mediated

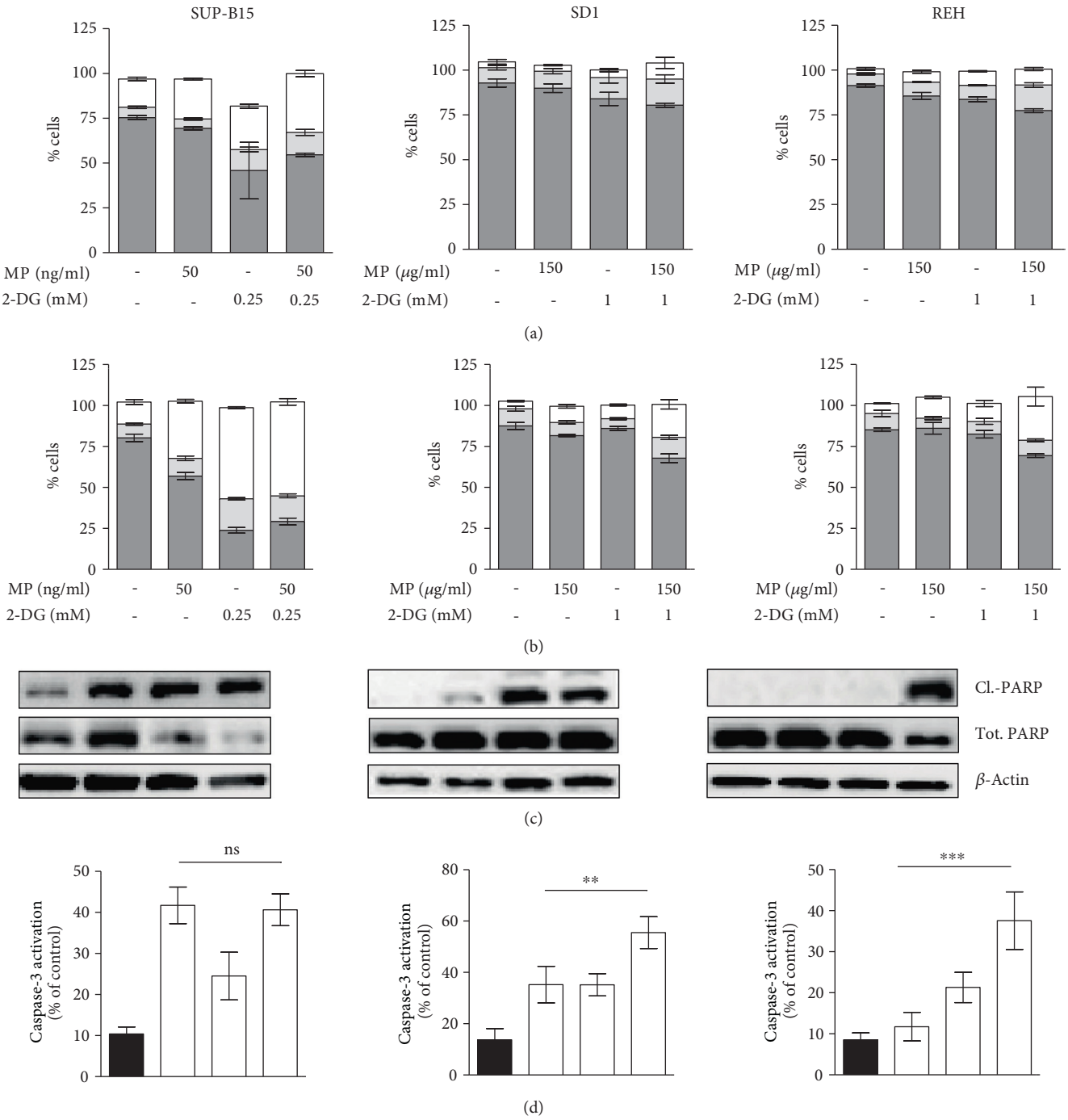

Figure 4: Induction of apoptosis upon MP, 2-DG, and combinatorial treatments. Apoptotic markers analysed by fluorescence-activated-cell-sorting (FACS) and western blot in a panel of ch-ALL after treatment with MP and 2-DG. FACS quantification of single (light grey) or double positive cells for Annexin-V and 7-AAD (white) after (a) 12 h and (b) 24 h treatment with MP and 2-DG. The percentage of living cells is represented in dark grey color. (c) Protein expression analysis by Western blot of cleaved-PARP in leukemia cell lines treated with MP, 2-DG, and MP+2-DG for 24 h is shown. (d) Caspase-3 activation was assessed by FACS in all three leukemia cell lines treated as described previously. Error bars represent the SD of the mean of at least two independent experiments ($n = 2$). $^{**}p \leq 0.01$, $^{***}p \leq 0.001$, two-way analysis of variance (ANOVA) using Bonferroni's multiple comparison test.

apoptosis induction. Since leukemic cell can circulate freely through normoxic and hypoxic environments, we investigated whether in normal and decreasing oxygen tension, 2-DG leads to the same biological effect. Upon treatment with 2-DG, the cells were incubated either in normoxia or in hypoxia (pO2 1%). No significant differences in the impact of 2-DG on cell viability were observed (Additional file 1: Figure 3). Thus, 2-DG treatment leads to cell viability impairment independently of the oxygen levels in ch-ALL cells. To confirm that HK is not crucial for the effects of 2-DG in

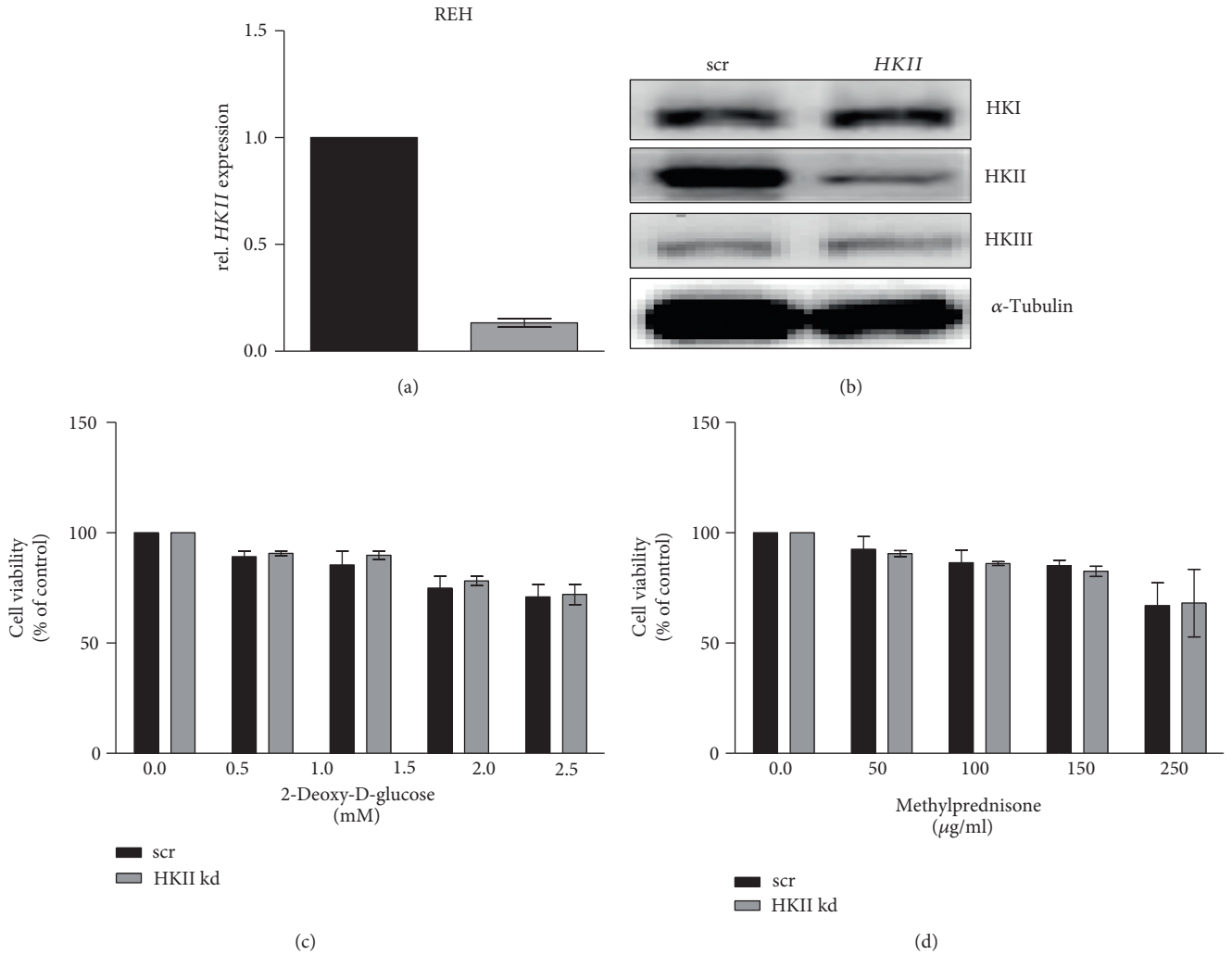

Figure 5: Gene expression analysis. REH transfection with siRNA was performed using nucleofection and gene expression was assessed. (a) Expression of HKII after silencing was measured in REH cells line at the mRNA level (24 h) and (b) at the protein level (48 h). The effects of (c) 2-DG or (d) MP on cell viability were measured in the presence or absence of HKII expression. The fold change was calculated via normalization to the scrambled control. Error bars represent the SD of the mean of at least three independent experiments ($n = 3$).

leukemia cell lines, we performed HKII silencing in all three leukemia cell lines (Figure 5 and Additional file 1: Figure 4). Due to low transfection efficiency in SUP-B15 and SD1 cell lines and since REH appeared to be the most resistant cell line, further experiments were carried out only in REH. The siRNA transfection efficiency at the mRNA level was measured after 24 h (Figure 5(a) and Additional file 1: Figure 4b) and confirmation of HKII silencing at the protein level was measured after 48 h by Western blot analysis (Figures 5(a) and 5(b)). To gain further insight on the role of HKII in REH cells, we performed cell viability assays after HKII knockdown. Silencing HKII did not significantly change the treatment response to either 2-DG (Figure 5(c)) or MP (Figure 5(d)), implying that the cytotoxic effect of 2-DG in this ch-ALL cell line is not dependent on its ability to inhibit glycolysis. Therefore, we focused our attention on identifying additional molecular targets of 2-DG in leukemia cell lines.

3.5. 2-DG Interferes with N-Linked Glycosylation (NLG) and Induces Changes in the Metabolic Profile of Leukemic Cells In Vitro. 2-DG is known as a structural analog of mannose and acts as a potent inhibitor of N-linked glycosylation (NLG), by competition with the endogenous substrate and by fraudulent incorporation into dolichol-pyrophosphate (lipid)-linked oligosaccharides, which are the precursors of NLG [23]. To investigate whether the antiproliferative effects of 2-DG in normoxia predominantly occur through inhibition of NLG and not through an HK-dependent block in glycolysis, we performed a cytotoxicity assay in the presence or absence of mannose (2.5 mM) (Figure 6(a)). Mannose treatment significantly reversed 2-DG-induced cytotoxicity, leading to the hypothesis that the effects of 2-DG in leukemia cells in normoxia are primarily due to interference with NLG. Moreover, a metabolomics analysis of the leukemia cell lines under study showed that a significant decrease in several metabolites involved in hexosamine

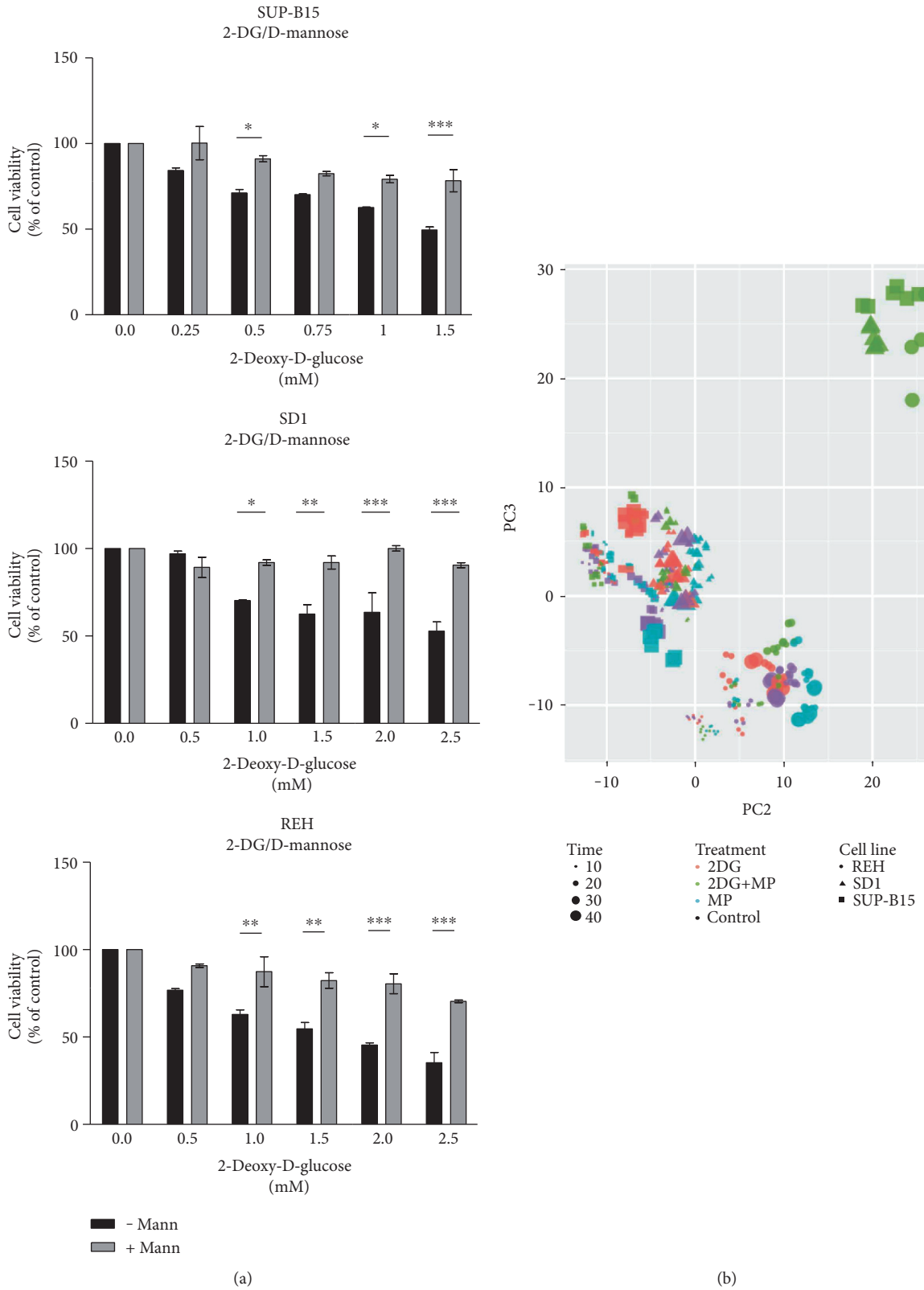

(a) (b)

Figure 6: Continued.

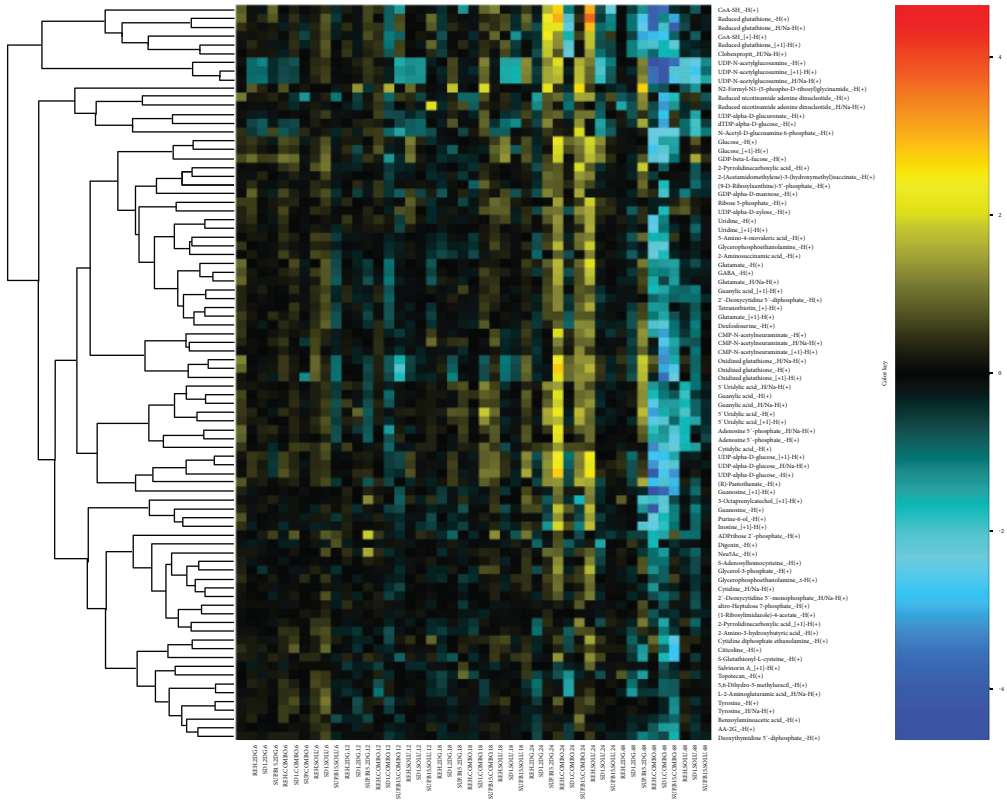

(c)

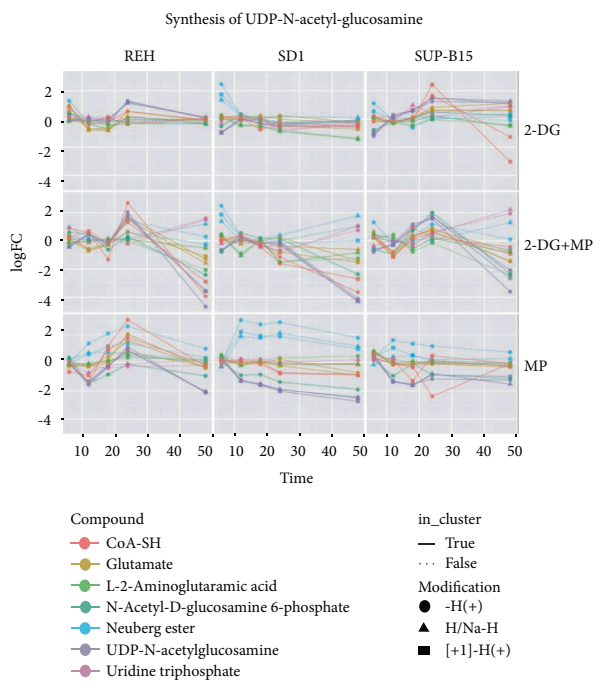

(d)

Figure 6: Metabolic profiles upon treatment with 2-DG and MP in ch-ALL. (a) Reversal effects of 2-DG on cell viability by exogenous mannose (2.5 mM). (b) Principal component analysis (PCA) score plot of SUP-B15 (●), SD1 (▲), and REH (■). Representative data are shown; the size of each condition is proportional to the treatment exposure. (c) The hierarchical clustering heat map shows consistent metabolic changes of ch-ALL cell lines upon 48 h of combinatorial treatment. (d) Enrichment in metabolites involves in the synthesis of the UDP-N-acetyl-glucosamine pathway in a matrix of 60 columns for 4 treatments (ctrl, 2-DG, MP, and 2-DG+MP) and 5 time points (0, 6, 12, 18, 24, and 48 h). Error bars represent the SD of the mean of at least three independent experiments ($n = 3$). $^{*}p \leq 0.05$, $^{**}p \leq 0.01$, $^{***}p \leq 0.001$, two-way analysis of variance (ANOVA) using Bonferroni's multiple comparison test.

biosynthesis pathway (HBP) and in the genesis of N-linked glycans was observed upon 48 h of combinatorial treatment (Figure 6(b)). UDP-N-acetyl-hexosamine, N-acetyl-hexosamine-phosphates, and UDP-hexosamine, which are all involved in the generation of glycosaminoglycans, proteoglycans, and glycolipids, were significantly downregulated upon combinatorial treatment (all p value $<10^{-15}$) (Figure 6(c)). As a consequence, the glycans are not transferred to the nascent products (e.g., glycoprotein), leading to a block in protein synthesis. As can be seen from Figure 6(c), the general trend of metabolites in UDP-N-acetyl-hexosamine pathway is upregulated at 24 h and downregulated at 48 h.

In addition, depending on the cell line used, UDP-N-acetyl-hexosamine levels stay the same or are increased upon treatment with 2-DG, apart from a slight decrease at 6 h. However, treatment with MP results in a general decrease in UDP-N-acetyl-hexosamine, with the exception of REH. The combined treatment shows a more complicated picture, with generally increased levels of the UDP-N-acetyl-hexosamine until 24 h and then falling sharply at 48 h (Figure 6(d)). Together, these results demonstrate the importance of the deregulation of NLG for the biological effects of 2-DG in ch-ALL. It has been described that impaired NLG leads to the accumulation of unfolded proteins within the endoplasmic reticulum (ER) and to the induction of the unfolded protein response (UPR) [24–26]. To investigate whether 2-DG treatment alone or in combination with MP triggers the UPR, leukemia cell lines were exposed to both drugs as single agents or in combination. Moreover, treatments with 2-DG and mannose (2.5 mM) were assessed. The impact of these drugs on the UPR was evaluated by measuring the expression of glucose-regulated protein 78 (GRP78). In addition, the activation of the UPR-mediated apoptotic pathway was investigated after 24 h treatment by measuring the expression of DNA damage-inducible transcript 3 protein (also called CHOP) (Figure 7). 2-DG alone induced an increase in GRP78 expression leading to the activation of the UPR response, in particular in the REH resistant cell type (Figure 7(a)). Surprisingly, in this cell line, the combination of 2-DG and MP did not lead to any additional increment in the expression of GRP78. SUP-B15 and SD1 displayed a significant increase in the levels of GRP78 in cells cotreated with 2-DG and MP, compared to single treatments. Surprisingly, in SD1 cells treated with a single dose of MP (150 μg/ml), the level of GRP78 was increased to the same extent as for the 2-DG single treatment. The activation of UPR-mediated apoptosis via CHOP was evaluated and we were able to show that, for SUP-B15 and SD1, the cotreatment with 2-DG and MP led to a significant increase in the expression of CHOP. In contrast, in REH, the same trend was observed for GRP78, indicating that the treatment with 2-DG alone at 1 mM was sufficient to increase the expression of both genes (GRP78 and CHOP). Moreover, mannose (2.5 mM) cotreatment with 2-DG was able to reverse the effects of the latter drug on GRP78 and CHOP levels in all three leukemia cell lines (Figure 7). These results indicate that in the leukemic cell lines under study, 2-DG induces its biological effects by interfering with NLG leading to UPR induction and subsequent activation of the UPR-mediated apoptotic pathway.

3.6. High-Throughput Screen with 365 Protein Kinase Inhibitors Identifies GSK-3 as a Potential Target in Leukemia. To better understand the mechanism of action of MP in resistant leukemic cells, we screened 365-protein kinase inhibitors in SD1 and REH cells. The outcome of the screen revealed 57 hit compounds, which acted synergistically with MP. Surprisingly, the majority of those inhibitors targeted kinases involved in metabolism such as p38-mitogen-activated protein kinase (p38/MAPK), insulin-like growth factor-I receptor (IGF-IR), and inhibitor of nuclear factor kappa-B kinase subunit α and β (IKK-α/β). Interestingly, among these hit compounds, 14 targeted glycogen synthase kinase-3 (GSK-3). Considering the impact of MP on cell metabolism and the relevance of GSK-3 inhibition in our screen, we decided to investigate the role of this kinase in MP-resistant ch-ALL cells in more detail. We selected the GSK-3 inhibitor SB-360741, a 3-anilino-4-arylmalemide, for further analysis, due to its robust synergistic effects with MP ($F_{\text{syn}} = 0.47$ and 0.88 for REH and SD1, resp.) [27]. A significant decrease in REH cell viability was observed after 72 h of treatment (Figure 8(a)). Comparable results were observed in the SD1 cell line (data not shown). In order to investigate the mechanism of cell death induced by MP and SB-360741, we further analyzed the expression levels of several apoptotic markers, which revealed that this process is the main mechanism underlying the observed cytotoxicity. Upon 24 h of single SB-360741 treatment, we observed a slight increment in cells in early apoptosis (Annexin-V-positive cells). However, when SB-360741 was combined with MP, the apoptotic rate increased significantly in comparison to single treatments (Additional file 1: Figure 5). Interestingly, we observed similar biological effects of SB-360741 and 2-DG when coadministrated with MP. We hypothesize a possible link between these two pathways. Therefore, we investigated the effect of 2-DG treatment on GSK-3 activity more in details. Upon single treatment with 2-DG, GSK-3 phosphorylation status remained unchanged, while the combinatorial treatment with MP led to the inhibition of GSK-3 activity via phosphorylation at Ser21 of the α isoform. Together, these results reveal the existence of 2-DG- and/or GSK-3-mediated pathway acting synergistically with MP, leading to the induction of cell death and apoptosis in ch-ALL.

4. Discussion

Within the last years, a large variety of different solid tumors have been associated with increased metabolic activity [8, 28]. Although there are many examples of solid tumors having altered metabolism, it has been only recently reported that this phenomenon also occurs in hematological malignancies [21, 22, 29, 30]. Therefore, targeting the metabolic pathways could represent an innovative approach to sensitize leukemic cells to chemotherapeutic drugs and potentially lead to a better patient outcome [31, 32]. One of the most important prognostic factors in ch-ALL is the response to the GCs treatment. Thus, strategies aiming to reverse GCs

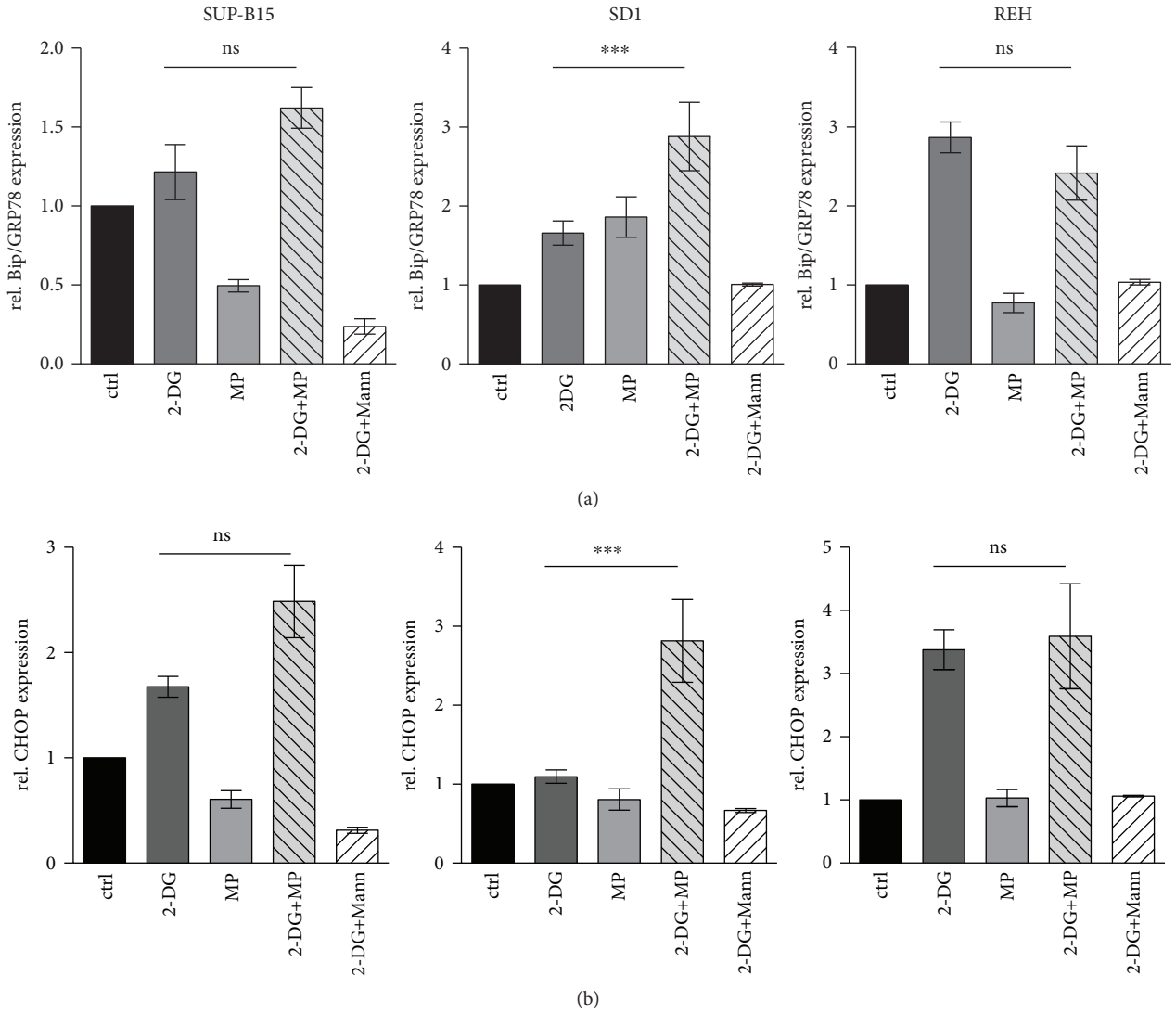

Figure 7: UPR induction by 2-DG in sensitive and resistant ch-ALL cell lines. (a) GRP78/Bip and (b) CHOP mRNA expression was assessed by real-time RT-PCR (SYBR-green) in leukemia cells treated with 2-DG (dark grey bar), MP (light grey bar), 2-DG+MP (grey striped bar), or 2-DG+Mann (white striped bar). Error bars represent the SD of the mean of at least three independent experiments ($n = 3$). β-Actin was used as a control to normalize the samples. $p < 0.05$ (ns), $^{***}p \leq 0.001$ using two-way analysis of variance (ANOVA) with Bonferroni's multiple comparison test.

resistance could improve the survival of children suffering from leukemia. Recent data investigating the mechanisms involved in MP resistance showed a tight correlation between rapid leukemic growth and a high glycolytic ratio [5]. Therefore, it is of interest to further analyze the impact of glycolysis inhibitors in leukemia, since several in vitro and in vivo studies have demonstrated their efficacy as anticancer drugs [33]. Moreover, some of these inhibitors have been already selected as candidates for clinical trials [21, 29, 34, 35]. In our study, the glucose analog 2-DG was selected principally because of its strong activity in depleting the production of ATP at the first limiting step of glycolysis. The investigation of the impact of 2-DG, as an antileukemic agent led us to the hypothesis that leukemia cells, like solid tumors, might have an altered metabolism, a phenomenon termed as "aerobic glycolysis" [36]. Indeed, the inhibition of the glucose consumption by 2-DG was paralleled by a decrease in cell viability and enhanced apoptosis in our in vitro leukemia model. However, a general downregulation of the expression of genes involved in glycolysis was revealed by cDNA microarray data analysis performed on a cohort of ch-ALL patients. A remarkable decrease was particularly observed in the expression of HK isoforms responsible for the biological effect of 2-DG. Furthermore, the cytotoxic effects of 2-DG in cancer appears to be higher under hypoxic conditions, or in cells presenting mitochondrial defects [37, 38]. Since leukemia cells have the capacity to circulate freely through normoxic and hypoxic environments, it was of importance to investigate the different mechanisms involved in 2-DG-induced cytotoxicity. Our data show that the glucose analog acts in an HKII-independent manner to reduce cell growth in leukemia. In support of our findings,

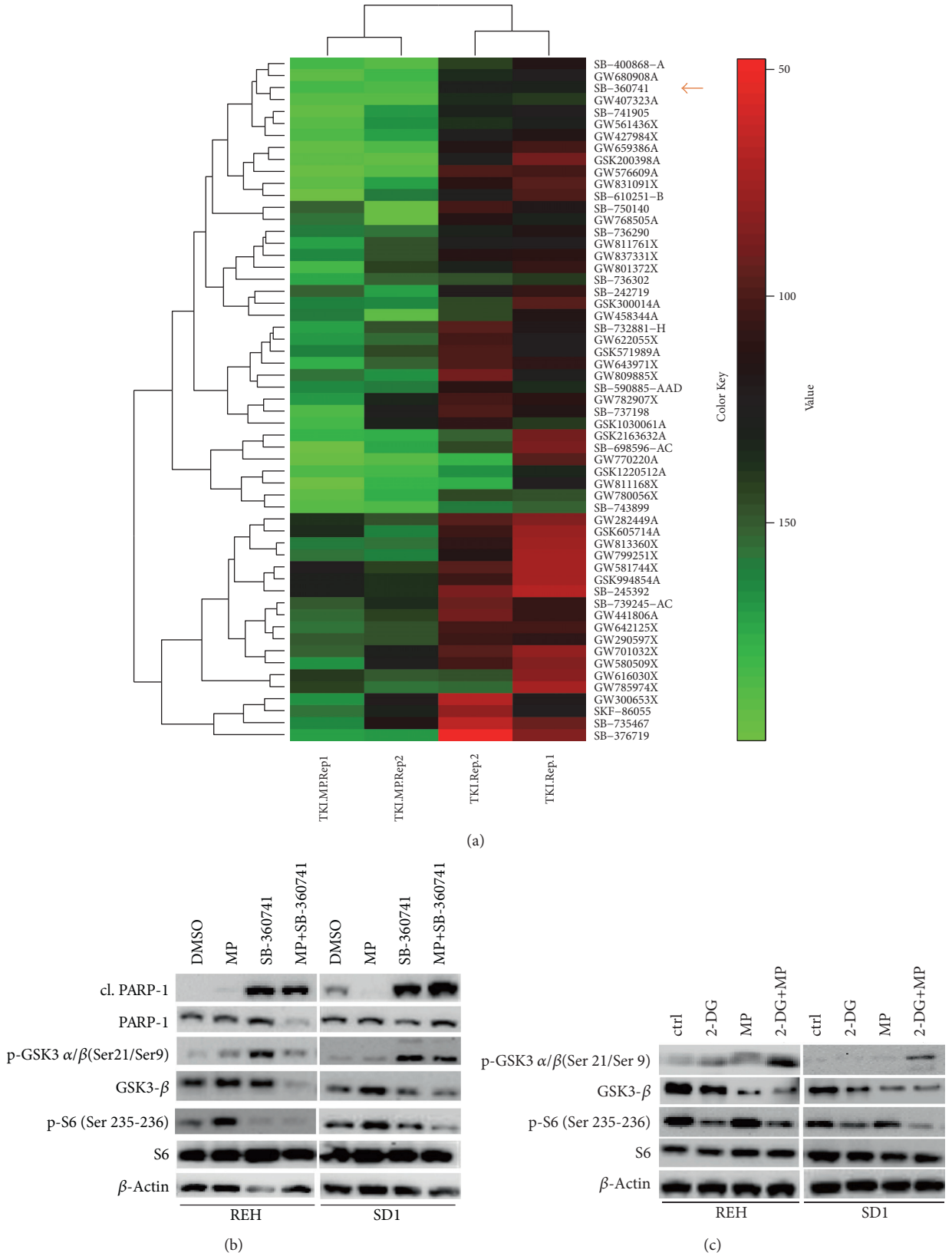

Figure 8: High-throughput screen of protein kinase inhibitors in SD1 and REH leukemia cells. (a) Heat map of REH representing the top candidates from the drug screen upon single and cotreatment with MP. SB-360741, a powerful GSK-3 inhibitor, is indicated by a red arrow. The values shown were calculated as a percentage of the DMSO-treated control. Protein expression profiles of leukemia cell lines, SD1 and REH, upon single or combinatorial treatment with (b) MP and SB-360741or (c) MP and 2-DG.

several reports have suggested a more complex mechanism of action of 2-DG [12, 39, 40]. In this context, we were able to show that a significant fraction of the 2-DG-mediated cell death can be rescued by coadministration of exogenous mannose. These data suggest that the observed antileukemic effects of 2-DG potentially involve NLG. By interfering with this process and consequently with protein folding, 2-DG promotes ER stress leading to UPR induction and protein synthesis inhibition [41, 42]. In addition, prolonged ER stress triggers an irreversible UPR-mediated apoptotic response [43]. The deregulation of NLG via 2-DG might serve as a sensor linking metabolism with the activation of oncogenic pathways. In line with this, a screen of 365 protein kinase inhibitors performed in two leukemia cell lines revealed that most of the kinases synergistically acting with MP were involved in metabolism. The selected kinase inhibitor targeting GSK-3 (SB-360741) was able to induce the same biological effects as 2-DG in combination with MP. GSK-3 is known to regulate apoptosis and proliferation in cancer and its role appears to be distinct, not only between physiological and pathological conditions but also depending on cell type and tissue context [44–46]. Moreover, in neuroblastoma, 2-DG exposure triggered an energy depletion in a GSK-3-mediated manner resulting in attenuation of the mitochondrial biogenesis, a particular form of stress adaptation [47]. In leukemia cell lines, we were unable to show a direct regulation of GSK-3 by 2-DG. Nevertheless, the combinatorial treatment of the glucose analog with MP highly affected the activity of the kinase. In conclusion, this study provides new insights into the intimate connection between GCs resistance and altered metabolism in ch-ALL. Therefore, it will be of a great interest to investigate alternative roles of 2-DG in a wider metabolic context, besides its function as a glucose analog. In addition, investigating of the role of GSK-3 in leukemia metabolism will provide further essential knowledge about the mechanisms underlying MP resistance. This research work provides evidence of the intimate connection between GCs resistance and altered metabolism in ch-ALL. Therefore, the current and the future challenge in the field of cancer metabolism is to dissect these complex metabolic changes and interpret them as a result of global metabolic interactions.

Conflicts of Interest

The authors declare that there is no conflict of interests regarding the publication of this paper.

Acknowledgments

The authors would like to thank the Graduate School of Cellular and Biomedical Science (GCB) of the University of Bern. Zaira Leni, Paulina Ćwiek, Valeriya Dimitrova, and Geetha Rossi were members of the GCB.

References

[1] C.-H. Pui, C. G. Mullighan, W. E. Evans, and M. V. Relling, "Pediatric acute lymphoblastic leukemia: where are we going and how do we get there?" *Blood*, vol. 120, pp. 1165–1174, 2012.

[2] A. L. Samuels, J. Y. Heng, A. H. Beesley, and U. R. Kees, "Bioenergetic modulation overcomes glucocorticoid resistance in T-lineage acute lymphoblastic leukaemia," *British Journal of Haematology*, vol. 165, pp. 57–66, 2014.

[3] D. S. Shah and R. Kumar, "Steroid resistance in leukemia," *World Journal of Experimental Medicine*, vol. 3, pp. 21–25, 2013.

[4] J. A. P. Spijkers-Hagelstein, S. S. Pinhanços, P. Schneider, R. Pieters, and R. W. Stam, "Chemical genomic screening identifies LY294002 as a modulator of glucocorticoid resistance in MLL-rearranged infant ALL," *Leukemia*, vol. 28, pp. 761–769, 2014.

[5] E. Hulleman, K. M. Kazemier, A. Holleman et al., "Inhibition of glycolysis modulates prednisolone resistance in acute lymphoblastic leukemia cells," *Blood*, vol. 113, pp. 2014–2021, 2009.

[6] C. Stäubert, H. Bhuiyan, A. Lindahl et al., "Rewired metabolism in drug-resistant leukemia cells: a metabolic switch hallmarked by reduced dependence on exogenous glutamine," *The Journal of Biological Chemistry*, vol. 290, no. 13, pp. 8348–8359, 2015.

[7] E. Buentke, A. Nordström, H. Lin et al., "Glucocorticoid-induced cell death is mediated through reduced glucose metabolism in lymphoid leukemia cells," *Blood Cancer Journal*, vol. 1, article e31, 2011.

[8] S. Ganapathy-Kanniappan and J.-F. H. Geschwind, "Tumor glycolysis as a target for cancer therapy: progress and prospects," *Molecular Cancer*, vol. 12, p. 152, 2013.

[9] E. Poteet, G. R. Choudhury, A. Winters et al., "Reversing the Warburg effect as a treatment for glioblastoma," *The Journal of Biological Chemistry*, vol. 288, pp. 9153–9164, 2013.

[10] A. M. Giammarioli, L. Gambardella, C. Barbati et al., "Differential effects of the glycolysis inhibitor 2-deoxy-D-glucose on the activity of pro-apoptotic agents in metastatic melanoma cells, and induction of a cytoprotective autophagic response," *International Journal of Cancer*, vol. 131, pp. E337–E347, 2012.

[11] J. M. Boag, A. H. Beesley, M. J. Firth et al., "Altered glucose metabolism in childhood pre-B acute lymphoblastic leukaemia," *Leukemia*, vol. 20, pp. 1731–1737, 2006.

[12] M. Kurtoglu, N. Gao, J. Shang et al., "Under normoxia, 2-deoxy-D-glucose elicits cell death in select tumor types not by inhibition of glycolysis but by interfering with N-linked glycosylation," *Molecular Cancer Therapeutics*, vol. 6, pp. 3049–3058, 2007.

[13] J. DeSalvo, J. N. Kuznetsov, J. Du et al., "Inhibition of Akt potentiates 2-DG-induced apoptosis via downregulation of UPR in acute lymphoblastic leukemia," *Molecular Cancer Research*, vol. 10, pp. 969–978, 2012.

[14] M. C. Berenbaum, "Synergy, additivism and antagonism in immunosuppression. A critical review," *Clinical and Experimental Immunology*, vol. 28, pp. 1–18, 1977.

[15] T. Haferlach, A. Kohlmann, L. Wieczorek et al., "Clinical utility of microarray-based gene expression profiling in the diagnosis and subclassification of leukemia: report from the International Microarray Innovations in Leukemia Study Group," *Journal of Clinical Oncology*, vol. 28, pp. 2529–2537, 2010.

[16] M. Dai, P. Wang, A. D. Boyd et al., "Evolving gene/transcript definitions significantly alter the interpretation of GeneChip data," *Nucleic Acids Research*, vol. 33, pp. e175–e175, 2005.

[17] G. K. Smyth, "Linear models and empirical Bayes methods for assessing differential expression in microarray experiments," *Statistical Applications in Genetics and Molecular Biology*, vol. 3, pp. 3–25, 2004.

[18] M. Kanehisa, S. Goto, Y. Sato, M. Kawashima, M. Furumichi, and M. Tanabe, "Data, information, knowledge and principle: back to metabolism in KEGG," *Nucleic Acids Research*, vol. 42, Database issue, pp. D199–D205, 2014.

[19] D. Croft, A. F. Mundo, R. Haw et al., "The reactome pathway knowledgebase," *Nucleic Acids Research*, vol. 42, Database issue, pp. D472–D477, 2014.

[20] O. Fedorov, S. Müller, and S. Knapp, "The (un)targeted cancer kinome," *Nature Chemical Biology*, vol. 6, pp. 166–169, 2010.

[21] L. E. Raez, K. Papadopoulos, A. D. Ricart et al., "A phase I dose-escalation trial of 2-deoxy-D-glucose alone or combined with docetaxel in patients with advanced solid tumors," *Cancer Chemotherapy and Pharmacology*, vol. 71, pp. 523–530, 2013.

[22] G. Maschek, N. Savaraj, W. Priebe et al., "2-deoxy-D-glucose increases the efficacy of adriamycin and paclitaxel in human osteosarcoma and non-small cell lung cancers in vivo," *Cancer Research*, vol. 64, pp. 31–34, 2004.

[23] R. Datema and R. T. Schwarz, "Interference with glycosylation of glycoproteins. Inhibition of formation of lipid-linked oligosaccharides in vivo," *The Biochemical Journal*, vol. 184, pp. 113–123, 1979.

[24] M. Wang and R. J. Kaufman, "The impact of the endoplasmic reticulum protein-folding environment on cancer development," *Nature Reviews Cancer*, vol. 14, pp. 581–597, 2014.

[25] M. Aebi, "N-linked protein glycosylation in the ER," *Biochimica et Biophysica Acta*, vol. 1833, pp. 2430–2437, 2013.

[26] P. Walter and D. Ron, "The unfolded protein response: from stress pathway to homeostatic regulation," *Science*, vol. 334, pp. 1081–1086, 2011.

[27] D. G. Smith, M. Buffet, A. E. Fenwick et al., "3-Anilino-4-arylmaleimides: potent and selective inhibitors of glycogen synthase kinase-3 (GSK-3)," *Bioorganic & Medicinal Chemistry Letters*, vol. 11, pp. 635–639, 2001.

[28] Z. Leni, G. Parakkal, and A. Arcaro, "Emerging metabolic targets in the therapy of hematological malignancies," *BioMed Research International*, vol. 2013, Article ID 946206, 12 pages, 2013.

[29] M. Stein, H. Lin, C. Jeyamohan et al., "Targeting tumor metabolism with 2-deoxyglucose in patients with castrate-resistant prostate cancer and advanced malignancies," *Prostate*, vol. 70, pp. 1388–1394, 2010.

[30] F. Aghaee, J. Pirayesh Islamian, and B. Baradaran, "Enhanced radiosensitivity and chemosensitivity of breast cancer cells by 2-deoxy-d-glucose in combination therapy," *Journal of Breast Cancer*, vol. 15, pp. 141–147, 2012.

[31] Y.-Y. Pang, T. Wang, F.-Y. Chen et al., "Glycolytic inhibitor 2-deoxy-d-glucose suppresses cell proliferation and enhances methylprednisolone sensitivity in non-Hodgkin lymphoma cells through down-regulation of HIF-1α and c-MYC," *Leukemia & Lymphoma*, vol. 56, pp. 1821–1830, 2015.

[32] K. Eberhart, K. Renner, I. Ritter et al., "Low doses of 2-deoxy-glucose sensitize acute lymphoblastic leukemia cells to glucocorticoid-induced apoptosis," *Leukemia*, vol. 23, pp. 2167–2170, 2009.

[33] Z. Zhu, W. Jiang, J. N. McGinley, and H. J. Thompson, "2-Deoxyglucose as an energy restriction mimetic agent: effects on mammary carcinogenesis and on mammary tumor cell growth *in vitro*," *Cancer Research*, vol. 65, pp. 7023–7030, 2005.

[34] L. J. Akers, W. Fang, A. G. Levy, A. R. Franklin, P. Huang, and P. A. Zweidler-McKay, "Targeting glycolysis in leukemia: a novel inhibitor 3-BrOP in combination with rapamycin," *Leukemia Research*, vol. 35, pp. 814–820, 2011.

[35] F. Zhang and R. L. Aft, "Chemosensitizing and cytotoxic effects of 2-deoxy-D-glucose on breast cancer cells," *Journal of Cancer Research and Therapeutics*, vol. 5, no. 1, pp. 41–43, 2009.

[36] S. Y. Lunt and M. G. Vander Heiden, "Aerobic glycolysis: meeting the metabolic requirements of cell proliferation," *Annual Review of Cell and Developmental Biology*, vol. 27, pp. 441–464, 2011.

[37] H. Pelicano, D. S. Martin, R.-H. Xu, and P. Huang, "Glycolysis inhibition for anticancer treatment," *Oncogene*, vol. 25, pp. 4633–4646, 2006.

[38] B. S. Dwarakanath, "Cytotoxicity, radiosensitization, and chemosensitization of tumor cells by 2-deoxy-D-glucose in vitro," *Journal of Cancer Research and Therapeutics*, vol. 5, no. 1, pp. 27–31, 2009.

[39] K. Urakami, V. Zangiacomi, K. Yamaguchi, and M. Kusuhara, "Impact of 2-deoxy-D-glucose on the target metabolome profile of a human endometrial cancer cell line," *Biomedical Research*, vol. 34, pp. 221–229, 2013.

[40] H. Xi, M. Kurtoglu, H. Liu et al., "2-Deoxy-D-glucose activates autophagy via endoplasmic reticulum stress rather than ATP depletion," *Cancer Chemotherapy and Pharmacology*, vol. 67, pp. 899–910, 2011.

[41] W. Mi, Y. Gu, C. Han et al., "O-GlcNAcylation is a novel regulator of lung and colon cancer malignancy," *Biochimica et Biophysica Acta*, vol. 2011, pp. 514–519, 1812.

[42] S.-M. Yu and S.-J. Kim, "Endoplasmic reticulum stress (ER-stress) by 2-deoxy-D-glucose (2DG) reduces cyclooxygenase-2 (COX-2) expression and N-glycosylation and induces a loss of COX-2 activity via a Src kinase-dependent pathway in rabbit articular chondrocytes," *Experimental & Molecular Medicine*, vol. 42, pp. 777–786, 2010.

[43] A. Raiter, R. Yerushalmi, and B. Hardy, "Pharmacological induction of cell surface GRP78 contributes to apoptosis in triple negative breast cancer cells," *Oncotarget*, vol. 5, pp. 11452–11463, 2014.

[44] F. Gao, A. Al-Azayzih, and P. R. Somanath, "Discrete functions of GSK3α and GSK3β isoforms in prostate tumor growth and micrometastasis," *Oncotarget*, vol. 6, no. 8, pp. 5947–5962, 2015.

[45] F. Piazza, S. Manni, and G. Semenzato, "Novel players in multiple myeloma pathogenesis: role of protein kinases CK2 and GSK3," *Leukemia Research*, vol. 37, pp. 221–227, 2013.

[46] P. Cohen and S. Frame, "The renaissance of GSK3," *Nature Reviews Molecular Cell Biology*, vol. 2, pp. 769–776, 2001.

[47] P. Ngamsiri, P. Watcharasit, and J. Satayavivad, "Glycogen synthase kinase-3 (GSK3) controls deoxyglucose-induced mitochondrial biogenesis in human neuroblastoma SH-SY5Y cells," *Mitochondrion*, vol. 14, pp. 54–63, 2014.

Hindawi
Oxidative Medicine and Cellular Longevity
Volume 2017, Article ID 2597581, 18 pages
https://doi.org/10.1155/2017/2597581

Review Article

Oxidative Stress Gene Expression Profile Correlates with Cancer Patient Poor Prognosis: Identification of Crucial Pathways Might Select Novel Therapeutic Approaches

Alessandra Leone, Maria Serena Roca, Chiara Ciardiello, Susan Costantini, and Alfredo Budillon

Experimental Pharmacology Unit, Istituto Nazionale Tumori Fondazione G. Pascale-IRCCS, Naples, Italy

Correspondence should be addressed to Alessandra Leone; a.leone@istitutotumori.na.it

Received 15 March 2017; Accepted 30 May 2017; Published 9 July 2017

Academic Editor: Lars Bräutigam

The role of altered redox status and high reactive oxygen species (ROS) is still controversial in cancer development and progression. Intracellular levels of ROS are elevated in cancer cells suggesting a role in cancer initiation and progression; on the contrary, ROS elevated levels may induce programmed cell death and have been associated with cancer suppression. Thus, it is crucial to consider the double-face of ROS, for novel therapeutic strategies targeting redox regulatory mechanisms. In this review, in order to derive cancer-type specific oxidative stress genes' profile and their potential prognostic role, we integrated a publicly available oxidative stress gene signature with patient survival data from the Cancer Genome Atlas database. Overall, we found several genes statistically significant associated with poor prognosis in the examined six tumor types. Among them, FoxM1 and thioredoxin reductase1 expression showed the same pattern in four out of six cancers, suggesting their specific critical role in cancer-related oxidative stress adaptation. Our analysis also unveiled an enriched cellular network, highlighting specific pathways, in which many genes are strictly correlated. Finally, we discussed novel findings on the correlation between oxidative stress and cancer stem cells in order to define those pathways to be prioritized in drug development.

1. Introduction

Reactive oxygen species (ROS) are commonly identified as oxygen reactive molecules associated with a wide variety of physiologic events [1] as well as cancer, diabetes, obesity, neurodegeneration, and other age-related diseases [2, 3]. A reduction-oxidation (redox) reaction concerns the transfer of electrons (reducing power) from a more reduced (nucleophilic) to more oxidized (electrophilic) molecules. ROS can be classified in two groups: (1) free radical ROS containing one or more unpaired electron(s) in their outer molecular orbitals (i.e., superoxide radicals and hydroxyl radicals); (2) nonradical ROS which are chemically reactive and can be converted to radical ROS (i.e., hydrogen peroxide), although they do not have unpaired electron(s). In both cases, ROS can be produced by either enzymatic reactions (i.e., NADPH oxidase, metabolic enzymes such as the cytochrome P450 enzymes, lipoxygenase, and cyclooxygenase) or by nonenzymatic reactions, such as during the mitochondrial respiratory chain. These considerations highlight the concept that the source of ROS is extremely heterogeneous. Indeed, ROS can be found in the environment, as pollutants, tobacco smoke, and iron salts, or generated inside the cells through multiple mechanisms [4]. Within cells, mitochondria, cytosol, single membrane-bound organelles (peroxisomes, endosomes, and phagosomes), or exosomes shed from plasma membranes, as well as extracellular fluids, including plasma, are all involved in ROS generation [3, 5, 6]. Mitochondria are the main ROS producers, principally because they are the site of the respiratory chain when electron leakage can react with molecular oxygen, resulting in the formation of superoxide, which can subsequently be converted to other ROS molecules. Then, generated ROS either can be detoxified or can leave the organelle through channels such as voltage-dependent anion channels

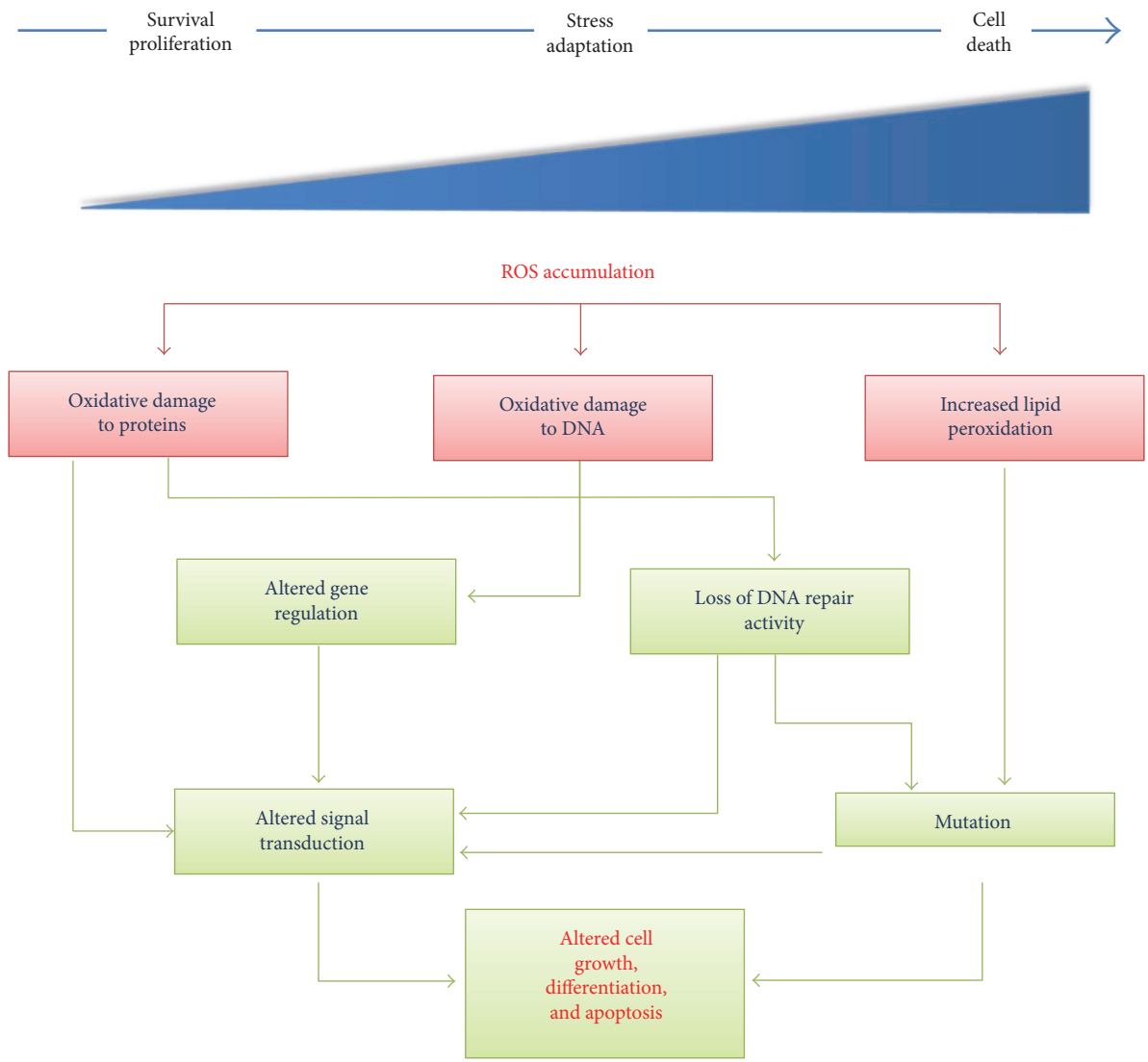

Figure 1: Redox stress activation in physiology. The production of abnormally large amounts of ROS leads to persistent changes in signal transduction and gene expression that, in the last instance, could give to cell death. The steady-state levels of ROS are determined by the rate of ROS production and their clearance by scavenging mechanisms.

(VDAC) or aquaporin, or by small vesicles such as exosomes [3, 5, 7]. However, ROS can also be the product of β-oxidation in peroxisomes, of prostaglandin synthesis and detoxification reactions by cytochrome P450, or of NADPH-mediated reaction in phagocytes [4, 5].

ROS are biologically important in a variety of physiological systems, including adaptation to hypoxia, regulation of autophagy, immunity, differentiation, and longevity. They regulate many signal transduction pathways by directly reacting with proteins and by modulating transcription factors and gene expression [1]. At low levels, ROS promote cellular proliferation, differentiation, and migration as well as cellular stress-responsive survival pathways such as nuclear factor-κB (NF-κB), thus inducing proinflammatory cytokines [4, 8]. Because of ROS' highly reactive potential toward biological molecules, excessive ROS levels can damage cellular components such as DNA, proteins, and lipids. To counteract these effects, cells activate "ROS adaption" mechanisms, involving several antioxidant ROS scavengers, as glutathione peroxidase (GPx), thioredoxin (Trx), catalase (CAT), superoxide-dismutase (SOD), and the nuclear factor erythroid 2 (NRF2) pathway [4, 7]. If a further increase in ROS levels occurs, then the cells undergo apoptotic cell death (Figure 1). Therefore, under physiological conditions, in order to guarantee cellular redox homeostasis, cells regulated intracellular ROS levels by applying a tight regulation of ROS generation and of ROS detoxifying pathways.

In this review, we first summarized the role of oxidative stress molecules in cancer initiation and progression and the proposed oxidative stress-targeted anticancer approaches. Next, in order to derive cancer-type specific oxidative stress gene profiles and their potential prognostic role, we integrated a publicly available oxidative stress gene signature [9] with the data extracted from the Cancer Genome Atlas (TCGA) database. Then, we reviewed some of those genes/pathways correlating with patient's survival, in order to define potential novel

anticancer therapeutic targets. Finally, we highlighted novel findings on the correlation between oxidative stress and cancer stem cells (CSC).

2. The Role of Oxidative Stress Molecules in Cancer Initiation and Progression

A link between ROS and cancer progression dates back to 1981 when increased levels of H_2O_2, induced by insulin were shown to promote tumor cell proliferation. Almost three decades later, several studies sustained this hypothesis, reporting increased levels of oxidative damage products in clinical tumor specimens and plasma as well as in cancer cell lines [5]. Based on these evidences, to date, the idea that altered redox balance and deregulated redox signaling are strongly implicated in any steps of carcinogenesis as well as in the resistance to treatment, by affecting many, if not all, hallmarks of cancer is widely accepted [10, 11]. Indeed, currently, the role of ROS in cancer initiation and progression through the modulation of cell proliferation, apoptosis, angiogenesis, and the alteration of the migration/invasion program is well described [7, 12, 13]. For example, ROS may affect proliferation by a ligand-independent transactivation of different receptor tyrosine kinase via ERK activation and may induce tissue invasion and metastatic dissemination by activation of metalloproteinases. Moreover, the release of vascular endothelial growth factor and angiopoietin induced by ROS promote tumor angiogenesis and *anoikis* [12, 14].

Nonetheless, the exact origin of ROS generation during cancer development and disease progression and how this event could be druggable remains still unclear. Increasing evidences reported a link between ROS activation and the presence of some oncogenes, such as Ras, c-Myc, or Bcr-Abl [2, 15, 16]. Activation of oncogenic signaling might contribute to the increase of ROS levels, which in turn by promoting genomic instability could affect both nuclear and mitochondrial DNA. The consequent activation of antioxidants' signaling within tumor cells can also promote cancer progression and metastasis [2, 15–18]. Furthermore, cancer cells undergo metabolic changes to counteract the oxidative stress, also contributing to metastatic program [5, 19, 20].

Loss of functional p53 is involved in ROS induction, due to p53 "genome guardian" role in sensing and removing oxidative damage to DNA, thus preventing genetic instability [5, 21]. Anyhow, unlike oncogenes, the role of tumor suppressors in the modulation of ROS is more complex, depending on the specific tumor suppressor itself. For example, ataxia-telangiectasia mutated (ATM) is a cellular damage sensor that by regulating cell cycle and DNA repair preserves genomic integrity. Deficiency of ATM gene, either in patients or in mice, has been shown to produce elevated ROS levels and a chronic oxidative stress status. Recently, cytoplasmic ATM is described to activate a pathway leading to autophagy through repression of mammalian target of rapamycin complex 1 (mTORC1) in response to elevated ROS levels [22, 23]. Another example regards the loss of PTEN that determines AKT hyperactivation and inactivation of the forkhead homeobox type O (FoxO) transcription factor and therefore enhanced susceptibility to oxidative stress [24].

Less evidences are available about the regulation of ROS by microenvironment; however, new efforts have been recently focused in this field [5, 12]. In this regard, Chan et al. demonstrated that cancer-associated fibroblast- (CAF-) derived ROS are able to induce the acquisition of an oxidative CAF-like state on normal fibroblasts. Then, these oxidatively transformed normal fibroblasts promoted the development of aggressive tumors via a TGFβ1-mediated Smad3 signaling, suggesting an important relationship between the extracellular redox state and cancer aggressiveness [25].

3. Targeting Oxidative Stress as Anticancer Therapy

The first approach to prevent or treat cancer, by targeting ROS, was based on the use of antioxidant reagents [11, 15]. In one of the first trials, based on supplementation of selenium, vitamin E and β-carotene on the diet showed a reduction of overall mortality and cancer rates [26]. However, a following trial not only failed to obtain consistent results but also indicated that in certain cases, antioxidants can rather promote cancer initiation and progression. Concordantly, two trials of cancer prevention, the CARET on male smokers, treated with vitamin A and/or β-carotene and the SELECT trial, on older males treated with vitamin E and/or selenium, resulted in an increased incidence of lung and prostate tumors, respectively [27–29]. Similar contradictory results were shown in the trials using antioxidant treatment as adjuvant therapy [30].

Based on these results, almost a decade ago, ROS inducers were proposed as anticancer strategy, in order to overcome the specific threshold of ROS level beyond which cancer cells undergo ROS-mediated cell death [4, 5]. The first agents used are those improving electrons leak from the respiratory complexes in the mitochondria, such as the arsenic trioxide, or conventional chemotherapeutic drugs such as doxorubicin. Indeed, patients treated with those agents showed lipid peroxidation in their plasma as well as low levels of vitamin E, vitamin C, and β-carotene in the blood [4]. The mechanism of action of these agents seems to be related to their ability to generate ROS directly from the mitochondria. Indeed, doxorubicin and arsenic trioxide penetrate in the inner membrane of the mitochondria and induce superoxide radical production by modulating the electron transport chain. Also 5-fluorouracil increases mitochondrial ROS with a different mechanism, mediated by p53 [4, 31]. Ionizing radiations represent other important ROS inducers, because they are able to promote by themselves high level of ROS and also because they might increase NADPH oxidase, an important source of ROS [32]. Moreover, we and others have demonstrated, in different models and in different combination settings, that oxidative injury played a significant functional role in the antitumor effect of histone deacetylase inhibitors (HDACi), a class of epigenetic antitumor compounds currently in clinical practice in haematological malignancies [7, 13, 33–42].

Recently, a new ROS inducer compound, Elesclomol (STA-4783), has been developed and tested, both in in vitro and in vivo preclinical studies as well as in clinical

trials [5, 43]. Interestingly, the result from a phase II trial using Elesclomol in combination with chemotherapy, in malignant melanoma patients, showed ROS generation and oxidative damage associated with prolonged progression-free survival [44]. Unfortunately, these results were not replicated in a phase III trial, where Elesclomol treatment was suspended due to adverse toxic effects [45]. The reason of this failure could be ascribed, at least in part, to cancer cells' capability to activate ROS adaption mechanisms by increasing levels of ROS scavengers, especially at advanced stages. This event is particularly efficacious in CSC, as described in the last paragraph of this review. To counteract the ROS adaptation mechanisms, a plausible solution could be the combination of ROS inducers either with another ROS inducer or with compounds that suppress cellular antioxidants, to overcome the threshold useful to induce cell death, The latest approach was tested by using an inhibitor of the scavenger SOD2, 2-Me, in combination with arsenic trioxide in lymphocytic leukemia and urothelial carcinoma cells [46, 47]. Similarly, the combination between the inhibitor of the antiapoptotic protein bcl2 ABT-737 and the ROS inducer, N-(4-hydroxyphenyl) retinamide, or the combination between an NRF2 inhibitor and a glutathione-depleting agents, showed increasing therapeutic efficiency compared to single-agent treatment [48, 49]. Based on these data, several clinical trials of combination treatment between ROS inducers and scavenger inhibitors are ongoing, including a multicenter phase II trial with the iron chelator Triapine and gemcitabine in advanced non-small-cell lung cancer [5].

4. Bioinformatics Correlation between Oxidative Stress Gene Expression and Prognosis in Solid Cancer Patients

Although the biological role of oxidative stress pathways has been extensively demonstrated, it is still unclear which and how oxidative stress genes predict bad prognosis and if their modulation is cancer-type specific. Here, to address this question, we took advantage of Cancer Genome Atlas (TCGA) database that, by profiling RNA expression levels and DNA mutational status for thousands of genes, has generated comprehensive maps of the key genomic changes in several types of cancer, enabling correlative analysis of critical cellular pathways involved in each type of cancers [50, 51]. In details, we compared cancer patient overall survival (OS) and the mRNA levels of 73 oxidative stress genes, selected from a public available oxidative stress signature [9], in different solid tumors. Specifically, the signature included peroxidases, which are represented by glutathione peroxidases (GPx) and peroxiredoxins (TPx); genes implicated in ROS metabolism (i.e., DUSP1, FoxM1, and HMOX1); and genes involved in superoxide metabolism, such as superoxide dismutase (SOD). Starting from the selection of the 73 oxidative stress genes, bioinformatics investigations were performed as described in Figure 2.

In details, bioinformatics analysis was made by SynTarget online tool (http://www.bioprofiling.de/PPISURV) using the following public datasets: TCGA_PAAD for pancreatic cancer, TCGA_COAD for colon cancer, TCGA_HNSCC for head and neck cancer (HNSCC), GSE31210 for lung cancer, TCGA_PRAD for prostate cancer, and METABRIC for breast cancer [52, 53]. PPISURV automatically derives the currently known interactome for a gene of interest and correlates expression levels of its interactome, with survival outcome in multiple publicly available clinical expression data sets containing microarray expression data set annotated with survival data. In details, as reported by Antonov et al. [54], in the case of the option "single gene survival analyses on a single data set," the PPISURV program exploits rank information from expression data sets that reflect the relative mRNA expression level. The samples are grouped with respect to expression rank of the gene in order to correlate survival information to the expression level of a gene in a particular data set. The groups are then subdivided in basis to "low expression" and "high expression" where expression rank of the gene is less or more than average expression rank across the data set, respectively. This separation of patients into "low" and "high" groups in the data set along with survival information is then used to find any statistical differences in survival outcome and to draw Kaplan-Meier plot. Hence, PPISURV establishes a correlation of the selected gene with survival and assesses the sign of the effect and if the gene deregulation is associated with positive or negative outcome.

Notably, a significant number of oxidative stress genes were negatively correlated with survival in solid carcinomas, reinforced the idea that oxidative stress plays a crucial role in cancer cells (Figure 3). Furthermore, going deep to our bioinformatics analysis, we observed that breast, lung, and HNSCC cancers were those more susceptible to oxidative stress gene expression fluctuations. To explain these data, one hypothesis could be that all these tumors are more vulnerable to external insults (i.e., pollutants) that, as mentioned above, are an important source of ROS. Furthermore, we speculate that this phenomenon could be also related to the high mutational load of those tumors. Indeed, several studies showed that either breast (particularly triple-negative subgroup) or lung cancer exhibited an elevated mutational load which is closely associated to mutations in DNA damage repair genes as well as to intrinsic genomic instability [55–57]. Similarly, recently it has been demonstrated that the overall mutational load was higher in old HNSCC patients that represent a high percentage of all HNSCC cancers, compared to younger patients [58]. On the contrary, pancreatic, prostate, and even colon (with exception of microsatellite instability (MSI) high subgroup) cancers are described as less hypermutated and thus, we speculate, are also less dependent to the oxidative stress and genomic instability [59–61].

A further detailed analysis of our correlation between oxidative gene expression signature and OS unveiled that the behavior of modulated genes was different among the cancers examined, with the exception of two genes involved in ROS metabolism, such as FoxM1 and TXNRD1, found as statistically significantly high in poor prognosis patients in four out of six of the tumor types analyzed (Figures 3 and 4). For this reason, those two genes are described below in details in two specific sections of the review. Other five

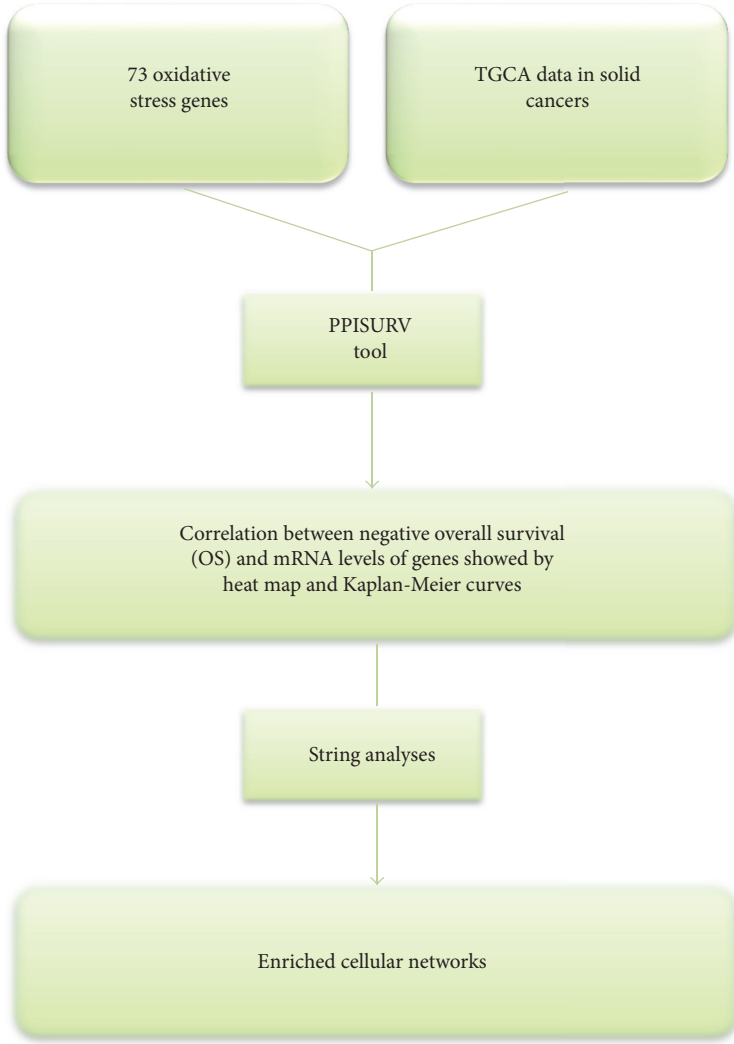

Figure 2: Bioinformatics analyses. Flow chart reporting step-by-step bioinformatics approach to unveil the most important genes/pathways involved in the correlation between oxidative stress and cancer.

genes, DUSP1, EPHX2, NUDT1, RNF7, and SEPP1, demonstrated a statistically significant modulation in poor prognosis patients in three out of six tumor types (Figure 3 and Suppl. Figure S1 available online at https://doi.org/10.1155/2017/2597581). Briefly, DUSP1 is a dual-specificity phosphatase-1, which is recognized as a key player for inactivating different MAPK isoforms. Recently, a role of DUSP-1 as central redox-sensitive regulator in monocytes has been demonstrated [62]. EPHX2 is a cytosolic epoxide hydrolase, implied in cancer progression and metastasis, in differentially manner based on the stages of carcinogenesis. Indeed, Bracalante et al. demonstrated that in A7 melanotic cells, resembling less aggressive tumor cells, anti-oxidant genes, including EPHX2, were upregulated in response to oxidative stress, while they were downregulated in G10 metastatic melanoma cells [63]. NUDT1, nudix hydrolase 1, is the most prominent mammalian enzyme among other enzymes responsible for hydrolyzing oxidized DNA precursors. NUDT1 is commonly upregulated in a wide variety of tumors to avoid incorporation of oxidized nucleotides that, in turn, induce DNA damage and cell death [64]. RNF7 (RING finger protein-7) acts as a metal chelating protein, a scavenger of ROS at the expense of self-oligomerization. RNF7 was found overexpressed in several tumor types, especially in lung carcinoma, and associated with poor prognosis [65].

SEPP1 is a selenoprotein 1, involved in cellular incorporation of the selenium circulating in the plasma. Moreover, SEPP1 has some antioxidant activity, as target of NRF2 family. In agreement, Bae et al. showed that some antioxidant genes known also as NRF2 targets, including SEPP1, were also transcriptionally modulated by the oncosuppressor BRCA1, thus suggesting that BRCA1 regulates the activity of NRF2 and protects cells against oxidative stress [66].

Finally, in order to identify a more relevant oxidative stress family in our setting, we performed an additional bioinformatics analysis where, independently from their trend of expression associated to poor prognosis, all modulated genes were analyzed in the biological database STRING, a resource of known and predicted protein-protein interaction. As shown in Figure 5, our analysis reveals an enriched

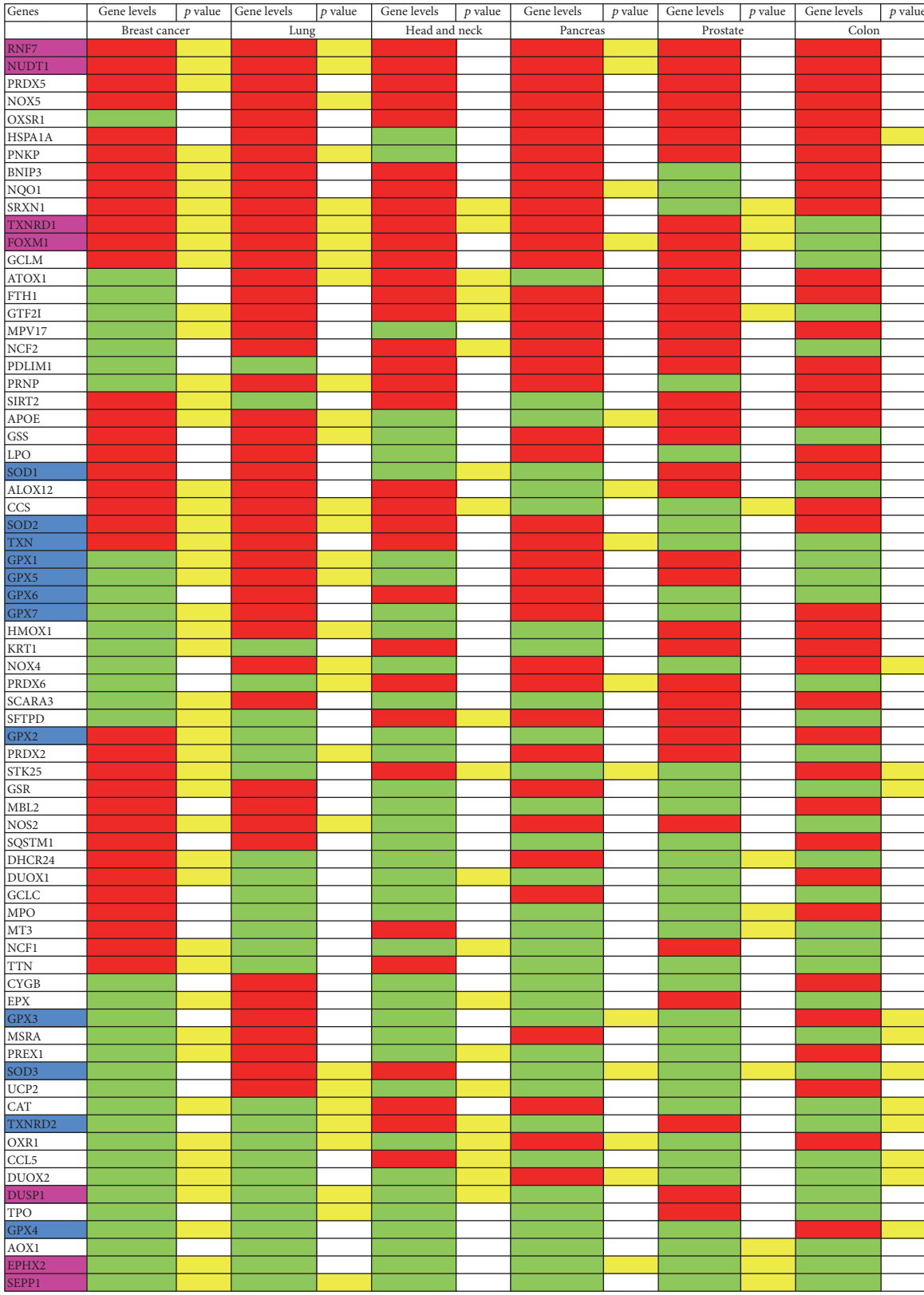

Figure 3: Bioinformatics correlation between oxidative stress gene expressions and poor prognosis in 6 different tumor types. Heat map in which we report in red or in green if the high or low expression of genes was negatively correlated with survival, respectively. Moreover, we evidenced in yellow when the correlation is statistically significant (with p value <0.05). In the first column, we evidenced in magenta, the genes similar modulated among cancers and in blue those oxidative stress family extracted from STRING analysis. Notably TXNRD1 showed a central role in both analyses.

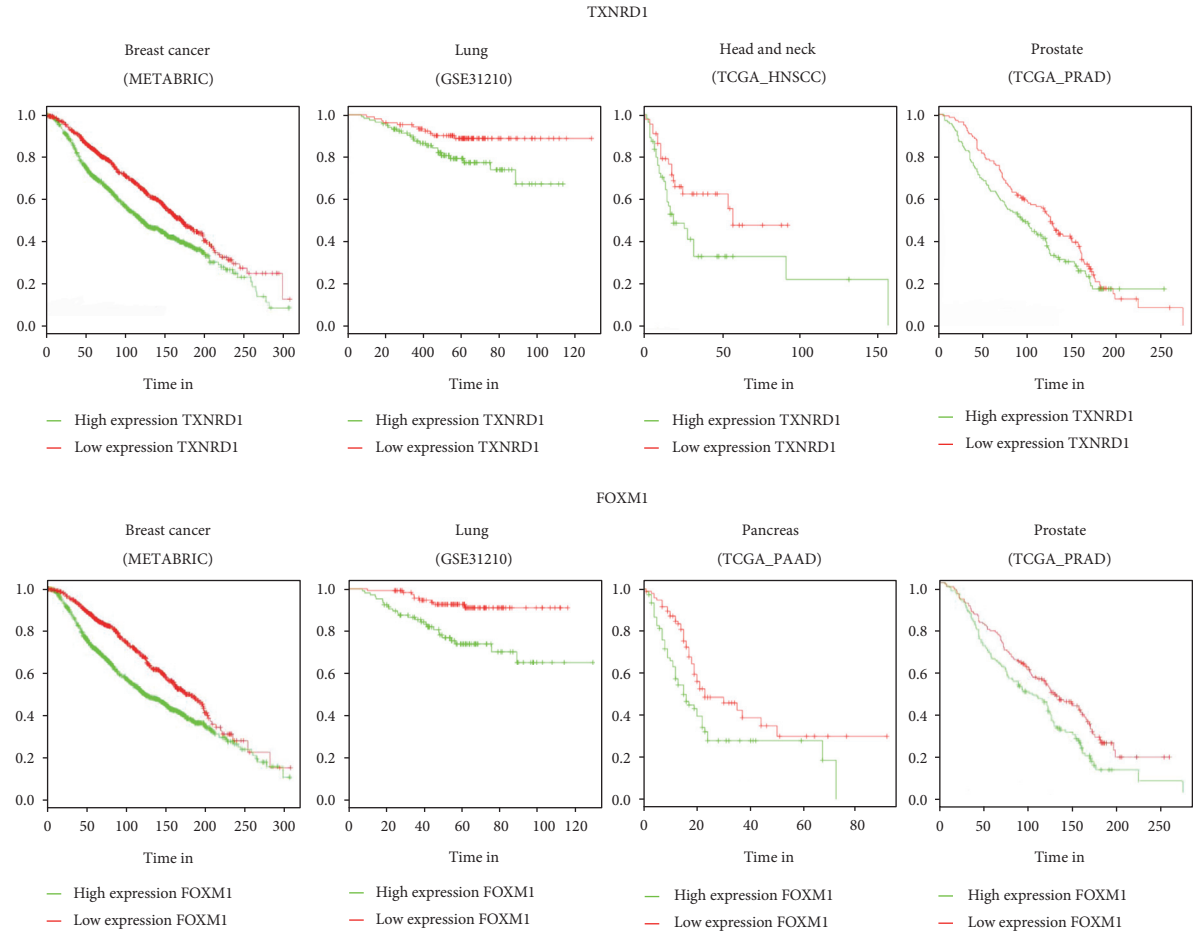

Figure 4: TXNRD1 and FoxM1 expression related to patient survival. Kaplan-Meier curves showing the survival in the case of high and low expression of TXNRD1 and FOXM1 in solid cancer patients.

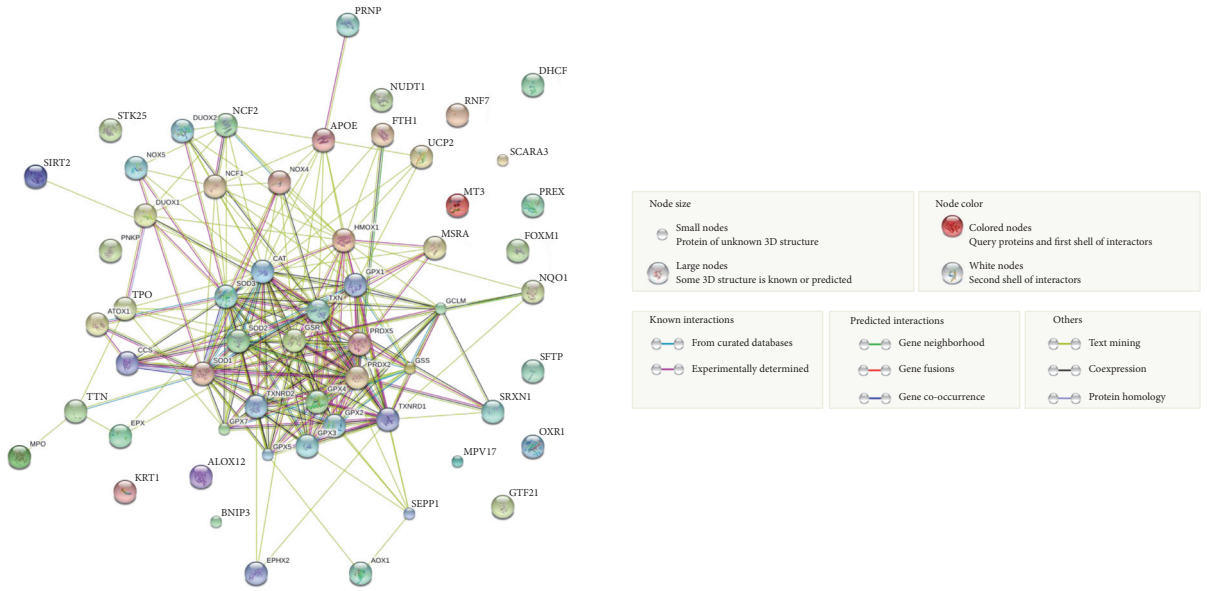

Figure 5: STRING analysis of the 58 oxidative stress genes. Association network in STRING analysis shows interactions of glutathione peroxidase, superoxide dismutase, and thioredoxin as principal oxidative stress signaling among six different tumor types.

cellular network, in which many genes, including GPx, SOD, and Trx pathways (the latter including TXNRD1), are strongly correlated, as demonstrated by both experimental studies and text mining (see red and green lines, resp.). Similar analyses were also performed for each tumor type separately, or considering high or low gene expression individually, confirming in almost all tumor types GPx, SOD, and Trx signaling as those predominant (Suppl. Figures S2 and S3).

Based on these analyses, together with TXNRD1, we decided to review the correlated pathways enriched in the network, in details (see below), analyzing their role in cancer and the possible therapeutic strategies to hit them.

5. FoxM1, a Critical Regulator of Oxidative Stress during Tumorigenesis

The highly conserved transcription factor FoxM1 belongs to the forkhead box transcription factor family, similarly to the best known member of FoxO family. However, different from the members of FoxO family, FoxM1 is expressed only in proliferative cells. Indeed, FoxM1 as a target of the cyclinD-CDK4/6 kinases, is reactivated when quiescent cells reenter in the cell cycle and reach a maximal level in S-phase which is maintained throughout G2 and mitosis [67, 68]. Beyond this role on proliferation, FoxM1 regulates metastasis, apoptosis, and DNA damage repair [69–71]. Furthermore, FoxM1 has been shown to prevent oxidative stress-dependent premature senescence. Park et al. showed how ROS themselves are inducers of FoxM1 expression, which in turn is able to stimulate antioxidant genes. The authors proposed the inhibition of FoxM1 as a new therapeutic strategy to kill cancer cells selectively [71]. In agreement, FoxM1 knocking-down was reported to sensitize human pluripotent stem cells to oxidative stress, as a consequence of activated-CAT5 downregulation, a FoxM1 antioxidant target gene [69].

A growing body of evidences reported high FoxM1 as frequently related to poor prognosis in multiple cancers, concordantly with our bioinformatic results [50]. To date, several mechanisms have been proposed to explain the activity of FoxM1 in cancer progression, including the activation of FoxM1 by several oncogenic protein and signalling pathways, such as c-Myc, Ras, and PI3K/AKT [72].

Hereafter, we discussed the role of FoxM1 in the four tumor types where we found statistically significant association of FoxM1 expression and poor prognosis.

The impact of FoxM1 in breast cancer progression is widely demonstrated. Indeed, its high level has been correlated with large tumor size, lymphovascular invasion, lymph-node metastases, and high stage. Two independent studies carried out on ER+ patients, reported that low FoxM1 expression, compared to high FoxM1 expression, is associated to better survival. Another study proved a positive correlation between HER2 status and FoxM1 expression in breast cancer tissue compared to normal breast counterpart [73–75], suggesting that FoxM1 is a downstream target of HER2 and could be used as a marker of HER2 overexpression. However, molecular basis underling the described roles of FoxM1 in cancer progression still needs to be clarified and different mechanisms have been proposed. For example, the induction of EMT by activation of Slug [76], stabilization of Smad3/Smad4 complex, and activation of TGFβ pathway [77] as well as the modulation of extracellular matrix by affecting the levels of uPA, uPAR, MMP-2, MMP-9, and VEGF have been proposed [78, 79]. Moreover, FoxM1 cooperates with survivin and nuclear XIAP in the promotion of chemoresistance [80]. Finally, further studies demonstrated that FoxM1 induces resistance to all the therapeutics tested in breast cancer (including cisplatin, paclitaxel, and trastuzumab) by several mechanisms: (1) acting on DNA-damage repair pathways, (2) promotion of cell cycle progression, (3) inhibition of cell cycle checkpoints, and (4) apoptosis induction [72].

FoxM1 gene is widely described as amplified also in lung cancer, regulating cell proliferation by promoting both G1/S and G2/M transition, differentiation, and transformation [81] as well as inhibition of apoptosis [82]. Recently, a direct link between FoxM1-induced ROS and lung cancer progression has been proposed by Tahmasbpoura et al. Their study showed elevated rate of lung cell proliferation related to high FoxM1 expression in patients exposed to sulfur mustard, a well known agent able to induce ROS [83].

Beyond the mechanisms described, the molecular basis of FoxM1 dysregulation has been also related to the capability of vitamin D receptor (VDR)/FoxM1 axis to affect cell stemness and to induce an invasive and metastatic phenotypes in pancreatic cancer. Indeed, the authors observed that VDR activation reduced the levels of FoxM1, inducing nuclear accumulation of β-catenin [84].

In prostate cancer (PCa), only few studies focused on the role of FoxM1; for instance, FoxM1 and its target CENPF, a structural protein of kinetochore, have been both proposed as critical drivers of PCa development and as prognostic markers of poor survival [85]. Concordantly, Lin et al. unveiled different miRNAs regulating FoxM1-CENPF axis taking advantage of miRNA expression profile available in Taylor dataset of prostate specimens (normal, localized, and metastatic tissues) [86]. Notably, since CENPF regulates several genes important for metastasis, including MMP2, MMP9, LOX, CXCR4, and CXCL12, dysregulation of the miRNA-COUP-TFII-FoxM1-CENPF axis can inhibit also PCa metastatization [86].

Overall, these considerations identified FoxM1 as a potential anticancer therapeutic target. Unfortunately, the druggability of FoxM1 remains a big challange because of the lack of substrate-binding pockets and hydrophobic surfaces [72, 87]. Several in vitro studies proposed RNA interference (RNAi) as a strategy to knockdown FoxM1, either alone or in combination with ROS inducers, in order to provoke ROS-mediated cell death [82]. Some studies reported that proteasome inhibitors, including bortezomib or thiostrepton, directly reduce both FoxM1 expression and its transcriptional activity with the same efficacy as that obtained by FoxM1 silencing [82, 88]. This latter approach is very promising, considering that bortezomib is already in clinical practice to treat multiple myeloma, and that RNAi treatment, so far, is not a reasonable therapeutic approach in patients [50, 82, 88]. Thus, bortezomib treatment has been proposed

as effective therapeutic strategy in highly expressing FoxM1 solid tumor, also in association with ROS inducers.

6. Thioredoxin, Glutathione Peroxidase, and Superoxide Dismutase Families as Mediators of Carcinogenesis

Thioredoxin system, composed of thioredoxin reductase (TrxR), thioredoxin (Trx), and NADPH, senses and responds to oxidative stress and modulates the redox status by scavenging ROS and by regulating several redox enzymes and signaling proteins. Mammalian genomes encode two main Trx systems: Trx1 and Trx reductase (TrxR) 1, which together constitutes the cytosolic system; Trx2 and TrxR2, which are localized in mitochondria (a Trx3 isoform has been also reported, as a testis-specific form, mainly expressed in male germ cells and associated to reproductive disorders) [89]. Trx1 reducing power allows the transfer of two electrons from its dithiol motif to an acceptor, then the oxidized disulfide form of the enzyme is recycled to the dithiol form by TrxR1, thereby oxidizing one molecule of NADPH.

Interestingly, our analysis revealed that TXNRD1, the gene encoding TrxR1, is upregulated and correlates with bad prognosis in pancreatic, colon, HNSCC, lung, prostate, and breast cancers. Trx1 enzyme has been shown to regulate NF-κB, playing opposite roles, depending to its intracellular localization: overexpression of Trx in cytoplasm reduced NF-κB activity, blocking the degradation of the NF-κB inhibitor IκB; in the nucleus, Trx directly reduces the cysteine(s) of NF-κB allowing the NF-κB-dependent gene expression [90]. Following NF-κB stimuli, such as UVB irradiation and TNFα treatment, Trx quickly translocates from the cytoplasm into the nucleus. Trx1 has also been reported as a secreted protein by normal and neoplastic cells [91], but not via exosomes [92]. Notably, Trx-increased secretion contributed to high ROS production in cisplatin-resistant lung tumors, both in vitro and in vivo [93].

Trx1 itself is regulated both by hypoxia and by oxidative stress conditions via binding of NRF2 to an antioxidant responsive element in the Trx promotor [94]. Moreover, Trx1 complex functions as a molecular switch turning the cellular redox state into kinase signaling. Thus, the system is able to regulate DNA synthesis, cell proliferation [95, 96], apoptosis, and transcription. In details, the reduced form of Trxs binds to apoptosis signal-regulating kinase 1 (ASK1) and inhibits its activity to prevent stress- and cytokine-induced apoptosis; when Trx is oxidized, it dissociates from ASK1 and apoptosis is stimulated [97–100]. The impact of Trx1 intracellular localization on its role may be taken into account especially in tumors (as colon and prostate) where a low expression of TXNRD1 correlates to poor patient outcome (as described in Figure 3). In fact, although increased Trx1 protein expression has been associated to hypoxic regions of certain tumours, tumor grade and chemoresistence, for instance by scavenging ROS species generated by various anticancer agents [101, 102], its localization and activity have to be both taken into account. In prostate cancer, Shan and colleagues identified constitutive nuclear and transiently increased cytoplasmic Trx1 oxidation by androgen but decreased Trx1 activities with the progression of prostate cancer, despite high levels of Trx1 protein expression in cancer cells [103]. The role of TrxR1 in dysplastic transformation has been pointed out in human breast epithelial cells, triggered by chronic oxidative stress [104]. In addition, Trx1 has been proposed as serum biomarker for either early diagnosis or prognosis of breast cancer in association with CEA and CA15-3 [105]. In non-small-cell lung cancer, Trx1 is able to modulate transcription of cyclooxygenase-2 via hypoxia-inducible factor- (HIF-) 1α [106]. It is actually worth to mention that many human cancers have low levels of thioredoxin-binding protein-2 (TBP-2), a Trx regulator which is able to bind Trx, blocking its reducing activity. These mechanisms have been identified as druggable: histone deacetylase inhibitors (HDACi) have been demonstrated to upregulate TBP-2 in various transformed cells, associated with a decrease in Trx levels [102].

Recently, Park and colleagues observed that TrxR2 is a novel binding protein for ribonucleotide reductase small subunit p53R2, which is involved in nuclear and mitochondrial DNA replication and repair, stimulating the enzymatic activity of TrxR in vitro. Their findings also suggest that p53R2 acts as a positive regulator of TrxR2 activity in the mitochondria both under normal physiological conditions and during the cellular response to DNA damage [107].

Although STRING analyses highlighted glutathione peroxidases (GPx) as one of the main family involved in oxidative stress adaptation, we found high heterogeneity in the disregulation of GPx family members among the tumor types we have investigated (Figure 5). GPx reduces either free hydrogen peroxide to water or lipid hydroperoxides to their corresponding alcohols. So far, eight different isoforms of GPx, 1 to 8, have been identified in humans, carrying different affinities for their substrates and different localizations. GPx1, found in the cytoplasm of mammalian cells, is mainly able to target the hydrogen peroxide, while GPx4 showed high affinity for lipid hydroperoxides. GPx2 is an intestinal and extracellular enzyme, while GPx3 is extracellularly secreted [99].

GPx1 allelic loss or polymosphisms have been known for years to contribute to both lung [108] and breast cancers [109]. Interestingly, in HNSCC cancer, almost all the isoforms showed low expression (Figure 3). In agreement, a decrease in GPx activity accompanied by SOD and CAT decrease as well as higher levels of oxidative DNA damage was found in HNSCC patients compared to healthy donors [110].

An increase of both Trx and GSH metabolism is a mechanism widely implicated in the resistance of cancer cells to chemotherapy. Loss of TXNRD1 makes tumors highly susceptible to pharmacological GSH deprivation, and concomitant inhibition of both GSH and TxrR systems was recently proposed as an anticancer strategy [18, 111]. Recently, Rodman and colleagues demonstrated that depletion of GSH and inhibition of TrxR activity enhanced radiation responses in human breast cancer stem cells by a mechanism involving thiol-dependent oxidative stress [112]. Furthermore, Scarbrough and colleagues reported that simultaneous

GSH/Trx inhibition sensitizes human breast and prostate cancer cells to 2DG + 17AAG-mediated killing [113].

Among the most important antioxidant enzymes, it is also important to highlight the role of SOD. SOD is able to convert the superoxide (O_2^-) radical into either oxygen (O_2) or the less reactive hydrogen peroxide (H_2O_2) which can then be removed by CAT, GPx, or TPx. Among the three major families of SOD, those we single out in humans are the copper and zinc (Cu-Zn) SOD1, whose localization is in cytosol, nucleus, peroxisome, and intermembrane space of the mitochondria [114], the mitochondrial enzyme manganese SOD2 (MnSOD), and the (Cu-Zn) extracellular SOD3. SOD enzymes are able to exert a strong antioxidant activity. In a recent study, Elchuri and colleagues observed that mice deficient in CuZn SOD1 (which contributes to the majority of cellular SOD activity [115]) showed a reduced lifespan and increased incidence of neoplastic changes in the liver [116]. Conversely, it has been also observed by several authors that SOD1 overexpression makes tumor cells resistant to oxidative stress and chemotherapy [117]. Increased expression and activity of MnSOD has been correlated with cancer aggressiveness in several tumors and through different pathways [118]. Recently, dysregulation of MnSOD function has been linked to an acetylation-mediated impairment [119, 120] which triggers an increase in oxidative stress, leading to AKT activation via oxidative inactivation of PTEN [119]. MnSOD acetylation (and activity) is regulated by the deacetylase Sirt3, a mitochondrial fidelity protein. Interestinlgly, Zou et al. showed that loss of Sirt3 results in endocrine therapy resistance of human luminal B breast cancer [120]. In agreement, we and others demonstrated that HDAC inhibition increases MnSOD protein expression in both solid and haematological diseases [121, 122].

Overall, similar to FoxM1, the described antioxidant systems represent putative good targets to improve therapeutical oxidative stress-dependent strategies. In details, several recent efforts have focused on the targeting of Trx/TrxR system [123–130]. Moreover, increasing evidences on a putative key role of HDAC inhibitors in the modulation of these pathways may deserve further investigations. In this regard, our recent study on the effect of HDACi in regulating NRF2/Keap1 pathway is of interest, considering the interplay between this pathway and thioredoxin [7].

7. Oxidative Stress and Cancer Stem Cells

In the multitude of morphological, functional, and responsive cancer cells, a subset of the so-called "cancer stem cells" (CSC), carrying peculiar features, was identified almost ten years ago in solid cancers [131]. However, the name CSC is not referred to an origin from normal stem counterpart but rather represents a specific population that displays some exceptional properties normally attributed to stem cells. Specific features, like hierarchical differentiation, self-renewal, enhanced invasive capacity, metastatic proficiency, and tumorigenicity, make CSC critical for tumor initiation and growth [132], while CSC elevated apoptosis resistance, drug-efflux pumps, enhanced DNA repair efficiency, detoxification enzyme expression, and quiescence are all identified as prosurvival mechanisms associated with resistance to chemotherapy and tumor relapse [133].

Few studies reported the behavior of cancer stem cells in oxidative stress condition, but notably in contrast to their normal stem cell counterparts, cancer stem cells are characterized by increased ROS levels, reduced oxidative damage, and thus longer survival [134, 135]. For example, Im and colleagues showed that significantly higher ROS levels were observed in the supernatant of glioblastoma cells, grown in serum-free sphere medium, either in polystyrene-treated tissue culture plates or in nonadherent plates. Moreover, it has been also shown that ROS is a critical factor for maintaining stemness, regulating the expression of the transcription factor SOX-2 [136]. This can be due to a combination of mechanisms that arise in the tumor, such as modulation of (1) multiple antioxidative enzyme systems [137] or (2) redox-sensitive signaling pathways, as NRF2, NF-κB, c-Jun, and HIFs, leading to the increased expression of antioxidant molecules [5].

The higher ROS levels in CSC could be associated with lower basal expression of ROS-scavenging systems, such as SODs, CAT, GPx, and TPx, compared to normal stem cells. In this regard, Yang et al. published those nonglioma stem cells which displayed significantly lower basal GPx1 expression and activity than glioma stem cells and that miR-153/NRF2/GPx1 pathway plays an important role in regulating radiosensitivity and stemness of glioma stem cells via ROS [138].

Due to the growing body of studies focused on the differential modulation of redox-sensitive signaling pathways (as summarized in Figure 6) in CSC subpopulation, compared to cancer cells or normal stem cells, in this paraghraph we discuss the relevance of the ROS-related pathways modulated in CSC phenotype.

In hypoxic environments, limited amount of oxygen leads to metabolic switches in both normal and malignant cells by HIFs. Paradoxically, recent studies have shown that CSC exhibit high HIF activity in normoxic environments and that HIF activity is critical in the maintenance of CSC as well as in the differentiation [139]. In agreement, Wang et al. found that overexpression of stem cell factor in hepatocellular carcinoma is regulated by hypoxic conditions through a selective HIF2α-dependent mechanism which promotes metastasis [140].

Several studies showed that HIF factors can enhance CSC population growth by modulating Notch signaling pathway in glioma [141], Hippo pathway through direct stabilization of TAZ in breast cancer [142], Ras-ERK-ELK3 in hepatocellular cancer, hypoxia-NOTCH1-SOX2 in ovarian cancer [143], and IL6-HIF1α in non-small-cell lung cancer [144]. Additionally, Yang et al. established that gastric CSC exhibited a marked increase in HIF1α expression and increased migration and invasion capabilities compared with the normoxic control upon hypoxia treatment. Also HIF-1α was responsible for activating EMT via increased expression of the transcription factor Snail in gastric CSC [145].

NF-κB is also related to hypoxia and HIF1α induction. It has been shown that inhibition of NFκB signaling promoted a significant reduction in the hypoxia-driven expansion of $CD44^+CD24^{-/low}$ CSC which was due to increased CD24

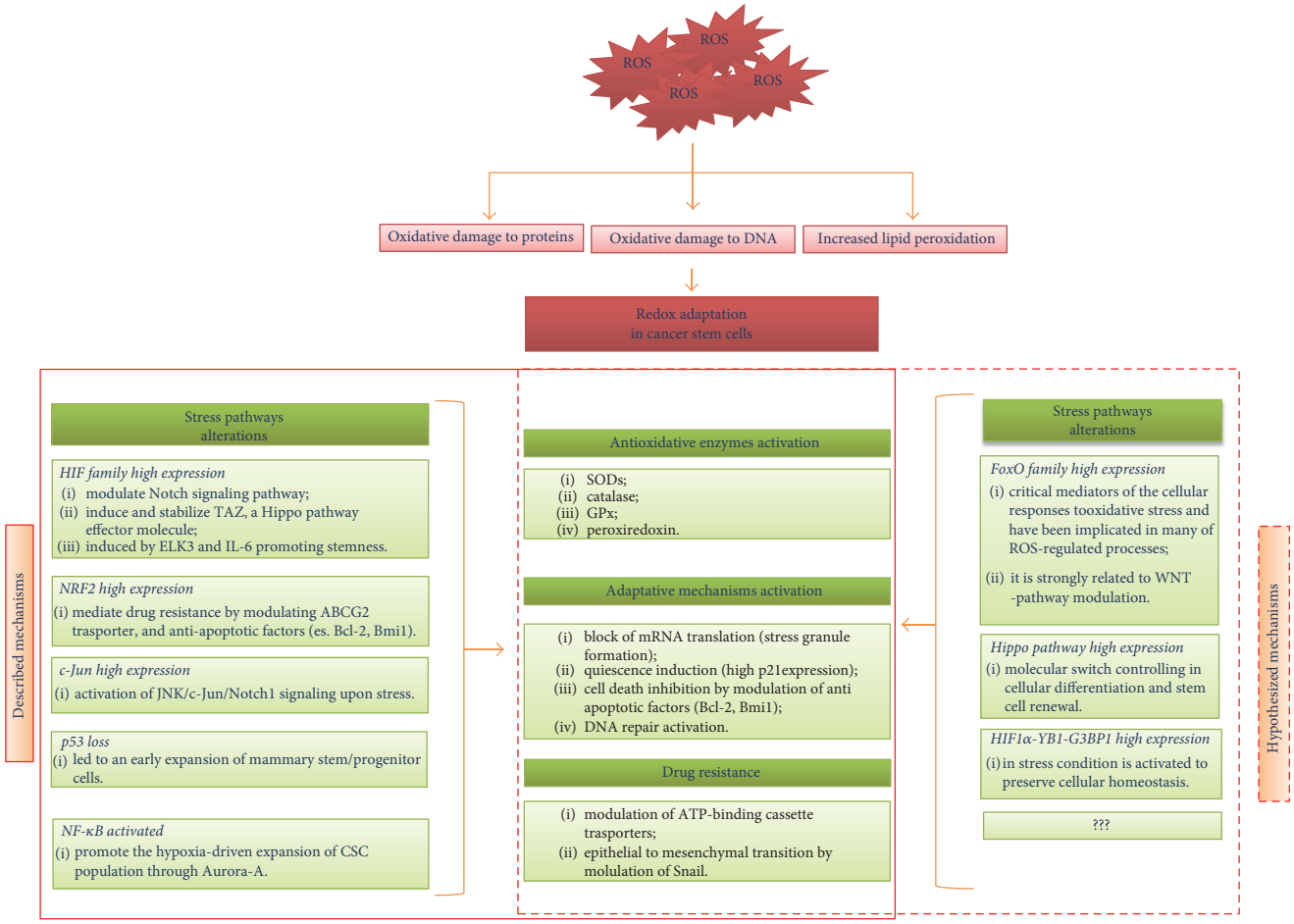

Figure 6: Redox stress in cancer stem cells. The persistent production of abnormally large amounts of ROS induced the mechanism of redox adaptation that, in turn, is translated in a various alteration in stress signaling. Here, we reported both known and hypothesized modulated pathways.

expression in breast cancer models [146]. Similarly, Aurora A kinase which can activate NF-κB pathway has been found highly expressed in ovarian CSC [147].

NRF2 represents another antioxidant system involved in the maintenance of quiescence as well as in the determination of differentiation fate in normal stem cells, as described and reviewed by Ryoo et al. [148]. For example, NRF2-deficient mice showed defective stem cell function. Indeed, haematopoietic stem cell, derived from those mice, dispayed lower levels of prosurvival cytochines and exibited spontaneous apoptosis related to wild-type cells [149].

Recently, several studies showed that high levels of NRF2 are related to CSC survival and anticancer drug resistance in HNSCC, cervical, breast, and ovarian cancers [150–153]. Notably, it was reported that NRF2 overexpression is related to an induction of ATP-binding cassette trasporters and thus drug resistance mechanisms. Other described redox-signaling pathway implicated in redox regulation in CSC could be c-Jun and/or p53 and NF-κB and FoxO family. In details, Chiche et al. showed that the loss of p53 in K5ΔNβcat (βcat activated) mice led to an early expansion of mammary stem/progenitor cells and accelerated the formation of triple-negative breast cancers. In particular, p53-deficient tumors expressed high levels of integrins and extracellular matrix components and were enriched in cancer stem cells [154].

Moreover, Xie et al. found that knockdown of JNK1 or JNK2 or treatment with JNK-IN-8, an adenosine triphosphate-competitive irreversible pan-JNK inhibitor, significantly reduced cell proliferation, the ALDH1+ and CD44 +/CD24- CSC subpopulations, and mammosphere formation, indicating that JNK family promotes CSC self-renewal and maintenance in triple-negative breast cancer [155].

However, other factors could be implicated in CSC capability to adapt high level of intracellular ROS and would be very interesting to better define them as potential therapeutic targets, mostly because many anticancer drugs increase intracellular ROS levels.

In this regard, the transcription factors FoxO1, FoxO3a, and FoxO4 are critical mediators of the cellular responses to oxidative stress and have been implicated in many of ROS-regulated processes [156]. It is also known that FoxO competes with TCF for the same binding site of β-catenin and suppresses β-catenin-TCF signaling toward proliferation, thus attenuating WNT-mediated signaling activities. Also, FoxO factors reduce mitochondrial output to prevent excess ROS production through inhibition of c-Myc function and alter the hypoxia response [157].

Another candidate is the Hippo pathway, which acts as a molecular switch controlling in cellular differentiation and stem cell renewal but is also modulated in stress condition and is described as highly mutated in cancer. Lehtinen and colleagues elegantly demonstrated the activation of Mst1, a serine/threonine kinase activated in the Hippo cascade, upon oxidative stress induced by exposure to increasing concentrations of exogenous H_2O_2. This was accompanied by phosphorylation of the transcription factor FoxO3a at S207, thereby disrupting its association with 14-3-3 binding protein and leading to its nuclear localization and transcriptional activation of the BH3- only Bcl-2 protein, Bim, which triggered neuronal apoptosis [158].

One of the first mechanisms modulated upon stress condition is messenger RNA translation, likely as a mean to limit energy demanding protein synthesis, leading to stress granule (SG) formation in cancer cells. Many evidences suggest that altered mRNA translational control is a critical factor in cancer progression, and in this regard, a new axis has been described. In details, Somasekharan et al. showed that under stress condition, a YB1, nuclease-sensitive element-binding protein 1, facilitates tumor metastasis through two mechanisms: first, it directly binds to HIF1α that drives stress adaptation and metastatic capacity in vivo; second, YB1 mediates formation of cytosolic SGs through translational activation of G3BP1, a SG nucleator [159]. Accumulating evidences suggest that SG formation is protective against stress-induced cell damage and death [160], and few studies suggested SG implication in cancer biology [161, 162].

8. Conclusions and Future Perspectives

The idea that the oxidative stress modulation has a crucial role in cancer cells to promote proliferation, adaptation, and resistance to therapy is now widely accepted [7, 12, 13]. Thus, modulating redox regulatory mechanisms represents an attractive therapeutic strategy. However, to date, the oxidative stress-related therapeutic strategies evaluated in preclinical and clinical studies did not produce homogenous results, due to several variables associated to ROS generation and redox adaptation mechanisms.

Furthermore, the identification of tumor-type specific oxidative stress gene profiles and how they could predict prognosis still represent critical challenges. Thanks to the increasing availability of cancer gene expression profile, mutation, epigenetic, and survival data from the TGCA dataset, it was possible to use bioinformatics to screen the role of oxidative stress genes from a publicly available signature in large cohorts of several solid cancer patients [52, 53].

The TCGA database provides correlative evidences suggesting the involvement of the FoxM1, thioredoxin, superoxide-dismutase, and glutathione pathways as principally and commonly modulated in breast, lung, HNSCC, pancreatic, prostate, and colon cancers. The differential expression levels of each gene observed in different settings revealed a precise spatial context where redox alterations may promote genome instability or redox adaptation.

For this reason, tumors should be classified into subclasses based on different oxidative stress alterations occurring in redox homeostasis genes, to guarantee the development of precision medicine-based approaches in selected subgroups of cancer patients. Further mechanistic studies are needed to identify either new compounds or molecules to be repositioned, in order to target the described redox pathways.

Conflicts of Interest

No potential conflicts of interest were disclosed.

Acknowledgments

This study was partially supported by the following Research Grant to Alfredo Budillon: Italian Ministry of Health (RF-2011-02346914).

References

[1] L. A. Sena and N. S. Chandel, "Physiological roles of mitochondrial reactive oxygen species," *Molecular Cell*, vol. 48, no. 2, pp. 158–167, 2012.

[2] J. G. Gill, E. Piskounova, and S. J. Morrison, "Cancer, oxidative stress, and metastasis," *Cold Spring Harbor Symposia on Quantitative Biology*, vol. 81, pp. 163–175, 2016.

[3] M. Tafani, L. Sansone, F. Limana et al., "The interplay of reactive oxygen species, hypoxia, inflammation, and sirtuins in cancer initiation and progression," *Oxidative Medicine and Cellular Longevity*, vol. 2016, Article ID 3907147, 18 pages, 2016.

[4] C. Gorrini, I. S. Harris, and T. W. Mak, "Modulation of oxidative stress as an anticancer strategy," *Nature Reviews Drug Discovery*, vol. 12, no. 12, pp. 931–947, 2013.

[5] D. Trachootham, J. Alexandre, and P. Huang, "Targeting cancer cells by ROS-mediated mechanisms: a radical therapeutic approach?," *Nature Reviews Drug Discovery*, vol. 8, no. 7, pp. 579–591, 2009.

[6] D. Hernandez-Garcia, C. D. Wood, S. Castro-Obregón, and L. Covarrubias, "Reactive oxygen species: a radical role in development?," *Free Radical Biology and Medicine*, vol. 49, no. 2, pp. 130–143, 2010.

[7] A. Leone, M. S. Roca, C. Ciardiello et al., "Vorinostat synergizes with EGFR inhibitors in NSCLC cells by increasing ROS via up-regulation of the major mitochondrial porin VDAC1 and modulation of the c-Myc-NRF2-KEAP1 pathway," *Free Radical Biology and Medicine*, vol. 89, pp. 287–299, 2015.

[8] G. B. Waypa, J. D. Marks, R. Guzy et al., "Hypoxia triggers subcellular compartmental redox signaling in vascular smooth muscle cells," *Circulation Research*, vol. 106, no. 3, pp. 526–535, 2010.

[9] https://www.qiagen.com/de/shop/pcr/primer-sets/rt2-profiler-pcr-arrays/?catno=PAHS-065Z#geneglobe.

[10] D. Hanahan and R. A. Weinberg, "Hallmarks of cancer: the next generation," *Cell*, vol. 144, no. 5, pp. 646–674, 2011.

[11] E. Panieri and M. M. Santoro, "ROS homeostasis and metabolism: a dangerous liason in cancer cells," *Cell Death & Disease*, vol. 7, no. 6, article e2253, 2016.

[12] T. Fiaschi and P. Chiarugi, "Oxidative stress, tumor microenvironment, and metabolic reprogramming: a diabolic liaison," *International Journal of Cell Biology*, vol. 2012, Article ID 762825, 8 pages, 2012.

[13] F. Bruzzese, B. Pucci, M. R. Milone et al., "Panobinostat synergizes with zoledronic acid in prostate cancer and multiple myeloma models by increasing ROS and modulating mevalonate and p38-MAPK pathways," *Cell Death & Disease*, vol. 4, article e878, 2013.

[14] S. F. Rodrigues and D. N. Granger, "Blood cells and endothelial barrier function," *Tissue Barriers*, vol. 3, no. 1-2, article e978720, 2015.

[15] J. Kim, J. Kim, and J. S. Bae, "ROS homeostasis and metabolism: a critical liaison for cancer therapy," *Experimental & Molecular Medicine*, vol. 48, no. 11, article e269, 2016.

[16] S. S. Sabharwal and P. T. Schumacker, "Mitochondrial ROS in cancer: initiators, amplifiers or an Achilles' heel?," *Nature Reviews Cancer*, vol. 14, no. 11, pp. 709–721, 2014.

[17] G. M. DeNicola, F. A. Karreth, T. J. Humpton et al., "Oncogene-induced Nrf2 transcription promotes ROS detoxification and tumorigenesis," *Nature*, vol. 475, no. 7354, pp. 106–109, 2011.

[18] I. S. Harris, A. E. Treloar, S. Inoue et al., "Glutathione and thioredoxin antioxidant pathways synergize to drive cancer initiation and progression," *Cancer Cell*, vol. 27, no. 2, pp. 211–222, 2015.

[19] A. Kuehne, H. Emmert, J. Soehle et al., "Acute activation of oxidative pentose phosphate pathway as first-line response to oxidative stress in human skin cells," *Molecular Cell*, vol. 59, no. 3, pp. 359–371, 2015.

[20] V. P. Sukhatme and B. Chan, "Glycolytic cancer cells lacking 6-phosphogluconate dehydrogenase metabolize glucose to induce senescence," *FEBS Letters*, vol. 586, no. 16, pp. 2389–2395, 2012.

[21] S. M. Wormann, L. Song, J. Ai et al., "Loss of P53 function activates JAK2-STAT3 signaling to promote pancreatic tumor growth, stroma modification, and gemcitabine resistance in mice and is associated with patient survival," *Gastroenterology*, vol. 151, no. 1, article e12, pp. 180–193, 2016.

[22] A. Alexander, S. L. Cai, J. Kim et al., "ATM signals to TSC2 in the cytoplasm to regulate mTORC1 in response to ROS," *Proceedings of the National Academy of Sciences of the United States of America*, vol. 107, no. 9, pp. 4153–4158, 2010.

[23] A. Alexander, J. Kim, and C. L. Walker, "ATM engages the TSC2/mTORC1 signaling node to regulate autophagy," *Autophagy*, vol. 6, no. 5, pp. 672-673, 2010.

[24] N. McCabe, S. M. Walker, and R. D. Kennedy, "When the guardian becomes the enemy: targeting ATM in PTEN-deficient cancers," *Molecular and Cellular Oncology*, vol. 3, no. 1, article e1053595, 2016.

[25] J. S. Chan, M. J. Tan, M. K. Sng et al., "Cancer-associated fibroblasts enact field cancerization by promoting extratumoral oxidative stress," *Cell Death & Disease*, vol. 8, no. 1, article e2562, 2017.

[26] Y. L. Qiao, S. M. Dawsey, F. Kamangar et al., "Total and cancer mortality after supplementation with vitamins and minerals: follow-up of the Linxian general population nutrition intervention trial," *Journal of the National Cancer Institute*, vol. 101, no. 7, pp. 507–518, 2009.

[27] G. S. Omenn, G. Goodman, M. Thornquist et al., "Chemoprevention of lung cancer: the beta-carotene and retinol efficacy trial (CARET) in high-risk smokers and asbestos-exposed workers," *IARC Scientific Publications*, vol. 136, pp. 67–85, 1996.

[28] G. S. Omenn, G. E. Goodman, M. D. Thornquist et al., "Risk factors for lung cancer and for intervention effects in CARET, the beta-carotene and retinol efficacy trial," *Journal of the National Cancer Institute*, vol. 88, no. 21, pp. 1550–1559, 1996.

[29] E. A. Klein, I. M. Thompson, C. M. Tangen et al., "Vitamin E and the risk of prostate cancer: the selenium and vitamin E cancer prevention trial (SELECT)," *JAMA*, vol. 306, no. 14, pp. 1549–1556, 2011.

[30] C. Jacobs, B. Hutton, T. Ng, R. Shorr, and M. Clemons, "Is there a role for oral or intravenous ascorbate (vitamin C) in treating patients with cancer? A systematic review," *The Oncologist*, vol. 20, no. 2, pp. 210–223, 2015.

[31] D. B. Longley, T. Latif, J. Boyer, W. L. Allen, P. J. Maxwell, and P. G. Johnston, "The interaction of thymidylate synthase expression with p53-regulated signaling pathways in tumor cells," *Seminars in Oncology*, vol. 30, no. 3, Supplement 6, pp. 3–9, 2003.

[32] T. Yoshida, S. Goto, M. Kawakatsu, Y. Urata, and T. S. Li, "Mitochondrial dysfunction, a probable cause of persistent oxidative stress after exposure to ionizing radiation," *Free Radical Research*, vol. 46, no. 2, pp. 147–153, 2012.

[33] F. Bruzzese, M. Rocco, S. Castelli, E. Di Gennaro, A. Desideri, and A. Budillon, "Synergistic antitumor effect between vorinostat and topotecan in small cell lung cancer cells is mediated by generation of reactive oxygen species and DNA damage-induced apoptosis," *Molecular Cancer Therapeutics*, vol. 8, no. 11, pp. 3075–3087, 2009.

[34] R. R. Rosato, J. A. Almenara, and S. Grant, "The histone deacetylase inhibitor MS-275 promotes differentiation or apoptosis in human leukemia cells through a process regulated by generation of reactive oxygen species and induction of p21CIP1/WAF1 1," *Cancer Research*, vol. 63, no. 13, pp. 3637–3645, 2003.

[35] X. Y. Pei, Y. Dai, and S. Grant, "Synergistic induction of oxidative injury and apoptosis in human multiple myeloma cells by the proteasome inhibitor bortezomib and histone deacetylase inhibitors," *Clinical Cancer Research*, vol. 10, no. 11, pp. 3839–3852, 2004.

[36] C. Yu, B. B. Friday, J. P. Lai et al., "Abrogation of MAPK and Akt signaling by AEE788 synergistically potentiates histone deacetylase inhibitor-induced apoptosis through reactive oxygen species generation," *Clinical Cancer Research*, vol. 13, no. 4, pp. 1140–1148, 2007.

[37] S. Bhalla, S. Balasubramanian, K. David et al., "PCI-24781 induces caspase and reactive oxygen species-dependent apoptosis through NF-kappaB mechanisms and is synergistic with bortezomib in lymphoma cells," *Clinical Cancer Research*, vol. 15, no. 10, pp. 3354–3365, 2009.

[38] N. Koshikawa, J. I. Hayashi, A. Nakagawara, and K. Takenaga, "Reactive oxygen species-generating mitochondrial DNA mutation up-regulates hypoxia-inducible factor-1alpha gene transcription via phosphatidylinositol 3-kinase-Akt/protein kinase C/histone deacetylase pathway," *The Journal of Biological Chemistry*, vol. 284, no. 48, pp. 33185–33194, 2009.

[39] I. M. Wolf, Z. Fan, M. Rauh et al., "Histone deacetylases inhibition by SAHA/Vorinostat normalizes the glioma microenvironment via xCT equilibration," *Scientific Reports*, vol. 4, p. 6226, 2014.

[40] K. F. Hui, P. L. Yeung, and A. K. Chiang, "Induction of MAPK- and ROS-dependent autophagy and apoptosis in

gastric carcinoma by combination of romidepsin and bortezomib," *Oncotarget*, vol. 7, no. 4, pp. 4454–4467, 2016.

[41] P. H. Liao, H. H. Hsu, T. S. Chen et al., "Phosphorylation of cofilin-1 by ERK confers HDAC inhibitor resistance in hepatocellular carcinoma cells via decreased ROS-mediated mitochondria injury," *Oncogene*, 2016.

[42] M. R. Makena, B. Koneru, T. H. Nguyen, M. H. Kang, and C. P. Reynolds, "Reactive oxygen species-mediated synergism of fenretinide and romidepsin in preclinical models of T-cell lymphoid malignancies," *Molecular Cancer Therapeutics*, 2017.

[43] J. R. Kirshner, S. He, V. Balasubramanyam et al., "Elesclomol induces cancer cell apoptosis through oxidative stress," *Molecular Cancer Therapeutics*, vol. 7, no. 8, pp. 2319–2327, 2008.

[44] S. O'Day, R. Gonzalez, D. Lawson et al., "Phase II, randomized, controlled, double-blinded trial of weekly elesclomol plus paclitaxel versus paclitaxel alone for stage IV metastatic melanoma," *Journal of Clinical Oncology*, vol. 27, no. 32, pp. 5452–5458, 2009.

[45] S. J. O'Day, A. M. Eggermont, V. Chiarion-Sileni et al., "Final results of phase III SYMMETRY study: randomized, double-blind trial of elesclomol plus paclitaxel versus paclitaxel alone as treatment for chemotherapy-naive patients with advanced melanoma," *Journal of Clinical Oncology*, vol. 31, no. 9, pp. 1211–1218, 2013.

[46] S. Takahashi, "Combination therapy with arsenic trioxide for hematological malignancies," *Anti-Cancer Agents in Medicinal Chemistry*, vol. 10, no. 6, pp. 504–510, 2010.

[47] K. L. Kuo, W. C. Lin, I. L. Ho et al., "2-methoxyestradiol induces mitotic arrest, apoptosis, and synergistic cytotoxicity with arsenic trioxide in human urothelial carcinoma cells," *PloS One*, vol. 8, no. 8, article e68703, 2013.

[48] S. Bruno, F. Ghiotto, C. Tenca et al., "N-(4-hydroxyphenyl)-retinamide promotes apoptosis of resting and proliferating B-cell chronic lymphocytic leukemia cells and potentiates fludarabine and ABT-737 cytotoxicity," *Leukemia*, vol. 26, no. 10, pp. 2260–2268, 2012.

[49] H. R. Lee, J. M. Cho, D. H. Shin et al., "Adaptive response to GSH depletion and resistance to L-buthionine-(S,R)-sulfoximine: involvement of Nrf2 activation," *Molecular and Cellular Biochemistry*, vol. 318, no. 1-2, pp. 23–31, 2008.

[50] B. Rotblat, T. G. Grunewald, G. Leprivier, G. Melino, and R. A. Knight, "Anti-oxidative stress response genes: bioinformatic analysis of their expression and relevance in multiple cancers," *Oncotarget*, vol. 4, no. 12, pp. 2577–2590, 2013.

[51] O. F. Kuzu, M. A. Noory, and G. P. Robertson, "The role of cholesterol in cancer," *Cancer Research*, vol. 76, no. 8, pp. 2063–2070, 2016.

[52] I. Amelio, P. O. Tsvetkov, R. A. Knight, A. Lisitsa, G. Melino, and A. V. Antonov, "SynTarget: an online tool to test the synergetic effect of genes on survival outcome in cancer," *Cell Death and Differentiation*, vol. 23, no. 5, p. 912, 2016.

[53] A. V. Antonov, "BioProfiling.de: analytical web portal for high-throughput cell biology," *Nucleic Acids Research*, vol. 39, pp. W323–W327, 2011.

[54] A. V. Antonov, M. Krestyaninova, R. A. Knight, I. Rodchenkov, G. Melino, and N. A. Barlev, "PPISURV: a novel bioinformatics tool for uncovering the hidden role of specific genes in cancer survival outcome," *Oncogene*, vol. 33, no. 13, pp. 1621–1628, 2014.

[55] J. Budczies, M. Bockmayr, C. Denkert et al., "Classical pathology and mutational load of breast cancer - integration of two worlds," *Journal of Pathology: Clinical Research*, vol. 1, no. 4, pp. 225–238, 2015.

[56] R. M. Chabanon, M. Pedrero, C. Lefebvre, A. Marabelle, J. C. Soria, and S. Postel-Vinay, "Mutational landscape and sensitivity to immune checkpoint blockers," *Clinical Cancer Research*, vol. 22, no. 17, pp. 4309–4321, 2016.

[57] N. B. Jamieson and A. V. Maker, "Gene-expression profiling to predict responsiveness to immunotherapy," *Cancer Gene Therapy*, 2016.

[58] S. Meucci, U. Keilholz, I. Tinhofer, and O. A. Ebner, "Mutational load and mutational patterns in relation to age in head and neck cancer," *Oncotarget*, vol. 7, no. 43, pp. 69188–69199, 2016.

[59] S. J. Murphy, S. N. Hart, J. F. Lima et al., "Genetic alterations associated with progression from pancreatic intraepithelial neoplasia to invasive pancreatic tumor," *Gastroenterology*, vol. 145, no. 5, pp. 1098–1109, 2013, e1.

[60] J. P. McCrow, D. C. Petersen, M. Louw et al., "Spectrum of mitochondrial genomic variation and associated clinical presentation of prostate cancer in South African men," *Prostate*, vol. 76, no. 4, pp. 349–358, 2016.

[61] F. Gelsomino, M. Barbolini, A. Spallanzani, G. Pugliese, and S. Cascinu, "The evolving role of microsatellite instability in colorectal cancer: a review," *Cancer Treatment Reviews*, vol. 51, pp. 19–26, 2016.

[62] H. S. Kim, S. L. Ullevig, D. Zamora, C. F. Lee, and R. Asmis, "Redox regulation of MAPK phosphatase 1 controls monocyte migration and macrophage recruitment," *Proceedings of the National Academy of Sciences of the United States of America*, vol. 109, no. 41, pp. E2803–E2812, 2012.

[63] C. Bracalente, I. L. Ibañez, A. Berenstein et al., "Reprogramming human A375 amelanotic melanoma cells by catalase overexpression: upregulation of antioxidant genes correlates with regression of melanoma malignancy and with malignant progression when downregulated," *Oncotarget*, vol. 7, no. 27, pp. 41154–41171, 2016.

[64] S. Waz, T. Nakamura, K. Hirata et al., "Structural and kinetic studies of the human nudix hydrolase MTH1 reveal the mechanism for its broad substrate specificity," *The Journal of Biological Chemistry*, vol. 292, no. 7, pp. 2785–2794, 2017.

[65] Y. Sun and H. Li, "Functional characterization of SAG/RBX2/ROC2/RNF7, an antioxidant protein and an E3 ubiquitin ligase," *Protein & Cell*, vol. 4, no. 2, pp. 103–116, 2013.

[66] I. Bae, S. Fan, Q. Meng et al., "BRCA1 induces antioxidant gene expression and resistance to oxidative stress," *Cancer Research*, vol. 64, no. 21, pp. 7893–7909, 2004.

[67] S. N. Mowla, E. W. Lam, and P. S. Jat, "Cellular senescence and aging: the role of B-MYB," *Aging Cell*, vol. 13, no. 5, pp. 773–779, 2014.

[68] M. Katoh, M. Igarashi, H. Fukuda, H. Nakagama, and M. Katoh, "Cancer genetics and genomics of human FOX family genes," *Cancer Letters*, vol. 328, no. 2, pp. 198–206, 2013.

[69] C. T. Kwok, M. H. Leung, J. Qin et al., "The forkhead box transcription factor FOXM1 is required for the maintenance of cell proliferation and protection against oxidative stress in human embryonic stem cells," *Stem Cell Research*, vol. 16, no. 3, pp. 651–661, 2016.

[70] I. Wierstra, "The transcription factor FOXM1 (forkhead box M1): proliferation-specific expression, transcription factor

function, target genes, mouse models, and normal biological roles," *Advances in Cancer Research*, vol. 118, pp. 97–398, 2013.

[71] H. J. Park, J. R. Carr, Z. Wang et al., "FoxM1, a critical regulator of oxidative stress during oncogenesis," *The EMBO Journal*, vol. 28, no. 19, pp. 2908–2918, 2009.

[72] R. Saba, A. Alsayed, J. P. Zacny, and A. Z. Dudek, "The role of forkhead box protein M1 in breast cancer progression and resistance to therapy," *International Journal of Breast Cancer*, vol. 2016, Article ID 9768183, 8 pages, 2016.

[73] H. Ahn, J. Sim, R. Abdul et al., "Increased expression of forkhead box M1 is associated with aggressive phenotype and poor prognosis in estrogen receptor-positive breast cancer," *Journal of Korean Medical Science*, vol. 30, no. 4, pp. 390–397, 2015.

[74] A. Bergamaschi, Z. Madak-Erdogan, Y. J. Kim, Y. L. Choi, H. Lu, and B. S. Katzenellenbogen, "The forkhead transcription factor FOXM1 promotes endocrine resistance and invasiveness in estrogen receptor-positive breast cancer by expansion of stem-like cancer cells," *Breast Cancer Research*, vol. 16, no. 5, p. 436, 2014.

[75] R. E. Francis, S. S. Myatt, J. Krol et al., "FoxM1 is a downstream target and marker of HER2 overexpression in breast cancer," *International Journal of Oncology*, vol. 35, no. 1, pp. 57–68, 2009.

[76] C. Yang, H. Chen, G. Tan et al., "FOXM1 promotes the epithelial to mesenchymal transition by stimulating the transcription of slug in human breast cancer," *Cancer Letters*, vol. 340, no. 1, pp. 104–112, 2013.

[77] J. Xue, X. Lin, W. T. Chiu et al., "Sustained activation of SMAD3/SMAD4 by FOXM1 promotes TGF-beta-dependent cancer metastasis," *The Journal of Clinical Investigation*, vol. 124, no. 2, pp. 564–579, 2014.

[78] A. Ahmad, Z. Wang, D. Kong et al., "FoxM1 down-regulation leads to inhibition of proliferation, migration and invasion of breast cancer cells through the modulation of extra-cellular matrix degrading factors," *Breast Cancer Research and Treatment*, vol. 122, no. 2, pp. 337–346, 2010.

[79] C. T. Karadedou, A. R. Gomes, J. Chen et al., "FOXO3a represses VEGF expression through FOXM1-dependent and -independent mechanisms in breast cancer," *Oncogene*, vol. 31, no. 14, pp. 1845–1858, 2012.

[80] G. N. de Moraes, D. Delbue, K. L. Silva et al., "FOXM1 targets XIAP and survivin to modulate breast cancer survival and chemoresistance," *Cellular Signalling*, vol. 27, no. 12, pp. 2496–2505, 2015.

[81] D. K. Yang, C. H. Son, S. K. Lee, P. J. Choi, K. E. Lee, and M. S. Roh, "Forkhead box M1 expression in pulmonary squamous cell carcinoma: correlation with clinicopathologic features and its prognostic significance," *Human Pathology*, vol. 40, no. 4, pp. 464–470, 2009.

[82] M. Halasi, B. Pandit, M. Wang, V. Nogueira, N. Hay, and A. L. Gartel, "Combination of oxidative stress and FOXM1 inhibitors induces apoptosis in cancer cells and inhibits xenograft tumor growth," *The American Journal of Pathology*, vol. 183, no. 1, pp. 257–265, 2013.

[83] E. Tahmasbpour, M. Ghanei, A. Qazvini, E. Vahedi, and Y. Panahi, "Gene expression profile of oxidative stress and antioxidant defense in lung tissue of patients exposed to sulfur mustard," *Mutation Research, Genetic Toxicology and Environmental Mutagenesis*, vol. 800-801, pp. 12–21, 2016.

[84] Z. Li, Y. Gao, D. Xie et al., "Activation of vitamin D receptor signaling downregulates the expression of nuclear FOXM1 protein and suppresses pancreatic cancer cell stemness," *Clinical Cancer Research*, vol. 21, no. 4, pp. 844–853, 2015.

[85] A. Aytes, A. Mitrofanova, C. Lefebvre et al., "Cross-species regulatory network analysis identifies a synergistic interaction between FOXM1 and CENPF that drives prostate cancer malignancy," *Cancer Cell*, vol. 25, no. 5, pp. 638–651, 2014.

[86] S. C. Lin, C. Y. Kao, H. J. Lee et al., "Dysregulation of miRNAs-COUP-TFII-FOXM1-CENPF axis contributes to the metastasis of prostate cancer," *Nature Communications*, vol. 7, article 11418, 2016.

[87] M. Halasi and A. L. Gartel, "Targeting FOXM1 in cancer," *Biochemical Pharmacology*, vol. 85, no. 5, pp. 644–652, 2013.

[88] A. L. Gartel, "Suppression of the oncogenic transcription factor FOXM1 by proteasome inhibitors," *Scientifica*, vol. 2014, Article ID 596528, 5 pages, 2014.

[89] A. Jimenez, W. Zu, V. Y. Rawe et al., "Spermatocyte/spermatid-specific thioredoxin-3, a novel Golgi apparatus-associated thioredoxin, is a specific marker of aberrant spermatogenesis," *The Journal of Biological Chemistry*, vol. 279, no. 33, pp. 34971–34982, 2004.

[90] K. Hirota, M. Murata, Y. Sachi et al., "Distinct roles of thioredoxin in the cytoplasm and in the nucleus. A two-step mechanism of redox regulation of transcription factor NF-kappaB," *The Journal of Biological Chemistry*, vol. 274, no. 39, pp. 27891–27897, 1999.

[91] A. Rubartelli, A. Bajetto, G. Allavena, E. Wollman, and R. Sitia, "Secretion of thioredoxin by normal and neoplastic cells through a leaderless secretory pathway," *The Journal of Biological Chemistry*, vol. 267, no. 34, pp. 24161–24164, 1992.

[92] Y. Manabe, M. Takagi, M. Nakamura-Yamada et al., "Redox proteins are constitutively secreted by skeletal muscle," *The Journal of Physiological Sciences*, vol. 64, no. 6, pp. 401–409, 2014.

[93] M. Wangpaichitr, E. J. Sullivan, G. Theodoropoulos et al., "The relationship of thioredoxin-1 and cisplatin resistance: its impact on ROS and oxidative metabolism in lung cancer cells," *Molecular Cancer Therapeutics*, vol. 11, no. 3, pp. 604–615, 2012.

[94] Y. C. Kim, H. Masutani, Y. Yamaguchi, K. Itoh, M. Yamamoto, and J. Yodoi, "Hemin-induced activation of the thioredoxin gene by Nrf2. A differential regulation of the antioxidant responsive element by a switch of its binding factors," *The Journal of Biological Chemistry*, vol. 276, no. 21, pp. 18399–18406, 2001.

[95] J. S. Song, H. H. Cho, B. J. Lee, Y. C. Bae, and J. S. Jung, "Role of thioredoxin 1 and thioredoxin 2 on proliferation of human adipose tissue-derived mesenchymal stem cells," *Stem Cells and Development*, vol. 20, no. 9, pp. 1529–1537, 2011.

[96] J. R. Prigge, S. Eriksson, S. V. Iverson et al., "Hepatocyte DNA replication in growing liver requires either glutathione or a single allele of txnrd1," *Free Radical Biology and Medicine*, vol. 52, no. 4, pp. 803–810, 2012.

[97] A. Matsuzawa and H. Ichijo, "Redox control of cell fate by MAP kinase: physiological roles of ASK1-MAP kinase pathway in stress signaling," *Biochimica et Biophysica Acta*, vol. 1780, no. 11, pp. 1325–1336, 2008.

[98] M. Saitoh, H. Nishitoh, M. Fujii et al., "Mammalian thioredoxin is a direct inhibitor of apoptosis signal-regulating

kinase (ASK) 1," *The EMBO Journal*, vol. 17, no. 9, pp. 2596–2606, 1998.

[99] E. M. Hanschmann, E. M. Hanschmann, J. R. Godoy, C. Berndt, C. Hudemann, and C. H. Lillig, "Thioredoxins, glutaredoxins, and peroxiredoxins—molecular mechanisms and health significance: from cofactors to antioxidants to redox signaling," *Antioxidants & Redox Signaling*, vol. 19, no. 13, pp. 1539–1605, 2013.

[100] J. Lu and A. Holmgren, "Thioredoxin system in cell death progression," *Antioxidants & Redox Signaling*, vol. 17, no. 12, pp. 1738–1747, 2012.

[101] A. Mukherjee and S. G. Martin, "The thioredoxin system: a key target in tumour and endothelial cells," *The British Journal of Radiology*, vol. 81, no. 1, pp. S57–S68, 2008.

[102] P. A. Marks, "Thioredoxin in cancer–role of histone deacetylase inhibitors," *Seminars in Cancer Biology*, vol. 16, no. 6, pp. 436–443, 2006.

[103] W. Shan, W. Zhong, R. Zhao, and T. D. Oberley, "Thioredoxin 1 as a subcellular biomarker of redox imbalance in human prostate cancer progression," *Free Radical Biology and Medicine*, vol. 49, no. 12, pp. 2078–2087, 2010.

[104] C. Dong, L. Zhang, R. Sun et al., "Role of thioredoxin reductase 1 in dysplastic transformation of human breast epithelial cells triggered by chronic oxidative stress," *Scientific Reports*, vol. 6, article 36860, 2016.

[105] B. J. Park, M. K. Cha, and I. H. Kim, "Thioredoxin 1 as a serum marker for breast cancer and its use in combination with CEA or CA15-3 for improving the sensitivity of breast cancer diagnoses," *BMC Research Notes*, vol. 7, p. 7, 2014.

[106] I. Csiki, K. Yanagisawa, N. Haruki et al., "Thioredoxin-1 modulates transcription of cyclooxygenase-2 via hypoxia-inducible factor-1alpha in non-small cell lung cancer," *Cancer Research*, vol. 66, no. 1, pp. 143–150, 2006.

[107] S. J. Park, H. B. Kim, C. Piao et al., "p53R2 regulates thioredoxin reductase activity through interaction with TrxR2," *Biochemical and Biophysical Research Communications*, vol. 482, no. 4, pp. 706–712, 2017.

[108] J. A. Moscow, L. Schmidt, D. T. Ingram, J. Gnarra, B. Johnson, and K. H. Cowan, "Loss of heterozygosity of the human cytosolic glutathione peroxidase I gene in lung cancer," *Carcinogenesis*, vol. 15, no. 12, pp. 2769–2773, 1994.

[109] Y. J. Hu and A. M. Diamond, "Role of glutathione peroxidase 1 in breast cancer: loss of heterozygosity and allelic differences in the response to selenium," *Cancer Research*, vol. 63, no. 12, pp. 3347–3351, 2003.

[110] J. Milonski, H. Zielinska-Bliźniewska, J. Olszewski, I. Majsterek, and M. Mrowicka, "DNA damage and oxidant-antioxidant status in blood of patients with head and neck cancer," *DNA and Cell Biology*, vol. 34, no. 3, pp. 213–219, 2015.

[111] P. K. Mandal, M. Schneider, P. Kölle et al., "Loss of thioredoxin reductase 1 renders tumors highly susceptible to pharmacologic glutathione deprivation," *Cancer Research*, vol. 70, no. 22, pp. 9505–9514, 2010.

[112] S. N. Rodman, J. M. Spence, T. J. Ronnfeldt et al., "Enhancement of radiation response in breast cancer stem cells by inhibition of thioredoxin- and glutathione-dependent metabolism," *Radiation Research*, vol. 186, no. 4, pp. 385–395, 2016.

[113] P. M. Scarbrough, K. A. Mapuskar, D. M. Mattson, D. Gius, W. H. Watson, and D. R. Spitz, "Simultaneous inhibition of glutathione- and thioredoxin-dependent metabolism is necessary to potentiate 17AAG-induced cancer cell killing via oxidative stress," *Free Radical Biology and Medicine*, vol. 52, no. 2, pp. 436–443, 2012.

[114] S. Zhang, J. Xue, J. Zheng et al., "The superoxide dismutase 1 3'UTR maintains high expression of the SOD1 gene in cancer cells: the involvement of the RNA-binding protein AUF-1," *Free Radical Biology and Medicine*, vol. 85, pp. 33–44, 2015.

[115] J. D. Crapo, T. Oury, C. Rabouille, J. W. Slot, and L. Y. Chang, "Copper,zinc superoxide dismutase is primarily a cytosolic protein in human cells," *Proceedings of the National Academy of Sciences of the United States of America*, vol. 89, no. 21, pp. 10405–10409, 1992.

[116] S. Elchuri, T. D. Oberley, W. Qi et al., "CuZnSOD deficiency leads to persistent and widespread oxidative damage and hepatocarcinogenesis later in life," *Oncogene*, vol. 24, no. 3, pp. 367–380, 2005.

[117] D. P. Brown, H. Chin-Sinex, B. Nie, M. S. Mendonca, and M. Wang, "Targeting superoxide dismutase 1 to overcome cisplatin resistance in human ovarian cancer," *Cancer Chemotherapy and Pharmacology*, vol. 63, no. 4, pp. 723–730, 2009.

[118] A. Piecuch, M. Brzozowa-Zasada, B. Dziewit et al., "Immunohistochemical assessment of mitochondrial superoxide dismutase (MnSOD) in colorectal premalignant and malignant lesions," *Przeglad Gastroenterologiczny*, vol. 11, no. 4, pp. 239–246, 2016.

[119] V. Vidimar, D. Gius, D. Chakravarti, S. E. Bulun, J. J. Wei, and J. J. Kim, "Dysfunctional MnSOD leads to redox dysregulation and activation of prosurvival AKT signaling in uterine leiomyomas," *Science Advances*, vol. 2, no. 11, article e1601132, 2016.

[120] X. Zou, C. A. Santa-Maria, J. O'Brien, D. Gius, and Y. Zhu, "Manganese superoxide dismutase acetylation and dysregulation, due to loss of SIRT3 activity, promote a luminal B-like breast carcinogenic-permissive phenotype," *Antioxidants & Redox Signaling*, vol. 25, no. 6, pp. 326–336, 2016.

[121] L. Bianchi, F. Bruzzese, A. Leone et al., "Proteomic analysis identifies differentially expressed proteins after HDAC vorinostat and EGFR inhibitor gefitinib treatments in Hep-2 cancer cells," *Proteomics*, vol. 11, no. 18, pp. 3725–3742, 2011.

[122] R. R. Rosato, S. S. Kolla, S. K. Hock et al., "Histone deacetylase inhibitors activate NF-kappaB in human leukemia cells through an ATM/NEMO-related pathway," *The Journal of Biological Chemistry*, vol. 285, no. 13, pp. 10064–10077, 2010.

[123] P. V. Raninga, G. Di Trapani, S. Vuckovic, M. Bhatia, and K. F. Tonissen, "Inhibition of thioredoxin 1 leads to apoptosis in drug-resistant multiple myeloma," *Oncotarget*, vol. 6, no. 17, pp. 15410–15424, 2015.

[124] L. Xie, Z. Luo, Z. Zhao, and T. Chen, "Anticancer and antiangiogenic iron(II) complexes that target thioredoxin reductase to trigger cancer cell apoptosis," *Journal of Medicinal Chemistry*, vol. 60, no. 1, pp. 202–214, 2017.

[125] H. Hwang-Bo, J. Cheong, W. J. Kim, Y. H. Yoo, and Y. H. Choi, "Auranofin, an inhibitor of thioredoxin reductase, induces apoptosis in hepatocellular carcinoma Hep3B cells by generation of reactive oxygen species," *General Physiology and Biophysics*, 2017.

[126] H. L. Ng, X. Ma, E. H. Chew, and W. K. Chui, "Design, synthesis, and biological evaluation of coupled bioactive scaffolds as potential anticancer agents for dual targeting of dihydrofolate reductase and thioredoxin reductase," *Journal of Medicinal Chemistry*, vol. 60, no. 5, pp. 1734–1745, 2017.

[127] J. Y. Zhu, C. Y. Zhang, J. J. Dai, K. Rahman, and H. Zhang, "Diterpenoids with thioredoxin reductase inhibitory activities from Jatropha multifida," *Natural Product Research*, pp. 1–6, 2017.

[128] D. Duan, J. Zhang, J. Yao, Y. Liu, and J. Fang, "Targeting thioredoxin reductase by parthenolide contributes to inducing apoptosis of HeLa cells," *The Journal of Biological Chemistry*, vol. 291, no. 19, pp. 10021–10031, 2016.

[129] J. Zhang, S. Peng, X. Li, R. Liu, X. Han, and J. Fang, "Targeting thioredoxin reductase by plumbagin contributes to inducing apoptosis of HL-60 cells," *Archives of Biochemistry and Biophysics*, vol. 619, pp. 16–26, 2017.

[130] A. Schroeder, U. Warnken, D. Röth et al., "Targeting thioredoxin-1 by dimethyl fumarate induces ripoptosome-mediated cell death," *Scientific Reports*, vol. 7, article 43168, 2017.

[131] J. P. Medema, "Cancer stem cells: the challenges ahead," *Nature Cell Biology*, vol. 15, no. 4, pp. 338–344, 2013.

[132] J. E. Visvader and G. J. Lindeman, "Cancer stem cells: current status and evolving complexities," *Cell Stem Cell*, vol. 10, no. 6, pp. 717–728, 2012.

[133] S. Colak and J. P. Medema, "Cancer stem cells—important players in tumor therapy resistance," *The FEBS Journal*, vol. 281, no. 21, pp. 4779–4791, 2014.

[134] D. Trachootham, H. Zhang, W. Zhang et al., "Effective elimination of fludarabine-resistant CLL cells by PEITC through a redox-mediated mechanism," *Blood*, vol. 112, no. 5, pp. 1912–1922, 2008.

[135] E. D. Lagadinou, A. Sach, K. Callahan et al., "BCL-2 inhibition targets oxidative phosphorylation and selectively eradicates quiescent human leukemia stem cells," *Cell Stem Cell*, vol. 12, no. 3, pp. 329–341, 2013.

[136] C. N. Im, H. H. Yun, H. J. Yoo, M. J. Park, and J. H. Lee, "Enhancement of SOX-2 expression and ROS accumulation by culture of A172 glioblastoma cells under non-adherent culture conditions," *Oncology Reports*, vol. 34, no. 2, pp. 920–928, 2015.

[137] J. Liu and Z. Wang, "Increased oxidative stress as a selective anticancer therapy," *Oxidative Medicine and Cellular Longevity*, vol. 2015, Article ID 294303, 12 pages, 2015.

[138] W. Yang, Y. Shen, J. Wei, and F. Liu, "MicroRNA-153/Nrf-2/GPx1 pathway regulates radiosensitivity and stemness of glioma stem cells via reactive oxygen species," *Oncotarget*, vol. 6, no. 26, pp. 22006–22027, 2015.

[139] G. Peng and Y. Liu, "Hypoxia-inducible factors in cancer stem cells and inflammation," *Trends in Pharmacological Sciences*, vol. 36, no. 6, pp. 374–383, 2015.

[140] X. Wang, J. Dong, L. Jia et al., "HIF-2-dependent expression of stem cell factor promotes metastasis in hepatocellular carcinoma," *Cancer Letters*, 2017.

[141] Z. Li, S. Bao, Q. Wu et al., "Hypoxia-inducible factors regulate tumorigenic capacity of glioma stem cells," *Cancer Cell*, vol. 15, no. 6, pp. 501–513, 2009.

[142] L. Xiang, D. M. Gilkes, H. Hu et al., "Hypoxia-inducible factor 1 mediates TAZ expression and nuclear localization to induce the breast cancer stem cell phenotype," *Oncotarget*, vol. 5, no. 24, pp. 12509–12527, 2014.

[143] E. J. Seo, D. K. Kim, I. H. Jang et al., "Hypoxia-NOTCH1-SOX2 signaling is important for maintaining cancer stem cells in ovarian cancer," *Oncotarget*, vol. 7, no. 34, pp. 55624–55638, 2016.

[144] F. Zhang, S. Duan, Y. Tsai et al., "Cisplatin treatment increases stemness through upregulation of hypoxia-inducible factors by interleukin-6 in non-small cell lung cancer," *Cancer Science*, vol. 107, no. 6, pp. 746–754, 2016.

[145] S. W. Yang, Z. G. Zhang, Y. X. Hao et al., "HIF-1alpha induces the epithelial-mesenchymal transition in gastric cancer stem cells through the snail pathway," *Oncotarget*, vol. 8, no. 6, pp. 9535–9545, 2017.

[146] O. Iriondo, M. Rábano, G. Domenici et al., "Distinct breast cancer stem/progenitor cell populations require either HIF1alpha or loss of PHD3 to expand under hypoxic conditions," *Oncotarget*, vol. 6, no. 31, pp. 31721–31739, 2015.

[147] I. Chefetz, J. C. Holmberg, A. B. Alvero, I. Visintin, and G. Mor, "Inhibition of aurora-a kinase induces cell cycle arrest in epithelial ovarian cancer stem cells by affecting NFkB pathway," *Cell Cycle*, vol. 10, no. 13, pp. 2206–2214, 2011.

[148] I. G. Ryoo, S. H. Lee, and M. K. Kwak, "Redox modulating NRF2: a potential mediator of cancer stem cell resistance," *Oxidative Medicine and Cellular Longevity*, vol. 2016, Article ID 2428153, 14 pages, 2016.

[149] A. A. Merchant, A. Singh, W. Matsui, and S. Biswal, "The redox-sensitive transcription factor Nrf2 regulates murine hematopoietic stem cell survival independently of ROS levels," *Blood*, vol. 118, no. 25, pp. 6572–6579, 2011.

[150] B. C. Lu, J. Li, W. F. Yu, G. Z. Zhang, H. M. Wang, and H. M. Ma, "Elevated expression of Nrf2 mediates multidrug resistance in CD133+ head and neck squamous cell carcinoma stem cells," *Oncology Letters*, vol. 12, no. 6, pp. 4333–4338, 2016.

[151] Y. Jia, J. Chen, H. Zhu, Z. H. Jia, and M. H. Cui, "Aberrantly elevated redox sensing factor Nrf2 promotes cancer stem cell survival via enhanced transcriptional regulation of ABCG2 and Bcl-2/Bmi-1 genes," *Oncology Reports*, vol. 34, no. 5, pp. 2296–2304, 2015.

[152] I. G. Ryoo, B. H. Choi, and M. K. Kwak, "Activation of NRF2 by p62 and proteasome reduction in sphere-forming breast carcinoma cells," *Oncotarget*, vol. 6, no. 10, pp. 8167–8184, 2015.

[153] T. Mizuno, N. Suzuki, H. Makino et al., "Cancer stem-like cells of ovarian clear cell carcinoma are enriched in the ALDH-high population associated with an accelerated scavenging system in reactive oxygen species," *Gynecologic Oncology*, vol. 137, no. 2, pp. 299–305, 2015.

[154] A. Chiche, M. Moumen, M. Romagnoli et al., "p53 deficiency induces cancer stem cell pool expansion in a mouse model of triple-negative breast tumors," *Oncogene*, 2016.

[155] X. Xie, T. S. Kaoud, R. Edupuganti et al., "c-Jun N-terminal kinase promotes stem cell phenotype in triple-negative breast cancer through upregulation of Notch1 via activation of c-Jun," *Oncogene*, 2016.

[156] P. Storz, "Forkhead homeobox type O transcription factors in the responses to oxidative stress," *Antioxidants & Redox Signaling*, vol. 14, no. 4, pp. 593–605, 2011.

[157] E. C. Ferber, B. Peck, O. Delpuech, G. P. Bell, P. East, and A. Schulze, "FOXO3a regulates reactive oxygen metabolism by inhibiting mitochondrial gene expression," *Cell Death and Differentiation*, vol. 19, no. 6, pp. 968–979, 2012.

[158] M. K. Lehtinen, Z. Yuan, P. R. Boag et al., "A conserved MST-FOXO signaling pathway mediates oxidative-stress responses and extends life span," *Cell*, vol. 125, no. 5, pp. 987–1001, 2006.

[159] S. P. Somasekharan, A. El-Naggar, G. Leprivier et al., "YB-1 regulates stress granule formation and tumor progression by translationally activating G3BP1," *The Journal of Cell Biology*, vol. 208, no. 7, pp. 913–929, 2015.

[160] K. Arimoto, H. Fukuda, S. Imajoh-Ohmi, H. Saito, and M. Takekawa, "Formation of stress granules inhibits apoptosis by suppressing stress-responsive MAPK pathways," *Nature Cell Biology*, vol. 10, no. 11, pp. 1324–1332, 2008.

[161] B. J. Moeller, Y. Cao, C. Y. Li, and M. W. Dewhirst, "Radiation activates HIF-1 to regulate vascular radiosensitivity in tumors: role of reoxygenation, free radicals, and stress granules," *Cancer Cell*, vol. 5, no. 5, pp. 429–441, 2004.

[162] M. J. Fournier, C. Gareau, and R. Mazroui, "The chemotherapeutic agent bortezomib induces the formation of stress granules," *Cancer Cell International*, vol. 10, p. 12, 2010.

Hindawi
Oxidative Medicine and Cellular Longevity
Volume 2017, Article ID 4396467, 12 pages
https://doi.org/10.1155/2017/4396467

Research Article

Toxicity and Immunogenicity in Murine Melanoma following Exposure to Physical Plasma-Derived Oxidants

Sander Bekeschus,[1] Katrin Rödder,[1] Bob Fregin,[2] Oliver Otto,[2] Maxi Lippert,[1] Klaus-Dieter Weltmann,[1] Kristian Wende,[1] Anke Schmidt,[1] and Rajesh Kumar Gandhirajan[1]

[1]*ZIK plasmatis, Leibniz Institute for Plasma Science and Technology (INP Greifswald), Felix-Hausdorff-Str. 2, 17489 Greifswald, Germany*
[2]*ZIK HIKE, Fleischmannstr. 42-44, 17489 Greifswald, Germany*

Correspondence should be addressed to Sander Bekeschus; sander.bekeschus@inp-greifswald.de

Received 3 March 2017; Accepted 4 May 2017; Published 27 June 2017

Academic Editor: Peeter Karihtala

Metastatic melanoma is an aggressive and deadly disease. Therapeutic advance has been achieved by antitumor chemo- and radiotherapy. These modalities involve the generation of reactive oxygen and nitrogen species, affecting cellular viability, migration, and immunogenicity. Such species are also created by cold physical plasma, an ionized gas capable of redox modulating cells and tissues without thermal damage. Cold plasma has been suggested for anticancer therapy. Here, melanoma cell toxicity, motility, and immunogenicity of murine metastatic melanoma cells were investigated following plasma exposure in vitro. Cells were oxidized by plasma, leading to decreased metabolic activity and cell death. Moreover, plasma decelerated melanoma cell growth, viability, and cell cycling. This was accompanied by increased cellular stiffness and upregulation of zonula occludens 1 protein in the cell membrane. Importantly, expression levels of immunogenic cell surface molecules such as major histocompatibility complex I, calreticulin, and melanocortin receptor 1 were significantly increased in response to plasma. Finally, plasma treatment significantly decreased the release of vascular endothelial growth factor, a molecule with importance in angiogenesis. Altogether, these results suggest beneficial toxicity of cold plasma in murine melanomas with a concomitant immunogenicity of potential interest in oncology.

1. Introduction

With over 70,000 new incidences and 10,000 deaths annually in the U.S. alone, melanoma is a highly prevalent type of cancer [1]. Advances have been made in melanoma therapy in the past decade but stage IV survival of nonresponder patients is still poor [2]. This owes partly to melanomas having the highest mutational burden but at the same time also having the most neoantigens among all types of cancers in humans [3]. Similar to other types of cancer, the majority of patients die due to metastasis spreading throughout the body [4]. This requires an understanding of cellular behavior and motility in response to therapy [5]. BRAF, NRAS, and MEK inhibitors improved end-stage melanoma patient survival [6]. Melanoma immunotherapy with anti-PD-(L)1 and anti-CTLA-4 antibodies further revolutionized therapy by abolishing cancer immunosuppression of tumor-specific T cells [7]. Moreover, increased immunogenicity correlates with $CD163^+$ cellular infiltrate that in combination with the number of $FOXP3^+$ cells is a predictor of survival [8]. Immunogenic cell death (ICD) is hallmarked by expression of calreticulin [9] which makes tumor cells visible to the immune system [10]. Of note, mitochondrial-derived reactive oxygen species (ROS) and reactive nitrogen species (RNS) and subsequent oxidative events seem to contribute to some molecular ICD events following chemo- and radiotherapy [11].

Cold physical plasma is an ionized gas and potently generates ROS and RNS of different kinds [12]. Several studies

indicated the involvement of mitochondria in plasma-mediated cancer cell death, underlining the notion that exogenous as well as endogenous reactive oxygen species may be at work [13–15]. Accordingly, cold plasma has been suggested as an interesting tool in skin cancer [16] and generally in tumor therapy [17] before. The first work also pointed at the plasma's potential to involve immunogenic cell death [18]. Interestingly, antioxidants were shown to enhance metastatic spreading in a murine melanoma model [19].

Hence, the effects of cold plasma-derived oxidants on cell motility, cytotoxicity, and immunogenicity were studied in murine melanoma cell line. It was found that all of these three important hallmarks of cancer were affected by exposure to plasma. These results are promising with regard to cold plasmas potentially having a future role in combination therapy in oncology.

2. Materials and Methods

2.1. Cell Culture and Plasma Treatment. Murine, metastatic B16F10 cells (ATCC CRL-6475) were maintained in Rosswell Park Memorial 1640 (RPMI1640) medium (Pan BioTech, Germany) containing 10% fetal bovine serum, 2% penicillin/streptomycin, and 1% glutamine (all Sigma, Germany). For plasma treatment in 24-well dishes (NUNC, Denmark), 5×10^4 cells were added per well. For treatment in 96-well plates (NUNC), 1×10^4 cells were given to each well. Cells were allowed to adhere overnight. As plasma source, an atmospheric pressure argon plasma jet (kINPen 11) was utilized. This plasma primarily acts via ROS and RNS and is not genotoxic [20, 21]. The device is technically similar to the kINPen MED that received accreditation as medical product for skin disease. Argon gas (99.999% pure; Air Liquide, France) was used to ignite the plasma at a frequency of about 1 MHz [22]. The jet was hovered over the cells for the indicated time using a computer-programed *xyz*-table (CNC, Germany).

2.2. Redox-Sensitive Probe and High-Content Imaging. Cells were loaded with CM-H_2DCF-DA (Thermo Fisher, USA) and treated with plasma or were left untreated. Fluorescent microscopy (Observer Z.1; Zeiss, Germany) was employed to image dye fluorescence facilitated by intracellular oxidases. Quantification of the cells' mean fluorescent intensities was facilitated using Fiji software. Metabolic activity was assessed by incubating the cells with 7-hydroxy-3H-phenox-azin-3-one-10-oxide (resazurin; Alfa Aesar, USA). Subsequently, fluorescent resorufin was quantified using a microplate reader measuring at λ_{ex} 535 nm and λ_{em} 590 nm (Tecan, Switzerland). To assess viability visually, propidium iodide (PI; Sigma) was added, and cells were imaged with a high-content imaging device (Operetta CLS; Perkin-Elmer, Germany) at different time points following treatment. For each time point, the total number of cells was quantified using digital phase contrast (DPC), and the number of PI positive were expressed as percent of that. In a similar manner, the total growth area was calculated for different time points following plasma treatment. DPC was used to identify cells, and only viable cells were included in the analysis before normalization to untreated control was calculated. To quantify cell motility, cells were plasma-treated and subsequently imaged every 20 min over three hours. Only PI^- cells (identified using DPC) were tracked. Mean displacement per cell over time was calculated. To identify mean nuclear area per cell for each treatment, B16F10 melanomas were fixed with PBS/PFA (4%, Sigma), permeabilized with 0.1% Triton X 100 (Sigma), and stained with DAPI. Nuclei area was quantified using automated image analysis. A similar protocol was applied to quantify cytosolic mean fluorescence intensity of zonula occludens 1 (ZO1 antibody; AbCam, UK) protein. The cytosolic area was determined using DPC, and the nuclear area was subtracted from that. Data analysis was performed using Harmony 4.5 software (PerkinElmer).

2.3. Real-Time Deformability Cytometry. Real-time deformability cytometry (Zellmechanik, Germany) allows analyzing the mechanical properties of cells with a throughput of up to 1000 cells per second [23]. The setup is built around an inverted microscope (Zeiss Observer, Germany) having a PDMS-based microfluidic chip assembled on the translation stage. One to two hours after plasma treatment, the cell suspension was driven through the central constriction of the chip by a syringe pump (Nemesys; Cetoni, Germany) at different flow rates between 0.16 μl/s and 0.32 μl/s. Inside the constriction, cell deformation was induced by a laminar flow profile and recorded by a high-speed camera (MC1362; Mikrotron, Germany) at 2000 frames per second. Image analysis was done on the fly enabling the quantification of size and deformation for each cell. For sample preparation, cells were centrifuged and resuspended in PBS containing 0.5% (*w*/*v*) methylcellulose to a final concentration of 10^6 cells per ml. For each sample, at least 5000 events were acquired. An analytical model calculating the hydrodynamic flow profile around a cell inside the channel allows to link cell deformation to material properties [24] and derivation of the cells' Young's modulus [25]. Here, cell deformation is calculated from

$$d = \frac{1 - (2\sqrt{\pi A})}{1}, \quad (1)$$

where A represents the area of the cell and l the perimeter. Statistical analysis was based on linear mixed models, which separates random effects, for example, biological variability, from fixed effects, for example, treatment of cells.

2.4. Cell Surface Marker Expression. Cells were detached using accutase (BioLegend, UK) and incubated with monoclonal antibodies directed against MHC I allophycocyanin (BioLegend), melanocortin receptor 1 (MC-1R) fluorescein isothiocyanate (Bioss, USA), and calreticulin (CRT) Alexa Fluor 647 (AbCam, UK). Cells were washed and resuspended in PBS containing 1% bovine serum albumin (Sigma) and 4′,6-diamidino-2-phenylindole (DAPI; Sigma). Cellular properties were acquired using multicolor flow cytometry (CytoFlex; Beckman-Coulter, Germany). Only viable ($DAPI^-$) cells were included for the analysis of cell surface marker mean fluorescent intensities. Kaluza 1.5a software (Beckman-Coulter) facilitated data analysis.

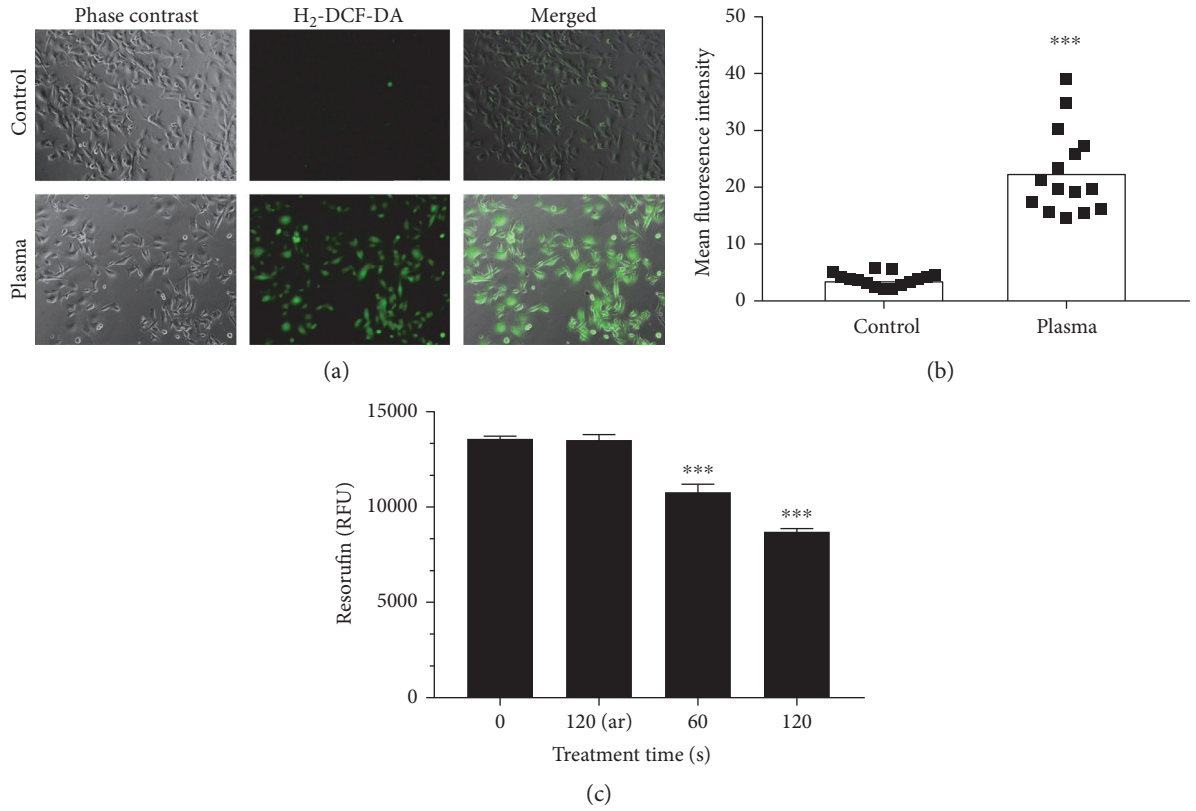

Figure 1: Oxidation and metabolic activity. (a) B16 melanoma cells were loaded with H_2-DCF-DA and subjected to plasma treatment (120 s) or not. (b) Quantification of mean fluorescence intensities of the cells. (c) Mean fluorescence intensity of resorufin representative for cellular metabolic activity. Data are one representative (a, b) and mean + S.E. (c). Statistical analysis was carried out using *t*-test.

2.5. Vascular Endothelial Growth Factor. Cell culture supernatants were stored at −80°C until analysis. Concentrations of vascular endothelial growth factor (VEGF) were assessed using an enzyme-linked immunosorbent assay (ELISA) kit (BMS619-2) according to the vendor's instructions (eBioscience, Germany).

2.6. Statistics. Graphing and statistical analysis was performed using prism 7.02 (GraphPad Software, USA). Mean and standard errors were calculated and analyzed according to statistical methods given in the figure legends. Groups or treatments differing significantly were marked with asterisks ($^*p < 0.05$; $^{**}p < 0.01$; and $^{***}p < 0.001$).

3. Results

3.1. Plasma Oxidized Melanoma Cell and Decreased Metabolic Activity and Viability. Cold physical plasma generated many different kinds of oxidants. In cells loaded with H_2-DCF-DA, plasma treatment increased total fluorescence in B16 melanoma cells compared to untreated controls (Figure 1(a)). Quantification of individual cellular fluorescence yielded a significantly enhanced mean fluorescence intensity (Figure 1(b)). To assess the cytotoxic effects, metabolic activity was assessed 3 hours after plasma treatment. Exposure to plasma for 60 s or 120 s but not 120 s of argon gas alone significantly decreased metabolic activity (Figure 1(c)). Subsequently, plasma-treated and control cells were imaged at different time points following in presence of PI indicative for cell membrane damage (Figure 2(a)). Utilization image-based quantification algorithms and the total number of cells as well as their mean fluorescence intensity of PI were determined (Figure 2(b)). Quantification and normalization to total cells revealed a significant increase in terminally dead cells in samples that had received 120 s of treatment (Figure 2(c)). Peak percent of dead cells was measured 12 h after treatment with a decrease after that. Altogether, plasma oxidized melanoma cells and decreased their metabolic activity by inducing terminal cell death.

3.2. Plasma Affected Cell Growth, Motility, and Biomechanical Properties. Next, total cell area and cell motility was assessed in PI^- (viable) cells. Total cell area was quantified at different time points postplasma treatment. Immediately following the treatment, the cell area was not affected (Figure 3(a)). By contrast, 60 s and 120 s of plasma treatment gave a significantly reduced cell area (Figures 3(b), 3(c), 3(d), and 3(e)). In the 120 s treated samples, the area was almost similar within the first hour (Figure 3(a)) compared to 6 h (Figure 3(b)) after treatment. This was not the case with all other samples where an increased cell area was observed. This suggested that also the viable cells were halting proliferation and possibly migration. Thus, the mean displacement of each viable cell was determined over three hours in controls and plasma-treated cells. In the 120 s plasma-treated sample, total displacement

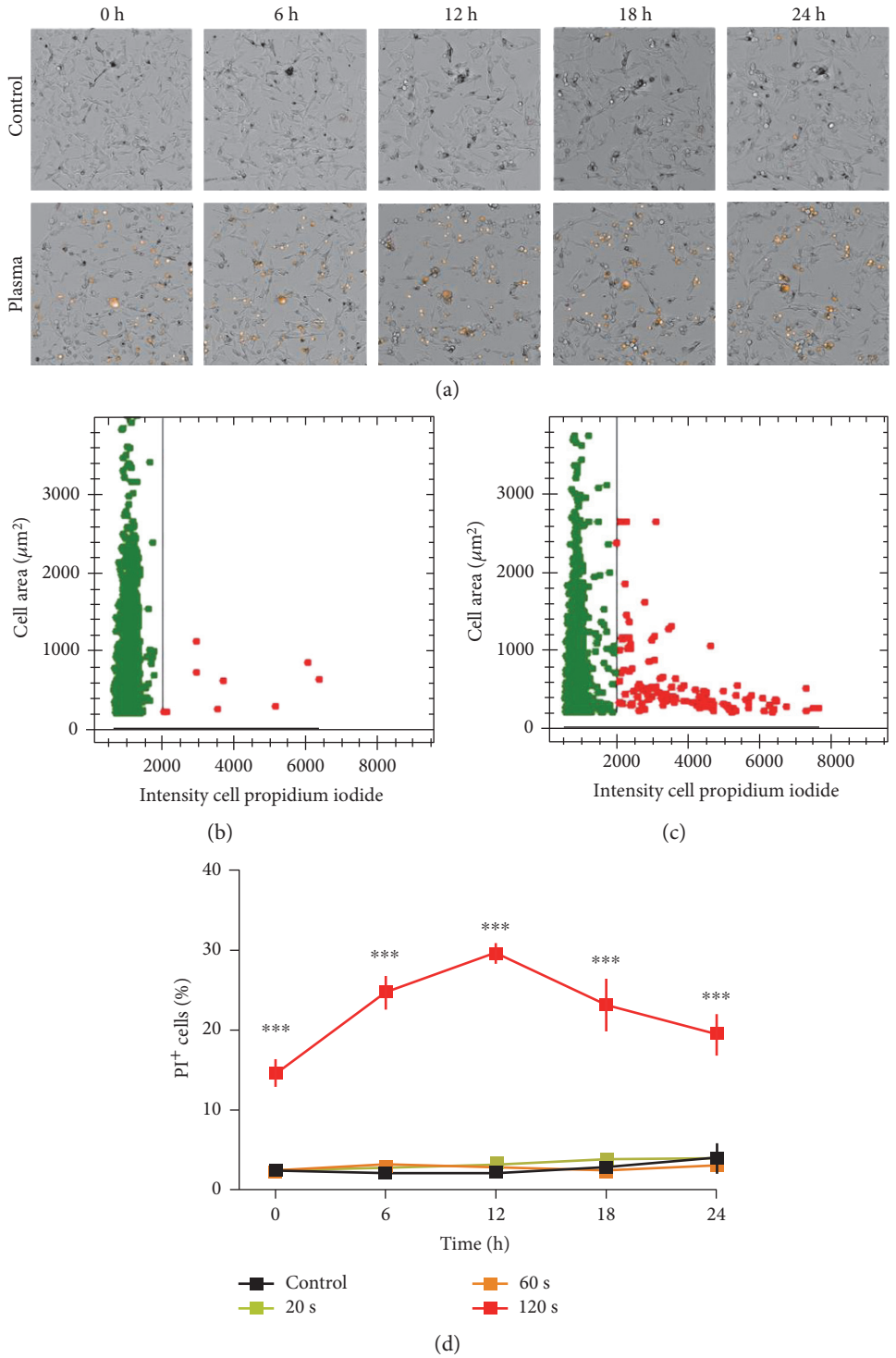

Figure 2: Cell death. (a) Representative bright field and PI overlay images of control (upper row) and plasma-treated (120 s, lower row) cells at different time points following exposure. (b) Representative dot plot of control cell area versus PI intensity per cell. (c) Representative dot plot of plasma-treated (120 s) cells and their area versus PI intensity per cell. Image quantification and normalization of PI$^+$ cells of all cells per field of view. Data are presented as mean ± S.E. of nine replicates. One representative of three independent experiments is shown. Statistical analysis was performed using *t*-test.

per viable cell was significantly decreased (Figure 3(f)). Concomitantly, mean nuclear area was significantly enlarged, arguing for cell cycle arrest. Both facts indicate decelerated cell motility, which is linked to biomechanical properties. Therefore, real-time deformability cytometry was performed in murine B16F10 control (Figure 4(a)) melanoma cells as well as following exposure to 60 s (Figure 4(b)) and 120 s (Figure 4(c)) of plasma treatment. After 60 s of plasma

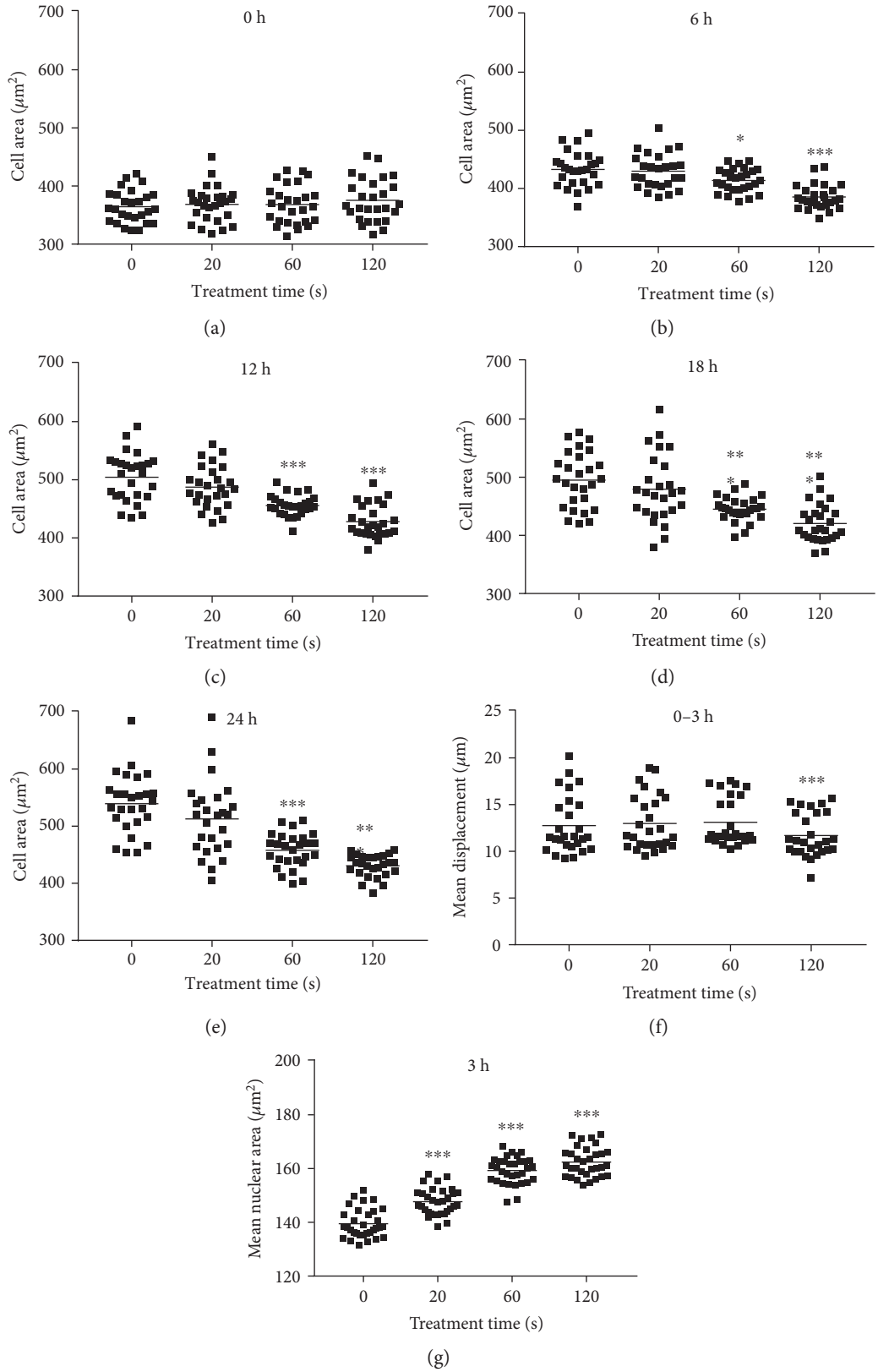

Figure 3: Melanoma growth kinetic and migration. (a–e) Total cell growth area per field of view was determined after several time points following plasma treatment and using automated image quantification. (f) PI^- melanoma motility as a function of mean cell displacement was calculated using time-lapse microscopy over 3 h and kinetic tracking algorithms. (g) Mean nuclear area of cells 3 h after plasma treatment. Data are presented as the mean of 9 replicates of each of the three independent experiments resulting in about 2000 single cells per treatment and time point. Statistical analysis was carried out using one-way ANOVA.

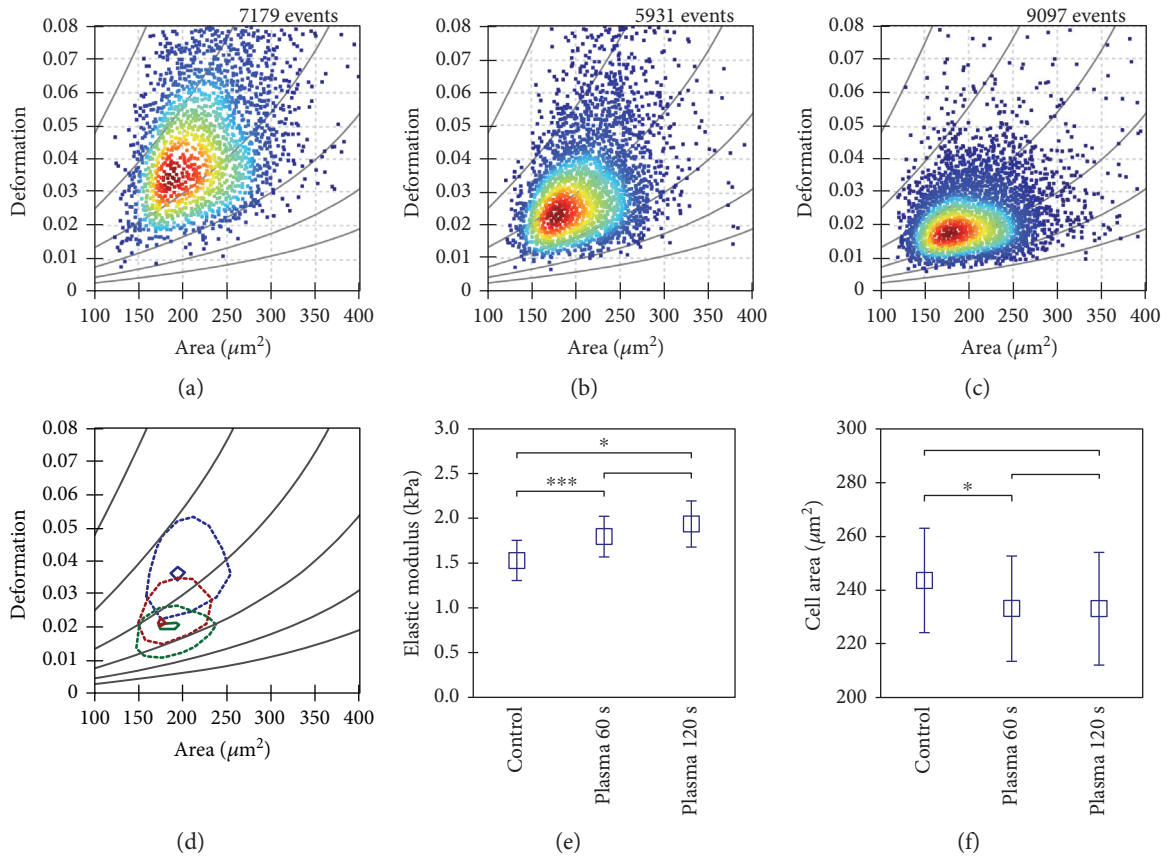

Figure 4: Real-time deformability cytometry. (a) Real-time deformability cytometry data of a control sample was compared to cells after 60 s (b) and 120 s (c) plasma treatment. (d) The 50% and 90% density lines of each population are given for control (blue) and plasma-treated (red 60 s, green 120 s) cells. (e) After plasma treatment, melanoma cells revealed a significant increase in Young's modulus whereas individual cell area (f) was nearly unaffected. Measurements have been carried out in a 30 μm channel at a frame rate of 2000 fps. Data shown are one representative (a–c) or mean (d) ± S.E. (e, f) of three independent experiments.

treatment, the median deformation and cell area changed from $d = 0.041$ to $d = 0.027$ and $A = 216.6\,\mu\text{m}^2$ to $A = 202.6\,\mu\text{m}^2$, respectively. A further reduction in median deformation to $d = 0.02$ was seen after 120 s of plasma treatment. This is summarized in Figure 4(d) by comparing the contour lines of each population. Overlay contour lines of each population clearly marked differences between all samples (Figure 4(d)). Application of an analytical model [25] allows for calculation of cellular properties. Significant differences were obtained between plasma-treated and control samples (Figure 4(e)). Sixty seconds of plasma treatment led to a significant increase in Young's modulus from 1.53 ± 0.22 kPa to 1.79 ± 0.23 kPa. Plasma exposure of 120 s resulted in an even higher elastic modulus of 1.94 ± 0.26 kPa. This alteration in mechanical properties was accompanied by a small decrease in cell area from $243.6 \pm 19.4\,\mu\text{m}^2$ to $233.1 \pm 19.1\,\mu\text{m}^2$ (Figure 4(f)). An integral part of tight junction formation, membrane-associated ZO1 expression is inversely linked to motility. Immunofluorescence staining gave an increase in cytosolic staining of ZO1 3 h following plasma treatment (Figure 5(a)). This increase was significant even with short, nontoxic plasma treatment times (Figure 5(b)). We also stained melanoma cells with antibodies targeted against occludin and e-cadherin but staining was weak, and changes upon plasma treatment were not observed (data not shown). Altogether, plasma decreased melanoma cell growth, motility, and deformability together with an increased ZO1 expression.

3.3. Plasma Increased the Immunogenicity and Decreased VEGF Release in Melanomas. Successful melanoma therapy is strongly linked to immunomodulation. Therefore, the expression of several cell surface molecules was investigated 4 h and 24 h following plasma treatment. Representative overlay histograms are given for each protein and time point (Figure 6). With MHC I, a significant increase was not seen after 4 h (Figure 6(c)) but was seen after 24 h (Figure 6(d)) in 120 s plasma-treated samples. This pointed to an increase in antigen presentation promoting immune recognition. For MC-1R, an important receptor in melanocyte biology, a subtle but significant increase was seen 4 h (Figure 6(e)) and 24 h (Figure 6(f)) after plasma treatment. Calreticulin (CRT) is the key molecule in immunogenic cell death (ICD). CRT was significantly increased after both 4 h (Figure 6(i)) as well as 24 h (Figure 6(j)) following exposure to plasma. Angiogenesis is important for tumor blood supply. VEGF—being a major molecule in the formation of blood vessels—was significantly decreased (Figure 7) 24 h

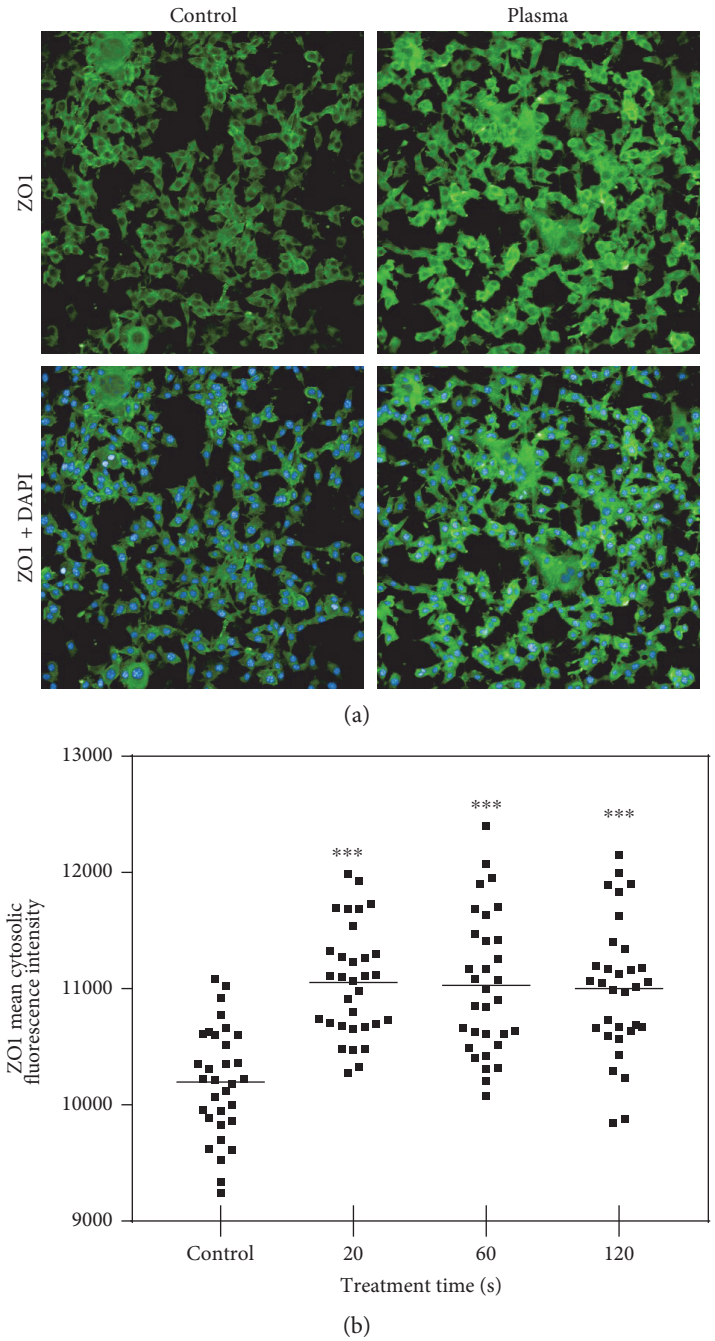

Figure 5: ZO1 expression. (a) Representative images of ZO1 and ZO1/DAPI immunofluorescence of control and plasma-treated (120 s) murine melanomas 3 h after exposure. (b) Quantification data are presented as mean of 8 replicates of each of the four experiments. Statistical analysis was performed using one-way ANOVA.

after plasma treatment. In our hands, VEGF decrease was greater than cell viable decrease (see Figure 2(d)).

4. Discussion

Cold plasma treatment affected melanoma cell viability, motility, and immunogenicity. Immunogenic properties such as therapy-induced upregulation MHCI and CRT are vital for antitumor immune responses [26]. MHCI is vital for presentation of endogenous and potentially tumor-specific (neo) antigens to cytotoxic T cells [27]. Vice versa, tumor cell elimination with high MHCI expression favors the generation of $MHCI^{low}$ cancer cells, especially in metastasis [28]. Therefore, upregulation of MHCI is viewed as a therapeutic goal in many types of tumors [29–31]. Similar to plasma, photodynamic therapy uses oxygen radicals and was shown to restore MHCI expression in human glioma [32]. Along similar lines, radiation upregulates MHCI expression in the breast [33], lung [34], and colon cancer [35]. Similar to downregulated MHCI, elevated levels of VEGF are also

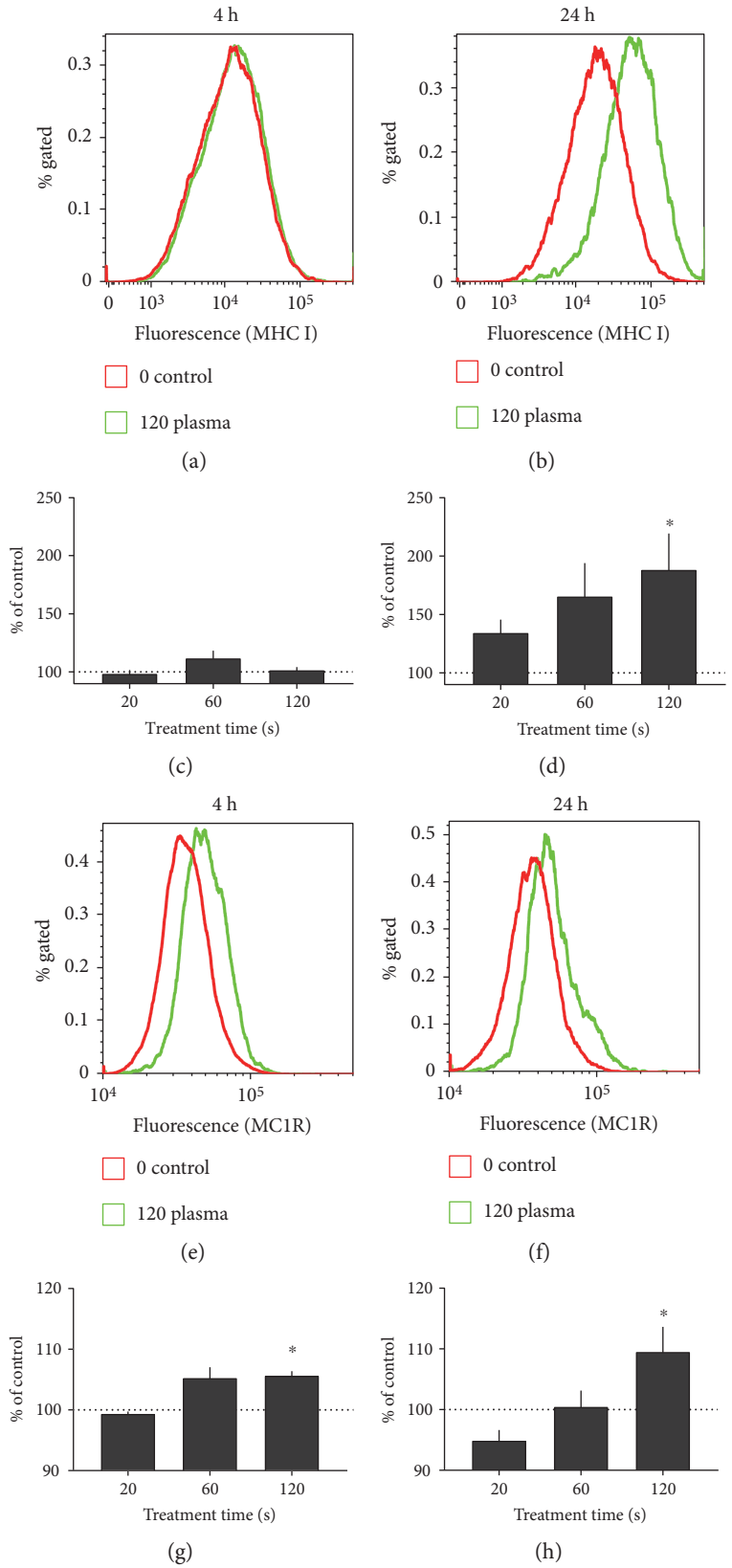

Figure 6: Continued.

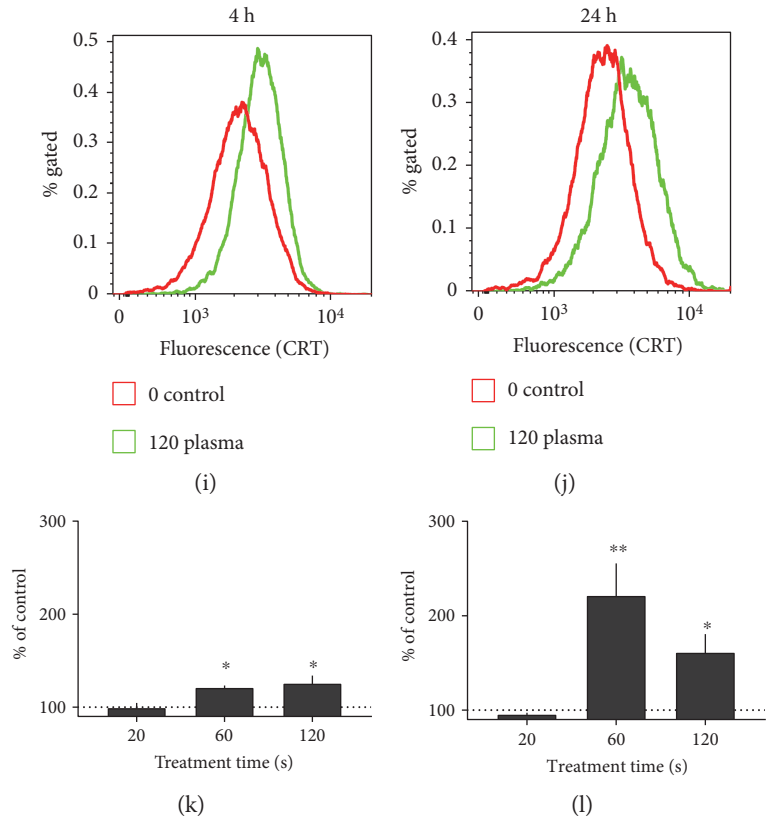

Figure 6: Cell surface marker expression. Cell surface marker expression of B16 melanoma cells 4 h (images on the left) or 24 h (images on the right) after plasma treatment. Representative overlay histograms of (a, b) MHC I, (e, f) MC1R, and (i, j) CRT are given. Quantification and normalization mean fluorescence intensity of each surface marker is shown for (c, d) MHC I, (g, h) MC1R, and (k, l) CRT. Data are presented as mean + S.E. of 3-4 independent experiments. Statistical analysis was performed using *t*-test.

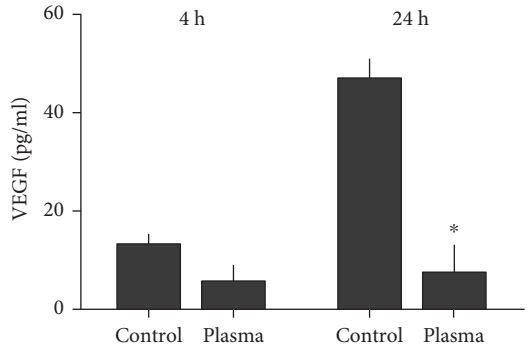

Figure 7: VEGF release. Cell culture supernatants were harvested 4 h and 24 h after plasma treatment, respectively. The concentration of VEGF was determined via ELISA. Data are presented as mean + S.E. of three independent experiments. Statistical analysis was performed using *t*-test.

important for tumorigenesis [36]. We saw a drastic decrease in VEGF release likely owing to cellular toxicity. Nonetheless, an Akt-mediated increase in intracellular oxidants was previously linked to enhanced VEGF release [37]. Hence, VEGF release might be redox controlled, and its reduction would be therapeutically desired [38]. By enhancing immunogenicity, also CRT correlates with favorable prognosis for patients with, for example, lung cancer [39], gastric cancer [40], and leukemia [41]. CRT on melanoma cells was also involved in dendritic cell vaccination in melanoma patients, although cell death was found to be dispensable for that effect [42]. Exogenously added CRT also potentiates the immunogenicity of melanomas in patients [43]. A CRT fusion-protein added to B16 cells evoked an antitumor immune response in mice [44]. Intriguingly, therapeutic intervention associated with upregulation of CRT involves the generation of reactive species [45–47].

Cold physical plasma expels reactive molecules known to be important in redox biology and medicine [48]. In contrast to intracellular generation with PDT and radio- or chemotherapy, plasma-generated species are applied exogenously from ambient air to cells and tissues [49]. kINPen plasma-generated reactive molecules include for example peroxynitrite, hydrogen peroxide, and hydroxyl radical [50–52]. Today's view is that most oxidative events in cells are translated by redox enzymes and thiol switches in transcription factors which then guide the cellular response [53]. For example, we previously identified activator protein 1 (AP1) family members such as FOSB and JUND in plasma-treated blood cancer cell lines to be crucial [54]. Both factors are redox-regulated [55], and their expression was dysregulated in metastatic melanoma [56]. This makes AP1 a crucial regulator of cell regulation and death [57], as observed in

our study with a decrease in metabolic activity and cell cycle arrest and increase in terminally dead cells. Interestingly, JUN proteins are involved in melanoma migration [58].

Cell mechanics is a major regulator and indicator of cell function and motility [59]. The main structural component linking function to mechanical properties is the cytoskeleton consisting of filamentous actin, microtubules, and intermediate filaments. For migration, cells require to alter their morphology, which is controlled by the cytoskeleton on a molecular and the emerging mechanical properties on a cellular scale [60]. In real-time deformability cytometry, an increase in elastic modulus after plasma treatment was observed. This effect could be originated from an alteration in actin polymerization subject to redox control [61], which is also supported by the retarded migration of the cells. This is in agreement with an earlier study on fibroblasts where a direct correlation between cell elasticity and migration was shown [62]. Enhanced cell motility and therefore invasiveness correlates with increased cytosolic ZO1 protein whereas noninvasive breast cancer cells showed elevated ZO1 in the cell membrane [63]. In pancreatic cancer cells, however, membrane-associated ZO1 was supporting invasiveness [64]. In our work, we saw an increase of ZO1 not only in the cytosolic fraction but also visually in the cell membrane. This implicates a de novo translation of ZO1 proteins in melanoma cells and not necessarily its specific translocation from the membrane to the cytosol. Underlining this idea, de novo generated ZO1 in breast cancer cells was previously shown to be present in the cytosol as well as to translocate to the cell membrane [65]. Another report describes the association of melanoma ZO1 with adherence junctions of nonepithelial cells such as fibroblasts instead of tight junctions [66]. The authors concluded that knockdown of ZO1 suppresses melanoma invasiveness. Similarly, an upregulation of MC1R increases B16F10 melanoma motility [67]. Yet, the authors transfected MC1R and induced an about twenty-fold increase. By contrast, MC1R upregulation after plasma was only 1.1-fold. The main function of MC1R is to control skin and hair pigmentation via eumelanin production [68]. MC1R is generally upregulated in melanoma cells [69]. This is used for therapeutic purposes to deliver target drugs into the cells, and pro-oxidant therapies such as PDT have been successfully employed in this strategy to increase survival in experimental animal models [70].

The utilization of only one cell line limits the specificity and/or generalization of our results that should be compared to nonmalignant melanocytes and confirmed in other cancer cell lines. Specifically, the relevance of our findings may increase if human cancer cells would be similarly affected. In addition, it would be valuable to identify the effects of other types of plasma sources in this model.

In summary, it was demonstrated that treatment of murine metastatic melanoma cells with cold physical plasma-derived oxidants exerted cytotoxic effects, decreased cell motility, and increased their immunogenicity. Animal models need to provide evidence whether plasma-inactivated melanoma experiences a vaccine-like immunogenic cell death (ICD) which would make plasma therapy an interesting new tool in oncology.

Conflicts of Interest

Oliver Otto is the cofounder and CEO of Zellmechanik Dresden GmbH Germany developing real-time deformability cytometry.

Acknowledgments

Funding was received from the German Federal Ministry of Education and Research (Grant nos. 03Z22DN11, 03Z22DN12, and 03Z22CN11).

References

[1] R. L. Siegel, K. D. Miller, and A. Jemal, "Cancer statistics, 2016," *CA: A Cancer Journal for Clinicians*, vol. 66, pp. 7–30, 2016.

[2] M. J. Smyth, S. F. Ngiow, A. Ribas, and M. W. Teng, "Combination cancer immunotherapies tailored to the tumour microenvironment," *Nature Reviews. Clinical Oncology*, vol. 13, pp. 143–158, 2016.

[3] T. N. Schumacher and R. D. Schreiber, "Neoantigens in cancer immunotherapy," *Science*, vol. 348, pp. 69–74, 2015.

[4] E. Quintana, E. Piskounova, M. Shackleton et al., "Human melanoma metastasis in NSG mice correlates with clinical outcome in patients," *Science Translational Medicine*, vol. 4, p. 159ra149, 2012.

[5] T. A. Martin and W. G. Jiang, "Loss of tight junction barrier function and its role in cancer metastasis," *Biochimica et Biophysica Acta*, vol. 1788, pp. 872–891, 2009.

[6] K. T. Flaherty, "Chemotherapy and targeted therapy combinations in advanced melanoma," *Clinical Cancer Research*, vol. 12, pp. 2366s–2370s, 2006.

[7] A. E. Vilgelm, D. B. Johnson, and A. Richmond, "Combinatorial approach to cancer immunotherapy: strength in numbers," *Journal of Leukocyte Biology*, vol. 100, pp. 275–290, 2016.

[8] S. Ladoire, L. Senovilla, D. Enot et al., "Biomarkers of immunogenic stress in metastases from melanoma patients: correlations with the immune infiltrate," *Oncoimmunology*, vol. 5, article e1160193, 2016.

[9] M. Obeid, A. Tesniere, F. Ghiringhelli et al., "Calreticulin exposure dictates the immunogenicity of cancer cell death," *Nature Medicine*, vol. 13, pp. 54–61, 2007.

[10] G. Kroemer, L. Galluzzi, O. Kepp, and L. Zitvogel, "Immunogenic cell death in cancer therapy," *Annual Review of Immunology*, vol. 31, pp. 51–72, 2013.

[11] A. D. Garg, S. Martin, J. Golab, and P. Agostinis, "Danger signalling during cancer cell death: origins, plasticity and regulation," *Cell Death & Differentiation*, vol. 21, pp. 26–38, 2014.

[12] K. D. Weltmann and T. von Woedtke, "Plasma medicine-current state of research and medical application," *Plasma Physics and Controlled Fusion*, vol. 59, p. 014031, 2017.

[13] S. Bekeschus, A. Schmidt, L. Bethge et al., "Redox stimulation of human THP-1 monocytes in response to cold physical plasma," *Oxidative Medicine & Cellular Longevity*, vol. 2016, Article ID 5910695, 2016.

[14] A. Zhunussova, E. A. Vitol, B. Polyak et al., "Mitochondria-mediated anticancer effects of non-thermal atmospheric plasma," *PloS One*, vol. 11, article e0156818, 2016.

[15] Y. Suzuki-Karasaki, "Tumor-targeting killing of multidrug-resistant human aggressive cancer cells by plasma-activated

media via mitochondrial and endoplasmic reticulum damages," *International Journal of Molecular Medicine*, vol. 38, pp. S50–S50, 2016.

[16] J. Gay-Mimbrera, M. C. Garcia, B. Isla-Tejera, A. Rodero-Serrano, A. V. Garcia-Nieto, and J. Ruano, "Clinical and biological principles of cold atmospheric plasma application in skin cancer," *Advances in Therapy*, vol. 33, pp. 894–909, 2016.

[17] D. Yan, J. H. Sherman, and M. Keidar, "Cold atmospheric plasma, a novel promising anti-cancer treatment modality," *Oncotarget*, vol. 5, 2016.

[18] V. Miller, A. Lin, and A. Fridman, "Why target immune cells for plasma treatment of cancer," *Plasma Chemistry and Plasma Processing*, vol. 36, pp. 259–268, 2016.

[19] K. Le Gal, M. X. Ibrahim, C. Wiel et al., "Antioxidants can increase melanoma metastasis in mice," *Science Translational Medicine*, vol. 7, p. 308re308, 2015.

[20] K. Wende, S. Bekeschus, A. Schmidt et al., "Risk assessment of a cold argon plasma jet in respect to its mutagenicity," *Mutation Research, Genetic Toxicology and Environmental Mutagenesis*, vol. 798-799, pp. 48–54, 2016.

[21] S. Kluge, S. Bekeschus, C. Bender et al., "Investigating the mutagenicity of a cold argon-plasma jet in an HET-MN model," *PloS One*, vol. 11, article e0160667, 2016.

[22] S. Bekeschus, A. Schmidt, K.-D. Weltmann, and T. von Woedtke, "The plasma jet kINPen – a powerful tool for wound healing," *Clinical Plasma Medicine*, vol. 4, pp. 19–28, 2016.

[23] O. Otto, P. Rosendahl, A. Mietke et al., "Real-time deformability cytometry: on-the-fly cell mechanical phenotyping," *Nature Methods*, vol. 12, pp. 199–202, 2015.

[24] M. Mokbel, D. Mokbel, A. Mietke et al., "Numerical simulation of real-time deformability cytometry to extract cell mechanical properties," *ACS Biomaterials Science & Engineering*, 2017.

[25] A. Mietke, O. Otto, S. Girardo et al., "Extracting cell stiffness from real-time deformability cytometry: theory and experiment," *Biophysical Journal*, vol. 109, pp. 2023–2036, 2015.

[26] H. Inoue and K. Tani, "Multimodal immunogenic cancer cell death as a consequence of anticancer cytotoxic treatments," *Cell Death & Differentiation*, vol. 21, pp. 39–49, 2014.

[27] C. M. Celluzzi, J. I. Mayordomo, W. J. Storkus, M. T. Lotze, and L. D. Falo Jr., "Peptide-pulsed dendritic cells induce antigen-specific CTL-mediated protective tumor immunity," *The Journal of Experimental Medicine*, vol. 183, pp. 283–287, 1996.

[28] E. Jager, M. Ringhoffer, M. Altmannsberger et al., "Immunoselection in vivo: independent loss of MHC class I and melanocyte differentiation antigen expression in metastatic melanoma," *International Journal of Cancer*, vol. 71, pp. 142–147, 1997.

[29] V. Shetty, G. Sinnathamby, Z. Nickens et al., "MHC class I-presented lung cancer-associated tumor antigens identified by immunoproteomics analysis are targets for cancer-specific T cell response," *Journal of Proteomics*, vol. 74, pp. 728–743, 2011.

[30] G. Ito, H. Tanaka, M. Ohira et al., "Correlation between efficacy of PSK postoperative adjuvant immunochemotherapy for gastric cancer and expression of MHC class I," *Experimental & Therapeutic Medicine*, vol. 3, pp. 925–930, 2012.

[31] A. Letsch, O. Elisseeva, C. Scheibenbogen et al., "Effect of vaccination of leukemia patients with a MHC class I peptide of Wilms tumor gene 1 (WT1) peptide with unspecific T helper stimulation on WT1-specific IgM responses and on IgG responses," *Journal of Clinical Oncology*, vol. 26, pp. 3054–3054, 2008.

[32] S. Y. Zhang, J. L. Li, X. K. Xu, M. G. Zheng, C. C. Wen, and F. C. Li, "HMME-based PDT restores expression and function of transporter associated with antigen processing 1 (TAP1) and surface presentation of MHC class I antigen in human glioma," *Journal of Neuro-Oncology*, vol. 105, pp. 199–210, 2011.

[33] S. Wan, S. Pestka, R. G. Jubin, Y. L. Lyu, Y. C. Tsai, and L. F. Liu, "Chemotherapeutics and radiation stimulate MHC class I expression through elevated interferon-beta signaling in breast cancer cells," *PloS One*, vol. 7, article e32542, 2012.

[34] X. Wang, J. E. Schoenhals, D. R. Valdecanas et al., "Suppression of major histocompatibility complex (MHC) class I and II mediates resistance to anti-PD-1 in lung adenocarcinoma tumors that can be overcome by radiation therapy," *International Journal of Radiation Oncology, Biology, Physics*, vol. 96, p. S89, 2016.

[35] E. A. Reits, J. W. Hodge, C. A. Herberts et al., "Radiation modulates the peptide repertoire, enhances MHC class I expression, and induces successful antitumor immunotherapy," *The Journal of Experimental Medicine*, vol. 203, pp. 1259–1271, 2006.

[36] N. Oka, A. Soeda, A. Inagaki et al., "VEGF promotes tumorigenesis and angiogenesis of human glioblastoma stem cells," *Biochemical & Biophysical Research Communications*, vol. 360, pp. 553–559, 2007.

[37] B. Govindarajan, J. E. Sligh, B. J. Vincent et al., "Overexpression of Akt converts radial growth melanoma to vertical growth melanoma," *The Journal of Clinical Investigation*, vol. 117, pp. 719–729, 2007.

[38] J. M. Mehnert, M. M. McCarthy, L. Jilaveanu et al., "Quantitative expression of VEGF, VEGF-R1, VEGF-R2, and VEGF-R3 in melanoma tissue microarrays," *Human Pathology*, vol. 41, pp. 375–384, 2010.

[39] J. Fucikova, E. Becht, K. Iribarren et al., "Calreticulin expression in human non-small cell lung cancers correlates with increased accumulation of antitumor immune cells and favorable prognosis," *Cancer Research*, vol. 76, pp. 1746–1756, 2016.

[40] C. N. Chen, C. C. Chang, T. E. Su et al., "Identification of calreticulin as a prognosis marker and angiogenic regulator in human gastric cancer," *Annals of Surgical Oncology*, vol. 16, pp. 524–533, 2009.

[41] J. Fucikova, I. Truxova, M. Hensler et al., "Calreticulin exposure by malignant blasts correlates with robust anticancer immunity and improved clinical outcome in AML patients," *Blood*, vol. 128, pp. 3113–3124, 2016.

[42] A. N. Cornforth, A. W. Fowler, D. J. Carbonell, and R. O. Dillman, "Resistance to the proapoptotic effects of interferon-gamma on melanoma cells used in patient-specific dendritic cell immunotherapy is associated with improved overall survival," *Cancer Immunology, Immunotherapy*, vol. 60, pp. 123–131, 2011.

[43] A. M. Dudek-Peric, G. B. Ferreira, A. Muchowicz et al., "Antitumor immunity triggered by melphalan is potentiated by melanoma cell surface-associated calreticulin," *Cancer Research*, vol. 75, pp. 1603–1614, 2015.

[44] Y. Qin, Y. Han, C. Cao, Y. Ren, C. Li, and Y. Wang, "Melanoma B16-F1 cells coated with fusion protein of mouse calreticulin and virus G-protein coupled receptor induced

the antitumor immune response in Balb/C mice," *Cancer Biology & Therapy*, vol. 11, pp. 574–580, 2011.

[45] M. Obeid, T. Panaretakis, N. Joza et al., "Calreticulin exposure is required for the immunogenicity of gamma-irradiation and UVC light-induced apoptosis," *Cell Death & Differentiation*, vol. 14, pp. 1848–1850, 2007.

[46] M. E. Rodriguez, I. S. Cogno, L. S. Milla Sanabria, Y. S. Moran, and V. A. Rivarola, "Heat shock proteins in the context of photodynamic therapy: autophagy, apoptosis and immunogenic cell death," *Photochemical & Photobiological Sciences*, vol. 15, pp. 1090–1102, 2016.

[47] T. Panaretakis, O. Kepp, U. Brockmeier et al., "Mechanisms of pre-apoptotic calreticulin exposure in immunogenic cell death," *The EMBO Journal*, vol. 28, pp. 578–590, 2009.

[48] D. B. Graves, "The emerging role of reactive oxygen and nitrogen species in redox biology and some implications for plasma applications to medicine and biology," *Journal of Physics D-Applied Physics*, vol. 45, article 263001, 2012.

[49] M. Dunnbier, A. Schmidt-Bleker, J. Winter et al., "Ambient air particle transport into the effluent of a cold atmospheric-pressure argon plasma jet investigated by molecular beam mass spectrometry," *Journal of Physics D-Applied Physics*, vol. 46, article 435203, 2013.

[50] S. Bekeschus, S. Iseni, S. Reuter, K. Masur, and K. D. Weltmann, "Nitrogen shielding of an argon plasma jet and its effects on human immune cells," *IEEE Transactions on Plasma Science*, vol. 43, pp. 776–781, 2015.

[51] H. Jablonowski and T. von Woedtke, "Research on plasma medicine-relevant plasma–liquid interaction: what happened in the past five years?" *Clinical Plasma Medicine*, vol. 3, pp. 42–52, 2015.

[52] S. Bekeschus, J. Kolata, C. Winterbourn et al., "Hydrogen peroxide: a central player in physical plasma-induced oxidative stress in human blood cells," *Free Radical Research*, vol. 48, pp. 542–549, 2014.

[53] E. M. Hanschmann, J. R. Godoy, C. Berndt, C. Hudemann, and C. H. Lillig, "Thioredoxins, glutaredoxins, and peroxiredoxins—molecular mechanisms and health significance: from cofactors to antioxidants to redox signaling," *Antioxidants & Redox Signaling*, vol. 19, pp. 1539–1605, 2013.

[54] A. Schmidt, K. Rödder, S. Hasse et al., "Redox-regulation of activator protein 1 family members in blood cancer cell lines exposed to cold physical plasma-treated medium," *Plasma Processes and Polymers*, vol. 13, pp. 1179–1188, 2016.

[55] C. Abate, L. Patel, F. J. Rauscher 3rd, and T. Curran, "Redox regulation of fos and jun DNA-binding activity in vitro," *Science*, vol. 249, pp. 1157–1161, 1990.

[56] D. T. Yamanishi, J. A. Buckmeier, and F. L. Meyskens Jr., "Expression of c-jun, jun-B, and c-fos proto-oncogenes in human primary melanocytes and metastatic melanomas," *The Journal of Investigative Dermatology*, vol. 97, pp. 349–353, 1991.

[57] E. Shaulian and M. Karin, "AP-1 as a regulator of cell life and death," *Nature Cell Biology*, vol. 4, pp. E131–E136, 2002.

[58] D. Wang, J. Y. Wang, N. Ding et al., "MAGE-A1 promotes melanoma proliferation and migration through C-JUN activation," *Biochemical & Biophysical Research Communications*, vol. 473, pp. 959–965, 2016.

[59] C. J. Chan, A. E. Ekpenyong, S. Golfier et al., "Myosin II activity softens cells in suspension," *Biophysical Journal*, vol. 108, pp. 1856–1869, 2015.

[60] J. Guck, F. Lautenschlager, S. Paschke, and M. Beil, "Critical review: cellular mechanobiology and amoeboid migration," *Integrative Biology (Camb)*, vol. 2, pp. 575–583, 2010.

[61] I. Dalle-Donne, R. Rossi, A. Milzani, P. Di Simplicio, and R. Colombo, "The actin cytoskeleton response to oxidants: from small heat shock protein phosphorylation to changes in the redox state of actin itself," *Free Radical Biology & Medicine*, vol. 31, pp. 1624–1632, 2001.

[62] J. S. Lee, C. M. Hale, P. Panorchan et al., "Nuclear lamin A/C deficiency induces defects in cell mechanics, polarization, and migration," *Biophysical Journal*, vol. 93, pp. 2542–2552, 2007.

[63] M. Polette, C. Gilles, B. Nawrocki-Raby et al., "Membrane-type 1 matrix metalloproteinase expression is regulated by zonula occludens-1 in human breast cancer cells," *Cancer Research*, vol. 65, pp. 7691–7698, 2005.

[64] E. Takai, X. Tan, Y. Tamori, M. Hirota, H. Egami, and M. Ogawa, "Correlation of translocation of tight junction protein zonula occludens-1 and activation of epidermal growth factor receptor in the regulation of invasion of pancreatic cancer cells," *International Journal of Oncology*, vol. 27, pp. 645–651, 2005.

[65] K. Aigner, B. Dampier, L. Descovich et al., "The transcription factor ZEB1 (deltaEF1) promotes tumour cell dedifferentiation by repressing master regulators of epithelial polarity," *Oncogene*, vol. 26, pp. 6979–6988, 2007.

[66] K. S. Smalley, P. Brafford, N. K. Haass, J. M. Brandner, E. Brown, and M. Herlyn, "Up-regulated expression of zonula occludens protein-1 in human melanoma associates with N-cadherin and contributes to invasion and adhesion," *The American Journal of Pathology*, vol. 166, pp. 1541–1554, 2005.

[67] H. Chung, J. H. Lee, D. Jeong, I. O. Han, and E. S. Oh, "Melanocortin 1 receptor regulates melanoma cell migration by controlling syndecan-2 expression," *The Journal of Biological Chemistry*, vol. 287, pp. 19326–19335, 2012.

[68] J. Y. Lin and D. E. Fisher, "Melanocyte biology and skin pigmentation," *Nature*, vol. 445, pp. 843–850, 2007.

[69] A. A. Rosenkranz, T. A. Slastnikova, M. O. Durymanov, and A. S. Sobolev, "Malignant melanoma and melanocortin 1 receptor," *Biochemistry (Mosc)*, vol. 78, pp. 1228–1237, 2013.

[70] T. A. Slastnikova, A. A. Rosenkranz, T. N. Lupanova, P. V. Gulak, N. V. Gnuchev, and A. S. Sobolev, "Study of efficiency of the modular nanotransporter for targeted delivery of photosensitizers to melanoma cell nuclei in vivo," *Doklady. Biochemistry and Biophysics*, vol. 446, pp. 235–237, 2012.

Hindawi Publishing Corporation
Oxidative Medicine and Cellular Longevity
Volume 2016, Article ID 9460462, 18 pages
http://dx.doi.org/10.1155/2016/9460462

Research Article

The Protective Roles of ROS-Mediated Mitophagy on ^{125}I Seeds Radiation Induced Cell Death in HCT116 Cells

Lelin Hu,[1,2] Hao Wang,[1] Li Huang,[1] Yong Zhao,[3] and Junjie Wang[1]

[1]*Department of Radiation Oncology, Peking University 3rd Hospital, Haidian District, Beijing 100191, China*
[2]*School of Medicine, Anhui University of Science and Technology, Huainan 232001, Anhui, China*
[3]*State Key Laboratory of Membrane Biology, Institute of Zoology, Chinese Academy of Sciences, Beijing 100101, China*

Correspondence should be addressed to Junjie Wang; junjiewangedu@163.com

Received 17 September 2016; Revised 18 November 2016; Accepted 24 November 2016

Academic Editor: Sander Bekeschus

For many unresectable carcinomas and locally recurrent cancers (LRC), ^{125}I seeds brachytherapy is a feasible, effective, and safe treatment. Several studies have shown that ^{125}I seeds radiation exerts anticancer activity by triggering DNA damage. However, recent evidence shows mitochondrial quality to be another crucial determinant of cell fate, with mitophagy playing a central role in this control mechanism. Herein, we found that ^{125}I seeds irradiation injured mitochondria, leading to significantly elevated mitochondrial and intracellular ROS (reactive oxygen species) levels in HCT116 cells. The accumulation of mitochondrial ROS increased the expression of HIF-1α and its target genes BINP3 and NIX (BINP3L), which subsequently triggered mitophagy. Importantly, ^{125}I seeds radiation induced mitophagy promoted cells survival and protected HCT116 cells from apoptosis. These results collectively indicated that ^{125}I seeds radiation triggered mitophagy by upregulating the level of ROS to promote cellular homeostasis and survival. The present study uncovered the critical role of mitophagy in modulating the sensitivity of tumor cells to radiation therapy and suggested that chemotherapy targeting on mitophagy might improve the efficiency of ^{125}I seeds radiation treatment, which might be of clinical significance in tumor therapy.

1. Introduction

Due to its low complication rates and high efficacy—which is comparable to that of radical surgery and external beam radiation therapy—^{125}I seeds implantation brachytherapy has become one of the most popular treatment modalities for many unresectable carcinomas and locally recurrent cancers [1–7]. A series of studies have explored the molecular mechanisms through which ^{125}I seeds radiation exerts anticancer activity. Most studies have focused on apoptosis and cell cycle arrest resulting from DNA damage after exposure to ^{125}I seeds radiation [8–10]. However, there is growing evidence that mitochondria, which account for up to 30% of the total cell volume, may also be important extranuclear mediators of the cytotoxic effects of radiation [11, 12]. Healthy mitochondria act as powerhouses, producing energy for cell function through the TCA cycle (tricarboxylic acid cycle) and oxidative phosphorylation [13]. Damage to mitochondria can lead to cell death and a variety of other problems [14].

Mitophagy, which refers to the selective removal of damaged or unwanted mitochondria, is crucial for mitochondrial quality control following stresses such as starvation, photo damage, hypoxia, and ROS production [15]. Certain physiological stresses can induce mitochondrial damage, which can cause oxidative stress and cell death triggered by the production of ROS from the mitochondrial electron transport chain (ETC). The high level of ROS can be selectively sequestered in autophagosomes and subjected to lysosomal degradation in a process termed mitophagy to promote cellular homeostasis and survival [16]. Mitophagy can thus alleviate cell injury following stress, acting as an effective antioxidant pathway and clearing increased mitochondrial or cytosolic ROS. Mitophagy has been reported to be involved in tumor resistance to therapy by maintaining healthy mitochondria [17, 18].

Mitophagy is mediated by specific receptors such as NIX, BNIP3, and FUNDC1 in mammalian systems [19]. BNIP3 and NIX are two important mitochondrial stressor sensors with homology to BCL2 in the BH3 domain. Once

mitophagy is triggered, BNIP3 and NIX are selectively recruited to dysfunctional mitochondria and then bound to the conserved LC3-interacting region (LIR) of LC3-II present on autophagosome to promote removal of damaged mitochondria by the autophagosome [16, 20, 21]. In addition, both BNIP3 and NIX facilitate mitophagy by promoting the release of Beclin1 from the Beclin1-Bcl2/Bcl-X complex [22]. NIX and BNIP3, two hypoxia-inducible proteins that target mitochondria for autophagosomal degradation, are the transcription products of HIF-1α [23]. HIF-1α is an important predictor of tumor progression for several types of solid cancers and can regulate the transcription of a number of genes (such as *BNIP3* and *NIX*) that are involved in mitophagy and apoptosis [24]. Several studies have shown that elevated mitochondrial ROS increases the expression of HIF-1α and its target genes BNIP3/NIX [17, 25].

In the present study, we have focused on the regulatory roles of autophagy in the radiosensitivity of tumors to ^{125}I seeds irradiation as well as the molecular mechanisms that underlie ^{125}I seeds radiation induced mitophagy. We found that mitophagy significantly decreased the sensitivity of tumor cells to ^{125}I seeds irradiation. Thus, targeting mitophagy combined with radiotherapy may improve the therapeutic efficiency in clinical patients with tumors, which needs to be confirmed by the clinical studies.

2. Materials and Methods

2.1. ^{125}I Radiation Source. The ^{125}I seeds used as the radiation source in this study were purchased from Ningbo Junan Pharmaceutical Technology Company (Ningbo, Zhe Jiang province, China) and were installed in an in-house model developed in our laboratory for in vitro ^{125}I seeds radiation. A detailed description of this model has been published earlier [26, 27]. ^{125}I seeds have a half-life of ~59.4 days. The experimentally applicable radiation dose rate of ^{125}I seeds ranged from 2.77 cGy/h to 1.385 cGy/h, which is approximate to the clinically applicable radiation dose rate used in permanent LRC brachytherapy. This model was validated by using thermoluminescent dosimetry (TLD) measurement, and the irradiation time was calculated according to the absorbed dose and initial radiation dose rate. The control cells were seeded and harvested at the same time points as the irradiated cells.

2.2. Reagents and Antibodies. Annexin V-FITC apoptosis detection kit I was purchased from Beijing Zoman Biotechnology (Beijing, China); the ROS assay kit and mitochondrial membrane potential assay kit with JC-1 were purchased from Beyotime (Shanghai, China); the mitochondrial ROS indicator MitoSOX was purchased from Invitrogen (Carlsbad, CA, USA); N-acetylcysteine (NAC) and chloroquine (CQ) were purchased from Sigma-Aldrich; 3-methyladenine (3-MA) was purchased from Selleck Chemicals LLC (Houston, TX, USA); Ly294002 was purchased from Invitrogen; Antimycin A was purchased from Sigma-Aldrich. LipofectamineTM 2000 was purchased from Invitrogen. Diphenyleneiodonium chloride (DPI) was purchased from Gene Operation Co., Ltd. (Wuxi, China). cDNA reverse transcription kit and real-time PCR kit were purchased from Takara Biotechnology (Dalian, China); and goat anti-rabbit IgG-horseradish peroxidase (HRP), goat anti-mouse IgG-HRP, anti-β-actin, and anti-LC3 polyclonal antibody were obtained from Sigma-Aldrich.

2.3. Cell Culture. Human colorectal cancer cells—HCT116 cells—were kindly provided by Dr. Xiaojuan Du of Peking University Health Science Center, Beijing, China. The HCT116 cells were grown in RPMI (Roswell Park Memorial Institute) 1640 medium supplemented with 10% fetal calf serum (FCS), 100 units/mL penicillin, and 100 μg/mL streptomycin, in a humidified atmosphere containing 5% CO_2 at 37°C.

2.4. Clonogenic Survival Assay. HCT116 cells in appropriate numbers were seeded in 35 mm dishes to ensure the formation of about 100 colonies per dish. After 24 hours, the cells were exposed to ^{125}I seeds irradiation in the model. At the desired time points, the cells were removed from the radiation source and cultured for 10–12 days [28]. They were then fixed with absolute ethanol and glacial acetic acid in a 1 : 1 ratio at 4°C for 30 minutes and stained with methylene blue for 2 hours. Finally, the samples were washed with cold phosphate-buffered saline (PBS) and dried at room temperature. The number of colonies per dish was counted and the survival fraction (SF) was calculated as PE (tested group)/PE (0-Gy group), where PE was (colony number/number of inoculating cells) × 100%. The experiment was repeated two times in duplicate. The survival fraction values were presented as the mean ± SD for the respective radiation doses.

2.5. Western Blot Analysis. Cells were lysed in a radio immunoprecipitation assay (RIPA) buffer (50 mM of pH-7.4 Tris-HCl, 1% NP-40, 0.25% Na-deoxycholate, 150 mM NaCl, and 1 mM of pH-7.4 EDTA) with protease and phosphatase inhibitor cocktails for 15 minutes on ice and then centrifuged for 30 minutes at 12,000g and 4°C. Bicinchoninic acid (BCA) protein assay kits (Beyotime Biotech, Shanghai, China) were used to measure the protein concentrations of protein supernatant. Equal amounts of the protein samples were denatured at 95°C for 5 minutes and then separated on dodecyl sulfate-polyacrylamide gel electrophoresis (SDS-PAGE) gel. Proteins were transferred onto polyvinylidene difluoride (PVDF) membranes (Hybond-P; Amersham, Buckinghamshire, UK) for 2 hours at 100 V on ice. Membranes were blocked with 5% nonfat milk in Tris-buffered saline and Tween 20 (TBST) for 1 hour at room temperature and then incubated overnight at 4°C with the indicated primary antibody. After washing thrice with TBST, the membranes were blotted with the respective secondary antibody for 1 hour at room temperature. The membranes were incubated with enhanced chemiluminescence (ECL) detection kits (Pierce Biotechnology, Rockford, IL, USA) to visualize proteins. Expression of human β-actin was detected as a loading control.

2.6. Flow Cytometry Analysis

2.6.1. Flow Cytometry Analysis of Apoptosis. After exposure to the 2 Gy of radiation, HCT116 cells were harvested and double-stained with fluorescein isothiocyanate- (FITC-)

labeled Annexin V and propidium iodide (PI) for 15 minutes in binding buffer according to the manufacturer's instructions to detect cell apoptosis. Then, fluorescence was detected by flow cytometry (Beckman Coulter, Miami, FL, USA) to assay the percentage of cell apoptosis.

2.6.2. Flow Cytometry Analysis of Intracellular ROS and Mitochondrial ROS. The ROS assay kit was used to assess intracellular ROS levels. After exposure to 2 Gy of radiation adherent HCT116 cells were washed with serum-free RPMI 1640 medium and stained with 5 μM of DCFH-DA at 37°C for 30 minutes. Then, labeled HCT116 cells were trypsinized and analyzed by flow cytometry.

MitoSOX™ Red mitochondrial superoxide indicator selectively targets mitochondria to detect mitochondrial ROS. Postirradiation adherent HCT116 cells were washed with serum-free RPMI 1640 medium and incubated with 10 μM of MitoSOX Red mitochondrial superoxide indicator at 37°C for 30 minutes. After the treatment, HCT116 cells were trypsinized and analyzed by flow cytometry.

2.6.3. Flow Cytometry Analysis of Mitochondrial Membrane Potential. One hundred thousand HCT116 cells were collected and washed once with PBS after irradiation. Mitochondrial membrane potential was detected by flow cytometry using a mitochondrial membrane potential assay kit with JC-1. Under normal conditions, JC-1 accumulates in the mitochondrial matrix in the form of J-aggregates, which emit a red fluorescence; however, when the mitochondrial membrane potential collapses, JC-1 exists as a monomer that cannot enter mitochondria and emits a green fluorescence. The ratio of the JC-1 red signal (J-aggregates) to the JC-1 green signal (monomer) was used as a measure of the mitochondrial membrane potential. Data were analyzed by FCS Express V3 software (De Novo Software, Glendale, CA, USA).

2.7. Immunofluorescence Analysis. Cells were cultured on coverslips in 35 mm dishes. After the indicated dose of ^{125}I seeds irradiation, the cells were fixed with 4% formaldehyde in PBS for 15 minutes at 37°C. The fixed cells were permeabilized with 0.2% Triton X-100 in PBS for 15 minutes on ice and subsequently blocked by goat serum. After incubation with primary antibodies overnight at 4°C, LC3 and TIM23 were detected with the polyclonal anti-LC3 antibody and the monoclonal antibody against TIM23, respectively. LC3 were detected with FITC- (Fluorescein Isothiocyanate-) conjugated goat anti-rabbit IgG. TIM23 were labeled with TRITC- (Tetramethylrhodamine Isothiocyanate-) conjugated goat anti-mouse IgG. Nuclei were stained with 4′,6-diamidino-2-phenylindole (Beyotime, China). Fluorescence images were captured with an LSM 510 Zeiss confocal microscope (Carl Zeiss Jena, Germany).

2.8. Detection of Cellular ATP Levels. Firefly luciferase-based ATP assay kit (Beyotime, China) was used to measure cellular ATP level. After exposure to the 2 Gy of radiation, HCT116 cells were lysed and centrifuged at 12,000g for 5 minutes. Cell lysates (100 μL) were mixed with 100 μL of ATP detection working dilution in a 96-well plate, and the cellular ATP levels were measured using the BioTek Synergy 2 Microplate Reader (BioTek Instruments Inc., Winooski, VT, USA). A BCA assay kit was used to determine the protein concentration of cell lysates (1 μL) of each group. The ratio of cellular ATP level to the protein concentration was used to evaluate total ATP level.

2.9. Reverse Transcription and Real-Time PCR. Total RNA was extracted from cells using Trizol (Invitrogen, Carlsbad, CA, USA) according to the manufacturer's instructions, and 1 μg of total RNA was used to reverse transcribe cDNA. Real-time PCR was performed using multiple kits (SYBR Premix Ex TaqTM, DRR041A, Takara Bio) on CFX96 (Bio-Rad, Hercules, CA, USA) [29]. The housekeeping gene hypoxanthine phosphoribosyl transferase (HPRT) was used as an endogenous control. The following primers were used: HPRT upstream primer 5′-CAGTATAATCCAAAGATGGTCAA-3′ and HPRT downstream primer 5′-TTAGGCTTTGTATTTTGCTTTTCC-3′; BNIP3 upstream primer 5′-CAGGGCTCCTGGGTAGAACT-3′ and BNIP3 downstream primer 5′-CTACTCCGTCCAGACTCATGC-3′; NIX upstream primer 5′-ATGTCGTCCCACCTAGTCGAG-3′ and NIX downstream primer 5′-TGAGGATGGTACGTGTTCCAG-3′; HIF-1α upstream primer 5′-GAACGTCGAAAAGAAAAGTCTCG-3′, and HIF-1α downstream primer 5′-CCTTATCAAGATGCGAACTCACA-3′.

2.10. Cell Transfection. LC3-specific siRNAs (small interference RNA) (5′-GAGUGAGCUCAUCAAGAUAtt-3′) and an unrelated control siRNA (5′-UUCUCCGAACGUGUCACGUtt-3′) [30] were synthesized from GenePharma Co., Ltd., to knockdown of LC3 expression. HCT116 cells were transfected with 100 nM LC3 siRNA or nonrelated control siRNA. Transfections were performed with LipofectamineTM 2000 in accordance with the manufacturer's instruction.

2.11. Statistical Analysis. Experiments were performed at least three times in duplicate. Statistical analyses were performed using the statistical software SPSS 17.0 (SPSS Inc., Chicago, IL, USA). The two-tailed t-test was applied to compare group means. Statistical significance was set at $p \leq 0.05$.

3. Results

3.1. Inhibition of Autophagy Enhanced the Sensitivity of Tumor Cells to ^{125}I Seeds Radiation. To investigate how autophagy affects the radiosensitivity of tumor cells, clonogenic survival assay was performed to assess the response to ^{125}I seeds radiation with and without pretreatment with autophagy inhibitors. HCT116 cells were pretreated with the autophagy inhibitors 3-MA (0.5 mM) or Ly294002 (10 μM) 2 hours prior to being exposed to 2 Gy and 4 Gy ^{125}I seeds radiation. The ratios of surviving fraction between 3MA group and control group were 0.81, 0.48 for total doses of 2 and 4 Gy, respectively (Figure 1(a)). What is more, the ratios of surviving fraction between Ly294002 and control group were 0.83 and 0.59 for total doses of 2 and 4 Gy, respectively (Figure 1(b)). We found a statistically significant decrease in the clonogenic survival

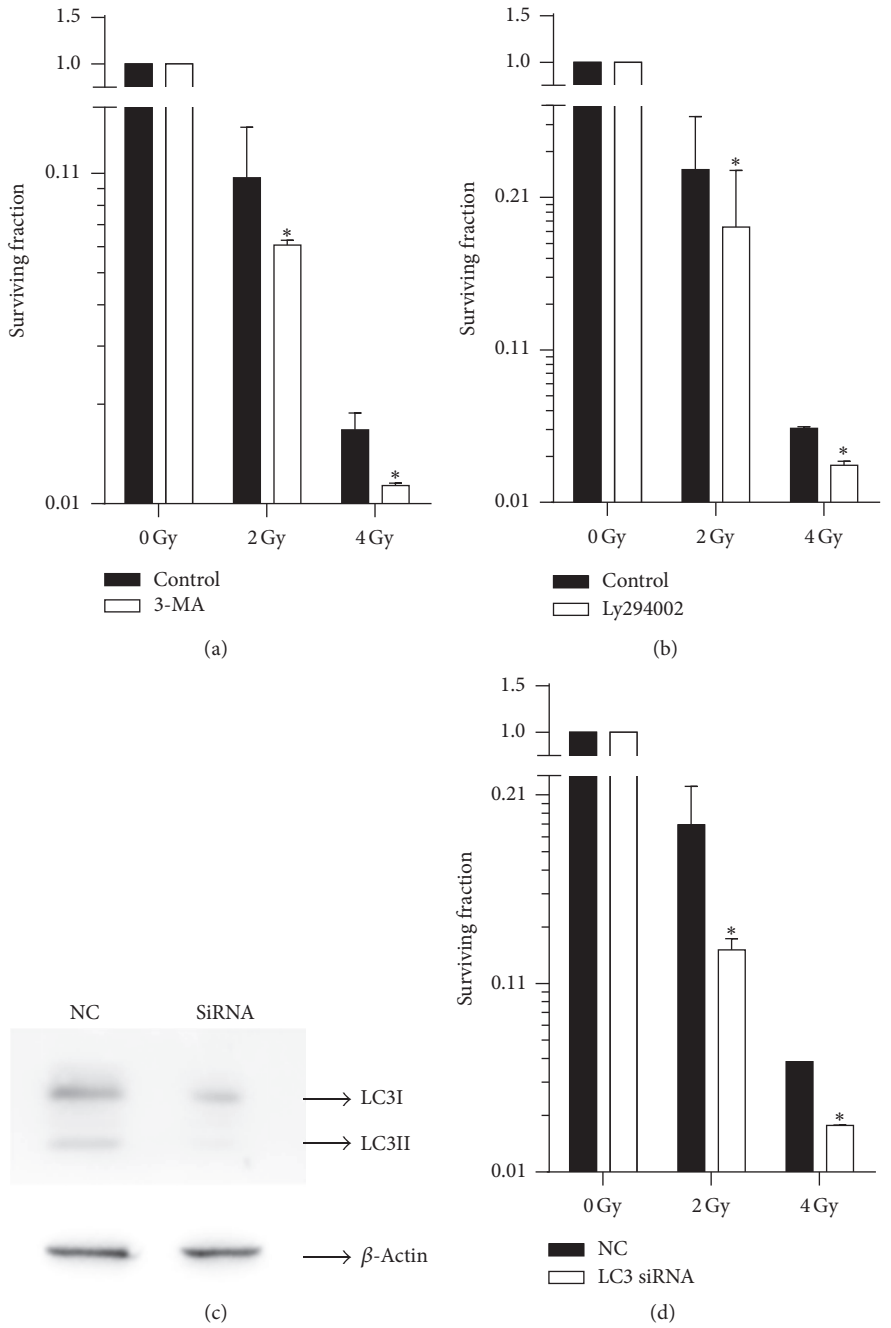

Figure 1: Inhibition of autophagy enhanced the sensitivity of HCT116 cells to ^{125}I seeds radiation. (a) HCT116 cells were pretreated with or without 3-MA before exposure to the indicated dose of ^{125}I seeds radiation. Clonogenic survival was assessed in the presence or and absence of 3-MA. (b) Clonogenic survival was assessed in HCT116 cells pretreated with or without Ly294002 before exposure to the indicated dose of ^{125}I seeds radiation. (c) HCT116 cells were transfected with LC3 siRNA or unrelated control siRNA. Western blot was performed to assess the expression of LC3 48 h after transfection. Representative Western blot analysis of LC3II/I is shown. (d) Clonogenic survival was assessed in HCT116 cells transfected with LC3 siRNA or unrelated control siRNA before exposure to the indicated dose of ^{125}I seeds radiation. The values are the means ± SD of three independent experiments. The two-tailed t-test was used for comparing the means. $*$ indicates significant difference ($p \leq 0.05$) as compared to the control group.

fraction in HCT116 cells pretreated with 3-MA or Ly294002 at 2 Gy and 4 Gy ($p \leq 0.05$), suggesting that these autophagy inhibitors have a radiosensitizing effect on HCT116 cells. Neither 3-MA nor Ly294002 was specific autophagy inhibitor. We further investigated whether knockdown of LC3 expression, a conserved gene required for mammalian autophagy, affected the radiosensitivity of HCT116 cells. Clonogenic survival assay was used to assess the response to ^{125}I seeds

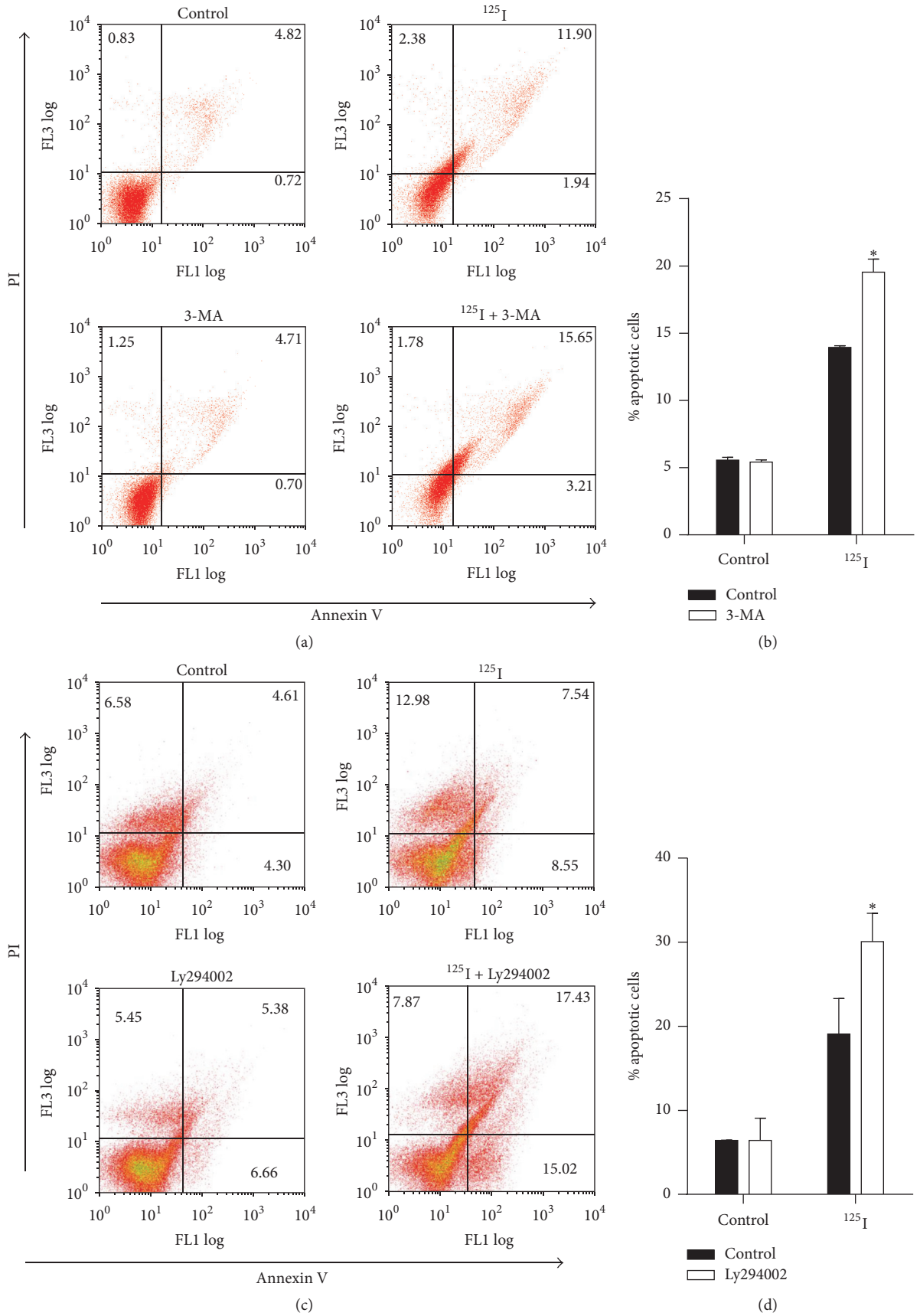

Figure 2: Continued.

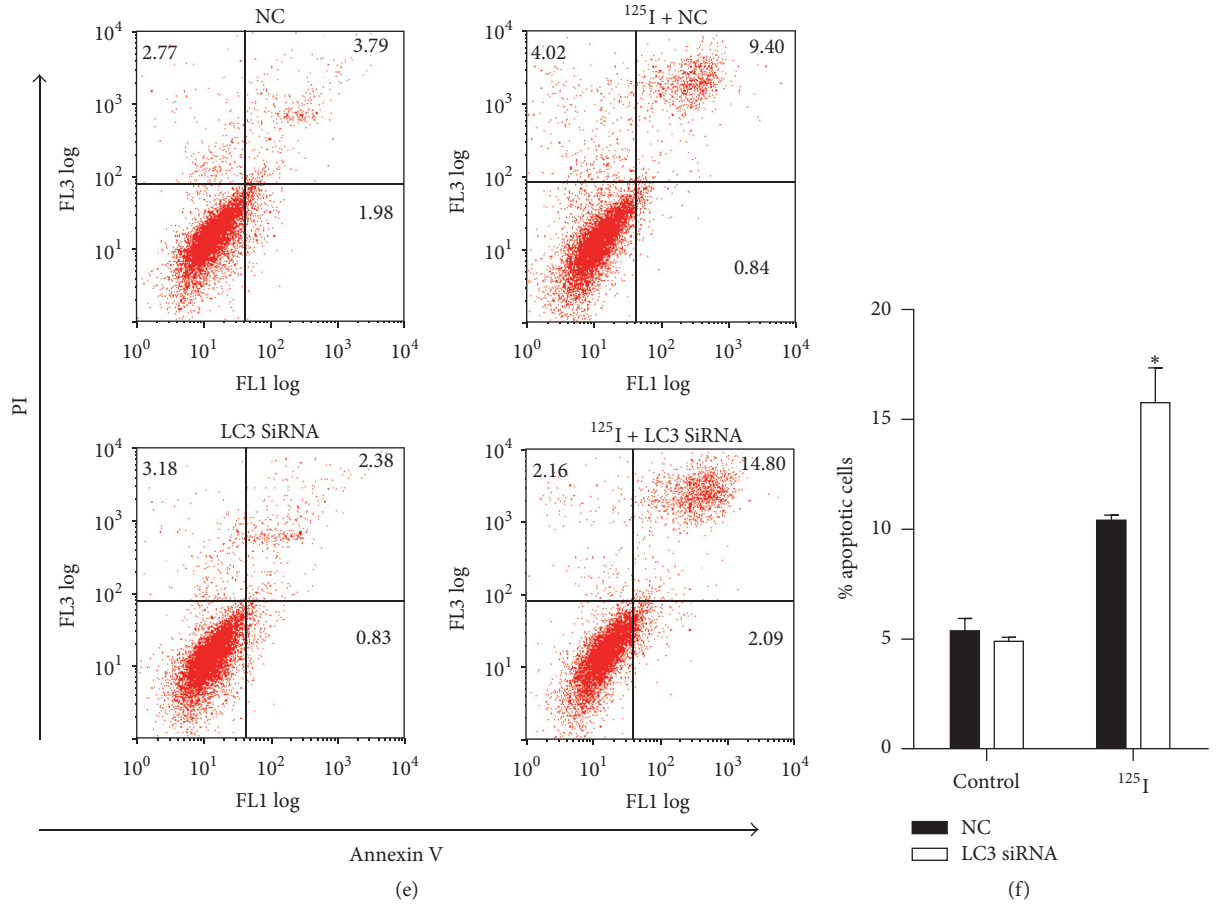

Figure 2: Inhibition of autophagy promoted apoptosis induced by ^{125}I seeds radiation. (a) Representative example of flow cytometry analysis pretreated with and without 3-MA before exposure to indicated doses of ^{125}I seeds radiation. Apoptotic cell death was detected by Annexin V and PI double staining. (b) The percentage of apoptosis with and without 3-MA was examined by flow cytometry after Annexin V and PI double staining. Annexin V^+/PI^- cell and anexin V^+/PI^+ cell populations were quantified and analyzed. (c) Typical example of flow cytometry analysis pretreated with and without Ly294002 before exposure to indicated doses of ^{125}I seeds radiation. (d) The percentage of apoptosis with and without Ly294002 was measured by flow cytometry with Annexin V and PI double staining. Annexin V^+/PI^- cell and anexin V^+/PI^+ cell populations were quantified and analyzed. (e) Typical example of flow cytometry analysis in HCT116 cells transfected with LC3 siRNA or unrelated control siRNA before exposure to the indicated dose of ^{125}I seeds radiation. (f) The percentage of apoptosis in HCT116 cells transfected with LC3 siRNA or unrelated control siRNA was measured by flow cytometry with Annexin V and PI double staining. Annexin V^+/PI^- cell and anexin V^+/PI^+ cell populations were quantified and analyzed. $*$ indicates significant difference ($p \leq 0.05$) between treated group or untreated group.

radiation after transfection with LC3 siRNA or nonrelated control siRNA duplex. The expression of LC3 in HCT116 cells transfected with LC3 siRNA duplex significantly decreased compared to nonrelated control siRNA group (Figure 1(c)). Following irradiation the ratios of surviving fraction between LC3 siRNA group and nonrelated control siRNA were 0.66, 0.51 for total doses of 2 and 4 Gy, respectively. We found that knockdown of LC3 expression sensitized HCT116 cells to ^{125}I seeds radiation at 2 Gy and 4 Gy ($p \leq 0.05$, Figure 1(d)), suggesting that inhibition of autophagy had a radiosensitizing effect on HCT116 cells.

3.2. Inhibition of Autophagy Promoted Apoptosis Induced by ^{125}I Seeds Radiation. In previous studies we had shown that ^{125}I seeds radiation induces apoptosis in colorectal cancer cells. To examine whether the enhanced radiosensitivity of autophagy inhibitors was due to increased apoptosis, the percentage of apoptotic cells was measured by double staining with Annexin V and PI and assayed by flow cytometry. We found that the proportion of PI^-/Annexin V^+ and PI^+/Annexin V^+ cell population in HCT116 cells increased from 13.9% to 19.5% following treatment with ^{125}I seeds radiation plus the autophagy inhibitor 3-MA ($p \leq 0.05$, Figures 2(a) and 2(b)). To confirm this phenomenon, the same experiments were duplicated with autophagy inhibitor Ly294002 instead of 3MA (Figure 2(c)). The percentage of apoptosis increased from 19.1% to 30.1% in cells treated with ^{125}I seeds radiation plus Ly294002 ($p \leq 0.05$, Figure 2(d)). We further investigated whether LC3 siRNA affected the apoptosis of HCT116 cells induced by ^{125}I seeds radiation. After transfection with LC3 siRNA duplex, the percentage of apoptotic cell induced by ^{125}I seeds radiation increased from 10.41 to 15.77

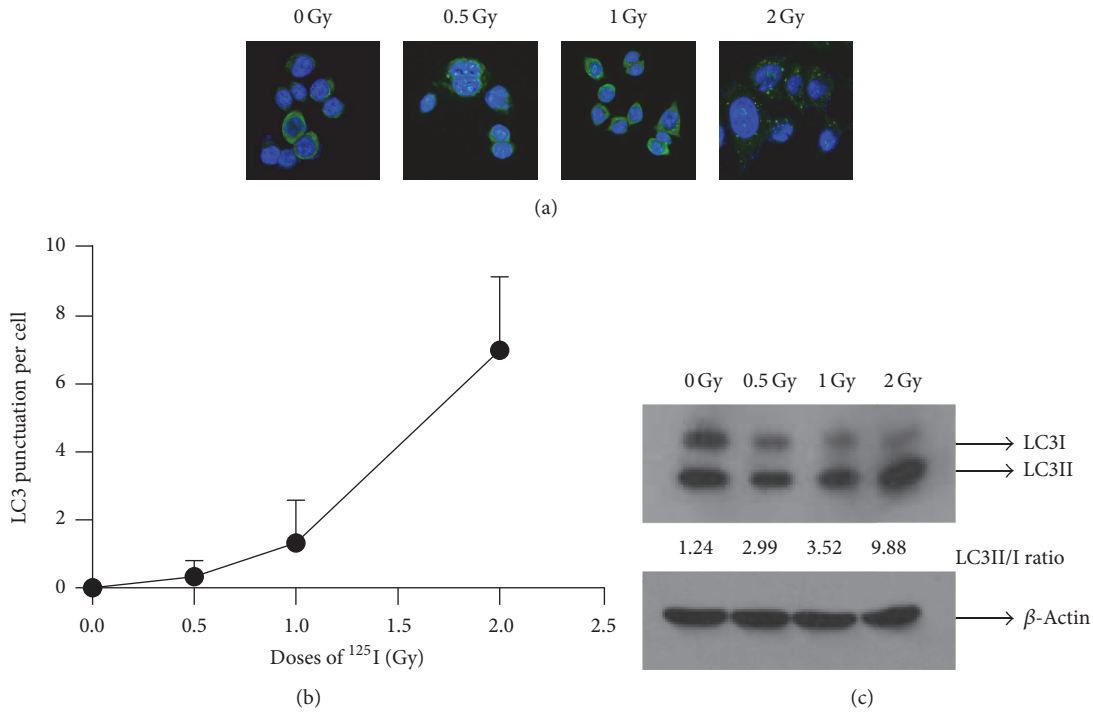

Figure 3: ^{125}I seeds radiation induced autophagy in HCT116 cells. (a) HCT116 cells were exposed to the indicated dose of ^{125}I seeds radiation. LC3 punctuation was measured using immunofluorescence with polyclonal anti-LC3 antibody. DAPI was used to stain nuclei. (b) The number of LC3 punctuations per cell after exposure to indicated doses of ^{125}I seeds radiation was quantified. The values are the mean (±SD) of at least three different cells. (c) HCT116 cells were exposed to the gradually increased dose of ^{125}I seeds radiation. The ratio of LC3II/I was analyzed by Western analysis with anti-LC3 antibody. β-Actin was evaluated as a loading control.

($p \leq 0.05$, Figures 2(e) and 2(f)). These results suggested that inhibition of autophagy increased the sensitivity to ^{125}I seeds radiation by enhancing apoptosis.

3.3. ^{125}I Seeds Radiation Induced Mitophagy in Tumor Cells. To investigate whether ^{125}I seeds radiation could induce autophagy in HCT116 cells, LC3-I and LC3-II were used as autophagy markers to estimate the induction of autophagy and the overall autophagic flux to permit correct interpretation of the results. Immunofluorescence staining with anti-LC3 antibody was performed with HCT116 cells following exposure to 0, 0.5, 1, and 2 Gy of ^{125}I seeds radiation (Figure 3(a)). As shown in Figure 3(b), the number of LC3 punctuations per cell increased gradually after exposure to 0, 0.5, 1, and 2 Gy of ^{125}I seeds radiation. Western blot analysis, performed to examine the transformation of soluble LC3 (LC3-I) to the LC3-II form, showed that the ratio of LC3-II to LC3-I increased gradually after treatment with indicated doses of ^{125}I seeds radiation (Figure 3(c)). This provided further evidence that ^{125}I seeds radiation induced autophagy in a dose-dependent manner in HCT116 cells.

Autophagy involves two key processes: the formation of autophagosomes and the formation of autolysosomes. In the initial stage, membrane distant from either the Golgi or ER sequesters cellular components to form autophagosome. At a relatively late stage of autophagy, autophagosome fuses with the lysosome to form an autolysosome, where LC3-II and sequestered cellular components were degraded by lysosomal hydrolytic enzymes [31–33]. There are two causes for the accumulation of LC3-II: one is increase of autophagosome formation and the other is inhibition of the formation of autolysosomes which is the site for degradation of autophagosomes [34]. To identify which of these two mechanisms was responsible for the autophagy caused by ^{125}I seeds radiation, we then investigated whether elevated LC3-II levels were due to the upregulation of autophagosome formation or the escape of autophagosome-lysosome fusion. Chloroquine (CQ), which acts as a late-stage autophagy inhibitor by blocking autophagosome-lysosome fusion, was used to treat the irradiated HCT116 cells for 6 hours before harvest, and the cells were examined under a confocal microscope (Figure 4(a)). As expected, treatment with CQ could make further increase of the number of LC3-II punctuations per cell induced by ^{125}I seeds radiation ($p \leq 0.05$, Figure 4(b)). Moreover, whole cell lysates from treated cells were analyzed by Western blotting in parallel at the same time. The results showed that CQ could make further increase of the ratio of LC3-II to LC3-I induced by ^{125}I seeds radiation (Figure 4(c)). These suggested that ^{125}I seeds radiation induced LC3-II punctuation accumulation was due to the increase of autophagosome formation rather than inhibition of lysosome-autophagosome fusion.

We also used electron microscopy, the gold standard for detecting autophagy, to investigate whether ^{125}I seeds radiation induced autophagy in HCT116 cells. Transmission electron microscope (TEM) analysis revealed that a large number

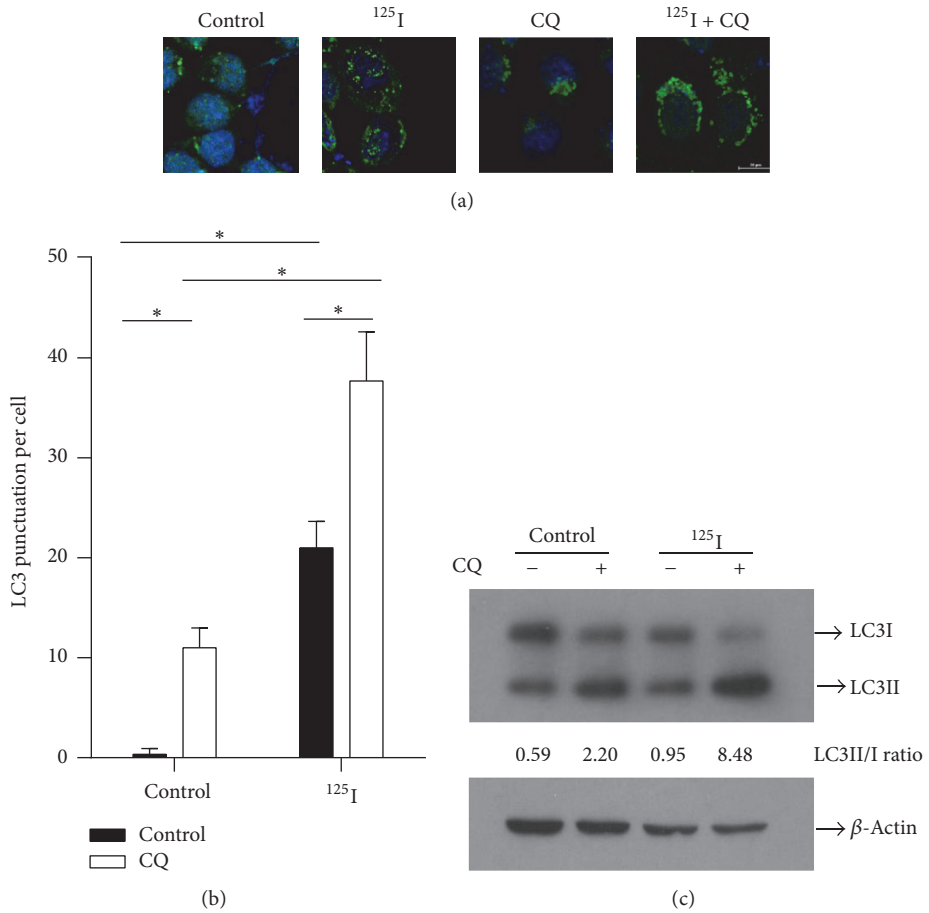

Figure 4: ^{125}I seeds radiation promoted autophagosome formation in HCT116 cells. (a) Irradiated HCT116 cells were treated with or without 40 μmol of chloroquine for 6 hours. LC3 punctuations were detected using immunofluorescence and images were captured by a confocal microscope. (b) The percentage of LC3 punctuation per cell was quantified. The values are the means ± SD of at least three different cells. (c) HCT116 cells were exposed to 125I seeds radiation (2 Gy) with or without chloroquine for 6 hours, respectively. The ratio of LC3II/I was measured by Western blotting analysis. $*$ indicates significant difference ($p \leq 0.05$) as compared to the control group.

of mitochondria in autophagosome-like vacuoles appeared in the cytoplasm after exposure to 2 Gy of ^{125}I seeds radiation (Figure 5(a)). This phenomenon was consistent with the result of immunofluorescence analysis. Following exposure to 2 Gy of ^{125}I seeds radiation, the cells were double indirect immunofluorescence staining with an anti-TIM23 antibody (red) and an anti-LC3 antibody (green) to detect the mitochondrial marker protein TIM23 and autophagosome marker protein LC3, respectively. The confocal image showed LC3 punctuation colocalized with mitochondria after ^{125}I seeds radiation. Besides, this colocalization induced by ^{125}I seeds radiation increased significantly after treatment with CQ, which could block autophagosome-lysosome fusion to amplify autophagy (Figure 5(b)). These results further supported that ^{125}I seeds radiation induced robust mitophagy by promoting autophagosome formation.

3.4. ^{125}I Seeds Radiation Impaired Mitochondria and Induced Oxidative Stress. To study whether ^{125}I seeds radiation could induce mitochondrial damage, we examined a series of indices that can reflect mitochondrial dysfunction. Immunofluorescence staining was performed with anti-TIM23 antibody to detect the mitochondrial marker protein TIM23. The fluorescence confocal image showed that ^{125}I seeds radiation induced changes in mitochondrial morphology, altering it from the elongated linear network form to a floccular and dot form (Figure 6(a)). In addition, mitochondrial membrane potential was analyzed with flow cytometry (Figure 6(b)); we found that ^{125}I seeds radiation impaired mitochondrial function and induced decrease in mitochondrial membrane potential ($p \leq 0.05$, Figure 6(c)).

It has been reported that mitochondrial dysfunction induced by radiation results in reduction of ATP synthesis owing to disruption of the proton gradient across the mitochondrial membrane [35, 36]. We next investigated whether ^{125}I seeds radiation induced mitochondrial dysfunction led to alterations in ATP production. Cellular ATP level was evaluated by firefly luciferase-based ATP assay kit; the results showed the level of total ATP decreased significantly after

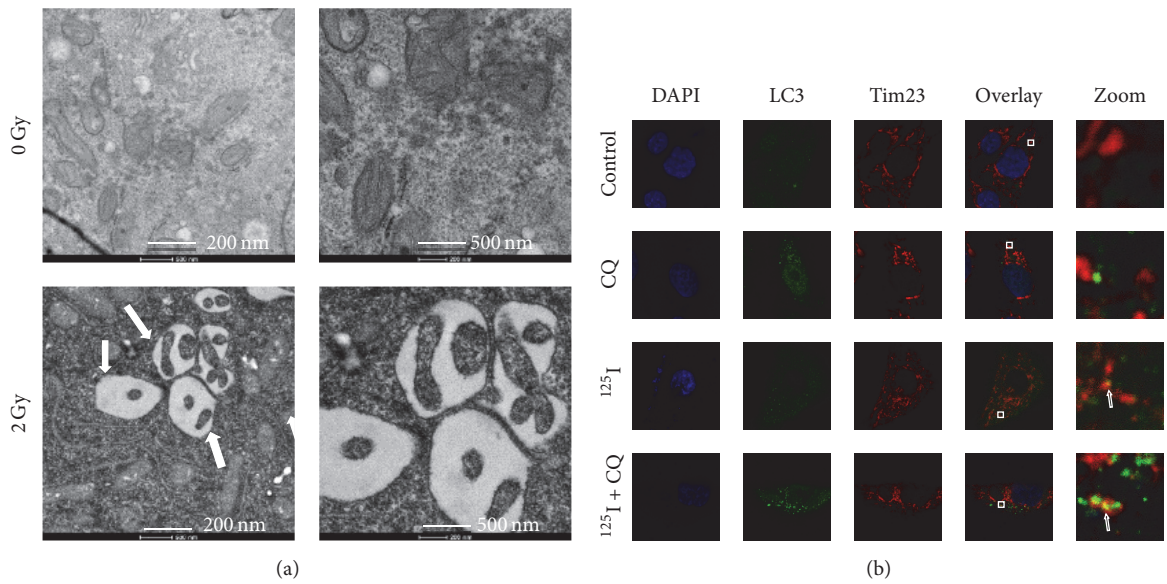

FIGURE 5: ^{125}I seeds radiation induced mitophagy in HCT116 cells. (a) HCT116 cells were exposed to ^{125}I seeds radiation (2 Gy); the representative transmission electron microscopic ultrastructures are shown. The arrows indicate an autophagic vacuole containing mitochondria (scale bars 200 nm and 500 nm). (b) HCT116 cells were exposed to ^{125}I seeds radiation alone or in combination with CQ (40 μmol) for 6 hours. Following fixation, the cells were immunostained with an anti-TIM23 antibody (red) and an anti-LC3 antibody (green) and visualized by confocal microscopy. The representative confocal microscopy images are shown. Small squares denoted the area zoomed in region of the images and white arrows denoted mitophagy punctuation induced by ^{125}I seeds radiation.

^{125}I seeds radiation ($p \leq 0.05$, Figure 6(d)). After exposure to 2 Gy of ^{125}I seeds radiation, cells were stained with the mitochondrial ROS and subjected to flow cytometry analysis (Figure 6(e)). Results showed that ^{125}I seeds radiation elevated levels of mitochondrial ROS in HCT116 cells ($p \leq 0.05$, Figure 6(f)). Similarly, postirradiation cells were stained with the intracellular ROS probes and analyzed by flow cytometry (Figure 6(g)). Results showed that ^{125}I seeds radiation elevated levels of intracellular ROS in HCT116 cells ($p \leq 0.05$, Figure 6(h)). Together, these data suggested that ^{125}I seeds radiation induced oxidative damage in mitochondria.

3.5. Elevated ROS Is Critical for Both Mitophagy and Apoptosis Induced by ^{125}I Seeds Radiation. There is increasing evidence that oxidative stress is responsible for autophagy [25]. To confirm the role of ROS in mitophagy and apoptosis induced by ^{125}I seeds radiation, we treated HCT116 cells with N-acetyl-L-cysteine (NAC; a ROS scavenger), ^{125}I seeds radiation, or both. Mitochondrial ROS and intracellular ROS generation were then analyzed using the corresponding probe for flow cytometry analysis. As shown in Figure 7(a), NAC decreased ^{125}I seeds radiation induced accumulation of mitochondrial ROS. Statistical results from three independent experiments in duplicate are shown in Figure 7(b) ($p \leq 0.05$). Besides, NAC decreased accumulation of intracellular ROS induced by ^{125}I seeds radiation (Figure 7(c)). Experiments were duplicated three times and data are shown in Figure 7(d) ($p \leq 0.05$). Protein levels of LC3-II and LC3-1 were determined by Western blotting in parallel. As shown in Figure 7(e), the rise in ratio of LC3-II to LC3-1 that was induced by ^{125}I seeds radiation lowered when the cells were treated with NAC. Moreover, immunofluorescence staining showed that NAC could decrease the LC3 punctuation accumulation induced by ^{125}I seeds radiation (Figure 7(h)).

We next utilized mitochondrial respiratory chain inhibitor to investigate the role of mitochondrial ROS on mitophagy induced by ^{125}I seeds radiation. DPI (50 uM) and Antimycin A (50 uM), which act as mitochondrial respiratory chain inhibitor by blocking electron flow at mitochondrial respiratory chain complexes I and III, respectively, were used to treat the irradiated HCT116 cells for 18 hours before harvest. As shown in Figures 6(f)–6(h), the treatment of DPI and Antimycin A could promote the accumulation of mitochondrial ROS and further increase mitophagy induced by ^{125}I seeds radiation.

We also used NAC, the ROS scavenger, to examine whether apoptosis correlated with the level of ROS induced by ^{125}I seeds radiation. Cells were doubled stained with the probes Annexin V and PI to evaluate the percentage of apoptosis by flow cytometry analysis (Figure 8(a)). Flow cytometry analysis showed that NAC decreased the proportion of apoptosis induced by ^{125}I seeds radiation ($p \leq 0.05$, Figure 8(b)), indicating that ROS play an important role in mitophagy and apoptosis in HCT116 cells.

3.6. The Accumulation of Mitochondrial ROS Induced by ^{125}I Seeds Irradiation Is Critical for mRNA Expression of HIF-1α and BNIP3/NIX. We investigated whether ^{125}I seeds radiation influenced the expression of HIF-1α and its target genes. Real-time PCR was performed to detect the expression of HIF-1α and its target genes BNIP3 and NIX. As shown in

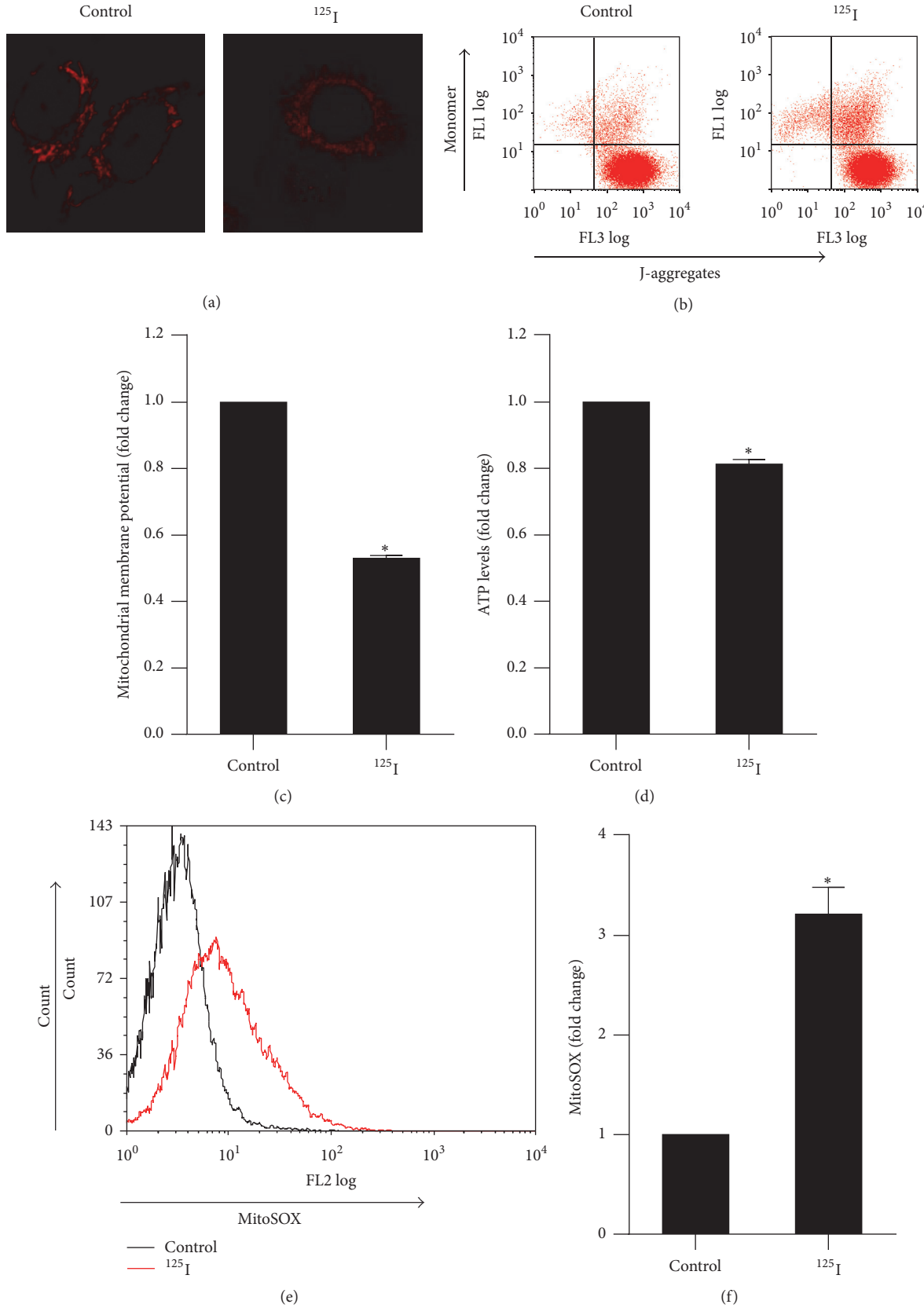

Figure 6: Continued.

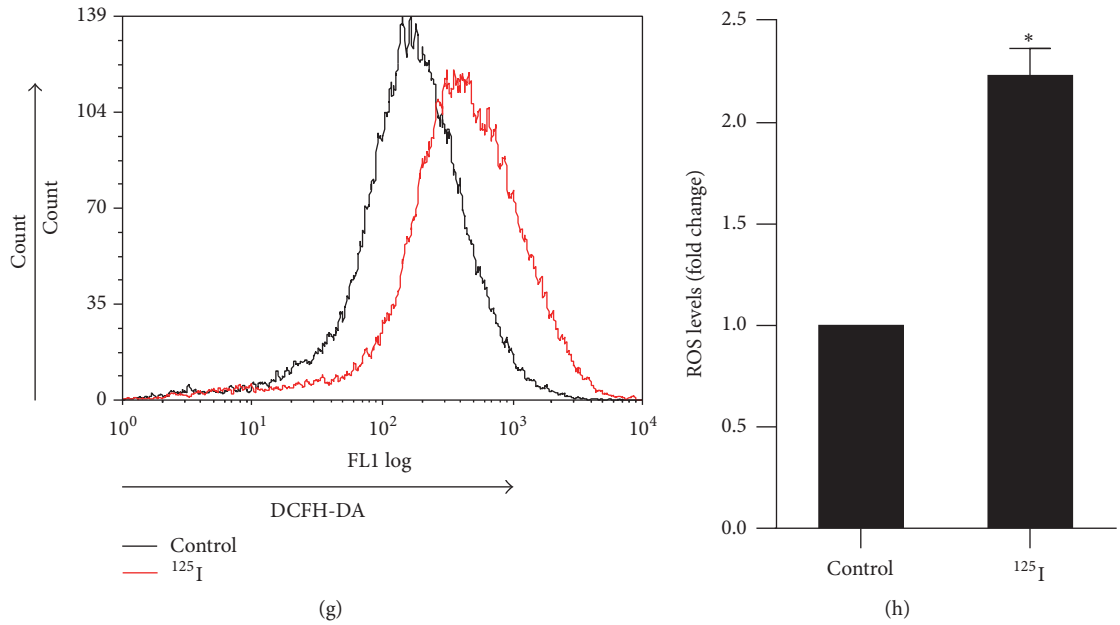

Figure 6: ^{125}I seeds radiation induced oxidative damage in mitochondria. HCT116 cells were exposed to 2 Gy of ^{125}I seeds radiation. (a) The cells were fixed and stained with anti-Tim23 antibody, and images were captured by a confocal microscope. The representative images are shown (scale bar 10 μm). (b) The mitochondrial potential was analyzed by flow cytometry with a JC-1 probe. Typical example of flow cytometry analysis was shown. (c) The ratio of J-aggregates and JC-1 monomers was used to evaluate the mitochondrial potential. The values are the means ± SD of three independent experiments. (d) Total ATP was evaluated by an ATP assay kit. The values are the means ± SD of three independent experiments. (e) Mitochondrial ROS were analyzed by flow cytometry after staining with MitoSOX. Typical example of flow cytometry analysis was shown. (f) Quantitative analysis of mitochondrial ROS. The values were derived from mean fluorescence intensity. The values are the means ± SD of three independent experiments. (g) Intracellular ROS were stained by DCFH-DA and analyzed by flow cytometry. (h) Quantitative analysis of intracellular ROS. The values were derived from mean fluorescence intensity. The values are the means ± SD of three independent experiments. $^*p \le 0.05$, as compared to the control group.

Figures 9(a)–9(c), ^{125}I seeds radiation significantly upregulated the mRNA expression of HIF-1α ($p \le 0.05$, Figure 9(a)), BNIP3 ($p \le 0.05$, Figure 9(b)), and NIX ($p \le 0.05$, Figure 9(c)).

To determine whether ROS induced by ^{125}I seeds radiation can raise the expression of BNIP3 and NIX, which is a crucial signal transduction pathway to regulate mitophagy, we examined the expression of HIF-1α, BNIP3, and NIX at the mRNA level by using real-time PCR. As shown in Figure 9, NAC decreased the expression of HIF-1α ($p \le 0.05$, Figure 9(d)), BNIP3 ($p \le 0.05$, Figure 9(e)), and NIX ($p \le 0.05$, Figure 9(f)). And the treatment of Antimycin A could further increase the mRNA expression of HIF-1α ($p \le 0.05$, Figure 9(g)), BNIP3 ($p \le 0.05$, Figure 9(h)), and NIX ($p \le 0.05$, Figure 9(i)) induced by ^{125}I seeds radiation, indicating that mitochondrial ROS induced by ^{125}I seeds irradiation might be critical for mitophagy and apoptosis through HIF-1α–BNP3/NIX pathways.

4. Discussion

Presently available evidence is in favor of autophagy as a novel cancer therapy target [37]. Autophagy is a dynamic process characterized by lysosomal degradation of cytoplasmic components such as cytoplasmic proteins and intracellular organelles [38]. The process requires the formation of the double-membrane autophagosome, which sequesters and transports the cytoplasmic cargo to the lysosome for degradation [39]. Recent studies show that autophagy plays an important role in cancer cell fate decisions following stress condition such as starvation, hypoxia, and chemotherapy [40]. Several studies have shown that elevated level of autophagy is associated with radio-resistance of various cancers [41, 42]. Multiple clinical trials have been performed to study the effects of conventional anticancer radiotherapy combined with autophagy inhibitors [37]. A number of autophagy inhibitors, such as chloroquine (CQ), hydroxychloroquine (HCQ), and 3-methyladenine (3-MA), have been applied in clinical trials. The combination of autophagy inhibitors and radiotherapy has been shown to provide survival benefits and increased lifespan in patients with cancer [43–45]; however, the specific role of autophagy induced by ^{125}I seeds radiation has not yet been determined.

In the present study, we first showed that both autophagy inhibitors 3-MA and Ly294002 could decrease the survival fraction of HCT116 cells after ^{125}I seeds radiation (Figures 1(a) and 1(b)). Moreover, knockdown of LC3 expression sensitizes HCT116 cells to ^{125}I seeds radiation, indication that inhibition of autophagy has a radiosensitizing effect on HCT116 cells (Figure 1(d)). Next, we explored how autophagy inhibitors

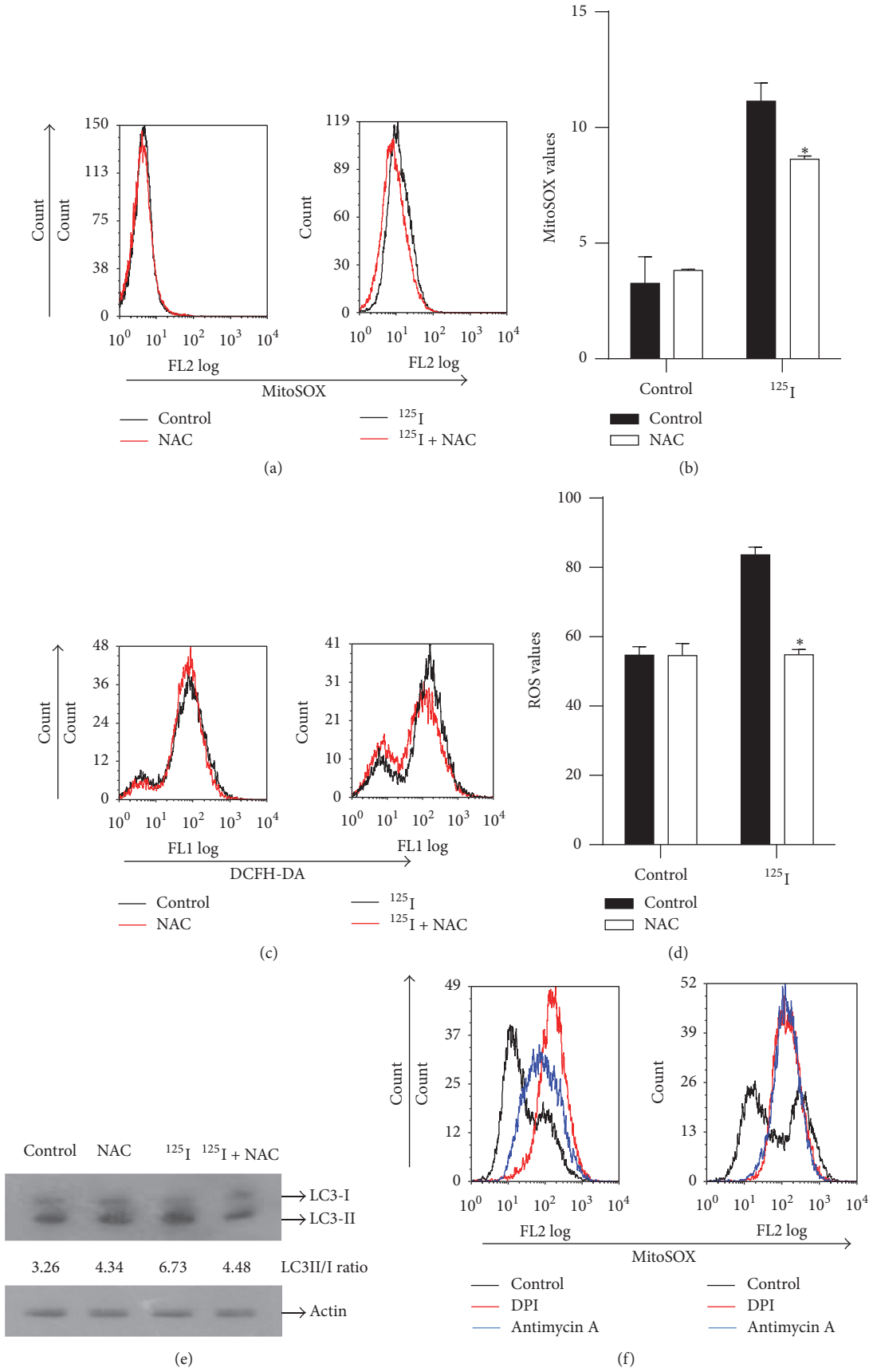

Figure 7: Continued.

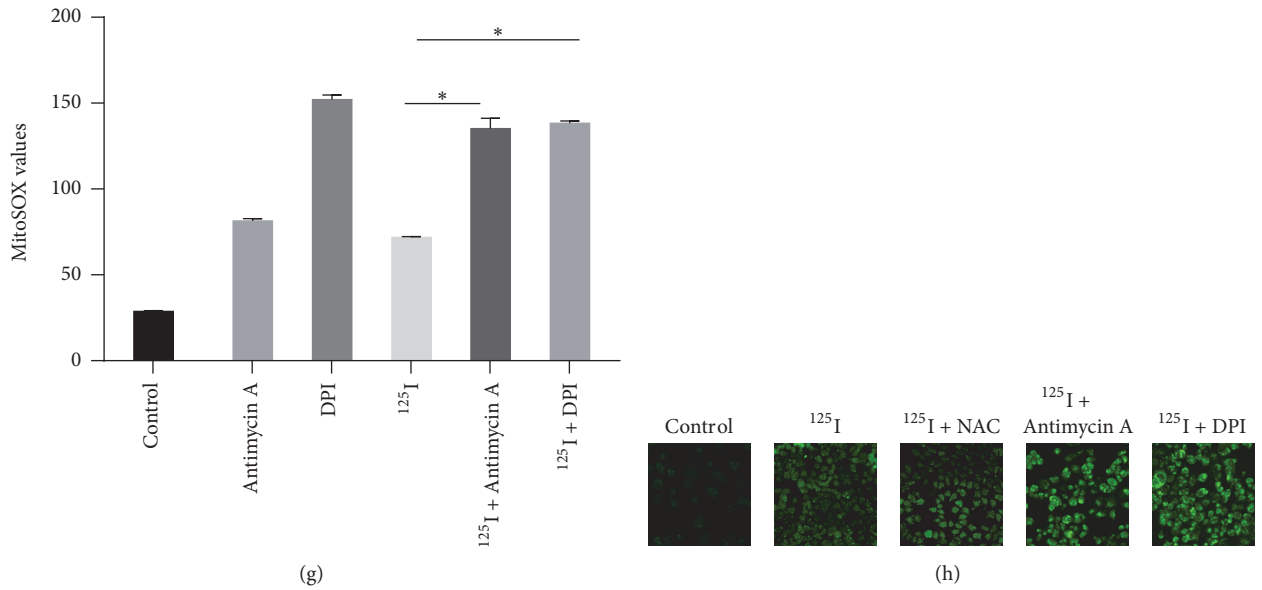

Figure 7: Accumulation of mitochondrial ROS is critical for ^{125}I seeds radiation induced mitophagy. (a–e) HCT116 cells were incubated with and without 5 mM of NAC for 4 hours and then either mock exposed or exposed to 2 Gy of ^{125}I seeds radiation. (a) Cells were stained with MitoSOX probe and then mitochondrial ROS were measured using flow cytometry. Typical example of flow cytometry analysis was shown. (b) Quantitative analysis of mitochondrial ROS. The values were derived from mean fluorescence intensity. The values are the means ± SD of three independent experiments. (c) Cells were stained by DCFH-DA probe and intracellular ROS were measured using flow cytometry. Typical example of flow cytometry analysis was shown. There are two peaks in the images which represented DCFH-DA negative peak and DCFH-DA positive peak, respectively. (d) Quantitative analysis of intracellular ROS. The values were derived from mean fluorescence intensity. (e) Representative Western blot analysis of LC3II/I is shown. (f–h). HCT116 cells were exposed to ^{125}I seeds radiation with or without Antimycin A (50 uM) or DPI (50 uM) for 18 hours. (f) Flow cytometry was performed to measure mitochondrial ROS with MitoSOX probe. Typical example of flow cytometry analysis was shown. (g) Quantitative analysis of mitochondrial ROS. The values were derived from mean fluorescence intensity. (h) Cells were immunostained with anti-LC3 antibody (green) and visualized by confocal microscopy. The typical confocal microscopy images are shown. The values are the means ± SD of three independent experiments. ∗ indicates a significant difference ($p \leq 0.05$) as compared to the control group.

modified the response of HCT116 cells to ^{125}I seeds radiation. We found that inhibition of autophagy increased the proportion of apoptosis induced by ^{125}I seeds radiation (Figures 2(a)–2(f)). Autophagy induced by multiple forms of cellular stress—such as hypoxia, ROS accumulation, DNA damage, protein aggregates, damaged organelles, or intracellular pathogens—interact with apoptosis to control cell survival and death [46]. We therefore consider it possible that ^{125}I seeds radiation triggers autophagy to protect colorectal cancer cells from apoptotic cell death.

LC3 is an important marker for detection of autophagy. It exists in two forms: LC3-I and LC3-II. LC3-I, a soluble cytosolic protein, is initially synthesized in an unprocessed form, proLC3. Once autophagy is triggered, LC3-I is modified to LC3-II which is recruited to autophagosomal membranes and showed punctuation-like distribution. The amount of LC3-II punctuation is reliably correlated with the extent of autophagosome formation [47]. LC3 lipidation can be evaluated by observing the ratio of LC3-II to LC3-1 on immunoblots. The accumulation of autophagosome can be measured by TEM image analysis or immunofluorescence analysis of LC3 punctuation [34]. In the present study, we identified ^{125}I seeds radiation induced autophagy (Figures 3(a)–3(c)) and autophagic flux (Figures 4(a)–4(c)) by immunofluorescence and Western blotting for the lipidation of LC3, respectively. Furthermore, the TEM images revealed the presence of autophagic vacuoles with mitochondria inside (Figure 5(a)), which was consistent with the results of immunofluorescence analysis (Figure 5(b)). On the basis of these findings we concluded that ^{125}I seeds radiation robustly induced mitophagy.

Mitophagy is a cargo-specific autophagy that selectively removes damaged mitochondria [48]. As a cell death executor, in addition to its more traditional roles in bioenergetics and metabolism, mitochondria are now recognized to play an important role in radiation induced cellular responses [11]. Mitochondrial damage could induce mitophagy to control mitochondrial number and quality to match metabolic demands [49]. Mitochondria are crucial energy organelles where large amounts of ATP are produced using the electrochemical gradient generated across mitochondrial inner membrane by the ETC [50]. Mitochondrial membrane potential supplies proton-motive force to promote translocation of proton from mitochondrial matrix to the intermembrane space, which is necessary for ATP synthesis. In addition to being the power center of the cell, mitochondria also generates reactive oxygen species (ROS), which originate from the electron leak from ETC. It has been well known that damage of mitochondria presented typical alterations

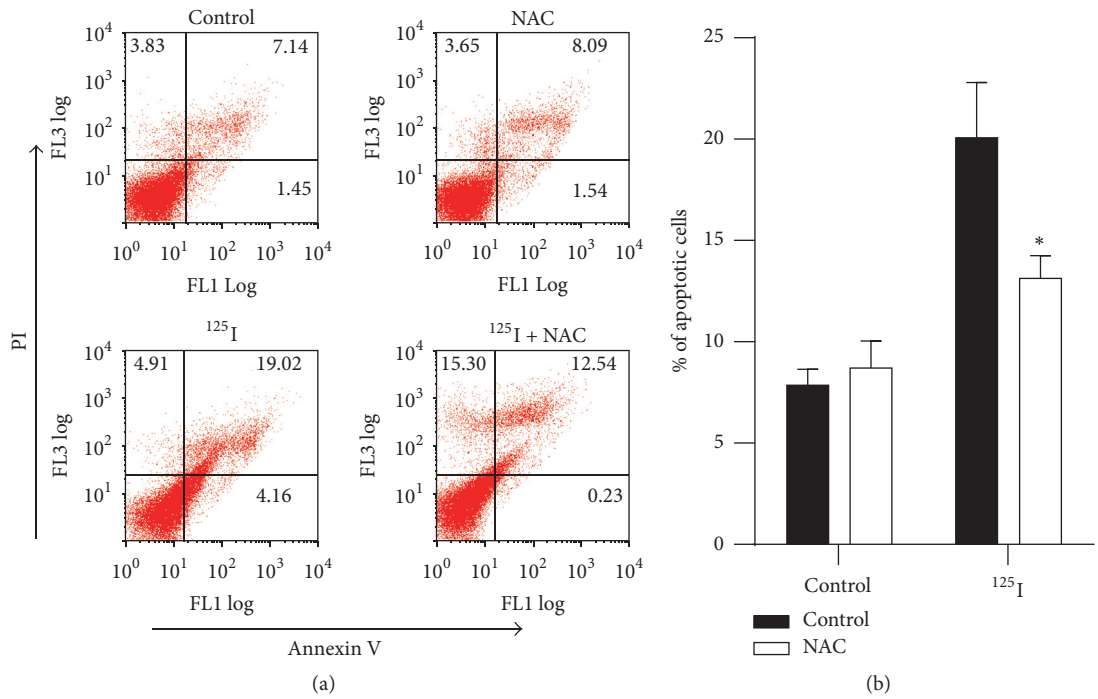

FIGURE 8: NAC decrease the proportion of apoptosis induced by ^{125}I seeds radiation. HCT116 cells were incubated with and without 5 mmol of NAC for 4 hours and then either mock exposed or exposed to 2 Gy of ^{125}I seeds radiation. (a) Annexin V and PI double staining was used to detect the distribution of cells after the indicated treatments. The typical examples of flow cytometry are shown. (b) Quantitative analysis of the percentage of apoptosis (PI^-/Annexin V^+ and PI^+/Annexin V^+ cell population). The values are the means ± SD of three independent experiments. ∗ indicates a significant difference ($p \leq 0.05$) as compared to the control group.

in mitochondrial morphology accompanied by biochemical changes, such as decreased ATP, decreased mitochondrial membrane potential, and increased mitochondrial ROS [51]. We therefore measured mitochondrial parameters after exposure to 2 Gy of ^{125}I seeds radiation. We demonstrated that ^{125}I seeds radiation had a significant impact on mitochondrial function, causing cell-specific disruption of mitochondrial membrane potential, reduction in the production of ATP, and accumulation of both cellular and mitochondrial ROS (Figure 6). These results indicated that oxidative stress induced by ^{125}I seeds radiation increased the concentration of reactive oxygen species and led to mitochondrial dysfunction by inhibiting mitochondrial respiration.

The sources of mitochondrial ROS overproduction are the electron leak from mitochondrial ETC. Complexes I and III of ETC are regarded as major sites of mitochondrial ROS producers [52]. Specific inhibitors can inhibit complexes I and III of ETC and induce the leak of electrons, which results in a higher rate of mitochondrial ROS [53]. We used ROS inhibitor or mitochondrial ROS enhancer to influence the level of mitochondrial ROS and investigate the role of mitochondrial ROS in mitophagy induced by ^{125}I seeds radiation. As a ROS scavenger NAC can block intracellular and mitochondrial ROS induced by ^{125}I seeds radiation. After treatment with NAC, LC3-II accumulation induced by ^{125}I seeds radiation decreased (Figures 7(a)–7(e)). Antimycin A, which blocks electron flow at complex III, is well known for increasing mitochondrial ROS and further increases mitophagy induced by ^{125}I seeds radiation [54]. Diphenyleneiodonium (DPI) acting as a cellular superoxide production inhibitor by inhibition of mitochondrial respiratory chain complex I NADH reductase resulted in the potential to increase the production of mitochondrial superoxide [55]. As shown in Figures 7(f)–7(h), the treatment of DPI and Antimycin A raised mitochondrial ROS and further raised mitophagy induced by ^{125}I seeds radiation. These results suggested that the accumulation of mitochondrial ROS induced by ^{125}I seeds radiation is an important intracellular factor that contributes to trigger mitophagy.

ROS can damage cellular components and activate numerous signaling pathways to induce mitophagy. HIF-1α activated by ROS is an important signaling protein that regulates mitophagy by transcriptional regulation of its target genes BNIP3 and its homologue NIX [17, 56]. ROS upregulates HIF-1α transcription by activating nonhypoxic factors in a redox-sensitive manner [57]. Therefore, we investigated whether the accumulation of ROS induced by ^{125}I seeds radiation activated HIF-1α and its target genes BNIP3 and NIX and thus triggered mitophagy. We demonstrated that ^{125}I seeds radiation elevated mitochondrial ROS and the expression of HIF-1α and its target genes BNIP3 and NIX (Figures 9(a)–9(c)). It was noteworthy that inhibition of ROS by NAC not only reduced the ROS level but also the expression of HIF-1α and its target genes BNIP3 and NIX (Figures 9(d)–9(f)). Furthermore, mitochondrial electron transport chain inhibitors (DPI and Antimycin A) raised the accumulation

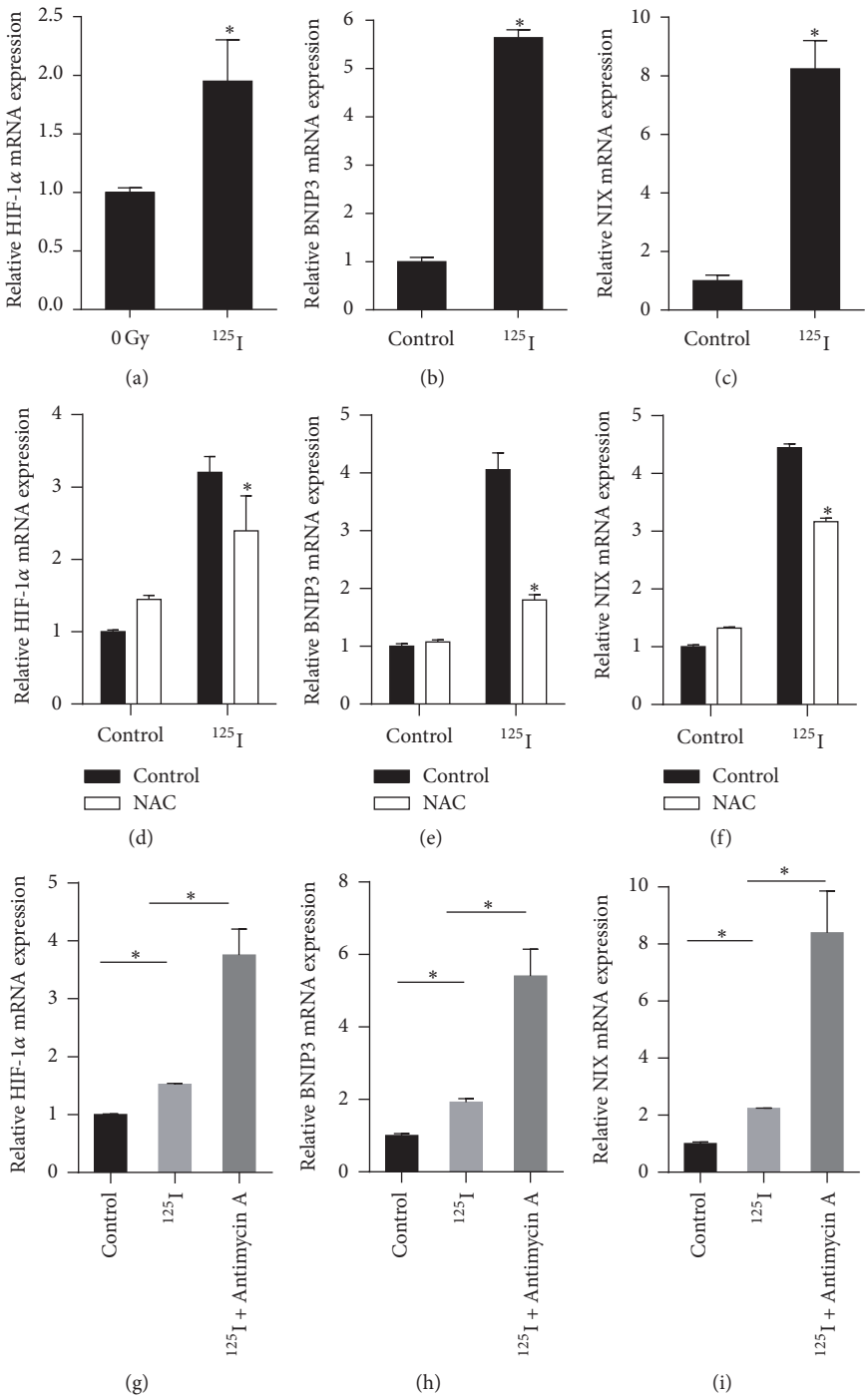

Figure 9: Mitochondrial ROS induced by ^{125}I seeds irradiation is critical for the expression of HIF-1α and its target gene. (a–c) HCT116 cells were exposed to 2 Gy of ^{125}I seeds radiation. Real-time PCR was performed to detect the expression of HIF-1α (a), BNIP3 (b), and NIX (c). (d–f) HCT116 cells were pretreated with and without 5 mM of NAC for 4 hours and then either mock exposed or exposed to 2 Gy of ^{125}I seeds radiation. The level of mRNA of HIF-1α (d), BNIP3 (e), and NIX (f) was detected by real-time PCR after treatment. (g–h) The irradiated HCT116 cells were treated with or without 50 uM of Antimycin A for 18 hours before harvest. The level of mRNA of HIF-1α (g), BNIP3 (h), and NIX (i) was detected by real-time PCR after treatment. $*$ indicates a significant difference ($p \leq 0.05$) between NAC treated and untreated cells.

of mitochondrial ROS level and the expression of HIF-1α and its target genes BNIP3 and NIX (Figures 9(g)–9(i)). These results suggested that mitochondrial ROS induced by ^{125}I seeds radiation upregulated the expression of HIF-1α and its target genes BNIP3 and NIX to trigger mitophagy.

BNIP3 and NIX can interact with BCL2 and BCL-XL to play a proapoptotic role. Deregulation of BNIP3 or NIX expression is associated with apoptosis [58]. We therefore hypothesized that ROS accumulation induced by ^{125}I seeds radiation might play a critical role in cell fate determination. To test this theory, we used NAC to explore how ROS accumulation affects cell fate. Strikingly, NAC inhibited the percentage of apoptosis induced by ^{125}I seeds radiation (Figures 8(a) and 8(b)), suggesting that mitochondrial ROS accumulation induced by ^{125}I seeds radiation not only triggered mitophagy through upregulation of the expression of HIF-1α and its target genes but was also involved in the cellular decision of apoptosis.

5. Conclusions

Our results show that the high level of mitochondrial ROS generated by ^{125}I seeds radiation induced mitochondrial damage upregulates the expression of HIF-1α and its target genes BNIP3 and NIX and triggers mitophagy. Mitophagy serves to reduce oxidative damage and ROS levels through the removal of damaged mitochondria, thus protecting HCT116 cells from apoptosis.

Competing Interests

All authors of the paper have no financial and personal relationships with other people or organizations that could inappropriately influence this work.

Authors' Contributions

Junjie Wang and Yong Zhao designed the study. Lelin Hu carried out the molecular biology experiment. Hao Wang and Li Huang participated in the statistical analysis. Lelin Hu wrote the manuscript. Junjie Wang and Yong Zhao revised the manuscript. All authors read and approved the final manuscript.

Acknowledgments

The authors thank Associate Professor Guopeng Wang, who worked in School of life Sciences, Peking University, for technical assistance and giving advice regarding transmission electron microscopy technology for this study. The authors thank Professor Xiaojuan Du, who worked in Peking University Health Science Center, for providing the HCT116 cell line. This work was supported by grants from the National Natural Science Foundation for Young Scholars (81402519, Hao Wang).

References

[1] J. J. Wang, H. S. Yuan, J. N. Li, W. J. Jiang, Y. L. Jiang, and S. Q. Tian, "Interstitial permanent implantation of 125I seeds as salvage therapy for re-recurrent rectal carcinoma," *International Journal of Colorectal Disease*, vol. 24, no. 4, pp. 391–399, 2009.

[2] J. Wang, Y. Jiang, J. Li, S. Tian, W. Ran, and D. Xiu, "Intraoperative ultrasound-guided iodine-125 seed implantation for unresectable pancreatic carcinoma," *Journal of Experimental and Clinical Cancer Research*, vol. 28, no. 1, article 88, 2009.

[3] J. Li, J. Wang, N. Meng et al., "Image-guided percutaneous ^{125}I seed implantation as a salvage treatment for recurrent soft tissue sarcomas after surgery and radiotherapy," *Cancer Biotherapy and Radiopharmaceuticals*, vol. 26, no. 1, pp. 113–120, 2011.

[4] L. Zhu, Y. Jiang, J. Wang et al., "An investigation of ^{125}I seed permanent implantation for recurrent carcinoma in the head and neck after surgery and external beam radiotherapy," *World Journal of Surgical Oncology*, vol. 11, article 60, 2013.

[5] L. Yao, J. Wang, Y. Jiang et al., "Permanent interstitial ^{125}I seed implantation as a salvage therapy for pediatric recurrent or metastatic soft tissue sarcoma after multidisciplinary treatment," *World Journal of Surgical Oncology*, vol. 13, no. 1, article 335, 2015.

[6] L. Yao, Y. Jiang, P. Jiang et al., "CT-guided permanent ^{125}I seed interstitial brachytherapy for recurrent retroperitoneal lymph node metastases after external beam radiotherapy," *Brachytherapy*, vol. 14, no. 5, pp. 662–669, 2015.

[7] Q. Cao, H. Wang, N. Meng et al., "CT-guidance interstitial ^{125}Iodine seed brachytherapy as a salvage therapy for recurrent spinal primary tumors," *Radiation Oncology*, vol. 9, no. 1, article 301, 2014.

[8] Y. Tian, Q. Xie, Y. Tian et al., "Radioactive ^{125}I seed inhibits the cell growth, migration, and invasion of nasopharyngeal carcinoma by triggering DNA damage and inactivating VEGF-A/ERK signaling," *PLoS ONE*, vol. 8, no. 9, Article ID e74038, 2013.

[9] J. Liu, H. Wang, A. Qu, J. Li, Y. Zhao, and J. Wang, "Combined effects of C225 and 125-iodine seed radiation on colorectal cancer cells," *Radiation Oncology*, vol. 8, no. 1, article 219, 2013.

[10] A. Qu, H. Wang, J. Li et al., "Biological effects of ^{125}I seeds radiation on A549 lung cancer cells: G2/M arrest and enhanced cell death," *Cancer Investigation*, vol. 32, no. 6, pp. 209–217, 2014.

[11] B. Zhang, M. M. Davidson, H. Zhou, C. Wang, W. F. Walker, and T. K. Hei, "Cytoplasmic irradiation results in mitochondrial dysfunction and DRP1-dependent mitochondrial fission," *Cancer Research*, vol. 73, no. 22, pp. 6700–6710, 2013.

[12] W. W.-Y. Kam and R. B. Banati, "Effects of ionizing radiation on mitochondria," *Free Radical Biology and Medicine*, vol. 65, pp. 607–619, 2013.

[13] M. Saraste, "Oxidative phosphorylation at the fin de siecle," *Science*, vol. 283, no. 5407, pp. 1488–1493, 1999.

[14] P. A. Ney, "Mitochondrial autophagy: origins, significance, and role of BNIP3 and NIX," *Biochimica et Biophysica Acta—Molecular Cell Research*, vol. 1853, no. 10, pp. 2775–2783, 2015.

[15] B. Cheng, A. Xu, M. Qiao et al., "BECN1s, a short splice variant of BECN1, functions in mitophagy," *Autophagy*, vol. 11, no. 11, pp. 2048–2056, 2015.

[16] L. Liu, K. Sakakibara, Q. Chen, and K. Okamoto, "Receptor-mediated mitophagy in yeast and mammalian systems," *Cell Research*, vol. 24, no. 7, pp. 787–795, 2014.

[17] A. H. Chourasia, K. Tracy, C. Frankenberger et al., "Mitophagy defects arising from BNip3 loss promote mammary tumor

progression to metastasis," *EMBO Reports*, vol. 16, no. 9, pp. 1145–1163, 2015.

[18] A. Viale, P. Pettazzoni, C. A. Lyssiotis et al., "Oncogene ablation-resistant pancreatic cancer cells depend on mitochondrial function," *Nature*, vol. 514, no. 7524, pp. 628–632, 2014.

[19] H. Wu, D. Xue, G. Chen et al., "The BCL2L1 and PGAM5 axis defines hypoxia-induced receptor-mediated mitophagy," *Autophagy*, vol. 10, no. 10, pp. 1712–1725, 2014.

[20] T. E. O'Sullivan, L. R. Johnson, H. H. Kang, and J. C. Sun, "BNIP3- and BNIP3L-mediated mitophagy promotes the generation of natural killer cell memory," *Immunity*, vol. 43, no. 2, pp. 331–342, 2015.

[21] N. Wilfinger, S. Austin, B. Scheiber-Mojdekhar et al., "Novel p53-dependent anticancer strategy by targeting iron signaling and BNIP3L-induced mitophagy," *Oncotarget*, vol. 7, no. 2, pp. 1242–1261, 2016.

[22] D. R. Green and B. Levine, "To be or not to be? How selective autophagy and cell death govern cell fate," *Cell*, vol. 157, no. 1, pp. 65–75, 2014.

[23] N. M. Mazure and J. Pouysségur, "Hypoxia-induced autophagy: cell death or cell survival?" *Current Opinion in Cell Biology*, vol. 22, no. 2, pp. 177–180, 2010.

[24] E. I. Braicu, H. Luketina, R. Richter et al., "HIF1α is an independent prognostic factor for overall survival in advanced primary epithelial ovarian cancer—a study of the OVCAD consortium," *OncoTargets and Therapy*, vol. 7, pp. 1563–1569, 2014.

[25] L. Li, J. Tan, Y. Miao, P. Lei, and Q. Zhang, "ROS and autophagy: interactions and molecular regulatory mechanisms," *Cellular and Molecular Neurobiology*, vol. 35, no. 5, pp. 615–621, 2015.

[26] H.-Q. Zhuang, J.-J. Wang, A.-Y. Liao, J.-D. Wang, and Y. Zhao, "The biological effect of ^{125}I seed continuous low dose rate irradiation in CL187 cells," *Journal of Experimental and Clinical Cancer Research*, vol. 28, no. 1, article 12, 2009.

[27] H. Wang, J. Li, A. Qu, J. Liu, Y. Zhao, and J. Wang, "The different biological effects of single, fractionated and continuous low dose rate irradiation on CL187 colorectal cancer cells," *Radiation Oncology*, vol. 8, no. 1, article 196, 2013.

[28] T. Yan, Y. Seo, and T. J. Kinsella, "Differential cellular responses to prolonged LDR-IR in MLH1-proficient and MLH1-deficient colorectal cancer HCT116 cells," *Clinical Cancer Research*, vol. 15, no. 22, pp. 6912–6920, 2009.

[29] L. Zhu, T. Yang, L. Li et al., "TSC1 controls macrophage polarization to prevent inflammatory disease," *Nature Communications*, vol. 5, Article ID 4696, 2014.

[30] L. Guo, H. Yu, W. Gu et al., "Autophagy negatively regulates transmissible gastroenteritis virus replication," *Scientific Reports*, vol. 6, Article ID 23864, 2016.

[31] L. Hu, H. Wang, L. Huang, Y. Zhao, and J. Wang, "Crosstalk between autophagy and intracellular radiation response (Review)," *International Journal of Oncology*, vol. 49, no. 6, pp. 2217–2226, 2016.

[32] Y. Jiang, J. Lee, J. H. Lee et al., "The arginylation branch of the N-end rule pathway positively regulates cellular autophagic flux and clearance of proteotoxic proteins," *Autophagy*, vol. 12, no. 11, pp. 2197–2212, 2016.

[33] M. J. Lee, J. H. Lee, and D. C. Rubinsztein, "Tau degradation: the ubiquitin-proteasome system versus the autophagy-lysosome system," *Progress in Neurobiology*, vol. 105, pp. 49–59, 2013.

[34] D. J. Klionsky, H. Abdalla, H. Abeliovich et al., "Guidelines for the use and interpretation of assays for monitoring autophagy," *Autophagy*, vol. 8, no. 4, pp. 445–544, 2012.

[35] S. Banerjee, N. Aykin-Burns, K. J. Krager et al., "Loss of C/EBPδ enhances IR-induced cell death by promoting oxidative stress and mitochondrial dysfunction," *Free Radical Biology and Medicine*, vol. 99, pp. 296–307, 2016.

[36] X. Wang, M. Yan, L. Zhao et al., "Low-dose methylmercury-induced apoptosis and mitochondrial DNA mutation in human embryonic neural progenitor cells," *Oxidative Medicine and Cellular Longevity*, vol. 2016, Article ID 5137042, 10 pages, 2016.

[37] M. B. E. Schaaf, B. Jutten, T. G. Keulers et al., "Canonical autophagy does not contribute to cellular radioresistance," *Radiotherapy and Oncology*, vol. 114, no. 3, pp. 406–412, 2015.

[38] H. Weidberg, E. Shvets, and Z. Elazar, "Biogenesis and cargo selectivity of autophagosomes," *Annual Review of Biochemistry*, vol. 80, pp. 125–156, 2011.

[39] B. B. Chandrika, C. Yang, Y. Ou et al., "Endoplasmic reticulum stress-induced autophagy provides cytoprotection from chemical hypoxia and oxidant injury and ameliorates renal ischemia-reperfusion injury," *PLoS ONE*, vol. 10, no. 10, Article ID e0140025, 2015.

[40] J. J. Jaboin, E. T. Shinohara, L. Moretti, E. S. Yang, J. M. Kaminski, and B. Lu, "The role of mTOR inhibition in augmenting radiation induced autophagy," *Technology in Cancer Research and Treatment*, vol. 6, no. 5, pp. 443–447, 2007.

[41] Q. Sun, T. Liu, Y. Yuan et al., "MiR-200c inhibits autophagy and enhances radiosensitivity in breast cancer cells by targeting UBQLN1," *International Journal of Cancer*, vol. 136, no. 5, pp. 1003–1012, 2015.

[42] N. Chen, L. Wu, H. Yuan, and J. Wang, "ROS/autophagy/Nrf2 pathway mediated low-dose radiation induced radio-resistance in human lung adenocarcinoma A549 cell," *International Journal of Biological Sciences*, vol. 11, no. 7, pp. 833–844, 2015.

[43] K. W. Kim, L. Moretti, L. R. Mitchell, K. J. Dae, and B. Lu, "Combined Bcl-2/mammalian target of rapamycin inhibition leads to enhanced radiosensitization via induction of apoptosis and autophagy in non-small cell lung tumor xenograft model," *Clinical Cancer Research*, vol. 15, no. 19, pp. 6096–6105, 2009.

[44] A. Apel, I. Herr, H. Schwarz, H. P. Rodemann, and A. Mayer, "Blocked autophagy sensitizes resistant carcinoma cells to radiation therapy," *Cancer Research*, vol. 68, no. 5, pp. 1485–1494, 2008.

[45] M. Chaurasia, A. N. Bhatt, A. Das, B. S. Dwarakanath, and K. Sharma, "Radiation-induced autophagy: mechanisms and consequences," *Free Radical Research*, vol. 50, no. 3, pp. 273–290, 2016.

[46] G. Kroemer, G. Mariño, and B. Levine, "Autophagy and the integrated stress response," *Molecular Cell*, vol. 40, no. 2, pp. 280–293, 2010.

[47] Y. Kabeya, N. Mizushima, T. Ueno et al., "LC3, a mammalian homologue of yeast Apg8p, is localized in autophagosome membranes after processing," *The EMBO Journal*, vol. 19, no. 21, pp. 5720–5728, 2000.

[48] C. De Duve and R. Wattiaux, "Functions of lysosomes," *Annual Review of Physiology*, vol. 28, pp. 435–492, 1966.

[49] R. J. Youle and D. P. Narendra, "Mechanisms of mitophagy," *Nature Reviews Molecular Cell Biology*, vol. 12, no. 1, pp. 9–14, 2011.

[50] S. Hekimi, Y. Wang, and A. Noë, "Mitochondrial ROS and the effectors of the intrinsic apoptotic pathway in aging cells: the discerning killers!," *Frontiers in Genetics*, vol. 7, article 161, 2016.

[51] L. Galam, A. Failla, R. Soundararajan, R. F. Lockey, and N. Kolliputi, "4-Hydroxynonenal regulates mitochondrial function in

human small airway epithelial cells," *Oncotarget*, vol. 6, no. 39, pp. 41508–41521, 2015.

[52] D. Babu, G. Leclercq, V. Goossens et al., "Mitochondria and NADPH oxidases are the major sources of TNF-α/cycloheximide-induced oxidative stress in murine intestinal epithelial MODE-K cells," *Cellular Signalling*, vol. 27, no. 6, pp. 1141–1158, 2015.

[53] P. R. Angelova and A. Y. Abramov, "Functional role of mitochondrial reactive oxygen species in physiology," *Free Radical Biology and Medicine*, vol. 100, pp. 81–85, 2016.

[54] D. Rakhmatullina, A. Ponomareva, N. Gazizova, and F. Minibayeva, "Mitochondrial morphology and dynamics in *Triticum aestivum* roots in response to rotenone and antimycin A," *Protoplasma*, vol. 253, no. 5, pp. 1299–1308, 2016.

[55] N. Li, K. Ragheb, G. Lawler et al., "DPI induces mitochondrial superoxide-mediated apoptosis," *Free Radical Biology and Medicine*, vol. 34, no. 4, pp. 465–477, 2003.

[56] S. Movafagh, S. Crook, and K. Vo, "Regulation of hypoxia-inducible factor-1a by reactive oxygen species: new developments in an old debate," *Journal of Cellular Biochemistry*, vol. 116, no. 5, pp. 696–703, 2015.

[57] S. Bonello, C. Zahringer, R. S. BelAiba et al., "Reactive oxygen species activate the HIF-1α promoter via a functional NFκB site," *Arteriosclerosis, Thrombosis, and Vascular Biology*, vol. 27, no. 4, pp. 755–761, 2007.

[58] J. Zhang and P. A. Ney, "Role of BNIP3 and NIX in cell death, autophagy, and mitophagy," *Cell Death and Differentiation*, vol. 16, no. 7, pp. 939–946, 2009.